Midwest Pooled Fund Research Program
Fiscal Year 2021
Research Project Number TPF-5(430) Supplement #16
NDOT Sponsoring Agency Code RPFP-21-CONC-2

MODIFICATION AND EVALUATION OF THE ASPHALT PIN TIE-DOWN FOR F-SHAPE PCB: TEST NO. WITD-4

Submitted by

Brandon J. Perry, M.E.M.E.
Research Engineer

Terrol T. Wilson, B.S.
Former Undergraduate Research Assistant

Robert W. Bielenberg, M.S.M.E.
Research Engineer

Ronald K. Faller, Ph.D., P.E.
Research Professor & MwRSF Director

MIDWEST ROADSIDE SAFETY FACILITY
Nebraska Transportation Center
University of Nebraska-Lincoln

Main Office
Prem S. Paul Research Center at Whittier School
Room 130, 2200 Vine Street
Lincoln, Nebraska 68583-0853
(402) 472-0965

Outdoor Test Site
4630 N.W. 36th Street
Lincoln, Nebraska 68524

Submitted to

MIDWEST POOLED FUND PROGRAM
Nebraska Department of Transportation
1500 Nebraska Parkway
Lincoln, Nebraska 68502

MwRSF Research Report No. TRP-03-488-24

December 17, 2024

TECHNICAL REPORT DOCUMENTATION PAGE

1. Report No.
TRP-03-488-24

2. Government Accession No.

3. Recipient's Catalog No.

4. Title and Subtitle
Modification and Evaluation of the Asphalt Pin Tie-Down for F-shape PCB: Test No. WITD-4

5. Report Date
December 17, 2024

6. Performing Organization Code

7. Author(s)
Perry, B.J., Wilson, T.T., Bielenberg, R.W., and Faller, R.K.

8. Performing Organization Report No.
TRP-03-488-24

9. Performing Organization Name and Address
Midwest Roadside Safety Facility (MwRSF)
Nebraska Transportation Center
University of Nebraska-Lincoln

Main Office:
Prem S. Paul Research Center at Whittier School
Room 130, 2200 Vine Street
Lincoln, Nebraska 68583-0853

Outdoor Test Site:
4630 N.W. 36th Street
Lincoln, Nebraska 68524

10. Work Unit No.

11. Contract
TPF-5(430) Supplement #136

12. Sponsoring Agency Name and Address
Midwest Pooled Fund Program
Nebraska Department of Transportation
1500 Nebraska Parkway
Lincoln, Nebraska 68502

13. Type of Report and Period Covered
Final Report: 2018-2024

14. Sponsoring Agency Code
RPFP-21-CONC-2

15. Supplementary Notes
Prepared in cooperation with U.S. Department of Transportation, Federal Highway Administration

16. Abstract

The objective of this research was to develop and evaluate potential design modifications for the F-shaped portable concrete barrier (PCB) with a steel pin tie-down anchorage system for asphalt surfaces. Previous full-scale crash testing of the original asphalt pin tie-down anchorage according to *Manual for Assessing Safety Hardware* (MASH) Test Level 3 (TL-3) test designation no. 3-11 criteria resulted in a failure due to wheel snag on the barrier joint that led to excess occupant compartment deformation. Potential design modifications were developed to mitigate wheel snag, and a preferred modification was selected for full-scale crash testing. The modified barrier system was full-scale crash tested and evaluated according to MASH TL-3 test designation no. 3-11 criteria.

Test no. WITD-4 consisted of sixteen F-shape PCB segments installed with a pinned tie-down configuration placed on a 2-in. thick asphalt pad. The rear toe of the PCBs was installed 18 in. from the edge of a 36-in. wide x 36-in. deep trench. Barrier nos. 5 through 13 were anchored on the traffic side of the system with three 1½-in. diameter x 38½-in. long steel pins placed through the bolt anchor pockets on each barrier segment and driven through the asphalt and into the underlying soil. A 5,019-lb quad cab pickup truck impacted the anchored PCB system at a speed of 61.9 mph and at an angle of 25.0 degrees. During test no. WITD-4, all occupant compart deformations recorded were within MASH limits and test no. WITD-4 was deemed successful according to MASH TL-3 test designation no. 3-11 safety criteria. However, due to the 2270P vehicle's left-front door snagging on a saddle cap, it was recommended that further evaluation of the system with MASH test designation no. 3-10 may be warranted.

17. Key Words
Highway Safety, Crash Test, Roadside Appurtenances, Compliance Test, MASH, Test Level 3, Portable Concrete Barrier, Pinned Barrier, Asphalt Foundation

18. Distribution Statement
No restrictions. This document is available through the National Technical Information Service.
5285 Port Royal Road
Springfield, VA 22161

19. Security Classification (of this report)
Unclassified

20. Security Classification (of this page)
Unclassified

21. No. of Pages
158

22. Price

Form DOT F 1700.7 (8-72) Reproduction of completed page authorized

DISCLAIMER STATEMENT

This material is based upon work supported by the Federal Highway Administration, U.S. Department of Transportation and the Midwest Pooled Fund Program under TPF-5(430) Supplement #16. The contents of this report reflect the views and opinions of the authors who are responsible for the facts and the accuracy of the data presented herein. The contents do not necessarily reflect the official views or policies of the state highway departments participating in the Midwest Pooled Fund Program nor the Federal Highway Administration, U.S. Department of Transportation. This report does not constitute a standard, specification, or regulation. Trade or manufacturers' names, which may appear in this report, are cited only because they are considered essential to the objectives of the report. The United States (U.S.) government and the state highway departments participating in the Midwest Pooled Fund Program do not endorse products or manufacturers.

UNCERTAINTY OF MEASUREMENT STATEMENT

The Midwest Roadside Safety Facility (MwRSF) has determined the uncertainty of measurements for several parameters involved in standard full-scale crash testing and non-standard testing of roadside safety features. Information regarding the uncertainty of measurements for critical parameters is available upon request by the sponsor and the Federal Highway Administration.

INDEPENDENT APPROVING AUTHORITY

The Independent Approving Authority (IAA) for the data contained herein was Dr. Andrew Loken, Associate Research Professor.

ACKNOWLEDGEMENTS

The authors wish to acknowledge several sources that made a contribution to this project: (1) the Midwest Pooled Fund Program funded by the California Department of Transportation, Florida Department of Transportation, Georgia Department of Transportation, Hawaii Department of Transportation, Illinois Department of Transportation, Indiana Department of Transportation, Iowa Department of Transportation, Kansas Department of Transportation, Kentucky Department of Transportation, Minnesota Department of Transportation, Missouri Department of Transportation, Nebraska Department of Transportation, New Jersey Department of Transportation, North Carolina Department of Transportation, Ohio Department of Transportation, South Carolina Department of Transportation, South Dakota Department of Transportation, Utah Department of Transportation, Virginia Department of Transportation, Wisconsin Department of Transportation, and Wyoming Department of Transportation for sponsoring this project; (2) MwRSF personnel for constructing the barriers and conducting the crash tests, and (3) the Holland Computing Center at the University of Nebraska, which receives support from the Nebraska Research Initiative, for providing computational resources.

Acknowledgement is also given to the following individuals who contributed to the completion of this research project.

Midwest Roadside Safety Facility
J.C. Holloway, M.S.C.E., Research Engineer & Assistant Director –Physical Testing Division
K.A. Lechtenberg, M.S.M.E., Research Engineer
S.K. Rosenbaugh, M.S.C.E., Research Engineer
C.S. Stolle, Ph.D., Research Associate Professor
J.S. Steelman, Ph.D., P.E., Associate Professor
M. Asadollahi Pajouh, Ph.D., P.E., Research Assistant Professor
A.E. Loken, Ph.D., Research Assistant Professor
T.Y. Yosef, Ph.D., Research Assistant Professor
A.T. Russell, B.S.B.A., Testing and Maintenance Technician II
E.W. Krier, B.S., Former Engineering Testing Technician II
D.S. Charroin, Engineering Testing Technician II
R.M. Novak, Engineering Testing Technician II
T.C. Donahoo, Engineering Testing Technician I
J.T. Jones, Engineering Testing Technician II
E.L. Urbank, Research Communication Specialist
Z.Z. Jabr, Engineering Technician
J.J. Oliver, Solidworks Drafting Coordinator
Undergraduate and Graduate Research Assistants

California Department of Transportation
Bob Meline, Chief, Roadside Safety Research Branch
David Whitesel, P.E., Transportation Engineer

Florida Department of Transportation
Derwood C. Sheppard, Jr., P.E., Design Standards Publication Manager, Roadway Design Engineer

Georgia Department of Transportation
Christopher Rudd, P.E., State Design Policy Engineer
Frank Flanders IV, P.E., Assistant State Design Policy Engineer

Hawaii Department of Transportation
James Fu, P.E., State Bridge Engineer
Dean Takiguchi, P.E., Engineer, Bridge Design Section
Kimberly Okamura, Engineer, Bridge Design Section

Illinois Department of Transportation
Filiberto Sotelo, P.E., Engineering Policy Unit Chief
Martha Brown, P.E., Safety Evaluation Unit Chief

Indiana Department of Transportation
Katherine Smutzer, P.E., Standards Engineer
Elizabeth Phillips, P.E., Highway Design Director

Iowa Department of Transportation
Daniel Harness, P.E., Transportation Engineer Specialist
Brian Smith, P.E., Methods Engineer
Mike Thiel, P.E., Transportation Engineer Specialist

Kansas Department of Transportation
Ron Seitz, P.E., Director of Design
Scott King, P.E., Road Design Bureau Chief

Kentucky Department of Transportation
Jason J. Siwula, P.E., Assistant State Highway Engineer
Kevin Martin, P.E., Transportation Engineer Specialist
Gary Newton, Engineering Tech III, Design Standards

Minnesota Department of Transportation
Michael Elle, P.E., Design Standards Engineer
Michelle Moser, P.E., Assistant Design Standards Engineer

Missouri Department of Transportation
Sarah Kleinschmit, P.E., Policy and Innovations Engineer

Nebraska Department of Transportation
Phil TenHulzen, P.E., Design Standards Engineer
Jim Knott, P.E., Construction Engineer
Mick Syslo, P.E., State Roadway Design Engineer
Brandon Varilek, P.E., Materials and Research Engineer & Division Head
Mark Fischer, P.E., PMP, Research Program Manager
Angela Andersen, Research Coordinator
David T. Hansen, Internal Research Coordinator

New Jersey Department of Transportation
Hung Tang, P.E., Principal Engineer, Transportation
Joseph Warren, Assistant Engineer, Transportation

North Carolina Department of Transportation
Neil Mastin, P.E., Manager, Transportation Program Management – Research and Development
D. D. “Bucky” Galloway, P.E., CPM, Field Operations Engineer
Brian Mayhew, P.E., State Traffic Safety Engineer

Ohio Department of Transportation
Don Fisher, P.E., Roadway Standards Engineer

South Carolina Department of Transportation
J. Adam Hixon, P.E., Design Standards Associate
Mark H. Anthony, P.E., Letting Preparation Engineer
Henry Cross, P.E., Design Standards Engineer
Jason Hall, P.E., Engineer

South Dakota Department of Transportation
David Huft, P.E., Research Engineer
Randy Brown, P.E., Standards Engineer

Utah Department of Transportation
Shawn Debenham, Traffic and Safety Specialist
Glenn Blackwelder, Operations Engineer

Virginia Department of Transportation
Charles Patterson, P.E., Standards/Special Design Section Manager
Andrew Zickler, P.E., Complex Bridge Design and ABC Support Program Manager

Wisconsin Department of Transportation
Erik Emerson, P.E., Standards Development Engineer
Rodney Taylor, P.E., Roadway Design Standards Unit Supervisor

Wyoming Department of Transportation
William Wilson, P.E., Architectural and Highway Standards Engineer

Federal Highway Administration
David Mraz, Division Bridge Engineer, Nebraska Division Office

SI* (MODERN METRIC) CONVERSION FACTORS

APPROXIMATE CONVERSIONS TO SI UNITS

Symbol	When You Know	Multiply By	To Find	Symbol
		LENGTH		
in.	inches	25.4	millimeters	mm
ft	feet	0.305	meters	m
yd	yards	0.914	meters	m
mi	miles	1.61	kilometers	km
		AREA		
in^2	square inches	645.2	square millimeters	mm^2
ft^2	square feet	0.093	square meters	m^2
yd^2	square yard	0.836	square meters	m^2
ac	acres	0.405	hectares	ha
mi^2	square miles	2.59	square kilometers	km^2
		VOLUME		
fl oz	fluid ounces	29.57	milliliters	mL
gal	gallons	3.785	liters	L
ft^3	cubic feet	0.028	cubic meters	m^3
yd^3	cubic yards	0.765	cubic meters	m^3
		NOTE: volumes greater than 1,000 L shall be shown in m^3		
		MASS		
oz	ounces	28.35	grams	g
lb	pounds	0.454	kilograms	kg
T	short ton (2,000 lb)	0.907	megagrams (or “metric ton”)	Mg (or "t")
		TEMPERATURE (exact degrees)		
°F	Fahrenheit	5(F-32)/9 or (F-32)/1.8	Celsius	°C
		ILLUMINATION		
fc	foot-candles	10.76	lux	lx
fl	foot-Lamberts	3.426	candela per square meter	cd/m^2
		FORCE & PRESSURE or STRESS		
lbf	poundforce	4.45	newtons	N
lbf/in^2	poundforce per square inch	6.89	kilopascals	kPa

APPROXIMATE CONVERSIONS FROM SI UNITS

Symbol	When You Know	Multiply By	To Find	Symbol
		LENGTH		
mm	millimeters	0.039	inches	in.
m	meters	3.28	feet	ft
m	meters	1.09	yards	yd
km	kilometers	0.621	miles	mi
		AREA		
mm^2	square millimeters	0.0016	square inches	in^2
m^2	square meters	10.764	square feet	ft^2
m^2	square meters	1.195	square yard	yd^2
ha	hectares	2.47	acres	ac
km^2	square kilometers	0.386	square miles	mi^2
		VOLUME		
mL	milliliter	0.034	fluid ounces	fl oz
L	liters	0.264	gallons	gal
m^3	cubic meters	35.314	cubic feet	ft^3
m^3	cubic meters	1.307	cubic yards	yd^3
		MASS		
g	grams	0.035	ounces	oz
kg	kilograms	2.202	pounds	lb
Mg (or "t")	megagrams (or “metric ton”)	1.103	short ton (2,000 lb)	T
		TEMPERATURE (exact degrees)		
°C	Celsius	1.8C+32	Fahrenheit	°F
		ILLUMINATION		
lx	lux	0.0929	foot-candles	fc
cd/m^2	candela per square meter	0.2919	foot-Lamberts	fl
		FORCE & PRESSURE or STRESS		
N	newtons	0.225	poundforce	lbf
kPa	kilopascals	0.145	poundforce per square inch	lbf/in^2

*SI is the symbol for the International System of Units. Appropriate rounding should be made to comply with Section 4 of ASTM E380.

TABLE OF CONTENTS

LIST OF FIGURES

LIST OF TABLES

1 INTRODUCTION

1.1 Background

Portable concrete barriers (PCBs) are often used in temporary applications where available space behind the barrier is limited, and it is desired that barrier deflection during vehicular impacts is reduced. Free-standing PCB systems develop redirective capacity through a combination of various forces and mechanisms. These include inertial resistance developed by the acceleration of barrier segments, lateral friction loads, and tensile loads developed from the mass and friction of the barrier segments upstream and downstream from the impacted region. Previous crash testing of the Midwest free-standing F-shape PCB with pin-and-loop connections in accordance with Test Level 3 (TL-3) impact safety standards published in the *Manual for Assessing Safety Hardware* (MASH) [1] demonstrated dynamic deflections in excess of 6.6 ft [2]. For many installations, this deflection is undesirable. Therefore, tie-down systems for anchoring PCB segments have been designed to limit dynamic barrier deflections.

The Midwest Roadside Safety Facility (MwRSF) previously developed and full-scale vehicle crash tested a tie-down system for PCBs on asphalt road surfaces that utilized three 1½-in. diameter x 38½-in. long ASTM A36 steel pins with 3-in. x 3-in. x ½-in. ASTM A36 steel caps installed in holes, or anchor pockets, on the front face of each barrier segment, as shown in Figure 1 [3]. The tie-down system was installed in combination with sixteen F-shape barriers on a 2-in. thick asphalt pad and crash tested according to the National Cooperative Highway Research Program (NCHRP) Report 350 [4] test designation no. 3-11. For the test, the F-shape PCBs were installed with the rear toe of the barrier 6 in. from a 3-ft deep vertical trench. The full-scale crash test showed that the vehicle was safely contained and redirected, and the test was deemed acceptable according to NCHRP Report 350 criteria. Barrier deflections for the system were reduced, and all the barriers in the system were safely restrained on the asphalt road surface. It was noted that a significant section of the asphalt and soil were fractured and separated in the impact region.

While this system successfully met NCHRP Report 350 criteria, it was anticipated that anchor and barrier loads would increase under MASH impact conditions. MASH testing may result in barrier deflections and barrier/anchorage damage not observed in NCHRP 350 testing. Thus, it was deemed necessary to evaluate the barrier system to MASH TL-3 criteria to determine if it would safely redirect errant vehicles under the updated criteria and to determine the working width of the barrier system.

A MASH TL-3 test of the F-shape barrier tie-down system for asphalt road surfaces was conducted at MwRSF [5]. The barrier system and setup for this test was identical to the previous NCHRP Report 350 full-scale crash test. In test no. WITD-2, the 2270P vehicle impacted the barrier system at a speed of 62.0 mph and an angle of 25.1 degrees. The impact point for this test was selected to maximize vehicle snag and loading of the barrier joint. The vehicle was captured and successfully redirected. The asphalt and soil behind the system failed, similar to the previous NCHRP Report 350 crash test. Dynamic deflection for test no. WITD-2 was 24.5 in., as compared to 18.4 in. in the NCHRP Report 350 crash test.

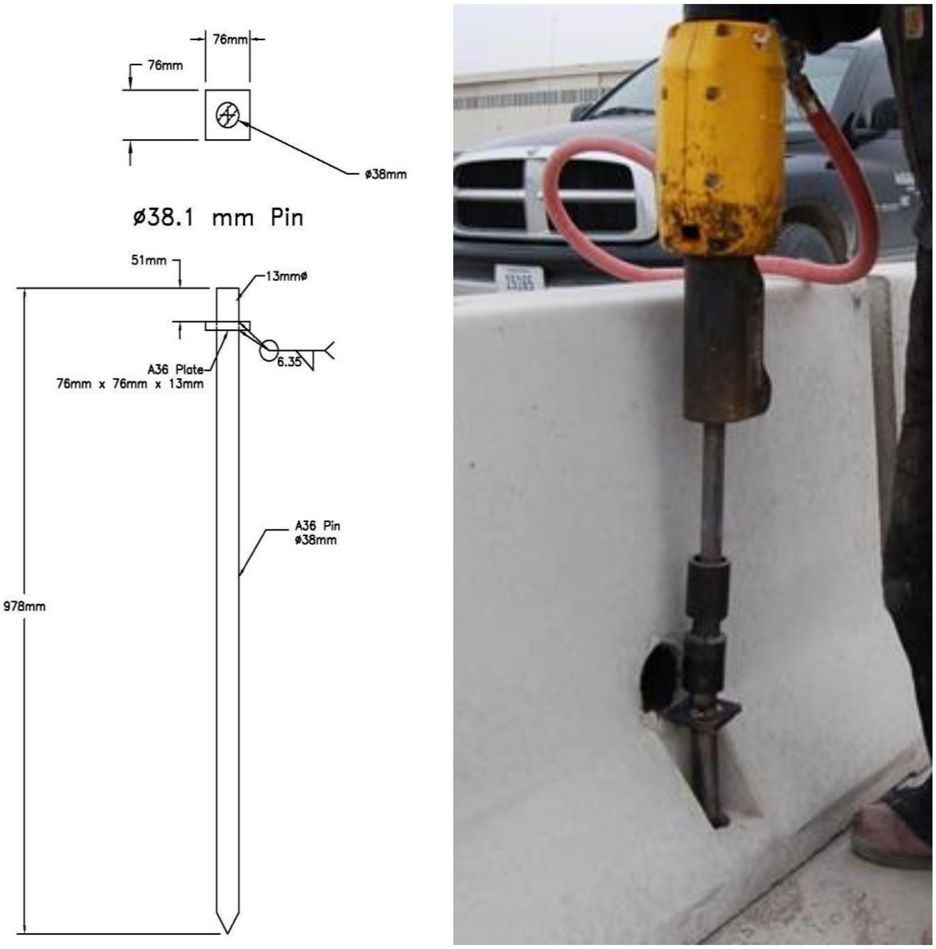

Figure 1. Asphalt Pin Tie-Down for F-Shape PCBs

During test no. WITD-2, the front-left tire snagged on the first barrier joint it encountered, as shown in Figure 2. The cause of the wheel snag was similar to what was observed in previous testing of the asphalt tie-down anchorage, in that the upstream barrier was loaded and deflected/rotated back laterally while the downstream barrier remained anchored. This exposed the face of the downstream barrier and promoted snagging of the wheel and tire as it traversed the joint. The front tire climbed the toe of the PCB barrier as well, which increased the exposure of the face of the downstream barrier to the wheel.

As a result of snagging on the joint, the front-left wheel rotated 90 degrees and was pushed back toward the floor pan of the pickup. This caused excessive floor pan deformations, opened a hole in the floor pan, and allowed a portion of the wheel to penetrate into the occupant compartment, as shown in Figure 3. The maximum deformation of the floor pan area was 13.2 in., which exceeded the 9-in. MASH limit for floor pan deformation. The combination of excessive occupant compartment deformation and the penetration of the wheel into the occupant compartment led to the test being deemed unacceptable under the MASH TL-3 safety requirements.

Figure 2. Barrier Joint Snag, Test No. WITD-3

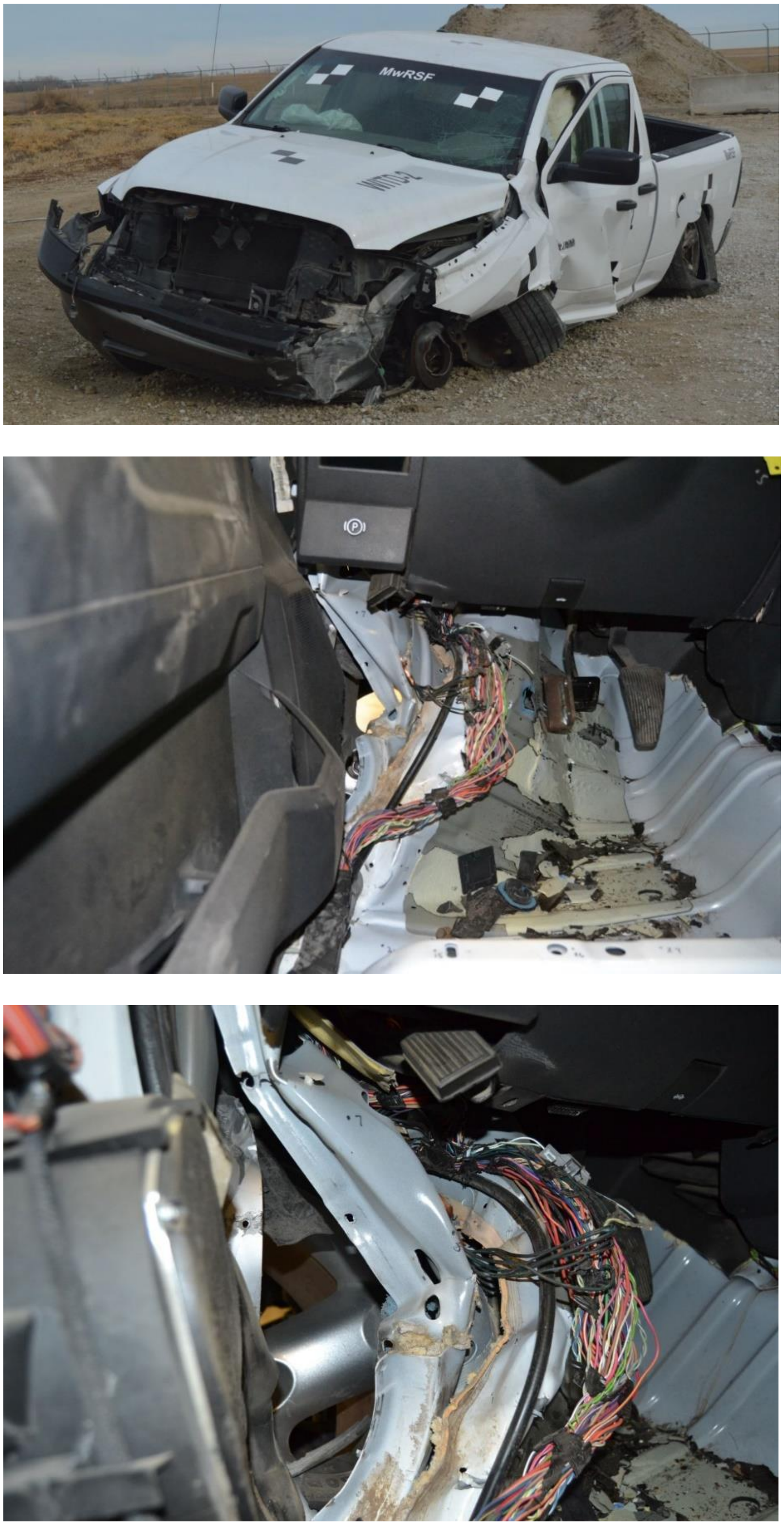

Figure 3. Occupant Compartment Damage, Test No. WITD-2

Following the test, it was noted that test no. WITD-1, a MASH TL-3 full-scale crash test of a concrete bolted tie-down anchorage for the F-shape PCB, had less severe wheel snag than test no. WITD-2, and that system satisfied MASH TL-3 performance requirements [5]. It was believed that the epoxied anchor rods used in that system more effectively reduced barrier motion and lessened the joint separation and wheel snag severity. This suggested that there may be ways to improve the barrier performance from test no. WITD-2 to mitigate the wheel snag. Potential options to improve the asphalt pin tie-down anchorage performance included increasing the offset of the barriers from the excavation and introducing a shear transfer element at the joint to prevent joint separation. The project sponsors opted to increase the barrier offset from 6 in. to 18 in. as this option required no additional hardware and was simple to implement.

In test no. WITD-3, wherein the barrier offset was increased from 6 in. to 18 in., the 2270P vehicle impacted the barrier system at a speed of 61.9 mph and an angle of 25.1 degrees. The impact point for this test was selected to maximize vehicle snag and loading of the barrier joint. The vehicle was captured and successfully redirected. There was little to no damage to the asphalt or soil disengagement as was seen in the NCHRP Report 350 and WITD-2 crash tests. Dynamic deflection for test no. WITD-3 was 16.3 in., as compared to 18.4 in. in NCHRP Report 350 and 24.5 in. in the WITD-2 crash tests. The right-front tire snagged on the upstream face of barrier no. 9, as shown in Figure 4. The cause of the wheel snag was similar to previous tests of the asphalt tie-down anchorage, in that the upstream barrier was loaded and deflected/rotated backward while the downstream barrier remained anchored. This exposed the face of the downstream barrier and promoted snagging of the wheel and tire as it traversed the joint. The front tire climbed the toe of the PCB segment, which also increased the exposure of the face of the downstream barrier to the wheel. As a result of the snagging behavior, the right-front wheel was pushed backward into the floor pan. This caused excessive floor pan deformations and a tear at the seam where the floor pan, toe pan, and kicker panel meet, as shown in Figure 5. Maximum deformation of the floor pan area was 10.4 in., which exceeded the 9-in. MASH floor pan deformation limit and led to the test being deemed unacceptable under MASH TL-3 safety requirements.

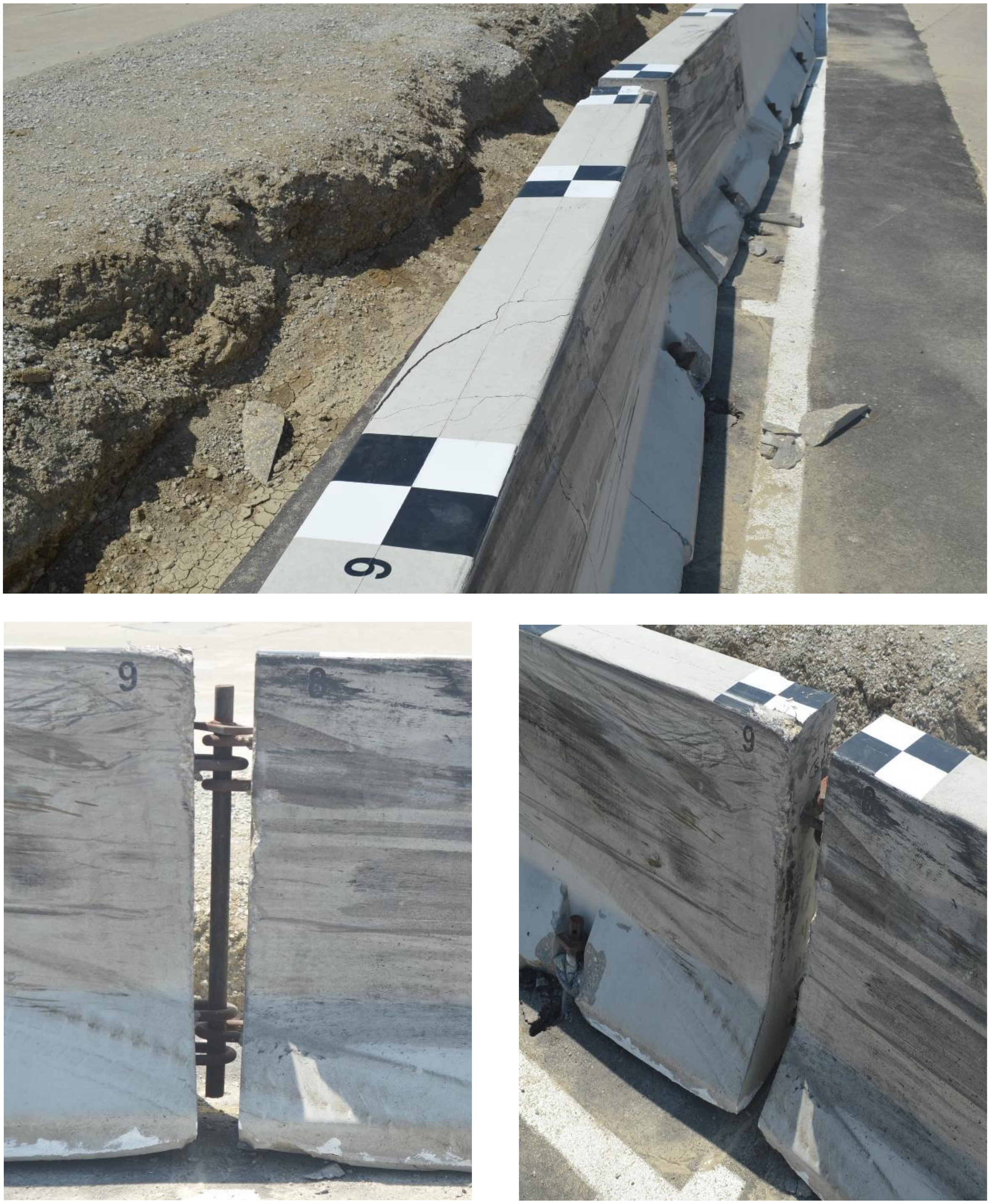

Figure 4. Barrier Joint Snag, Test No. WITD-3

Figure 5. Occupant Compartment Damage, Test No. WITD-3

1.2 Objective

The objective of this research was to review and evaluate modifications to the F-shape PCB with steel pin tie-down anchorages for asphalt road surfaces and evaluate the modified barrier system to MASH TL-3 safety criteria. In particular, this research effort aimed to develop a tied-down F-shape PCB system which did not produce the snagging behavior observed in previous crash testing of similar systems.

1.3 Scope

The research objective was achieved through the completion of several tasks. The study began with the development of potential design concepts to improve the safety performance of the steel pin tie-down system for asphalt surfaces for use with F-shape PCBs. The researchers brainstormed design concepts and evaluated their potential to reduce joint separation and wheel snag. The most promising concepts were presented to the sponsors for review and selection of a preferred design concept. The preferred design concept was evaluated and refined using engineering analysis and LS-DYNA computer simulation. The refined design concept was then implemented in a full-scale crash test. One full-scale crash test was conducted on the modified F-shape PCB anchorage system according to MASH test designation no. 3-11. The full-scale vehicle crash test results were analyzed, evaluated, and documented. Conclusions and recommendations were then made pertaining to the safety performance of the tie-down anchorage for the F-shape PCB.

2 ASPHALT TIE-DOWN ANCHORAGE DESIGN MODIFICATIONS

Design modifications for the steel pin tie-down system for asphalt surfaces for use with F-shape PCBs were developed based on concepts to mitigate the wheel snag observed in test nos. WITD-2 and WITD-3. These design modifications were then presented to the project sponsor along with their potential advantages and disadvantages, and the sponsor was asked to select their preferred concept for full-scale crash testing and evaluation.

2.1 Design Concepts

Design concepts to mitigate the wheel snag and excessive occupant compartment deformations observed in test nos. WITD-2 and WITD-3 focused on two main criteria. First, it was believed that minimizing the relative lateral barrier displacement between adjacent barrier segments at the joint would reduce the wheel snag by exposing the wheel to less contact area at the upstream end of the downstream barrier segment. The PCB anchorage system evaluated in test no. WITD-1, which utilized epoxied threaded rods anchored in concrete on the traffic face of the PCB segments, provided increased resistance to relative lateral barrier motion. This exposed less of the end of the downstream barrier segment to the vehicle wheel as it traversed the joint and allowed this system to meet MASH TL-3 requirements while the asphalt pin tie-down anchorage did not. Thus, design concepts were considered that further limited barrier segment rotation and displacement or provided shear transfer across barrier segment joints such that the relative lateral barrier displacement between the barrier segments was limited. Second, design concepts were considered to physically shield barrier segment joints and thus prevent wheel snag by placing some form of protection across the joint.

Previous studies have utilized front and backside attachments that span across the PCB joints. Backside attachments with large sections aid in shear transfer and have shown the ability to limit deflections and relative lateral barrier displacements [6]. It is necessary for front side attachments to have a smaller profile to prevent snag issues. As such, front side attachments do not provide as much shear transfer as backside attachments but aid in shielding the gap at the joint. Attachments on both the front and back side of the system are ideal to provide continuity across the joint, limiting deflections, and providing shear transfer [7, 8].

The potential barrier modifications also took several design considerations into account. First, the modification had to work as a retrofit to the existing F-shape PCB segment such that the joint design, segment geometry, and barrier reinforcement were unchanged. The system also needed to use readily available hardware and components to the extent possible. The proposed design modifications for the F-shape PCB with steel pin tie-down anchorage for asphalt road surfaces are outlined in the subsequent sections.

2.1.1 Design Concept A – Saddle Cap with Concrete Anchors

Design Concept A consisted of a steel saddle cap that spanned across the joint between adjacent barrier segments, as shown in Figures 6 and 7. The saddle cap was fabricated from a 37⅝-in. long x ⅛-in. thick, U-shaped, steel plate that sat on the top of the barrier segments and extended 6¾ in. down each side of the barrier. The saddle cap was anchored to the adjacent barrier segments with four ¾-in. diameter wedge bolt mechanical anchors along the sides of the saddle cap. Design Concept A was intended to provided shear transfer across the barrier segment joint and restrain relative lateral displacement of the barrier segments. Additionally, the sides of the saddle cap would provide a degree of physical shielding and wheel snag mitigation for the upper portion of the barrier joint. One benefit of this concept was that it was symmetric with respect to the front and back sides of the barrier, which would reduce the potential for the retrofit to be installed in an improper orientation. The primary drawback of this type of installation was the need for additional steel components and anchorage hardware at every joint in the PCB system.

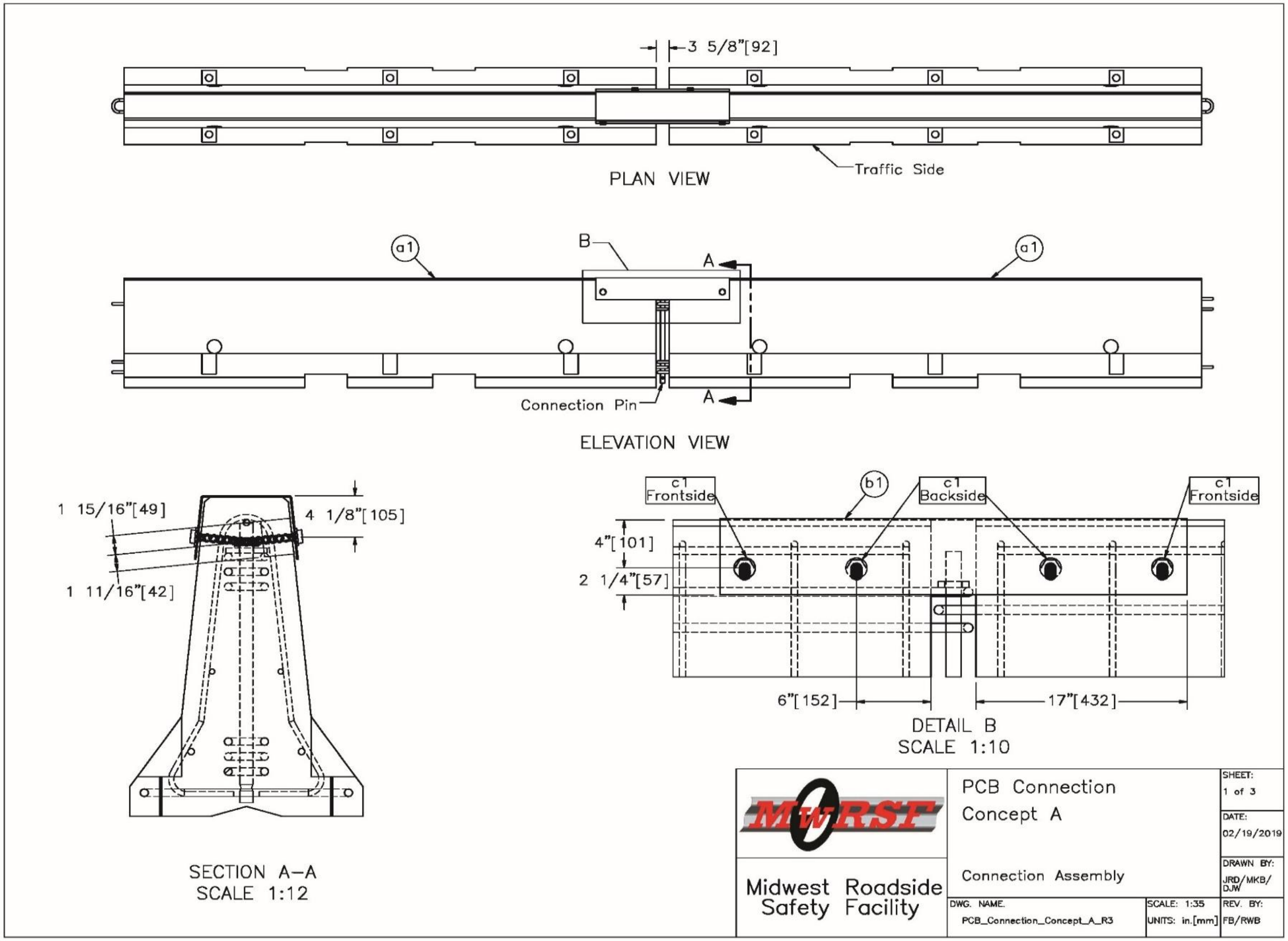

Figure 6. Design Concept A

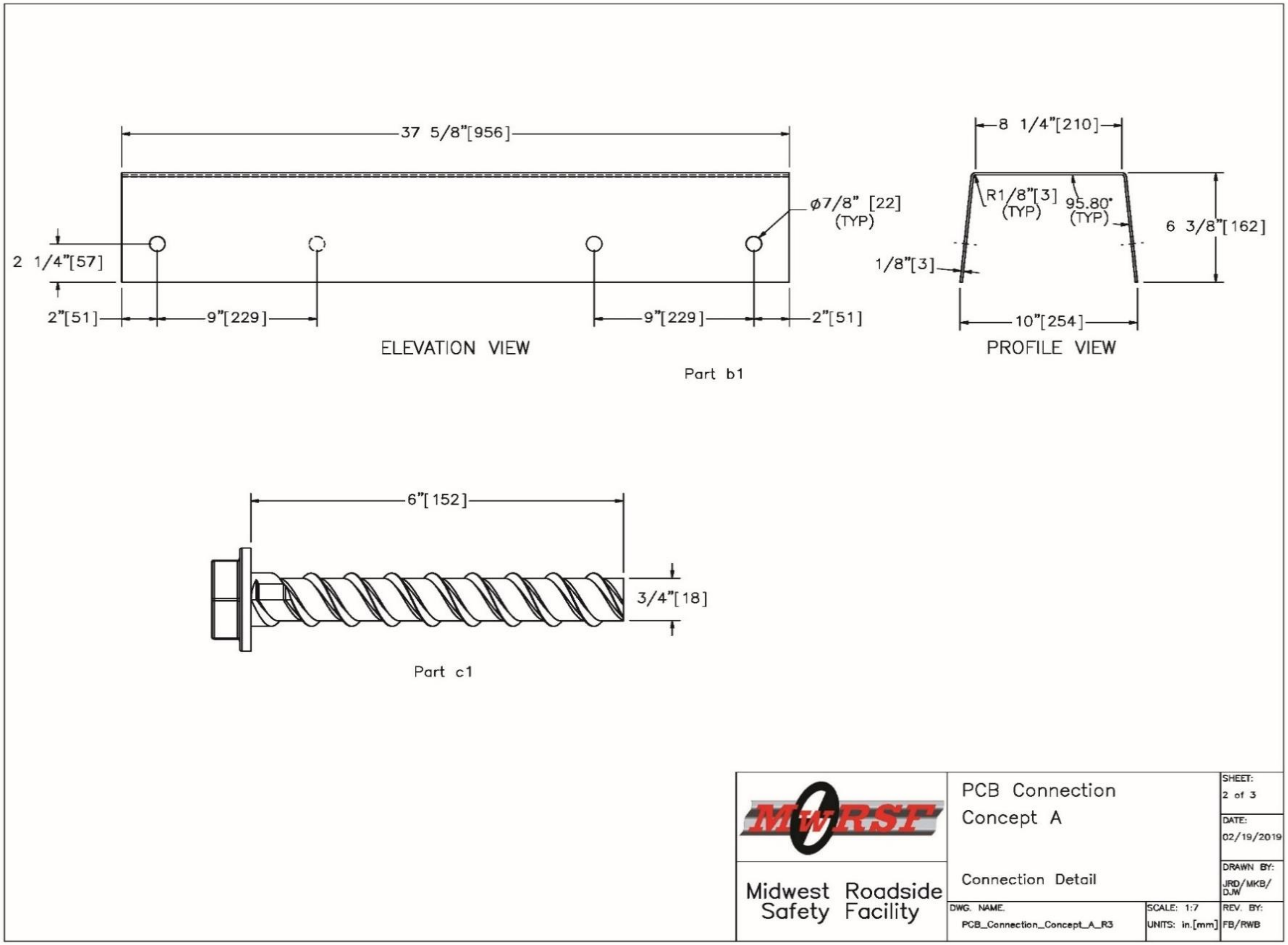

Figure 7. Design Concept A, Cont.

2.1.2 Design Concept B – Thick Rear Shear Plate

Design Concept B consisted of a steel shear plate that spanned across the joint between adjacent barrier segments, as shown in Figures 8 through 10. The 37⅝-in. long x 6-in. wide x 1-in. thick steel plate was mounted on the non-traffic side face of the barrier segment, centered 4 in. down from the top of the barrier segment, and centered longitudinally across the barrier joint. The shear plate was anchored to the barrier segments with four ¾-in. diameter wedge bolt mechanical anchors. Design Concept B was intended to provide shear transfer across the barrier segment joint and restrain relative lateral displacement of the barrier segments. The concept only required hardware mounted on the non-traffic side of the barrier segments and four anchors. The concept was not symmetric with respect to the front and back sides of the barrier, which could increase the potential for the retrofit to be installed in an improper orientation. Another drawback of this installation was the need for additional steel components and anchorage hardware at every joint in the PCB system.

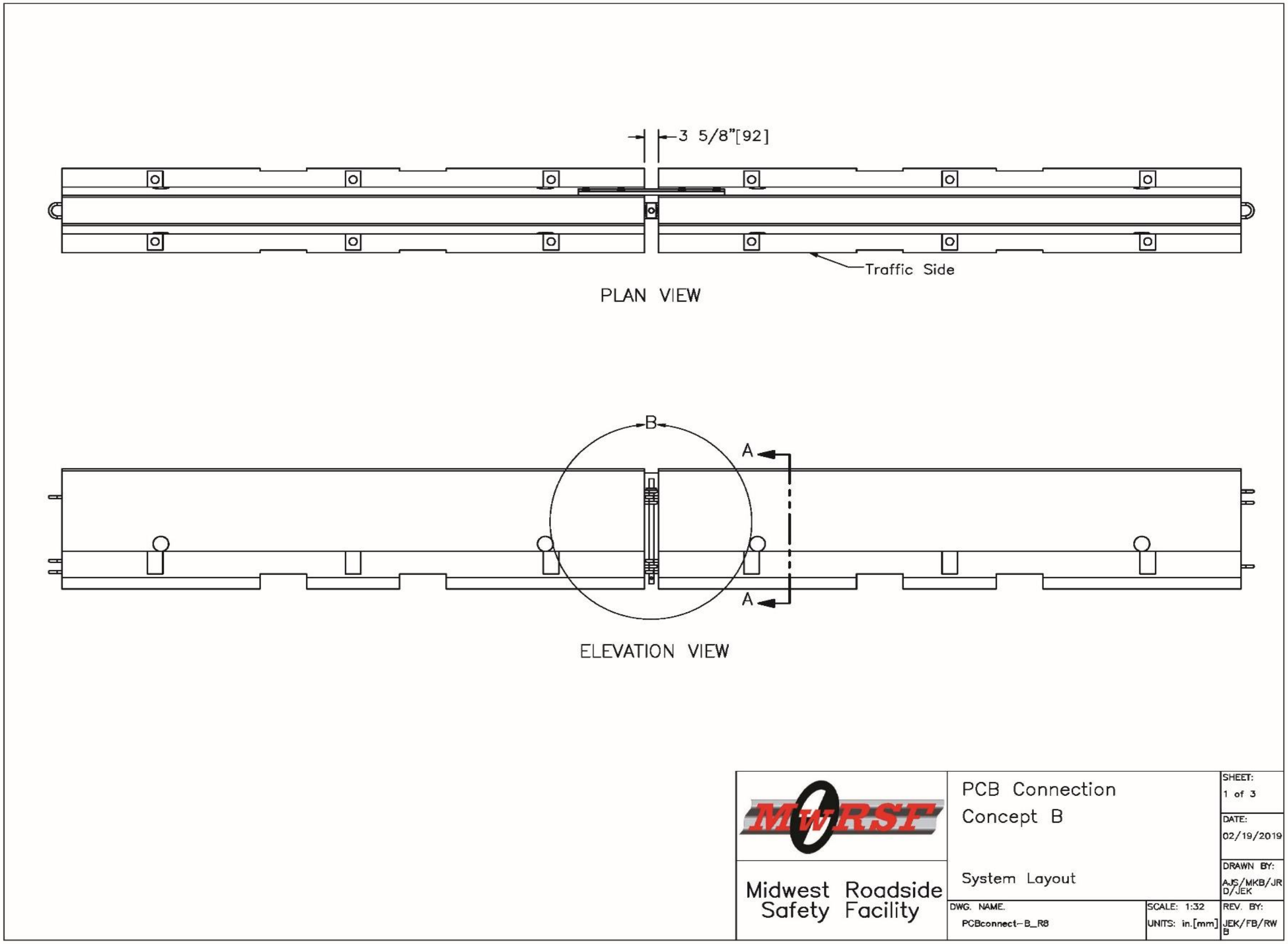

Figure 8. Design Concept B

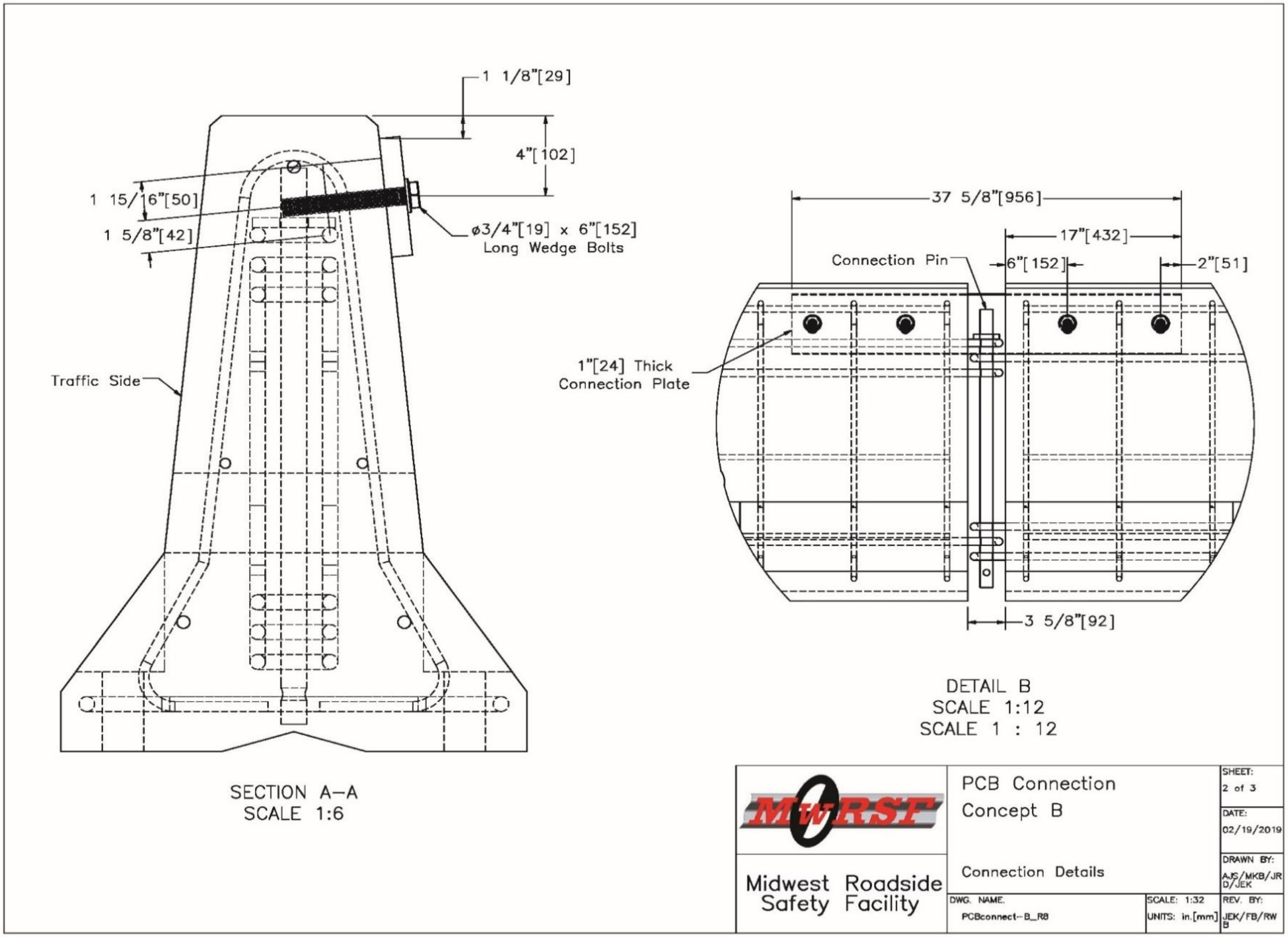

Figure 9. Design Concept B, Cont.

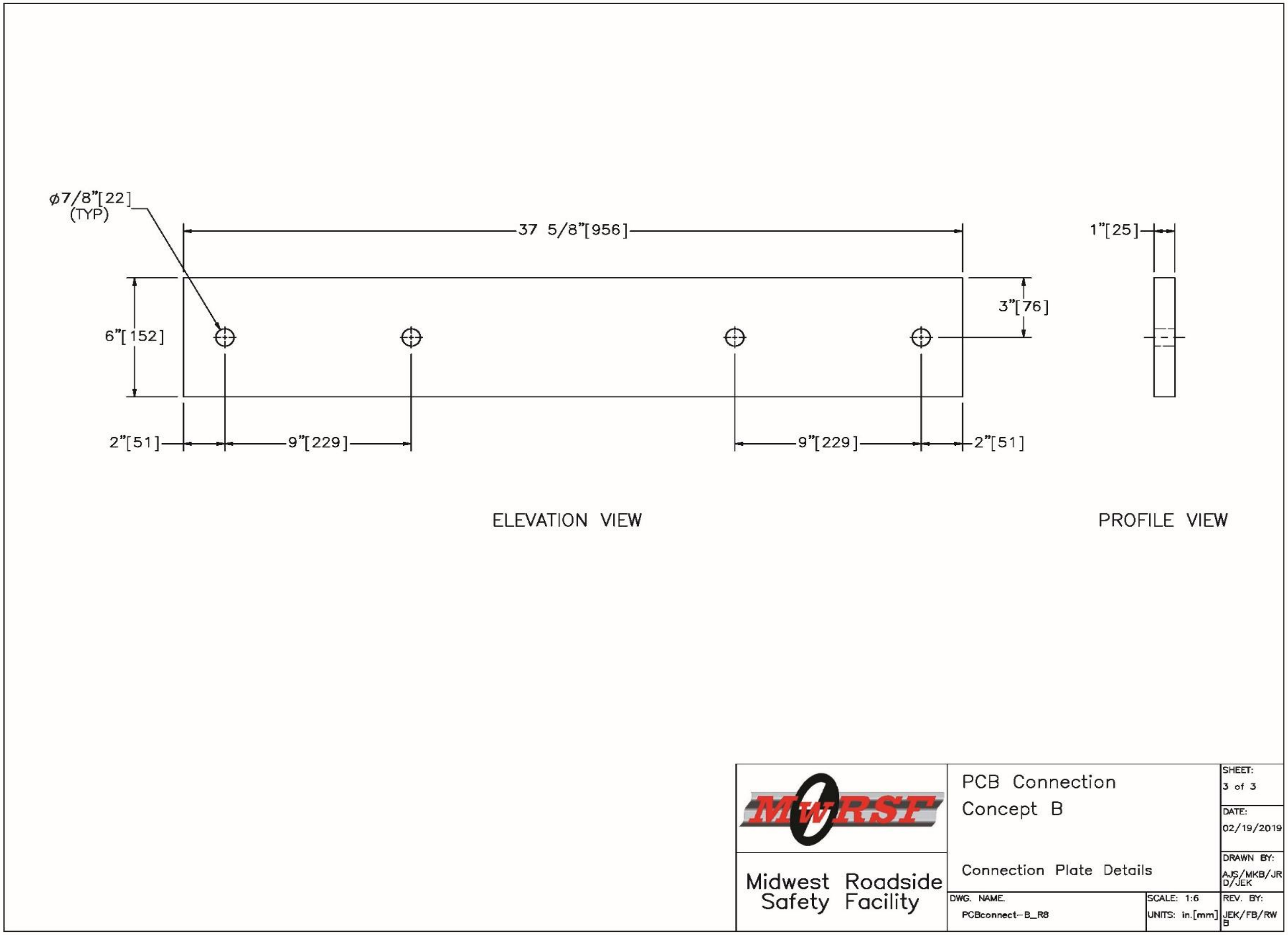

Figure 10. Design Concept B, Cont.

2.1.3 Design Concept C – Rear Shear Tube

Design Concept C consisted of a steel shear tube that spanned across the joint between adjacent barrier segments, as shown in Figures 11 through 13. The 37⅝-in. long HSS3½x3½x¼ tube was mounted on the non-traffic side face of the barrier segment, centered 4 in. down from the top of the barrier segment, and centered longitudinally across the barrier joint. The shear tube was anchored to the barrier segments with four ¾-in. diameter x 4¾-in. long hex bolts threaded into ¾ in. Red Head drop-in anchors. Design Concept C was intended to provide shear transfer across the barrier segment joint and restrain relative lateral displacement of the barrier segments. The concept only required hardware mounted on the non-traffic side of the barrier segments and four anchors. The concept was not symmetric with respect to the front and back sides of the barrier, which could increase the potential for the retrofit to be installed in an improper orientation. Another drawback of installation was the need for additional steel components and anchorage hardware at every joint in the PCB system.

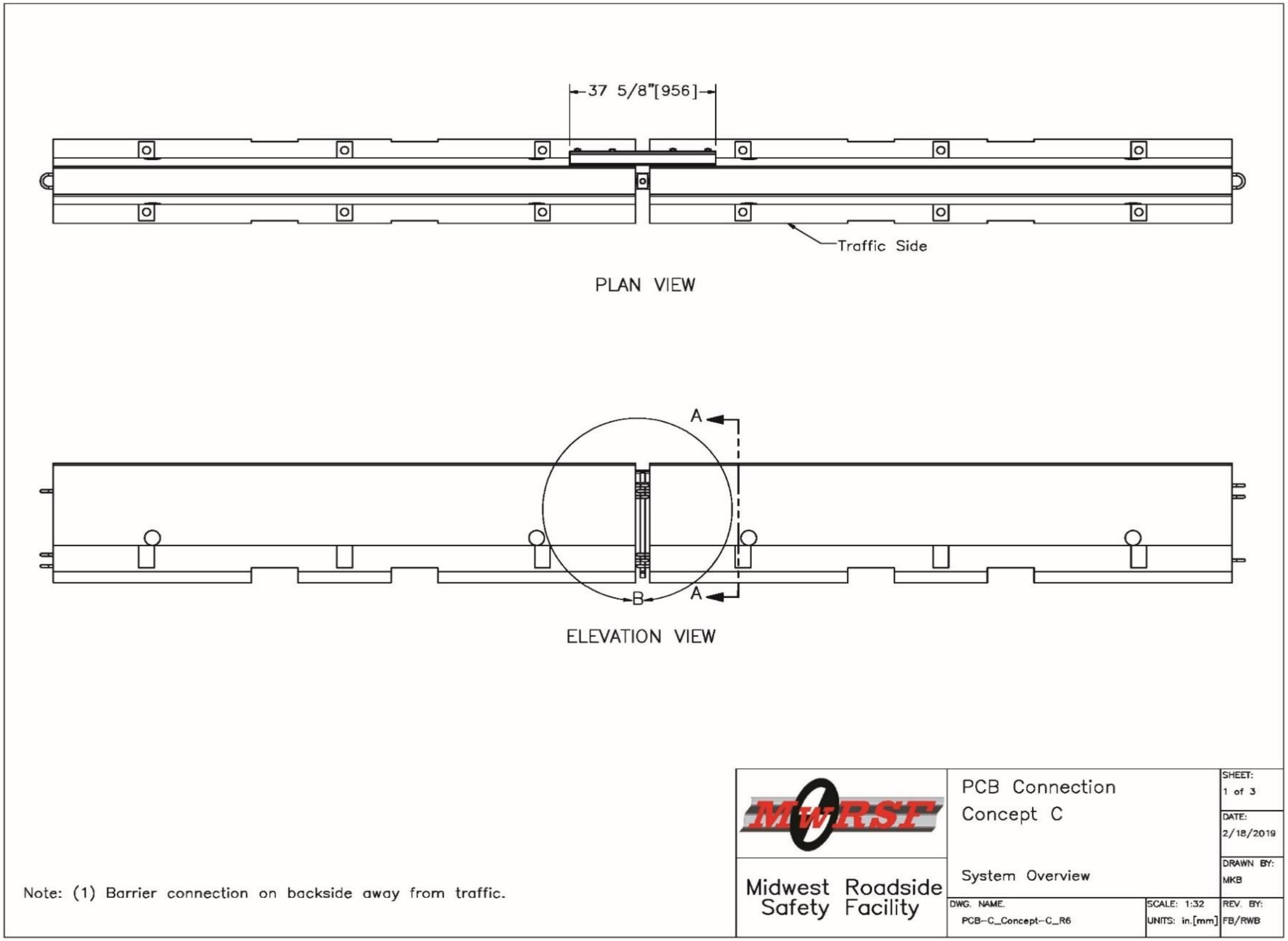

Figure 11. Design Concept C

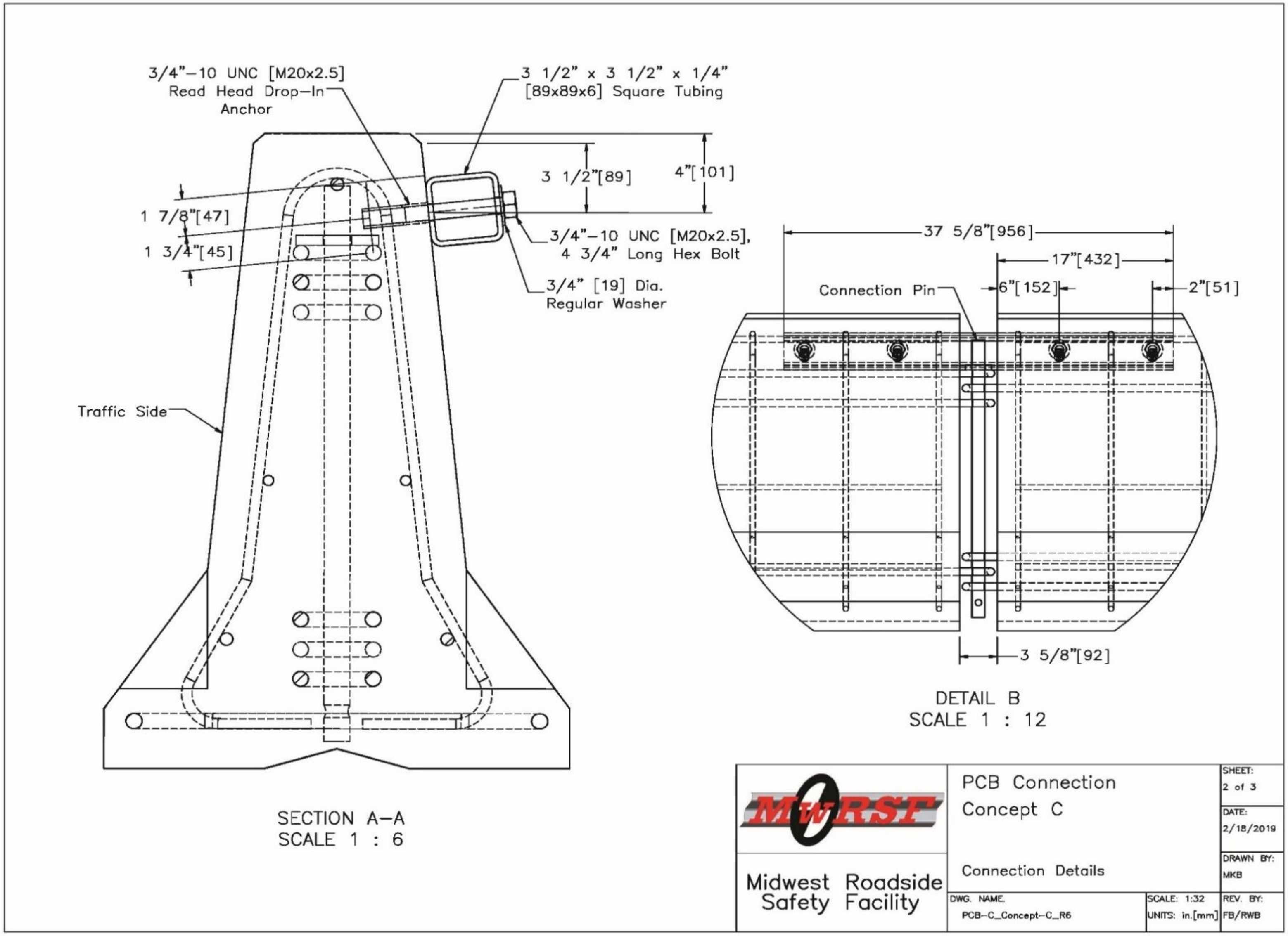

Figure 12. Design Concept C, Cont.

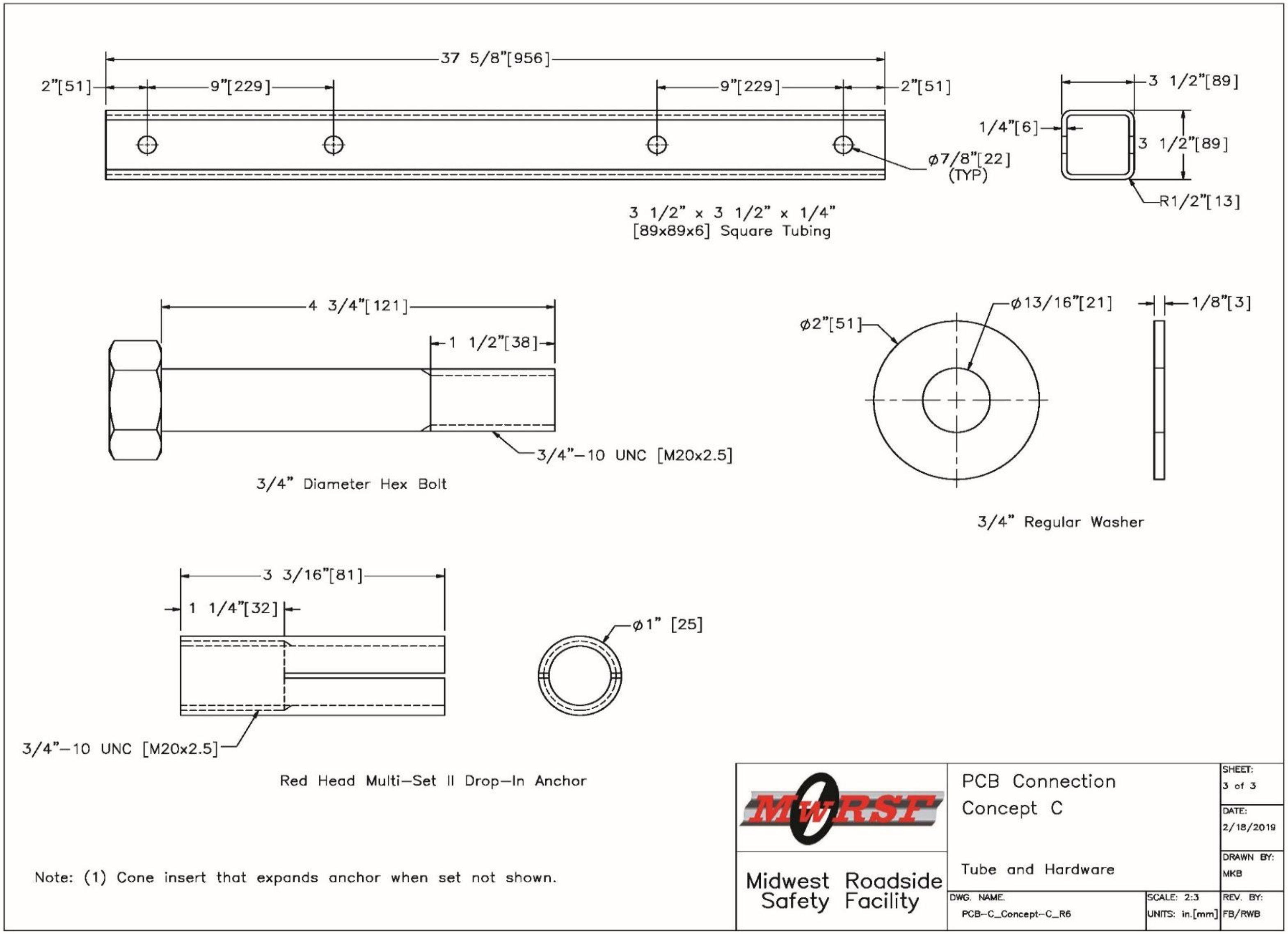

Figure 13. Design Concept C, Cont.

2.1.4 Design Concept D – Rear W-Beam

Design Concept D consisted of two 10-gauge W-beam terminal connectors that spanned across the joint between adjacent barrier segments, as shown in Figures 14 through 16. The 30-in. long W-beam terminal connectors were mounted on the non-traffic side face of the barrier segment, aligned vertically with the lower edge of the W-beam at the inflection point of the upper two sloped faces of the F-shape barrier, and centered longitudinally across the barrier joint. The W-beam terminal connectors were spliced together with standard splice bolts and anchored to the barrier segments with three ¾-in. diameter wedge bolt mechanical anchors. Design Concept D was intended to provide shear transfer across the barrier segment joint and restrain relative lateral displacement of the barrier segments. Ideally, the W-beam would have been mounted higher on the face of the barriers for more effective restraint of the upper section of the barrier segments, but the placement of the mechanical anchors interfered with the reinforcing steel. The concept only required hardware mounted on the non-traffic side of the barrier segments and used standard guardrail components. The concept was not symmetric with respect to the front and back sides of the barrier, which could increase the potential for the retrofit to be installed in an improper orientation. Another drawback of this installation was the need for additional steel components and anchorage hardware at every joint in the PCB system.

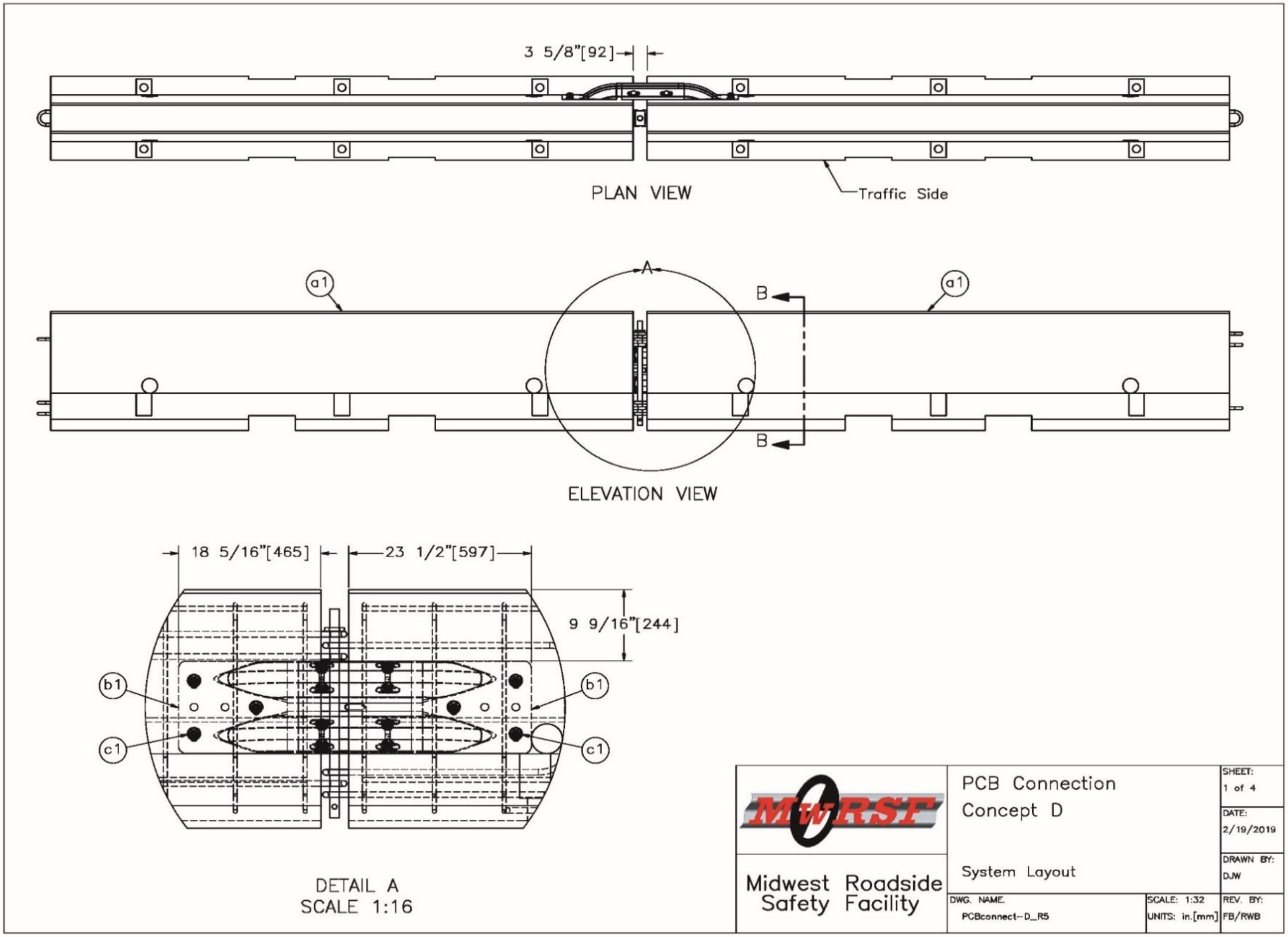

Figure 14. Design Concept D

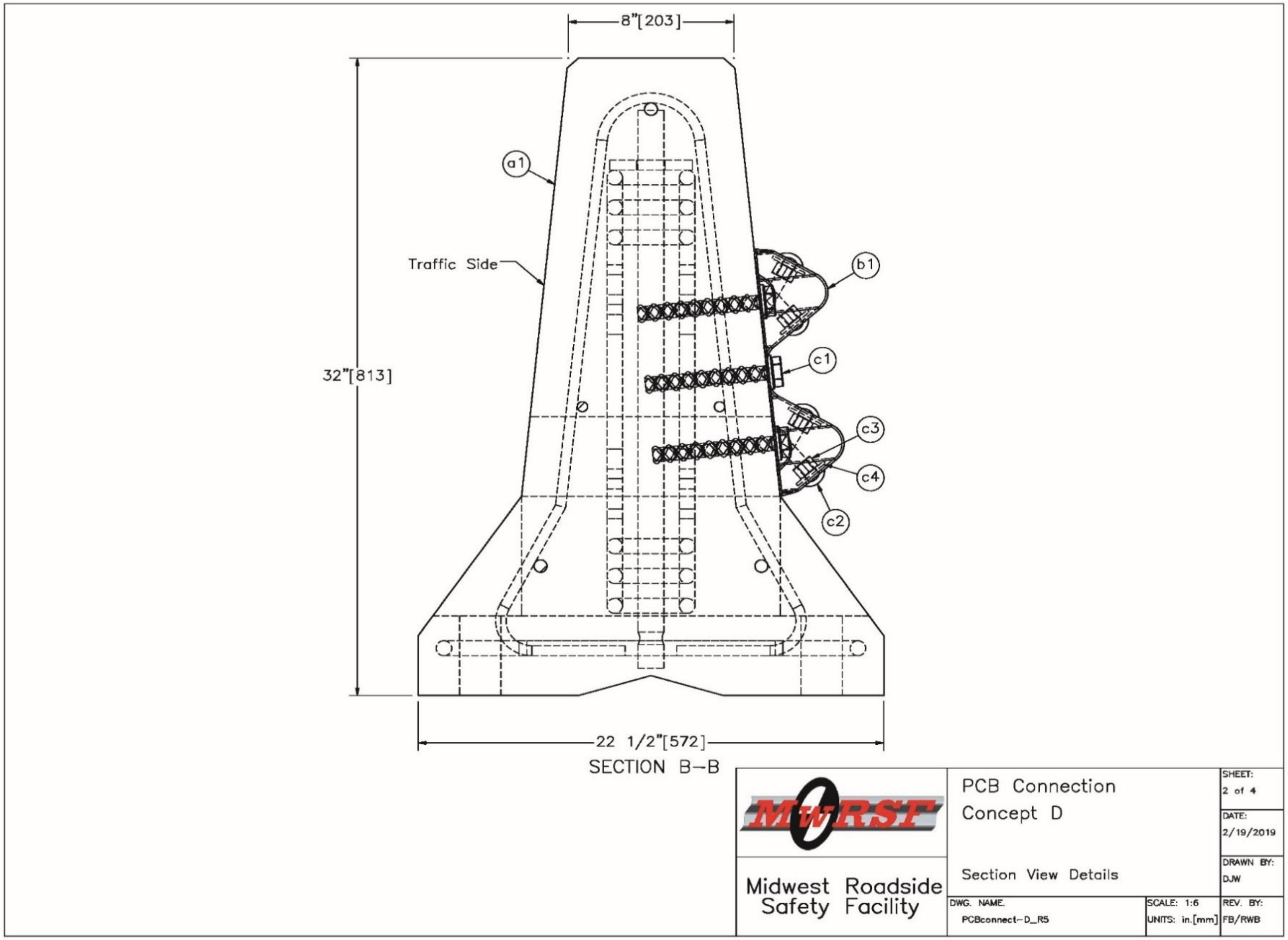

Figure 15. Design Concept D, Cont.

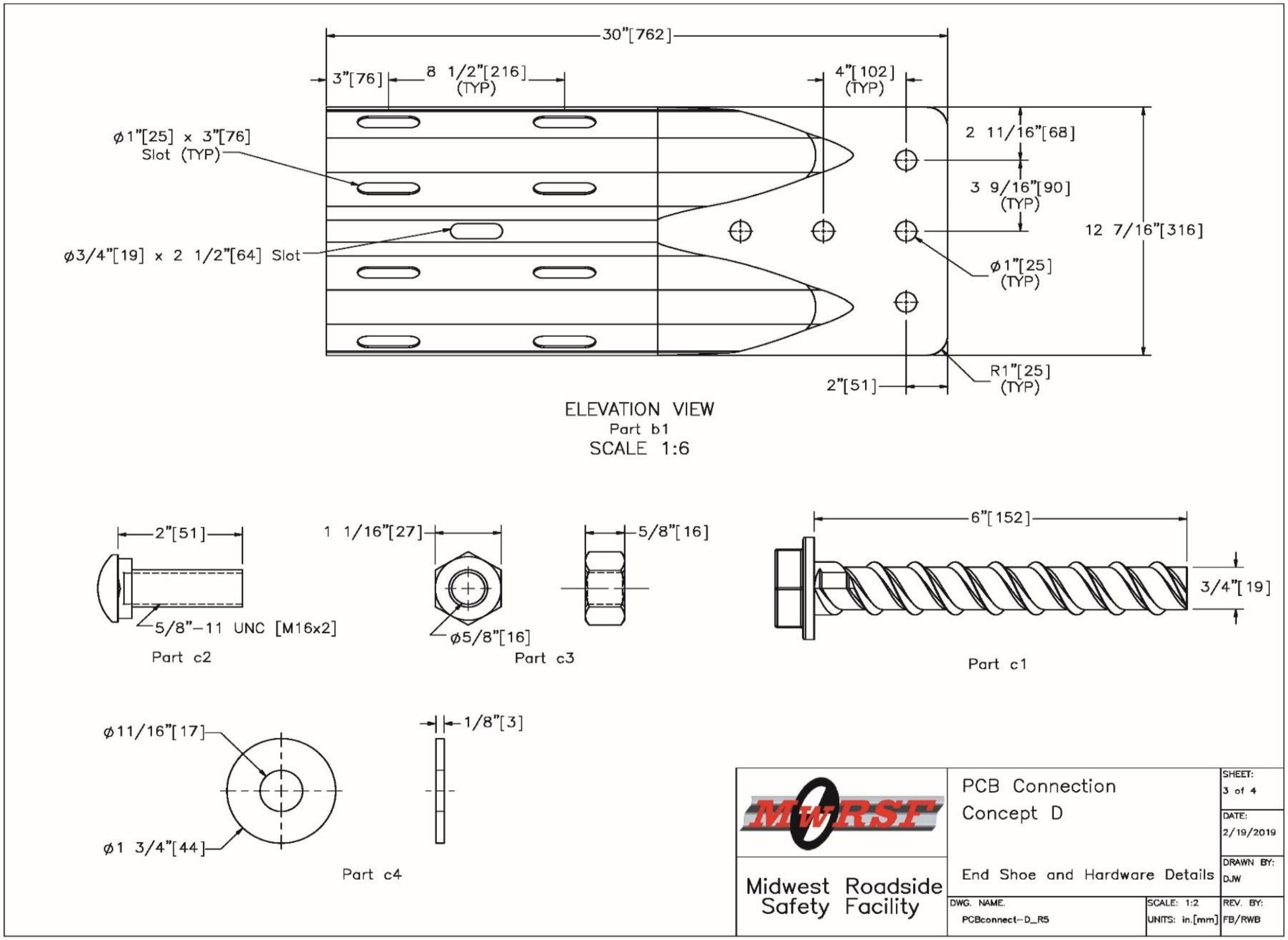

Figure 16. Design Concept D, Cont.

2.1.5 Design Concept E – Thin Front Shear Plate

Design Concept E consisted of a steel shear plate that spanned across the joint between adjacent barrier segments, as shown in Figures 17 through 19. The 23⅝-in. long x 21⅝-in. wide, 10-gauge steel plate was mounted on the traffic side face of the barrier segment, spanned the entire height of the upper sloped face of the barrier segments, and was centered longitudinally across the barrier joint. The shear plate was anchored to the barrier segments with four ¾-in. diameter wedge bolt mechanical anchors. Design Concept E was intended to provide shear transfer across the barrier segment joint and restrain relative lateral displacement of the barrier segments. Additionally, the plate would provide some degree of physical shielding and wheel snag mitigation for the upper portion of the barrier joint. The concept only required hardware mounted on the traffic side of the barrier segments and four anchors. The concept was not symmetric with respect to the front and back sides of the barrier, which could increase the potential for the retrofit to be installed in an improper orientation. Another drawback of this installation was the need for additional steel components and anchorage hardware at every joint in the PCB system.

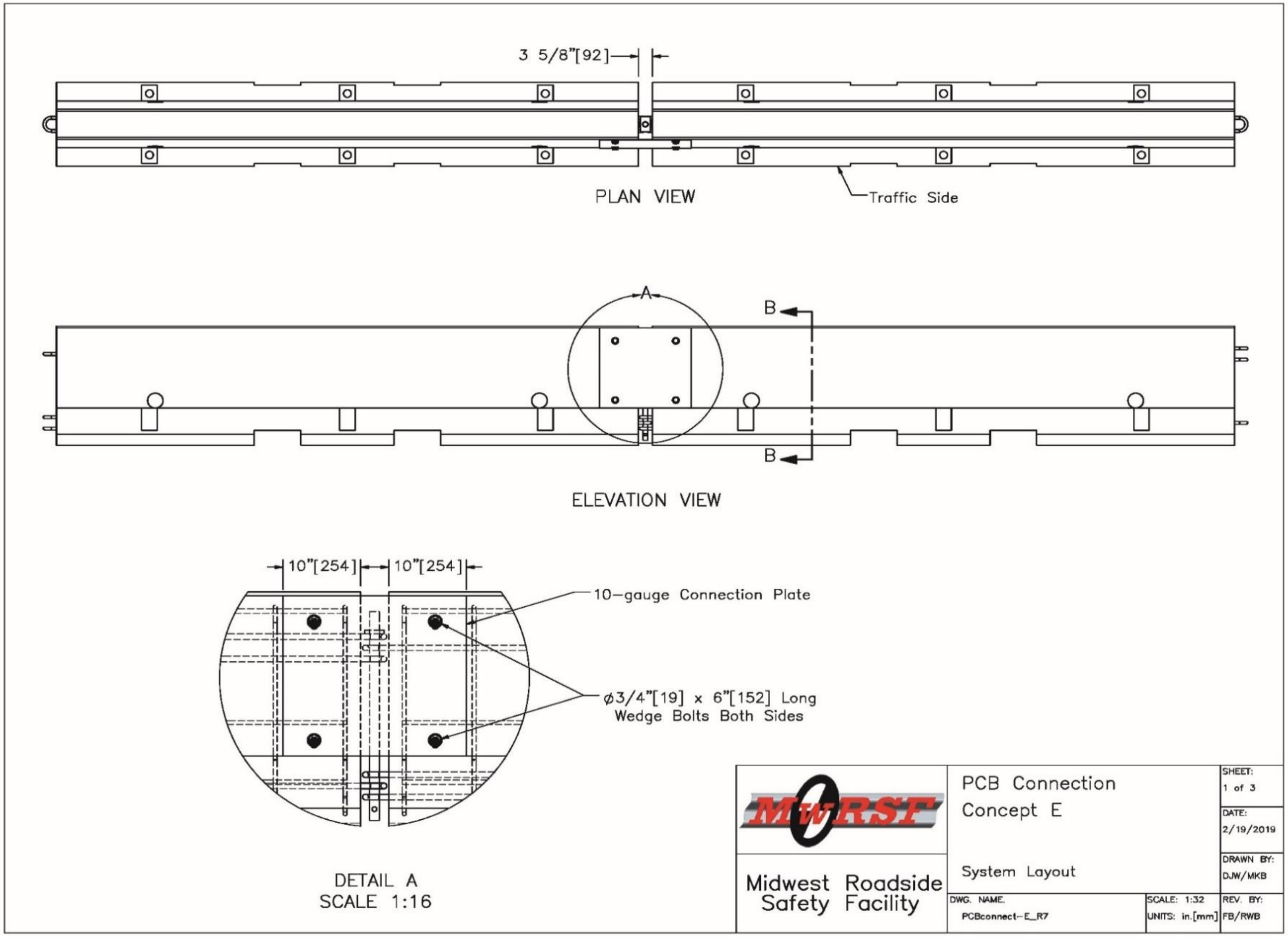

Figure 17. Design Concept E

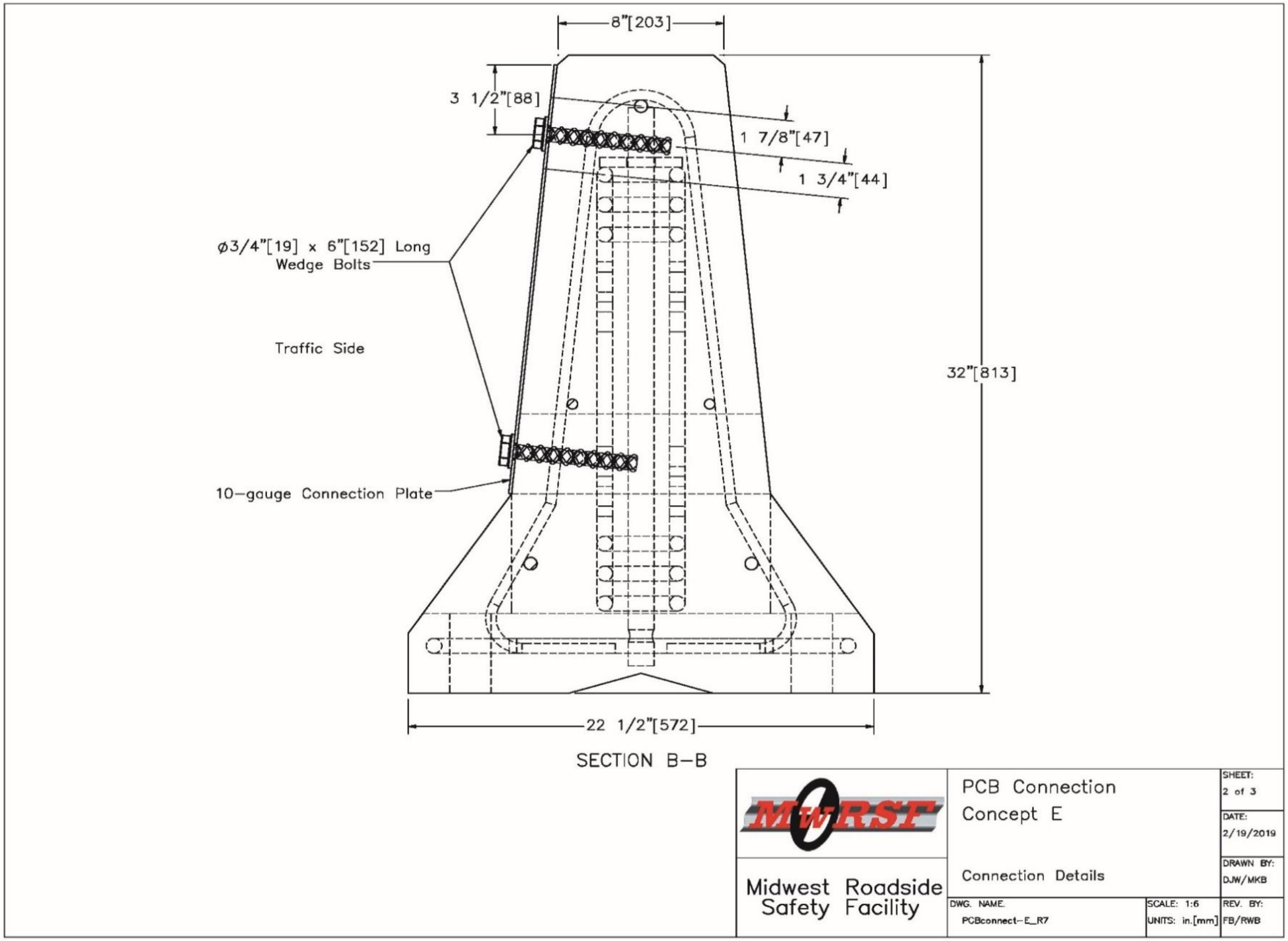

Figure 18. Design Concept E, Cont.

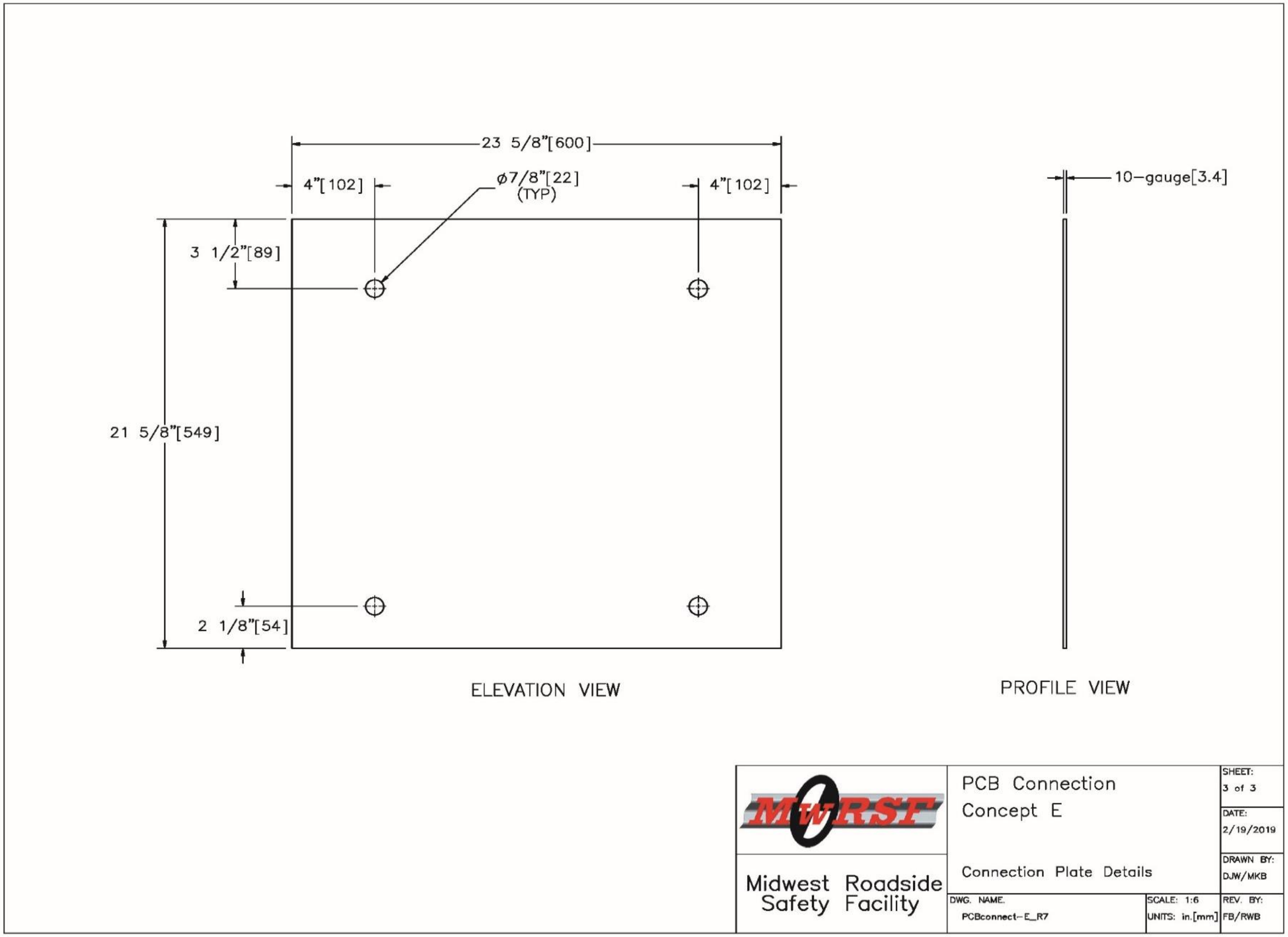

Figure 19. Design Concept E, Cont.

2.1.6 Design Concept F – Saddle Cap without Concrete Anchors

Design Concept F consisted of a steel saddle cap without concrete anchors that spanned across the joint between adjacent barrier segments, as shown in Figures 20 and 21. The saddle cap was a 6¼-in. tall x 6½-in. wide x ⅛-in. thick, U-shaped steel plate that sat on top of the barrier segments with a $^{3}/_{16}$-in. clearance between the interior of the saddle cap and lateral PCB surfaces. A 3-in. tall x 3-in. wide x ¼-in. thick steel square tube was welded to the inside of the saddle cap to stiffen the assembly and prevent saddle cap bulging during impact. A 30¾-in. tall x 1¼-in. diameter connection pin was inserted through holes drilled through the square tube, saddle cap top, and a weld plate, and welded to all three parts. The connection pin, inserted through barrier connection loops and centered longitudinally and laterally, was the only connection to the barrier, providing ease of installation. Design Concept F was intended to provide shear transfer across the barrier segment joints and restrain relative lateral displacement of the barrier segments. Additionally, there was potential for the sides of the saddle cap to provide some degree of physical shielding and wheel snag mitigation for the upper portion of the barrier joint. The benefits of this concept were that it was symmetric with respect to the front and back sides of the barrier and did not require concrete anchors, simplifying installation. The primary drawback of the saddle cap without concrete anchors was the concern that the saddle cap would bulge, allowing the barrier ends to slip out of the saddle cap, and thus expose the face of the downstream barrier allowing snag.

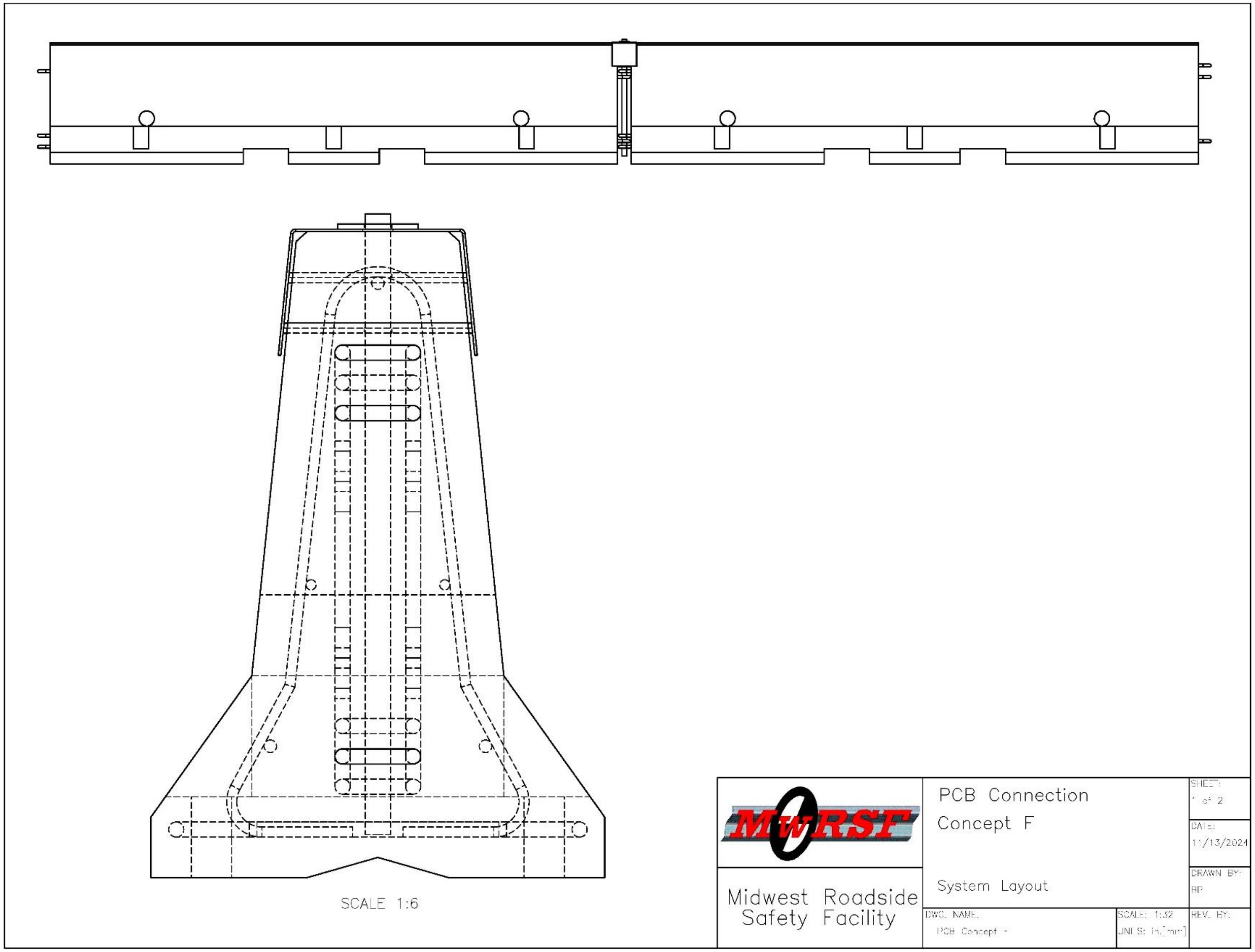

Figure 20. Design Concept F

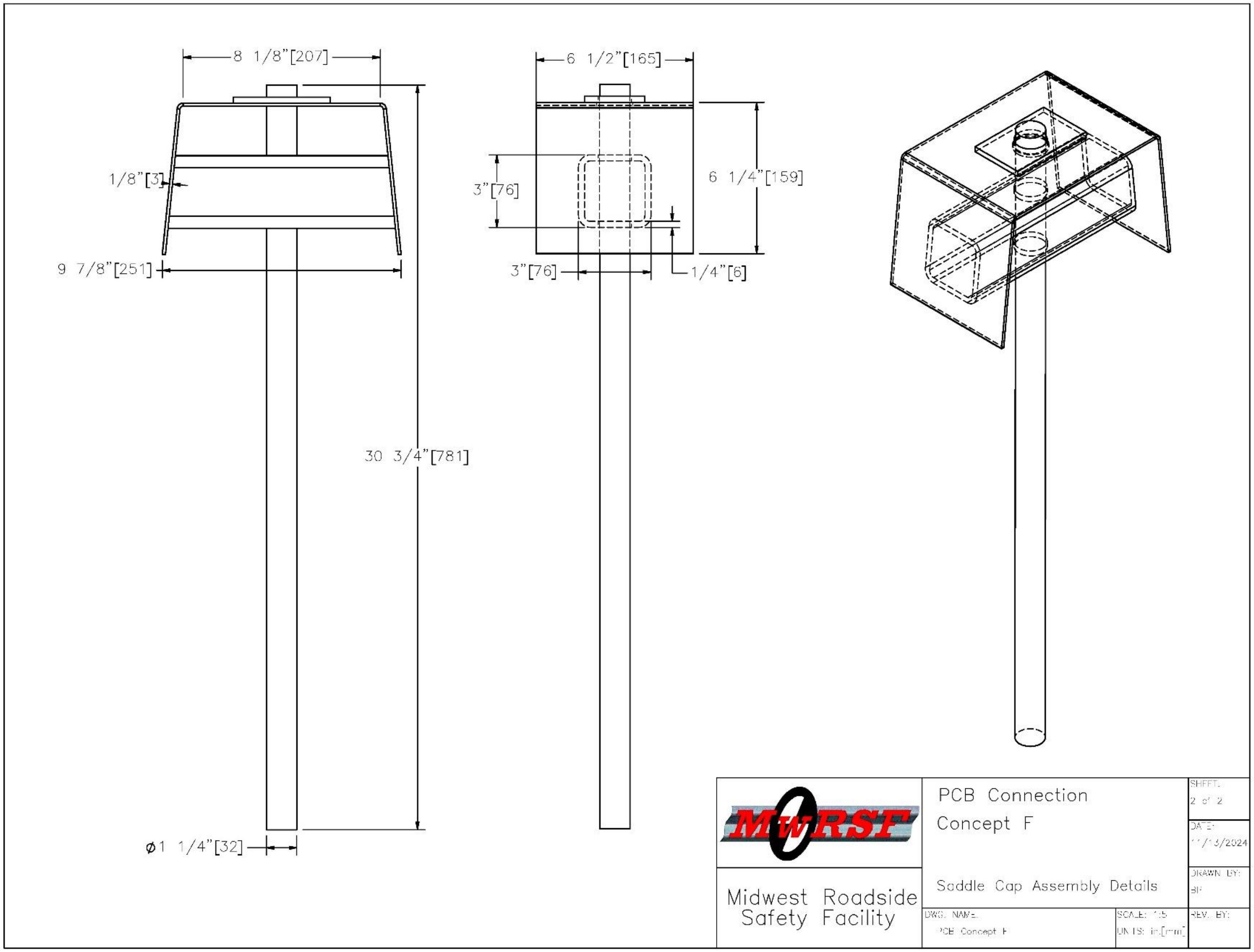

Figure 21. Design Concept F, Cont.

2.2 Selection of Preferred Design Concept

The proposed design modification concepts were presented to the research sponsor for review and selection of a preferred modification for development using finite element analysis (FEA) and evaluation through full-scale crash testing. All proposed concepts had the potential to improve system performance, but the sponsors preferred a design that could be installed from the non-traffic side of the barrier for safety purposes. Therefore, Design Concepts A (saddle cap with concrete anchors) and E (thin front shear plate) were eliminated. Further, the sponsors preferred a concept that did not require concrete anchors for ease of installation. Thus, the sponsors selected Design Concept F, the saddle cap without concrete anchors, for design development using LS-DYNA and eventual full-scale crash testing. Design concepts that were omitted internally prior to sponsor review and selection are included in Appendix A.

3 SIMULATION OF ASPHALT TIE-DOWN ANCHORAGE WITH SADDLE CAPS

3.1 Methodology

To evaluate the potential of saddle caps without concrete anchors as a deflection-limiting mechanism, a parametric study was conducted using LS-DYNA. LS-DYNA is a transient, nonlinear FEA code that has been widely used in the design and analysis of roadside safety hardware [9]. The methodology for evaluating the saddle cap began with the development of a baseline model of the WITD-3 system that produced similar deflections to previous MASH TL-3 full-scale crash testing with the 2270P vehicle. Next, the saddle cap model was included in the baseline model with varying saddle cap geometries. The results of the simulations of the various geometric changes to the saddle cap were then collected, compared, and used to select the best-performing saddle cap geometry for full-scale crash testing.

3.2 Baseline Model Development and Validation

The first step to using FEA for saddle cap development involved creating a baseline model and validating it to test no. WITD-3. The baseline model was created by incorporating previously developed models of PCBs, anchor pins in asphalt, and a 2270P pickup truck.

3.2.1 PCB Model

The F-shape portable concrete barrier model was based on models developed previously at MwRSF for simulation of PCBs [10]. The model consisted of the F-shape barrier, end connection loops, and connection pins, as shown in Figure 22.

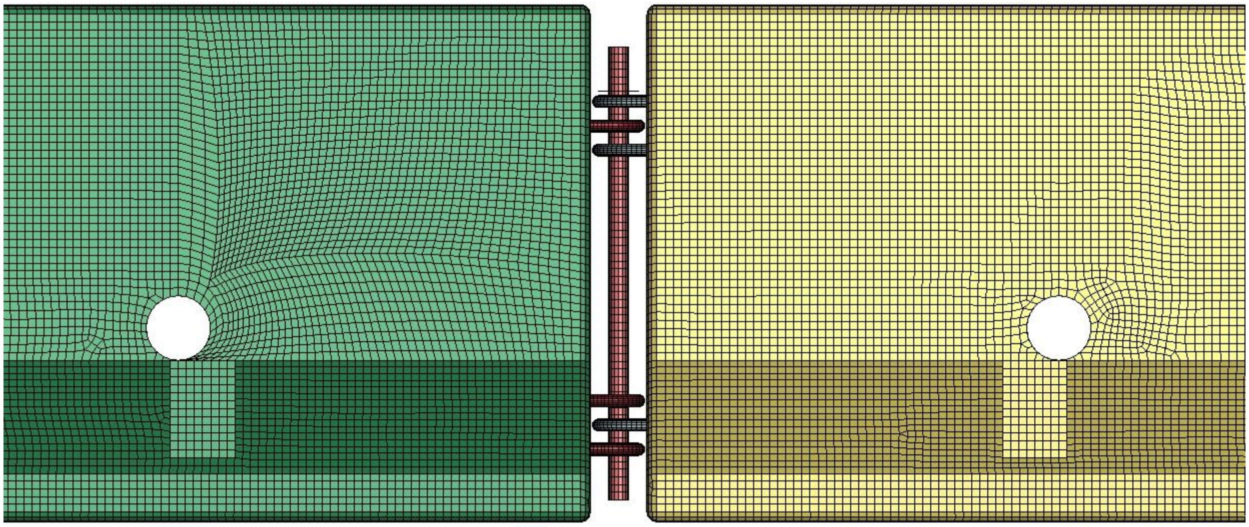

Figure 22. F-shape PCB Model

The main body of the F-shape barrier model was created using shell elements with a rigid material definition. The rigid material definition allowed the proper mass and rotational inertias to be defined for the barrier even though it was essentially hollow. The barrier segments were assigned a mass of 4,976 lb based on measurements taken from actual barrier segments. The rotational inertias were determined based on SolidWorks models of the PCB segment. The SolidWorks models used tended to overestimate the mass and rotational inertia of the PCB segment as the solid model included the mass of the concrete body and the reinforcing steel but did not account for the volume of concrete lost due to the reinforcing steel. Thus, the rotational inertias determined by the software were scaled down based on the ratio of the actual measured mass of the barrier segment to the software-estimated mass of the segment. The use of shell elements improved the overall contact between the barrier and the vehicle. In addition, the use of shell elements made it easier to fillet the corners and edges of the barrier. By rounding off the barrier edges, the edge contacts and penetrations were reduced, thus further improving the contact interface.

The connection loops in the barrier model consisted of two sets of three rebar loops. The connection loops were modeled with a rigid material as previous testing of the barrier in various configurations showed little to no deformation of the connection loops. The connection pin was modeled with the MAT_PIECEWISE_LINEAR_PLASTICITY material in LS-DYNA with the appropriate properties for A36 steel. The baseline barrier system model incorporated a total of sixteen barrier segments for a total barrier length of 200 ft.

A critical component of the baseline model of the free-standing, F-shape PCB was the definition of barrier-to-ground friction. PCB systems use a combination of inertial resistance and longitudinal tension to redirect impacting vehicles. The longitudinal tension in the barrier system is largely developed by barrier-to-ground friction. Previous research at Texas A&M Transportation Institute (TTI) and MwRSF measured the dynamic friction coefficient for a concrete PCB segment sliding on a concrete surface to be between 0.40 and 0.44 [11-12]. Further, MwRSF measured the dynamic friction coefficient for a concrete PCB segment sliding on an asphalt surface to be 0.51 [10]. The lower friction value of 0.40 was selected for use in the analysis as this value has provided accurate results in prior studies and to maximize relative lateral barrier displacements. This friction value was applied in the LS-DYNA baseline model between the barrier segments and the shell element ground. In addition to providing appropriate friction coefficients, the barrier model needed to develop the correct weight or normal forces on the ground. This was accomplished by allowing the barriers in the simulation model to reach quasi-static equilibrium on the ground prior to being impacted. Damping was used to help the barriers reach a steady normal force on the ground and was turned off prior to vehicle impact.

3.2.2 Pin in Asphalt Model

The pin in asphalt model was based on component testing of a 1½-in. diameter, A36 steel pin embedded 32 in. through 2-in. asphalt, replicating the pins used in previous full-scale testing, as shown in Figure 23 [3]. The model consisted of a solid element pin inserted into a rigid sleeve that was connected to two pairs of nonlinear springs, shown in Figure 24. The rigid sleeve and nonlinear springs were used to develop the proper force-deflection response of the pins when moving through soil and asphalt. The load curves for the springs were developed directly from the pin in asphalt component tests, and the force-deflection and pullout behaviors of the pins were compared to validate the model. The pin was modeled with the MAT_PIECEWISE_LINEAR_PLASTICITY material in LS-DYNA with the appropriate properties for A36 steel.

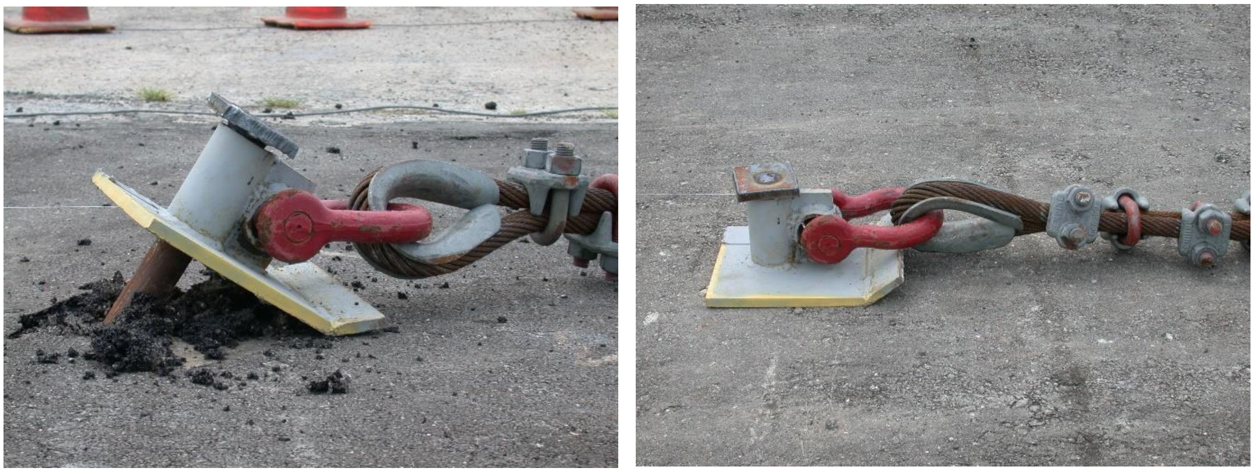

Figure 23. Component Testing of a Pin in Asphalt

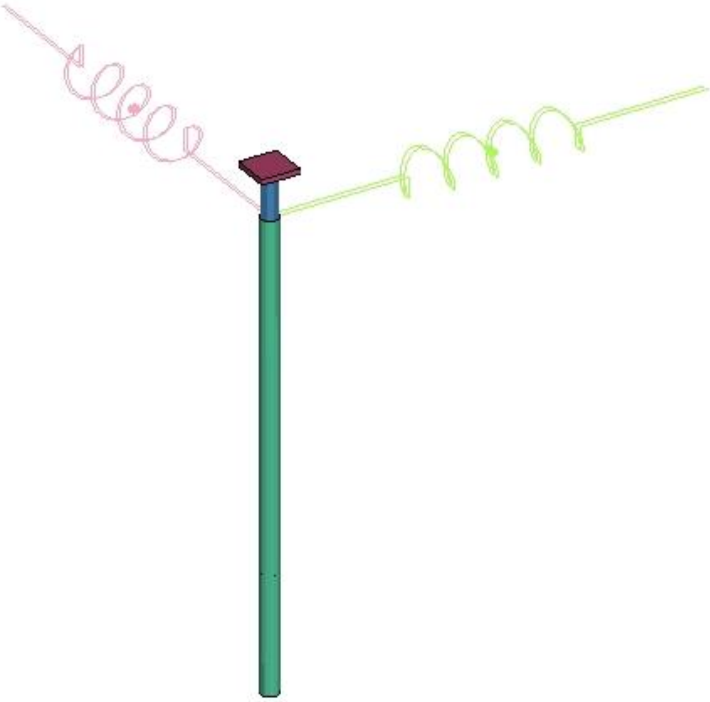

Figure 24. Pin in Asphalt Model

3.2.3 2270P Pickup Truck Model

The 2270P pickup truck model was a 2018 Dodge Ram originally developed by the Center for Collision Safety and Analysis Team at George Mason University [13] and modified by MwRSF personnel for use in roadside safety applications. An image of the Dodge Ram model is shown in Figure 25.

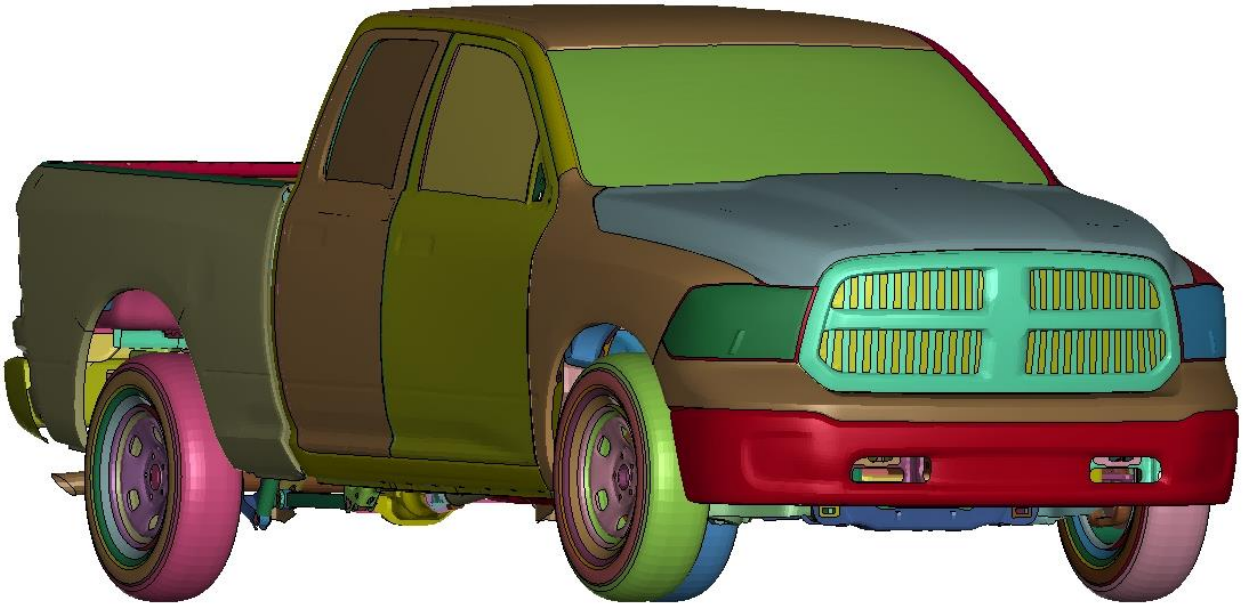

Figure 25. 2270P Pickup Truck Model

3.2.4 Baseline Model and Comparison to Test No. WITD-3

The baseline model was simulated with a 2270P pickup truck impacting the system at a speed of 62 mph and an angle of 25 degrees at a location 4.3 ft upstream from the joint center between barrier nos. 8 and 9, as shown in Figure 26. The system consisted of 16 F-shape PCBs with asphalt pins installed in all three traffic-side bolt pockets in each PCB, for a total of 48 asphalt pins. The barriers were positioned with a 4-in. joint spacing, leaving no gap between the connection loops and connection pins, as would be the appropriate joint spacing if the barriers were pulled taut.

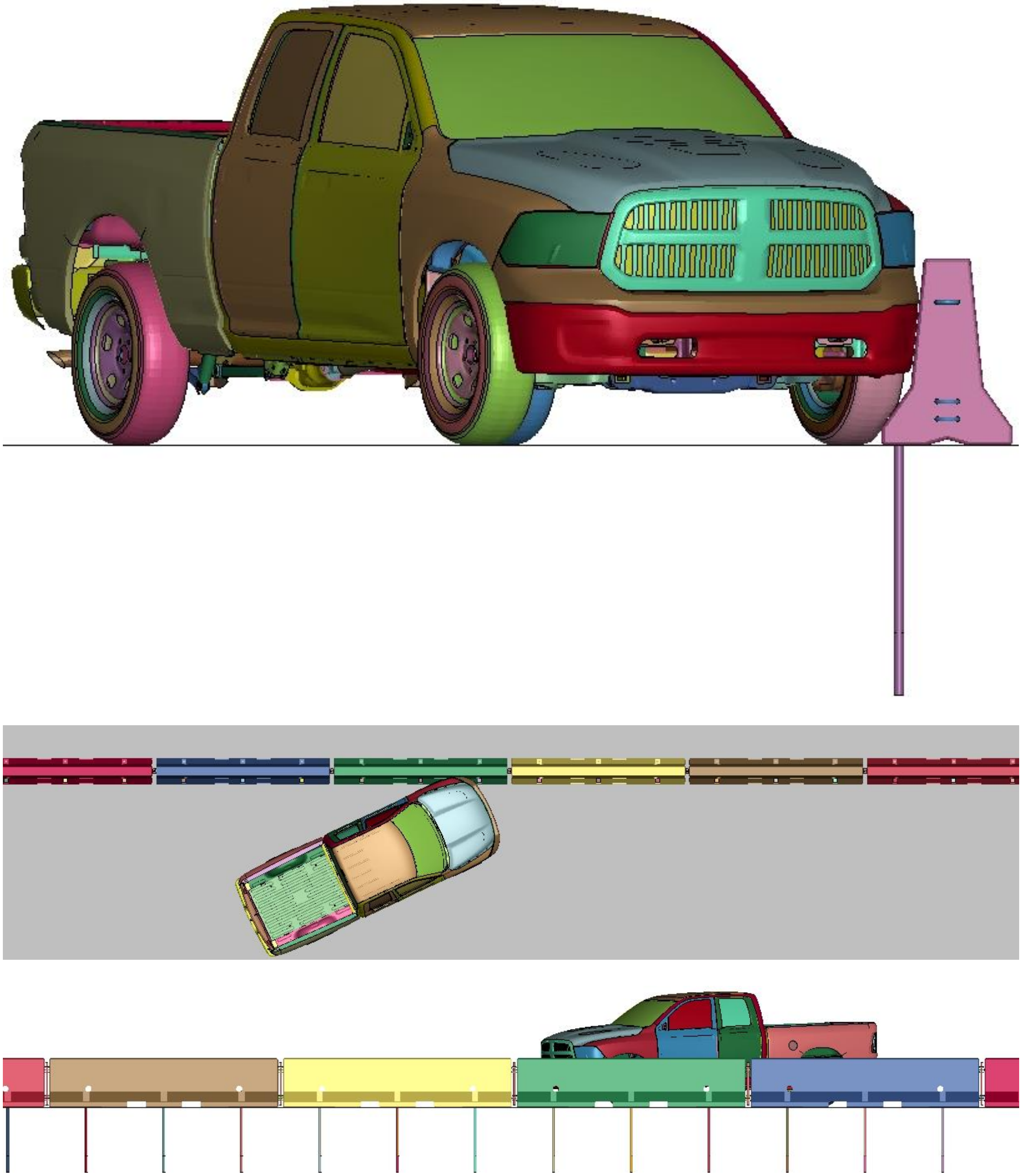

Figure 26. Baseline Model

The results of the baseline system simulation were compared to the results from test no. WITD-3. Test no. WITD-3 consisted of a 2270P vehicle impacting the PCB system at a speed of 61.9 mph and an angle of 25.1 degrees. The vehicle’s longitudinal and lateral velocities from test no. WITD-3 and the baseline model were compared using the Roadside Safety Simulation Validation Program (RSVVP) [14]. The RSVVP analysis showed that the model accurately predicted test no. WITD-3 longitudinal and lateral vehicle velocities, as shown in Appendix B. However, the dynamic deflection of the baseline model was 10.6 in., which underestimated the 16.3-in. dynamic deflection in test no. WITD-3.

The relative lateral barrier displacement was also compared between the model and test no. WITD-3. The relative lateral barrier displacement aids in quantifying the amount of exposed face of the downstream barrier and thus the snag hazard. The lateral barrier displacement at the time the left-front wheel was traversing the joint was 0.36 in. and 3.28 in. in the baseline model and test no. WITD-3, respectively.

The dynamic deflection and relative lateral barrier displacement discrepancies between the model and test no. WITD-3 could have potentially been caused by two factors: the barriers being modeled as rigid and the 4-in. joint spacing. Barrier nos. 8 and 9 both experienced fractures and toe break out at the anchor pins during test no. WITD-3, likely increasing the dynamic deflections, as shown in Figure 27. A non-rigid barrier model with damage would have likely produced more accurate deflections, however, the project scope did not account for creation of such a model. The 4-in. joint spacing may have also contributed to the deflection discrepancy. To reiterate, the 4-in. joint spacing only occurs when the barriers are pulled taut after the connection pin is installed between two adjacent barriers, which was performed prior to test no. WITD-3. However, given allowable barrier tolerances, joint spacing is often less than 4 in. Loop bar tolerances can cause certain loops to be pulled taut while others may have some gaps. To illustrate barrier tolerances, in test no. WITD-3 there is a visible gap between the connection loop of barrier no. 6 and the connection pin, although the barriers were pulled taut, as shown in Figure 28. As such, the joint spacing of the baseline model was decreased from 4 in. to 3.5 in.

Figure 27. Barrier Nos. 8 and 9 Damage, Test No. WITD-3

Figure 28. Gap Between Connection Loop and Pin, Test No. WITD-3

The RSVVP analysis showed that the model with 3.5-in. joint spacing was sufficient in predicting test no. WITD-3 lateral vehicle velocity, but not longitudinal velocity, as shown in Appendix B. Visual comparisons of the baseline model and test no. WITD-3, as shown in Figures 29 and 30, showed that the behavior of the vehicle and the barrier were similar between the full-scale test and the baseline simulation. The dynamic deflection of the model with 3.5-in. joint spacing was 16.3 in. as compared to 10.6 in. and 16.3 in. in the original baseline model and test no. WITD-3, respectively. Further, the relative lateral barrier displacement of the model with 3.5-in. joint spacing was 1.31 in. as compared to 0.36 in. and 3.28 in. in the original baseline model and test no. WITD-3, respectively. The baseline model with 3.5-in. joint spacing captured the wheel snag, as shown in Figure 31. For illustration purposes, the impacted barrier was hidden to highlight the severity of the wheel snag. Note the amount of overlap between the wheel and barrier, and the wheel's rotation as it traverses the joint.

Test nos. WITD-2 and WITD-3 both failed due to wheel snag on the upstream face of the barrier immediately downstream from the impacted barrier. As such, it is more crucial that the baseline model captures relative lateral barrier displacement and wheel snag behavior than other metrics such as vehicle velocities. Based on the wheel snag and improved dynamic deflection and relative lateral barrier displacement, it was believed that the baseline model with 3.5-in. joint spacing provided reasonable results, and the baseline model was deemed appropriate for use in further development of the saddle cap.

0.000 sec 0.000 sec

0.050 sec 0.050 sec

0.100 sec 0.100 sec

0.150 sec 0.150 sec

0.200 sec 0.200 sec

0.250 sec 0.250 sec

Figure 29. Overhead Sequential Photographs, Test No. WITD-3 (left) and Baseline Model (right)

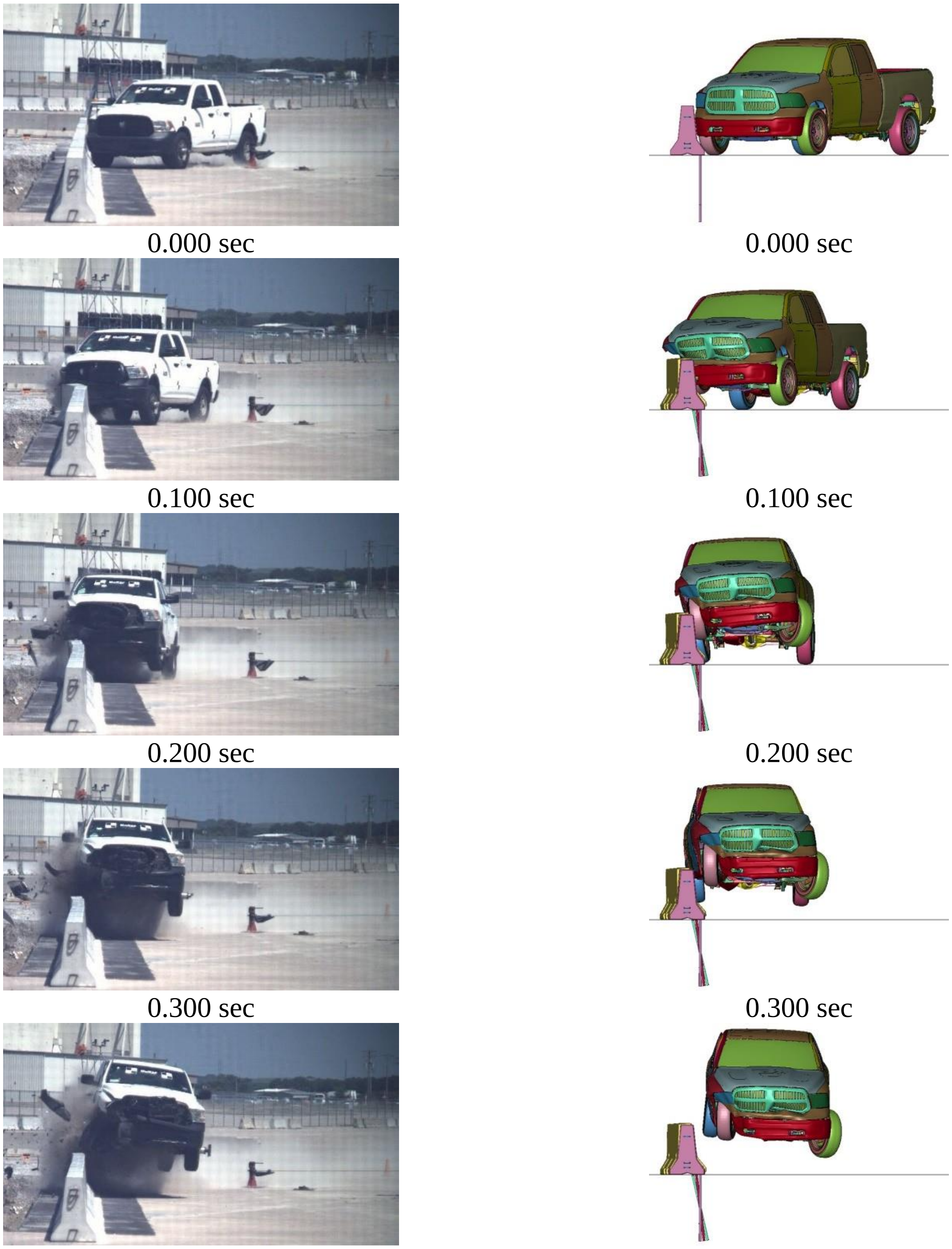

0.000 sec 0.000 sec

0.100 sec 0.100 sec

0.200 sec 0.200 sec

0.300 sec 0.300 sec

0.400 sec 0.400 sec

Figure 30. Downstream Sequential Photographs, Test No. WITD-3 (left) and Baseline Model (right)

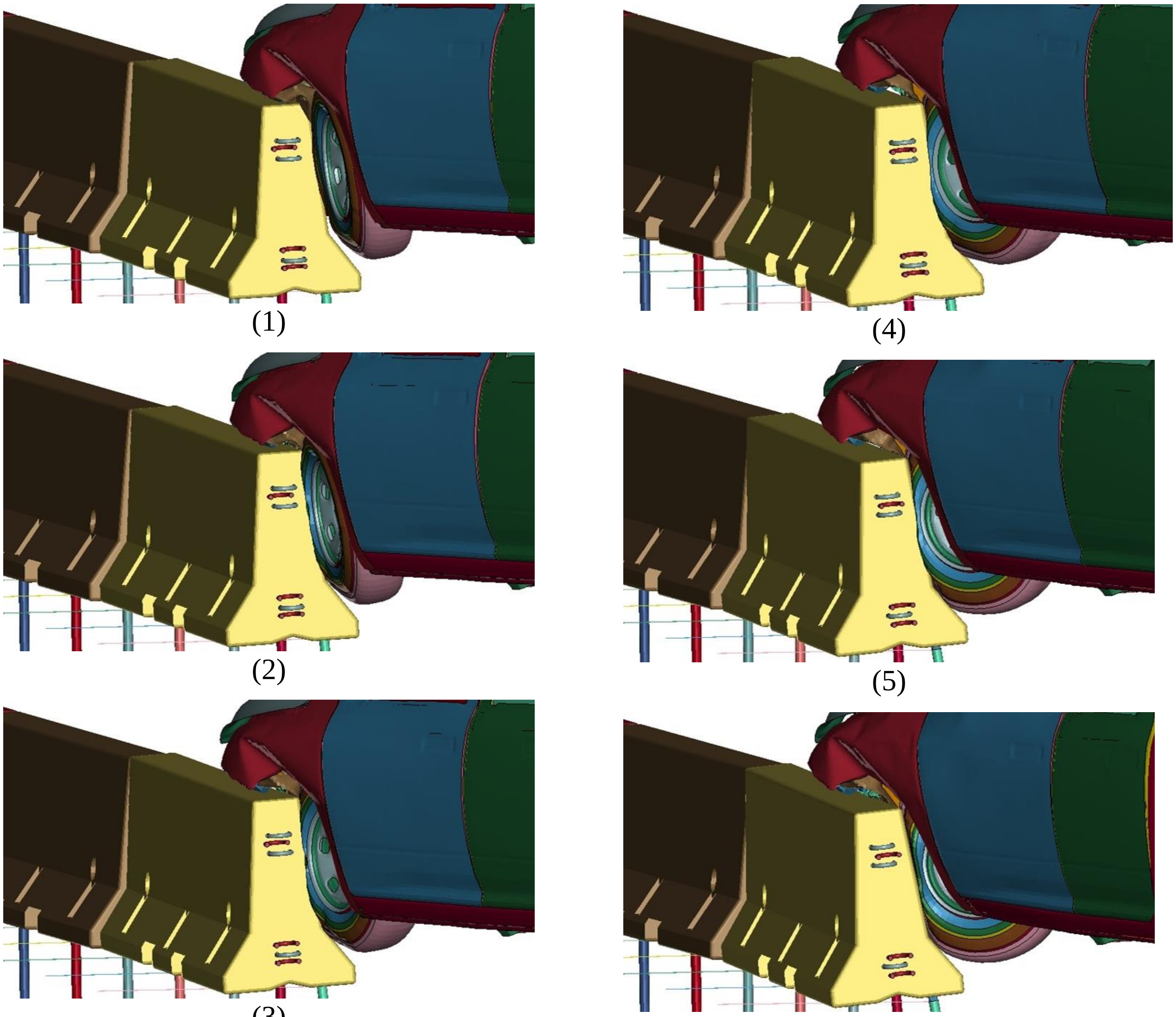

(1) (4)

(2) (5)

(3) (6)

Figure 31. Documentary Images, Baseline Model

3.3 Saddle Cap Development

Once the baseline model was deemed appropriate for the purposes of this study, the saddle cap was incorporated into the model, as shown in Figure 32. The initial saddle cap geometry was 6¼-in. tall x 6½-in. wide x ⅛-in. thick, with a $^{3}/_{16}$-in. clearance per side between the interior of the saddle cap and lateral PCB surfaces. Initial saddle cap geometry was minimized with expectations that geometric aspects, such as height, width, and thickness, would be increased as the simulation study progressed. All saddle cap assembly parts, consisting of the saddle cap, connection pin, weld plate, and square tube, were modeled with the MAT_PIECEWISE_LINEAR_PLASTICITY material card in LS-DYNA. The saddle cap, connection pin, and weld plates were assigned appropriate material properties for A572 Grade 50 steel whereas the square tube was assigned appropriate material properties for A500 Grade B steel.

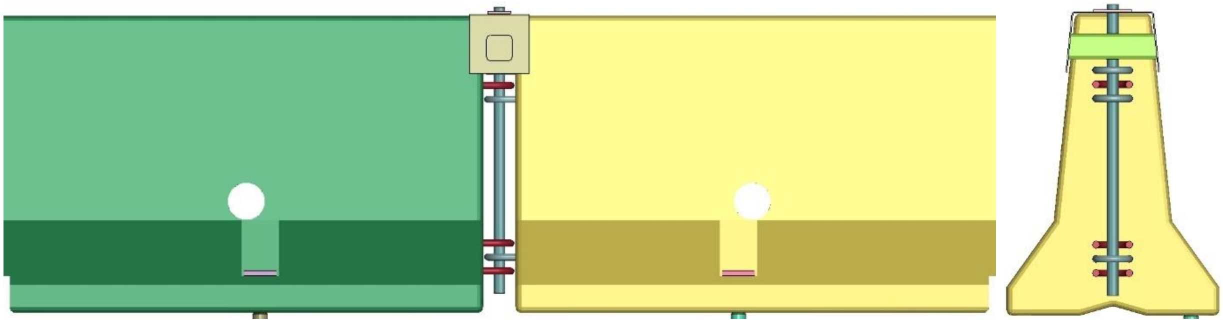

Figure 32. Baseline Model with Saddle Cap

The initial saddle cap model terminated early due to negative volumes in vehicle elements that interacted with the saddle cap. As such, the saddle cap geometry was altered to evaluate the effects of increased height and width on system performance and model stability. Three additional saddle caps were modeled with increased height (12½ in. tall x 6½ in. wide), increased width (6¼ in. tall x 13 in. wide), and increased height and width (12½ in. tall x 13 in. wide), as shown in Figure 33.

Dynamic deflections and relative lateral barrier displacements from the baseline and saddle cap models with altered geometry are provided in Table 1. All saddle cap models showed a decrease in deflections and relative lateral barrier displacements compared to the baseline model, with the increased height and width model providing the most improvement.

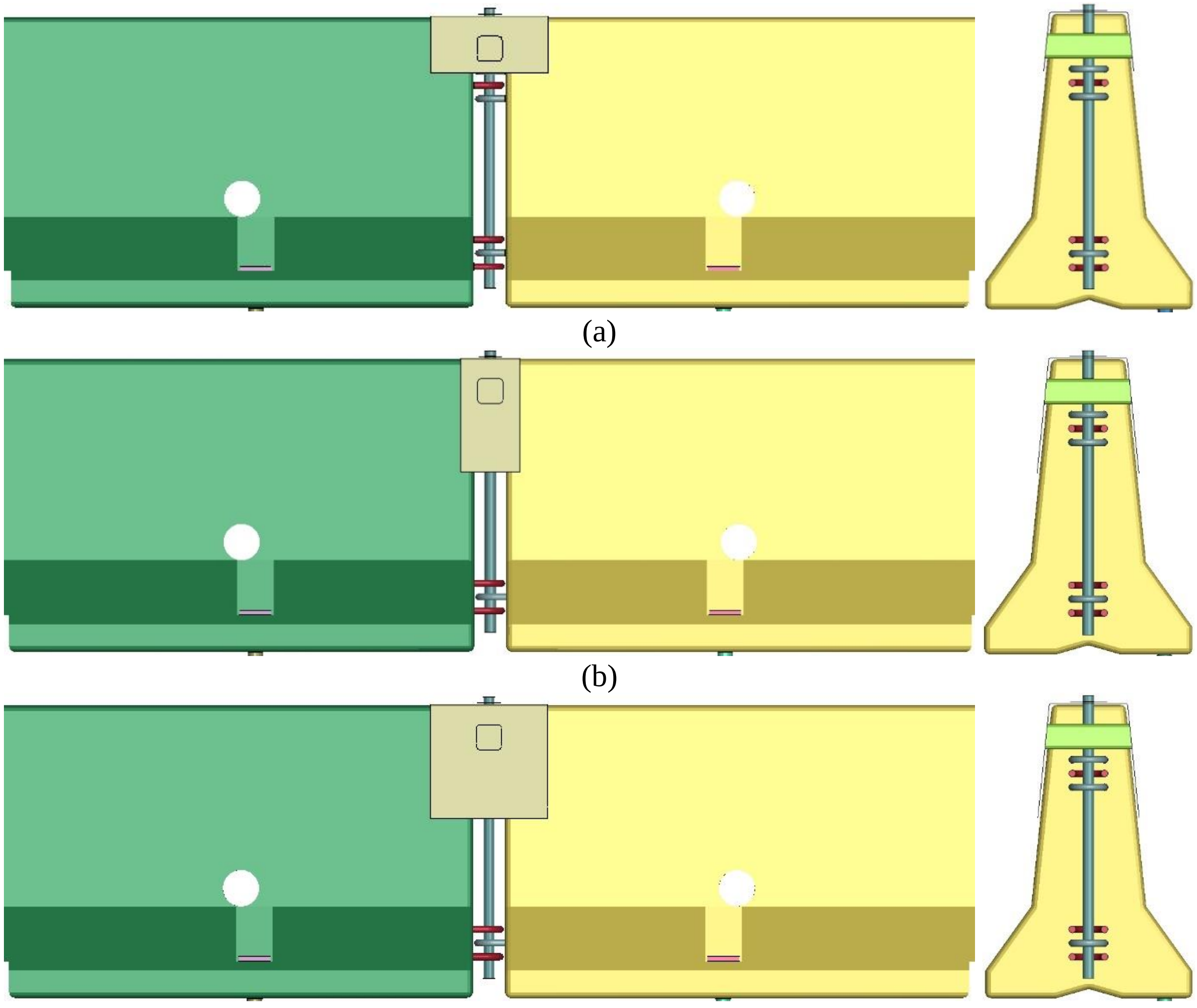

(a)

(b)

(c)

Figure 33. Saddle Cap Models with (a) Increased Width, (b) Increased Height, and (c) Increased Height and Width

Table 1. Dynamic Deflections and Relative Lateral Barrier Displacements, Baseline Model and Saddle Cap Models with Altered Geometry

Evaluation Criteria	Saddle Cap			
	None - Baseline	Increased Height	Increased Width	Increased Height and Width
Dynamic Deflection (in.)	16.3	13.6	15.0	13.5
Relative Lateral Barrier Displacement (in.)	1.31	1.10	1.04	1.01

Images comparing wheel-barrier overlap from the baseline model and saddle cap models with altered geometry are shown in Figure 34. The tire and rim snagged on the barrier in the baseline and increased width models whereas tire snag only occurred in the increased height and increased height and width models. This is because both models with increased height not only provided shear transfer, but also shielded the joint. However, the saddle cap with increased height began to bend outward during loading, exposing the upstream edge of the saddle cap. The lower leading edge of the front-left door snagged on the exposed saddle cap edge, leaving an opening between the frame of the vehicle and door, as shown in Figure 35. Saddle cap bending and snag caused concerns for occupant compartment penetration issues. Given that the saddle cap with increased height and width produced the smallest deflection and relative lateral barrier displacement, along with the ability to shield the gap and minimize wheel-barrier overlap, this saddle cap was selected for further refinement.

(a) Baseline - No Saddle Cap

(b) Increased Width

(c) Increased Height

(d) Increased Height and Width

Figure 34. Wheel-Barrier Overlap: (a) Baseline Model, (b) Saddle Cap Model with Increased Width, (c) Saddle Cap Model with Increased Height, and (d) Saddle Cap Model with Increased Height and Width

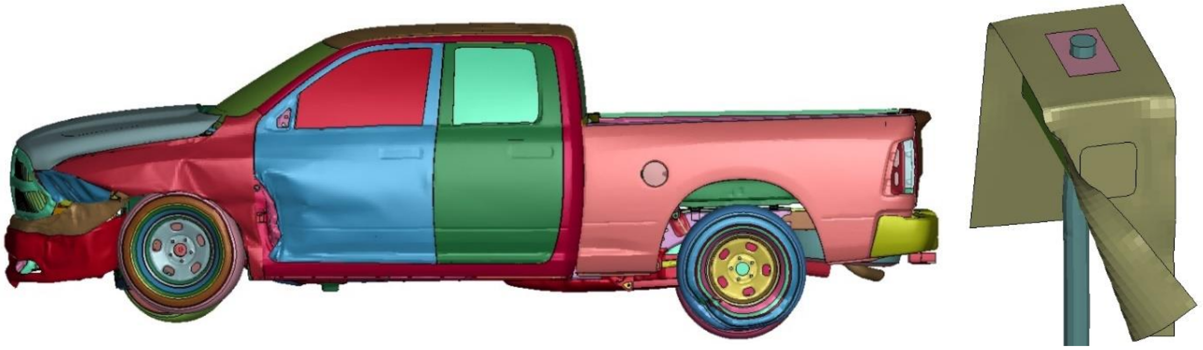

Figure 35. Door Snag on the Saddle Cap with Increased Height

The initial saddle cap models had a $^{3}/_{16}$-in. clearance per side between the interior of the saddle cap and lateral PCB surfaces. Due to known barrier tolerance issues [12], the clearance was increased from $^{3}/_{16}$ in. per side to ¼ in. to ensure that the saddle cap would fit onto the barriers without necessitating barrier material removal. The saddle cap model with increased height and width was altered to accommodate a ¼-in. clearance and compared to the previous model with a $^{3}/_{16}$-in. clearance. The dynamic deflections were 13.5 in. and 13.6 in. and the relative lateral barrier displacements were 1.01 in. and 1.03 in. for the $^{3}/_{16}$-in. clearance and ¼-in. clearance models, respectively. The front fender snagged on the lower upstream corner of the saddle cap with ¼-in. clearance, causing the saddle cap to deform outward toward the vehicle, as shown in Figure 36. The lower leading edge of the left-front door then snagged on the exposed upstream edge of the saddle cap, leaving an opening between the frame of the vehicle and door. This saddle cap deformation and snag caused concerns for occupant compartment penetration issues. As such, the next modification to the saddle cap model was to increase the saddle cap thickness from ⅛ in. to $^{3}/_{16}$ in. and ¼ in. in an attempt to prevent saddle cap snag.

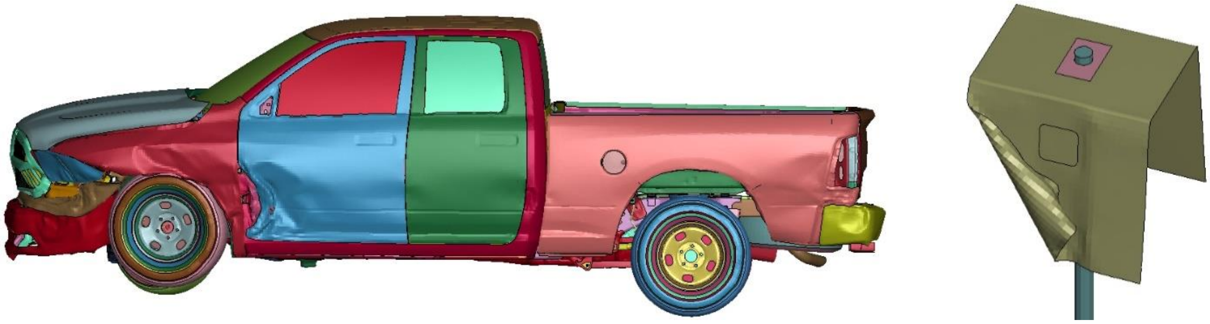

Figure 36. Door Snag on the Saddle Cap with Increased Clearance

Dynamic deflections and relative lateral barrier displacements from the 12½-in. tall x 13-in. wide saddle cap models with ¼-in. clearance and varying thickness are in Table 2. Dynamic deflections and relative lateral barrier displacements were reduced with increased saddle cap thickness. Further, door snag on the saddle cap did not occur in the models with increased thickness. The wheel overlap with the downstream barrier decreased with increased saddle cap thickness, as shown in Figure 37. Although the rim did not snag on the downstream barrier in any of these models, additional height changes were explored to further mitigate tire snag. As such, the ¼-in. thick saddle cap model height was increased from 12.5 in. to 16 in.

Table 2. Dynamic Deflections and Relative Lateral Barrier Displacements, Models with Varied Saddle Cap Thickness

Evaluation Criteria	Saddle Cap Thickness		
	⅛ in.	$^{3}/_{16}$ in.	¼ in.
Dynamic Deflection (in.)	13.6	13.4	13.2
Relative Lateral Barrier Displacement (in.)	1.03	0.95	0.85

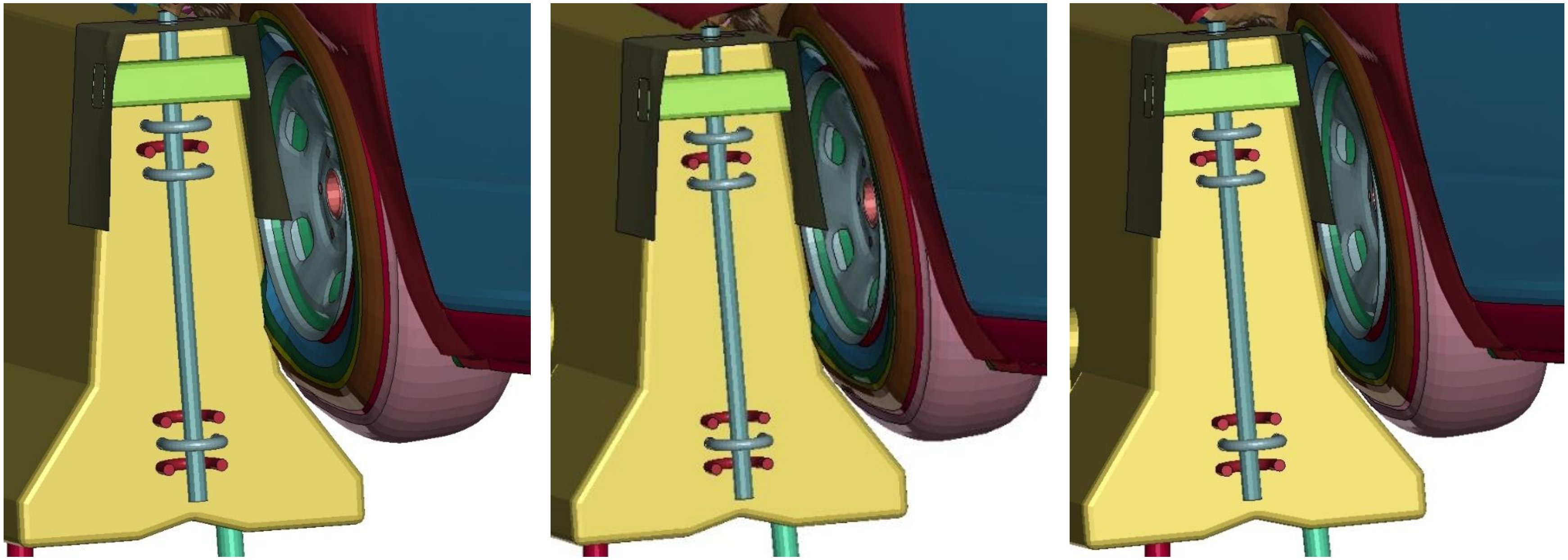

⅛-in. thick

$^{3}/_{16}$-in. thick

¼-in. thick

Figure 37. Wheel-Barrier Overlap, Models with Varied Saddle Cap Thickness

The dynamic deflections were 13.2 in. and 13.3 in. and the relative lateral barrier displacements were 0.85 in. and 0.89 in. for the 12.5-in. and 16-in. tall saddle cap models, respectively. Wheel-barrier overlap images comparing the 12.5-in. tall and 16-in. tall saddle caps are in Figure 38. Although tire snag occurred in the 16-in. tall saddle cap model, tire snag was reduced when compared to the 12.5-in. tall saddle cap model. The 16-in. tall saddle cap model was selected for further refinement due to the similarities in deflection and relative lateral barrier displacement and the improved tire snag mitigation.

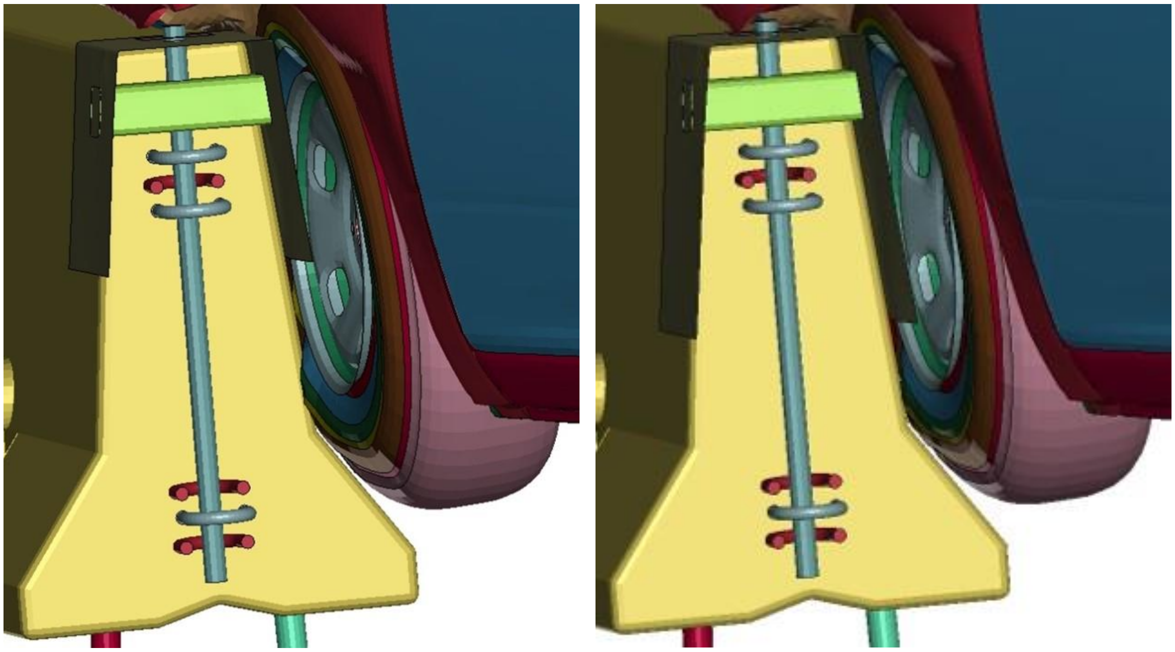

(a) 12.5-in. tall

(b) 16-in. tall

Figure 38. Wheel-Barrier Overlap, Saddle Cap Models Comparing Increased Height: (a) 12.5-in. tall and (b) 16-in. Tall

The next refinement was to change the saddle cap width from 13 in. to 12 in. for consistency with stock material. The weld plate on top of the saddle cap was originally included to improve the attachment of the connection pin to the ⅛-in. thick saddle cap. Because the saddle cap was increased to ¼ in. thick, the weld plate was no longer necessary and removed. The dynamic deflections were 13.3 in. and 13.5 in. and the relative lateral barrier displacements were 0.89 in. and 0.90 in. for the 13-in. and 12-in. wide saddle cap models, respectively. Wheel-barrier overlap from saddle cap models comparing saddle cap widths are in Figure 39. Deflections, relative lateral barrier displacements, and tire snag mitigation capabilities were similar between the two models. Therefore, the 16-in. tall x 12-in. wide x ¼-in. thick saddle cap model with a ¼-in. clearance between the saddle cap interior and lateral barrier faces was selected for full-scale crash testing to MASH test designation no. 3-11.

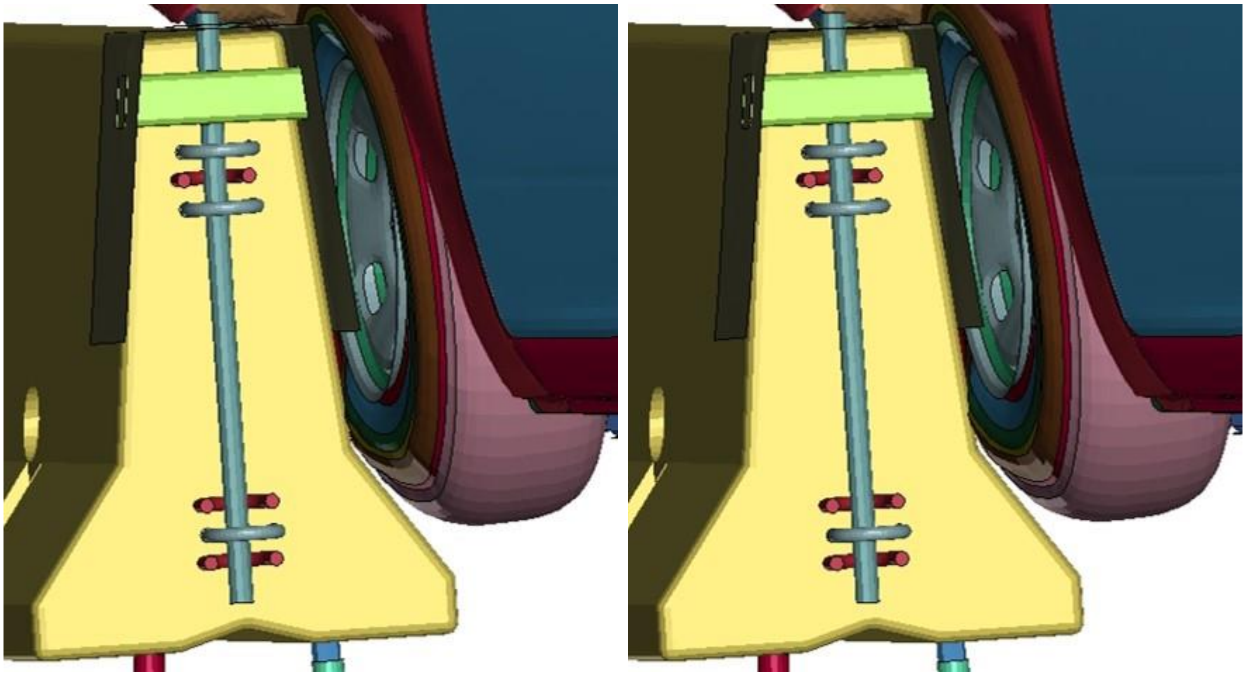

(a) 13-in. wide

(b) 12-in. wide

Figure 39. Wheel-Barrier Overlap, Saddle Cap Models Comparing Reduced Width: (a) 13-in. Wide and (b) 12-in. Wide

4 TEST REQUIREMENTS AND EVALUATION CRITERIA

4.1 Test Requirements

Longitudinal barriers, such as PCBs, must satisfy impact safety standards in order to be declared eligible for federal reimbursement by the Federal Highway Administration (FHWA) for use on the National Highway System. For new hardware, these safety standards consist of the guidelines and procedures published in MASH [1]. According to TL-3 of MASH, longitudinal barrier systems must be subjected to two full-scale vehicle crash tests, as summarized in Table 3.

Table 3. MASH TL-3 Crash Test Conditions for Longitudinal Barriers

Test Article	Test Designation No.	Test Vehicle	Vehicle Weight lb	Impact Conditions		Evaluation Criteria [1]
				Speed mph	Angle deg.	
Longitudinal Barrier	3-10	1100C	2,420	62	25	A,D,F,H,I
	3-11	2270P	5,000	62	25	A,D,F,H,I

[1] Evaluation criteria explained in Table 4.

However, only MASH test designation no. 3-11 was deemed necessary as other prior small car tests were used to support a decision to deem the 1100C crash test not critical for the evaluation of the F-shape PCB tie-down anchorage system for asphalt surfaces. TTI’s test no. 7069-3 [15, 16] performed under MASH TL-3 standards, indicated that safety-shape barriers can safely redirect 1100C vehicles. In test no. 2214NJ-1, found in MwRSF report no. TRP-03-177-06, MASH test designation no. 3-10 was successfully conducted on a permanent New Jersey shape concrete parapet under NCHRP Project 22-14(2) [17]. Additionally, the increased toe height of New Jersey shape barriers tends to produce increased vehicle climb and instability as compared to the F-shape geometry. Another successful MASH test designation no. 3-10 crash test was conducted by TTI on a free-standing F-shape PCB similar to the barrier used in this study [18]. These tests indicate that safety shape barriers are capable of successfully capturing and redirecting the 1100C vehicle in both free-standing PCB and permanent concrete parapet applications. The anchored F-shape PCB evaluated in this study would be expected to perform similarly to previous MASH 1100C vehicle tests in terms of capture and redirection. Therefore, test designation no. 3-10 with the 1100C vehicle was deemed non-critical for evaluation of the asphalt tie-down anchorage and saddle caps for use with F-shape PCBs. Accordingly, only MASH test designation no. 3-11 was conducted on the anchored PCB system.

It should be noted that the test matrix detailed herein represents the researchers’ best engineering judgement with respect to the MASH safety requirements and their internal evaluation of critical tests necessary to evaluate the crashworthiness of the anchored PCB system. Thus, any tests within the evaluation matrix deemed non-critical may eventually need to be evaluated based on additional knowledge gained over time or revisions to the MASH criteria.

Table 4. MASH Evaluation Criteria for Longitudinal Barriers

<table>
<tr><td>Structural Adequacy</td><td colspan="4">A. Test article should contain and redirect the vehicle or bring the vehicle to a controlled stop; the vehicle should not penetrate, underride, or override the installation although controlled lateral deflection of the test article is acceptable.</td></tr>
<tr><td rowspan="9">Occupant Risk</td><td colspan="4">D. Detached elements, fragments or other debris from the test article should not penetrate or show potential for penetrating the occupant compartment, or present an undue hazard to other traffic, pedestrians, or personnel in a work zone. Deformations of, or intrusions into, the occupant compartment should not exceed limits set forth in Section 5.2.2 and Appendix E of MASH.</td></tr>
<tr><td colspan="4">F. The vehicle should remain upright during and after collision. The maximum roll and pitch angles are not to exceed 75 degrees.</td></tr>
<tr><td colspan="4">H. Occupant Impact Velocity (OIV) (see Appendix A, Section A5.2.2 of MASH for calculation procedure) should satisfy the following limits:</td></tr>
<tr><td rowspan="3"></td><td colspan="3">Occupant Impact Velocity Limits</td></tr>
<tr><td>Component</td><td>Preferred</td><td>Maximum</td></tr>
<tr><td>Longitudinal and Lateral</td><td>30 ft/s</td><td>40 ft/s</td></tr>
<tr><td colspan="4">I. The Occupant Ride down Acceleration (ORA) (see Appendix A, Section A5.2.2 of MASH for calculation procedure) should satisfy the following limits:</td></tr>
<tr><td rowspan="3"></td><td colspan="3">Occupant Ride down Acceleration Limits</td></tr>
<tr><td>Component</td><td>Preferred</td><td>Maximum</td></tr>
<tr><td>Longitudinal and Lateral</td><td>15.0 g’s</td><td>20.49 g’s</td></tr>
</table>

4.2 Evaluation Criteria

Evaluation criteria for full-scale vehicle crash testing are based on three factors: (1) structural adequacy, (2) occupant risk, and (3) vehicle trajectory after collision. Criteria for structural adequacy are intended to evaluate the ability of the PCB system to contain and redirect impacting vehicles. In addition, controlled lateral deflection of the test article is acceptable. Occupant risk evaluates the degree of hazard to occupants in the impacting vehicle. Post-impact vehicle trajectory is a measure of the potential of the vehicle to result in a secondary collision with other vehicles and/or fixed objects, thereby increasing the risk of injury to the occupants of the impacting vehicle and/or other vehicles. These evaluation criteria are summarized in Table 4 and defined in greater detail in MASH. The full-scale vehicle crash test was conducted and reported in accordance with the procedures provided in MASH. In addition to the standard occupant risk measures, the Post-Impact Head Deceleration (PHD), the Theoretical Head Impact Velocity (THIV), and the Acceleration Severity Index (ASI) were determined and reported. Additional discussion on PHD, THIV and ASI is provided in MASH.

4.3 Soil Strength Requirements

In accordance with Chapter 3 and Appendix B of MASH, foundation soil strength must be verified before any full-scale crash testing can occur on soil-dependent systems. For test no. WITD-4, the F-shape PCBs were placed on top of an asphalt pad that covered in-situ soil, and the PCBs were anchored with steel pins that passed through the barrier and into the asphalt and soil. A static soil test was not completed for the following reasons: (1) the soil surrounding the anchors was not tamped in a similar method used to install a post for a static soil test, (2) although the soil surrounding the anchors was not tamped, standard MASH soil was used, (3) asphalt provides more resistance to anchor motion than soil, and (4) given the asphalt pad, this type of installation did not allow for a representative static soil test to be conducted in the critical area of the installation. As such, the lack of a static soil test did not violate MASH requirements for soil-dependent systems.

5 TEST CONDITIONS

5.1 Test Facility

The Outdoor Test Site is located at Lincoln Air Park on the northwest side of the Lincoln Municipal Airport and is approximately five miles northwest of the University of Nebraska-Lincoln.

5.2 Vehicle Tow and Guidance System

A reverse-cable tow system with a 1:2 mechanical advantage was used to propel the test vehicle. The distance traveled and the speed of the tow vehicle were one-half that of the test vehicle. The test vehicle was released from the tow cable before impact with the barrier system. A digital speedometer on the tow vehicle increased the accuracy of the test vehicle impact speed.

A vehicle guidance system developed by Hinch [19] was used to steer the test vehicles. A guide flag, attached to the left-front wheel and the guide cable, was sheared off before impact with the barrier system. The ⅜-in. diameter guide cable was tensioned to approximately 3,500 lb and supported both laterally and vertically every 100 ft by hinged stanchions. The hinged stanchions stood upright while holding up the guide cable, but as the vehicle was towed down the line, the guide flag struck and knocked each stanchion to the ground.

5.3 Test Vehicle

For test no. WITD-4, a 2017 Dodge Ram 1500 crew cab pickup truck was used as the test vehicle. The curb, test inertial, and gross static vehicle weights were 5,242 lb, 5,019 lb, and 5,183 lb, respectively. The test vehicle is shown in Figure 40, and photos of the pre-test floorboards and undercarriage are show in Figure 41. Vehicle dimensions are shown in Figure 42.

The longitudinal component of the center of gravity (c.g.) was determined using the measured axle weights. The Suspension Method [20] was used to determine the vertical component of the c.g. This method is based on the principle that the c.g. of any freely suspended body is in the vertical plane through the point of suspension. The vehicle was suspended successively in three positions, and the respective planes containing the c.g. were established. The intersection of these planes pinpointed the final c.g. location for the test inertial condition. The location of the final c.g. for test no. WITD-4 is shown in Figures 42 and 43. Data used to calculate the location of the c.g. and ballast information are shown in Appendix C.

Square, black-and-white checkered targets were placed on the vehicle, shown in Figure 43, to serve as reference in the high-speed digital video and aid in the video analysis. Round, checkered targets were placed at the c.g. on the left-side door, the right-side door, and the roof of the vehicle.

The front wheels of the test vehicle were aligned to vehicle standards except the toe-in value was adjusted to zero such that the vehicle would track properly along the guide cable. A 5B flash bulb was mounted under the vehicle’s left-side windshield wiper and was fired by a pressure tape switch mounted at the impact corner of the bumper. The flash bulb was fired upon initial impact with the test article to create a visual indicator of the precise time of impact on the high-speed digital videos. A radio-controlled brake system was installed in the test vehicle so the vehicle could be brought safely to a stop after the test.

Figure 40. Test Vehicle, Test No. WITD-4

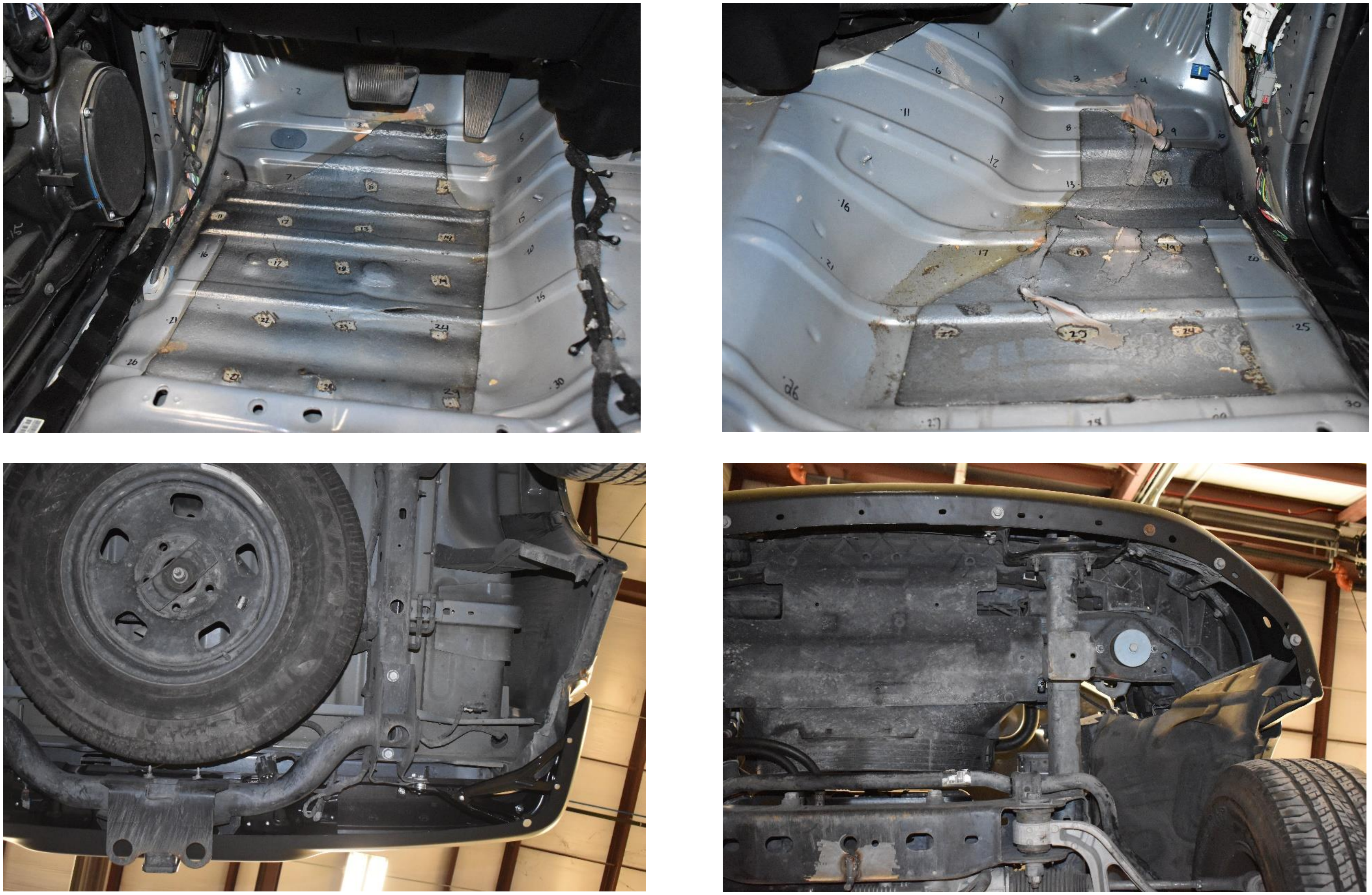

Figure 41. Test Vehicle’s Pre-Test Interior Floorboards and Undercarriage, Test No. WITD-4

Test Name: WITD-4
VIN No: 3C6RR6KT2JG118353

Model Year: 2017
Make: Dodge
Model: Ram 1500

Tire Size: 265/70R17
Tire Inflation Pressure: 40 psi
Odometer: 296879

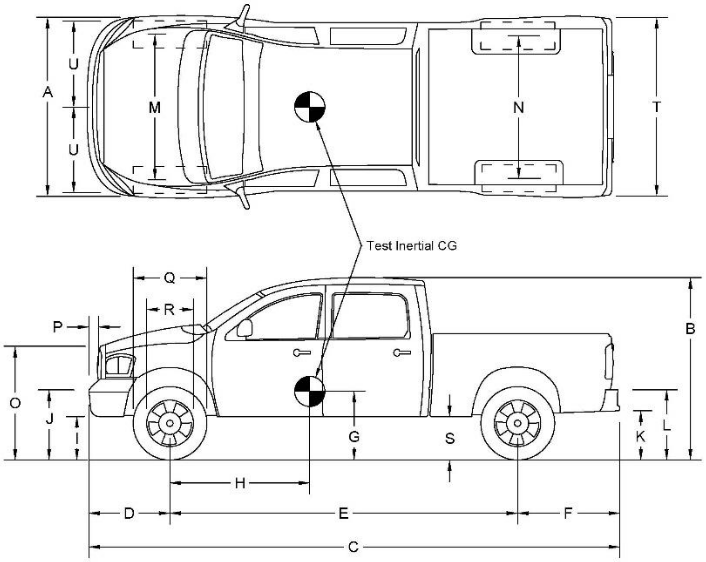

Vehicle Geometry - in. (mm)
Target Ranges listed below

A:	77 1/2	1968 1/2	78±2 (1950±50)	B:	74 1/4	1885 19/20	
C:	228 1/4	5797 11/20	237±13 (6020±325)	D:	38	965 1/5	39±3 (1000±75)
E:	140 3/4	3575 1/20	148±12 (3760±300)	F:	49 1/2	1257 3/10	
G:	28 1/8	714 3/8	min: 28 (710)	H:	61 1/4	1555 3/4	63±4 (1575±100)
I:	13	330 1/5		J:	24 1/4	615 19/20	
K:	20 1/2	520 7/10		L:	29 1/4	742 19/20	
M:	67 3/4	1720 17/20	67±1.5 (1700±38)	N:	67 7/8	1724 1/40	67±1.5 (1700±38)
O:	44 1/8	1120 31/40	43±4 (1100±75)	P:	4 1/4	107 19/20	
Q:	30 1/4	768 7/20		R:	18 1/2	469 9/10	
S:	15	381		T:	76 5/8	1946 11/40	

U (impact width): 36 914 2/5

Mass Distribution - lb (kg)

Gross Static	LF	1488 (675)	RF	1445 (655)
	LR	1122 (509)	RR	1128 (512)

Weights lb (kg)	Curb	Test Inertial	Gross Static
W-front	2927 (1328)	2835 (1286)	2933 (1330)
W-rear	2315 (1050)	2184 (991)	2250 (1021)
W-total	5242 (2378)	5019 (2277) 5000±110 (2270±50)	5183 (2351) 5165±110 (2343±50)

Wheel Center Height (Front):	14 3/4	374 13/20
Wheel Center Height (Rear):	14 3/4	374 13/20
Wheel Well Clearance (Front):	34 3/4	882 13/20
Wheel Well Clearance (Rear):	38	965 1/5
Bottom Frame Height (Front):	18	457 1/5
Bottom Frame Height (Rear):	25 1/2	647 7/10

Engine Type: Gasoline
Engine Size: 5.7L V8
Transmission Type: Automatic
Drive Type: RWD
Cab Style: Crew Cab
Bed Length: 67"

GVWR Ratings - lb

Front: 3700
Rear: 3900
Total: 6900

Surrogate Occupant Data

Type: Hybrid II
Mass: 164 lb
Seat Position: Driver

Note any damage prior to test: Passenger side dent on corner behind right behind second door, passenger side rear quarter bottom half of leading edge is dented, driver side rear quarter between wheel well and tail light is dented and scraped

Figure 42. Vehicle Dimensions, Test No. WITD-4

Test Name: WITD-4

VIN: 3C6RR6KT2JG118353

Model Year: 2017

Make: Dodge

Model: Ram 1500

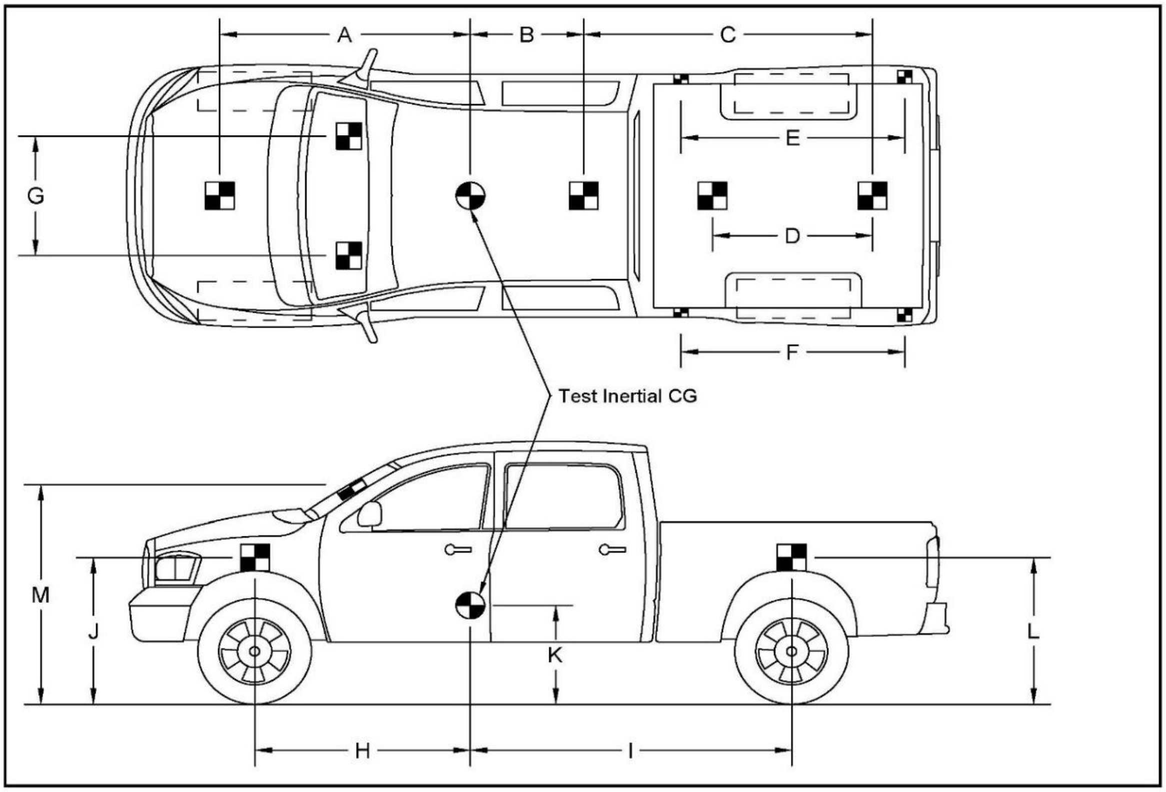

TARGET GEOMETRY-- in. (mm)

A: 69 13/16 (1773)
E: 54 1/2 (1384)
J: 38 7/8 (987)
B: 34 7/8 (886)
F: 54 5/8 (1387)
K: 28 1/8 (714)
C: 62 1/2 (1588)
G: 36 5/8 (930)
L: 42 3/16 (1072)
D: 25 3/8 (645)
H: 61 1/4 (1556)
M: 65 7/8 (1673)
I: 79 1/4 (2013)

Figure 43. Target Geometry, Test No. WITD-4

5.4 Simulated Occupant

For test no. WITD-4, a Hybrid II 50th-Percentile, Adult Male Dummy equipped with footwear was placed in the left-front seat of the test vehicle with the seat belt fastened. The dummy had a final weight of 164 lb. As recommended by MASH, the simulated occupant weight was not included in calculating the c.g. location.

5.5 Data Acquisition Systems

5.5.1 Accelerometers

Two environmental shock and vibration sensor/recorder systems were used to measure the accelerations in the longitudinal, lateral, and vertical directions. Both accelerometer systems were mounted near the c.g. of the test vehicle. The electronic accelerometer data obtained in dynamic testing was filtered using the SAE Class 60 and the SAE Class 180 Butterworth filter conforming to the SAE J211/1 specifications [21].

The two systems, the SLICE-1 and SLICE-2 units, were modular data acquisition systems manufactured by Diversified Technical Systems, Inc. of Seal Beach, California. The SLICE-2 unit was designated as the primary system. The acceleration sensors were mounted inside the bodies of custom-built, SLICE 6DX event data recorders and recorded data at 10,000 Hz to the onboard microprocessor. Each SLICE 6DX was configured with 7 GB of non-volatile flash memory, a range of ±500 g's, a sample rate of 10,000 Hz, and a 1,650 Hz (CFC 1000) anti-aliasing filter. The "SLICEWare" computer software programs and a customized Microsoft Excel worksheet were used to analyze and plot the accelerometer data.

5.5.2 Rate Transducers

Two identical angular rate sensor systems mounted inside the bodies of the SLICE-1 and SLICE-2 event data recorders were used to measure the rates of rotation of the test vehicle. Each SLICE MICRO Triax ARS had a range of 1,500 degrees/sec in each of the three directions (roll, pitch, and yaw) and recorded data at 10,000 Hz to the onboard microprocessors. The raw data measurements were then downloaded, converted to the proper Euler angles for analysis, and plotted. The "SLICEWare" computer software program and a customized Microsoft Excel worksheet were used to analyze and plot the angular rate sensor data.

5.5.3 Retroreflective Optic Speed Trap

A retroreflective optic speed trap was used to determine the speed of the test vehicle before impact. Five retroreflective targets, spaced at approximately 18-in. intervals, were applied to the side of the vehicle. When the emitted beam of light was reflected by the targets and returned to the Emitter/Receiver, a signal was sent to the data acquisition computer, recording at 10,000 Hz, as well as the external LED box activating the LED flashes. The speed was then calculated using the spacing between the retroreflective targets and the time between the signals. LED lights and high-speed digital video analysis are used as a backup if vehicle speeds cannot be determined from electronic data.

5.5.4 Digital Photography

Six AOS high-speed digital video cameras, eight GoPro digital video cameras, and four Panasonic digital video cameras were utilized to film test no. WITD-4. Camera details, camera operating speeds, lens information, and a schematic of the camera locations relative to the system are shown in Figure 44.

The high-speed videos were analyzed using the TEMA Motion software program. Actual camera speed and camera divergence factors were considered in the analysis of the high-speed videos. A Nikon digital still camera was also used to document pre- and post-test conditions for the test.

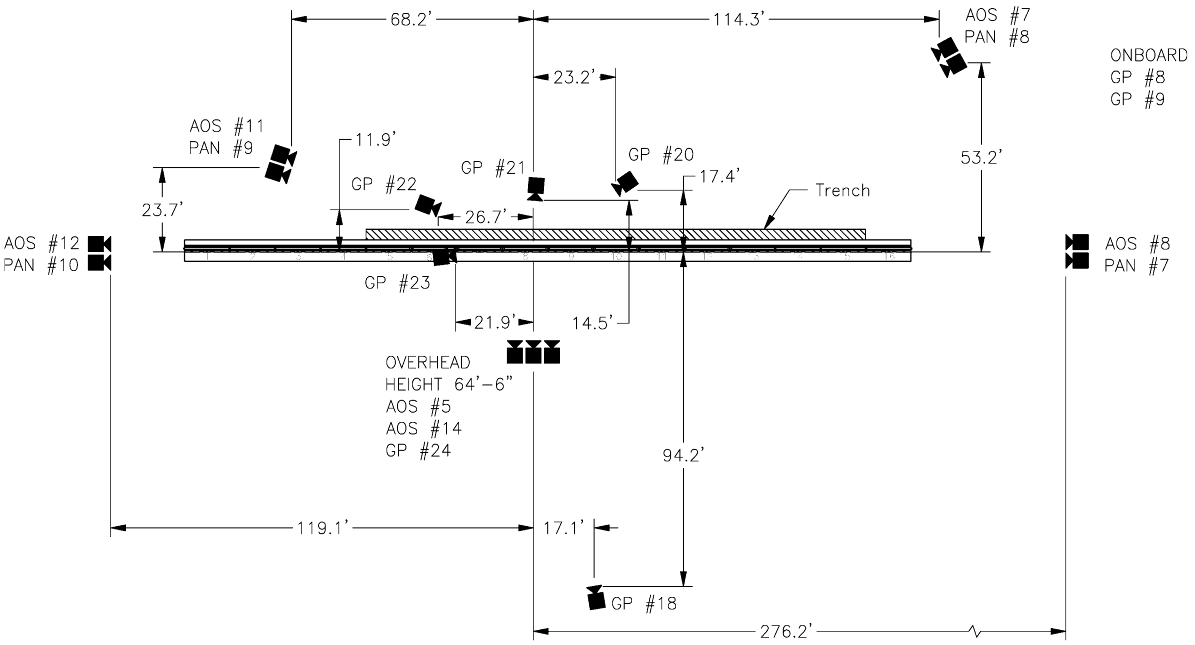

No.	Type	Operating Speed (frames/sec)	Lens	Lens Setting
AOS-5	AOS X-PRI	500	Kowa 12 mm Fixed	-
AOS-7	AOS X-PRI	500	Fujinon 75 mm Fixed	-
AOS-8	AOS S-VIT 1531	500	100 mm Fixed	-
AOS-11	AOS J-PRI	500	Sigma 17-50	50
AOS-12	AOS J-PRI	500	Nikon 50 mm Fixed	-
AOS-14	AOS J-PRI	500	Rokinon 12 mm Fixed	-
GP-8	GoPro Hero 4	120		
GP-9	GoPro Hero 4	120		
GP-18	GoPro Hero 6	240		
GP-20	GoPro Hero 6	240		
GP-21	GoPro Hero 6	240		
GP-22	GoPro Hero 7	240		
GP-23	GoPro Hero 7	240		
GP-24	GoPro Hero 7	240		
PAN-7	Panasonic HC-VX981	120		
PAN-8	Panasonic HC- VX981	120		
PAN-9	Panasonic HC- VX981	120		
PAN-10	Panasonic HC- VX981	120		

Figure 44. Camera Locations, Speeds, and Lens Settings, Test No. WITD-4

6 DESIGN DETAILS

The test installation consisted of sixteen 12-ft 6-in. long F-shape PCBs with a steel pin tie-down anchorage system for use with asphalt surfaces, as shown in Figures 45 through 59. The system was installed with the rear toe of the PCBs placed 18 in. away from the edge of both a 2-in. thick asphalt pad and a 36-in. wide x 36-in. deep trench. Photographs of the test installation are shown in Figures 60 and 61. Material specifications, mill certifications, and certificates of conformity for the system materials are shown in Appendix D.

The concrete mix for the barrier sections required a minimum compressive strength of 5,000 psi. A minimum concrete cover of 2 in. was specified for all reinforcement. Each PCB was reinforced with ASTM A615 Grade 60 rebar. Barrier segments were connected with a pin-and-loop system, as shown in Figure 49. Each connection pin had a length of 28 in., diameter of 1¼ in., and was used to interlock the ¾-in. diameter ASTM A709 Grade 70 connection loops.

The barrier installation was placed on top of a 2-in. thick asphalt pad composed of NE SPR Mix with 64-34 Grade binder. Barrier nos. 5 through 13 were each anchored to the ground surface through the anchor pockets on the traffic side with three 1½-in. diameter by 38½-in. long, ASTM A36 steel anchor pins driven through the 2-in. thick asphalt pad and into the underlying soil, as shown in Figures 45, 46, 48, and 49. During installation, the barrier segments were pulled in a direction parallel to their longitudinal axes, and slack was removed from all joints. After slack was removed from all joints, steel anchor pins were embedded to a depth of 32 in., as shown in Figures 46 and 49.

A saddle cap assembly was attached at the joints between barrier nos. 5 through 13. The assembly consisted of a 16-in. tall x 12-in. wide x ¼-in. thick saddle cap, a 31¼-in. long, 1¼-in. diameter connection pin, and a 3-in. tall x 3-in. wide x ¼-in. thick stiffening tube, as shown in Figures 55 and 56.

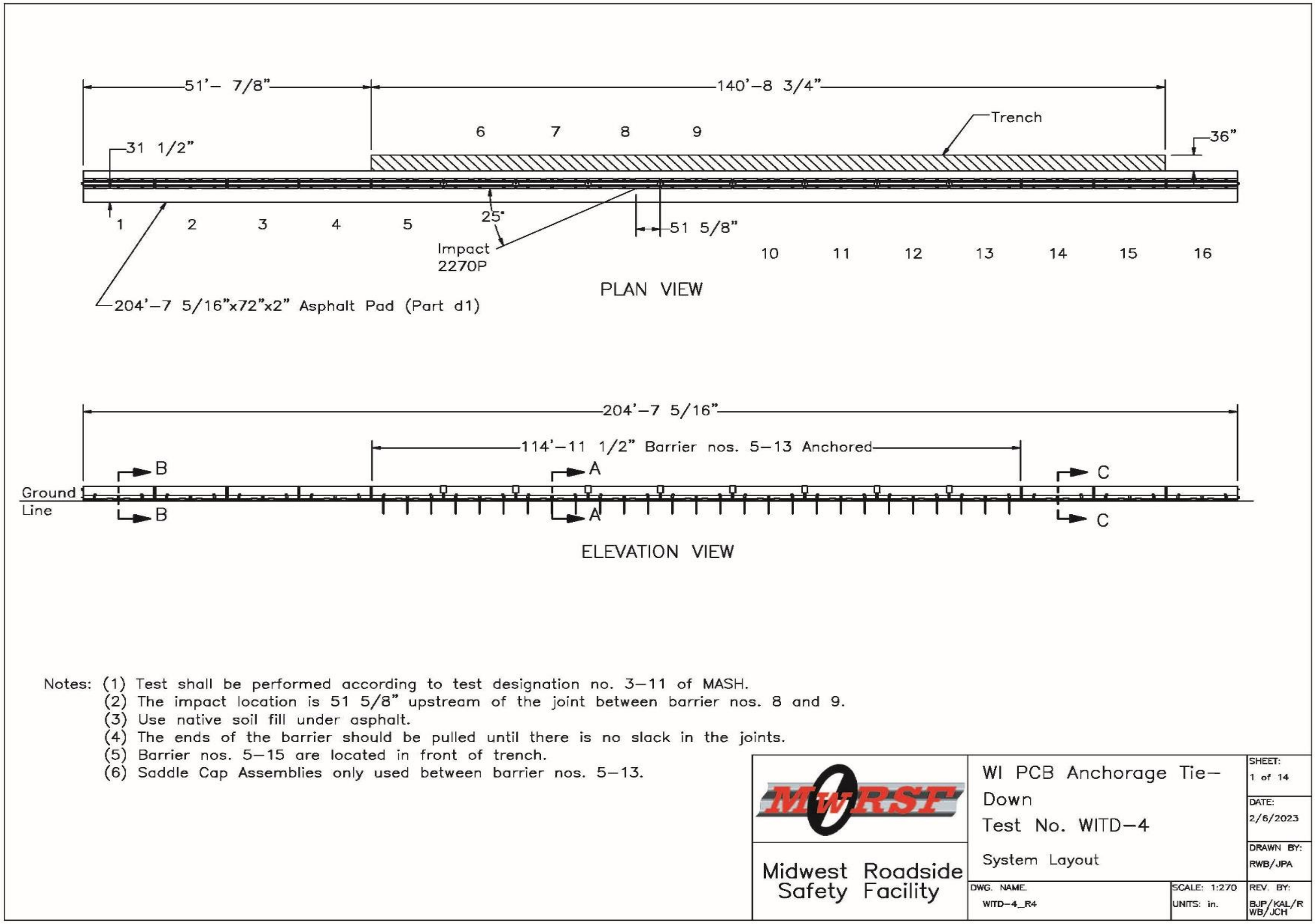

Notes:
(1) Test shall be performed according to test designation no. 3–11 of MASH.
(2) The impact location is 51 5/8" upstream of the joint between barrier nos. 8 and 9.
(3) Use native soil fill under asphalt.
(4) The ends of the barrier should be pulled until there is no slack in the joints.
(5) Barrier nos. 5–15 are located in front of trench.
(6) Saddle Cap Assemblies only used between barrier nos. 5–13.

Figure 45. System Layout, Test No. WITD-4

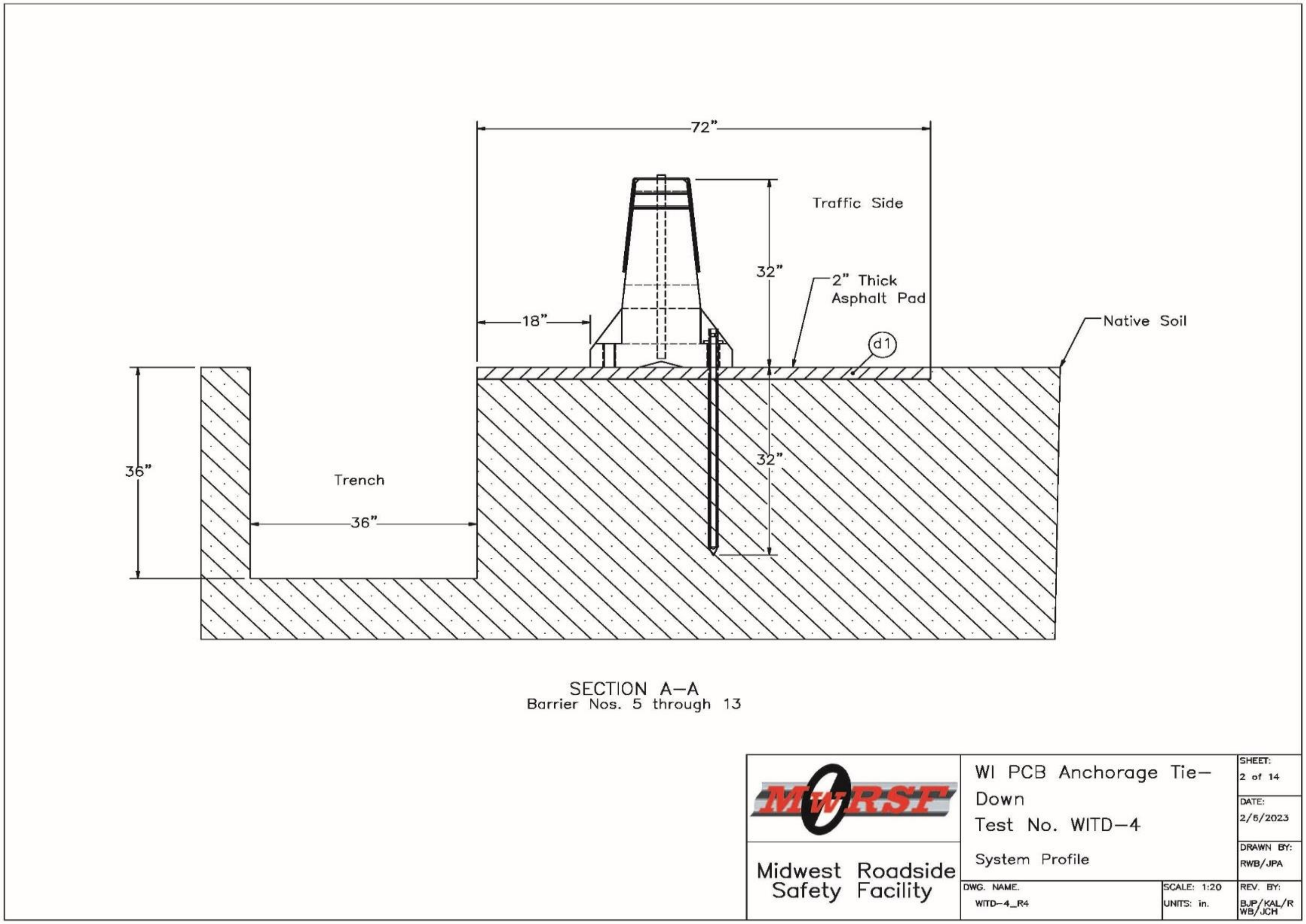

Figure 46. System Profile, Test No. WITD-4

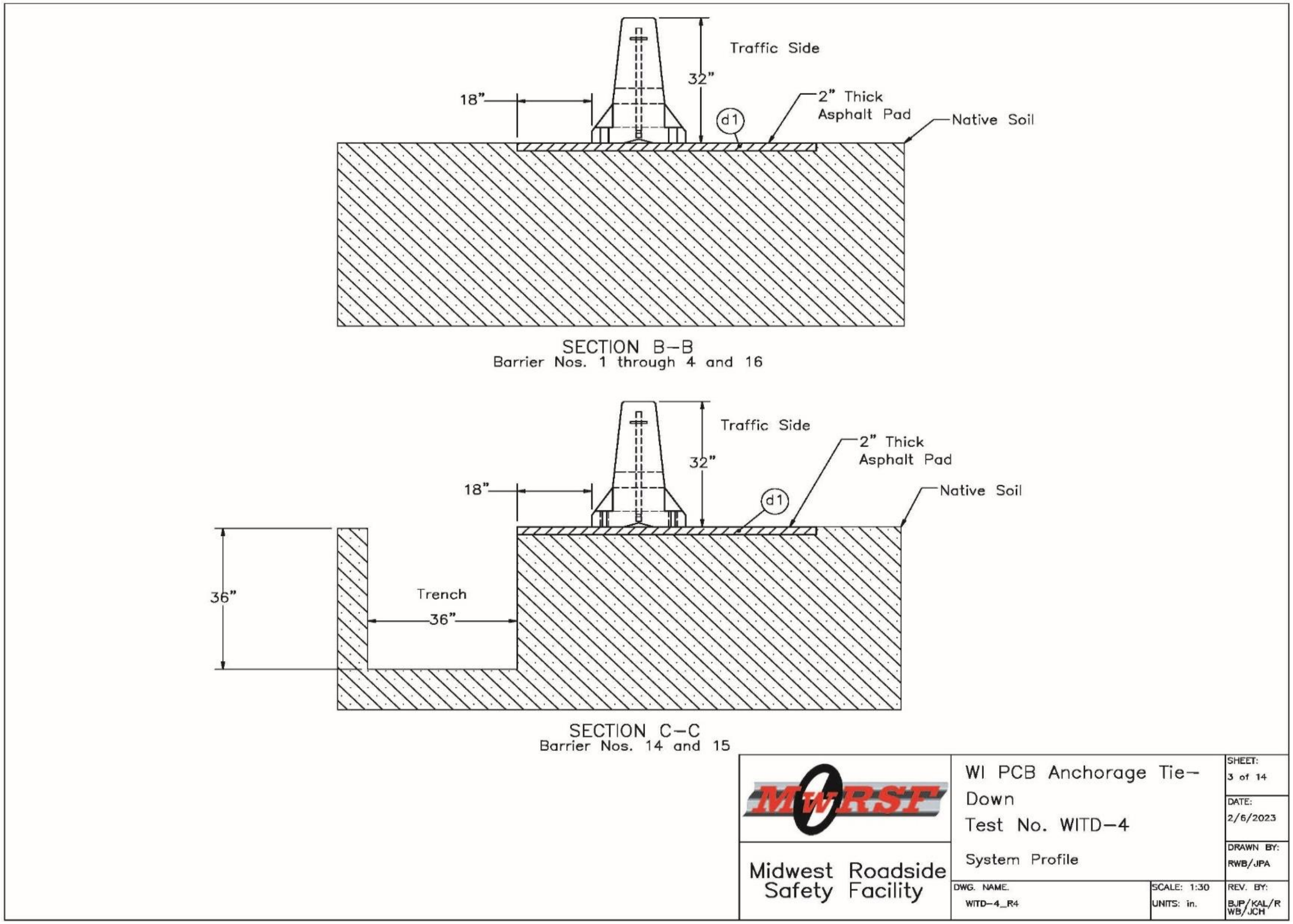

Figure 47. System Profile, Test No. WITD-4

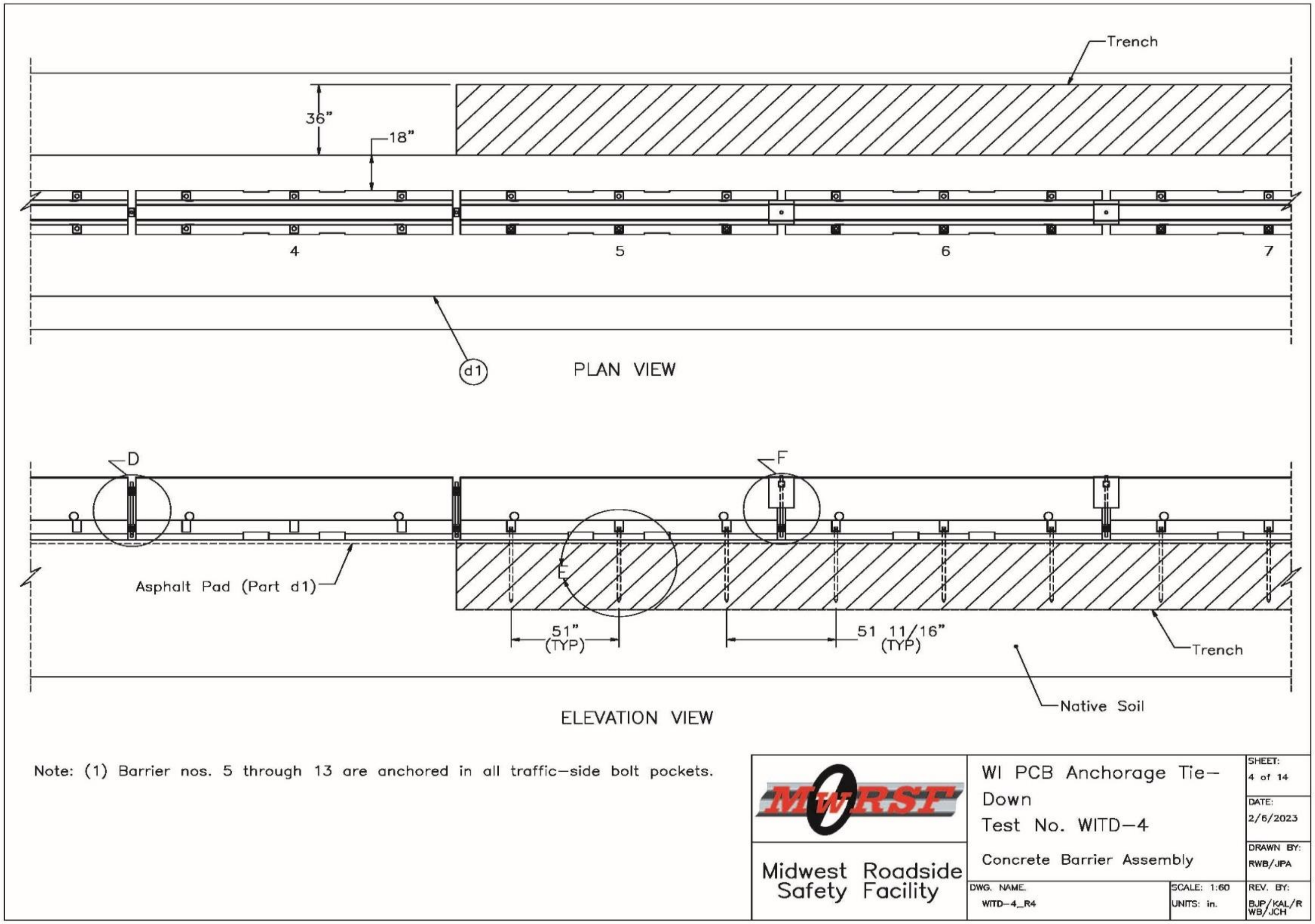

Figure 48. Concrete Barrier Assembly, Test No. WITD-4

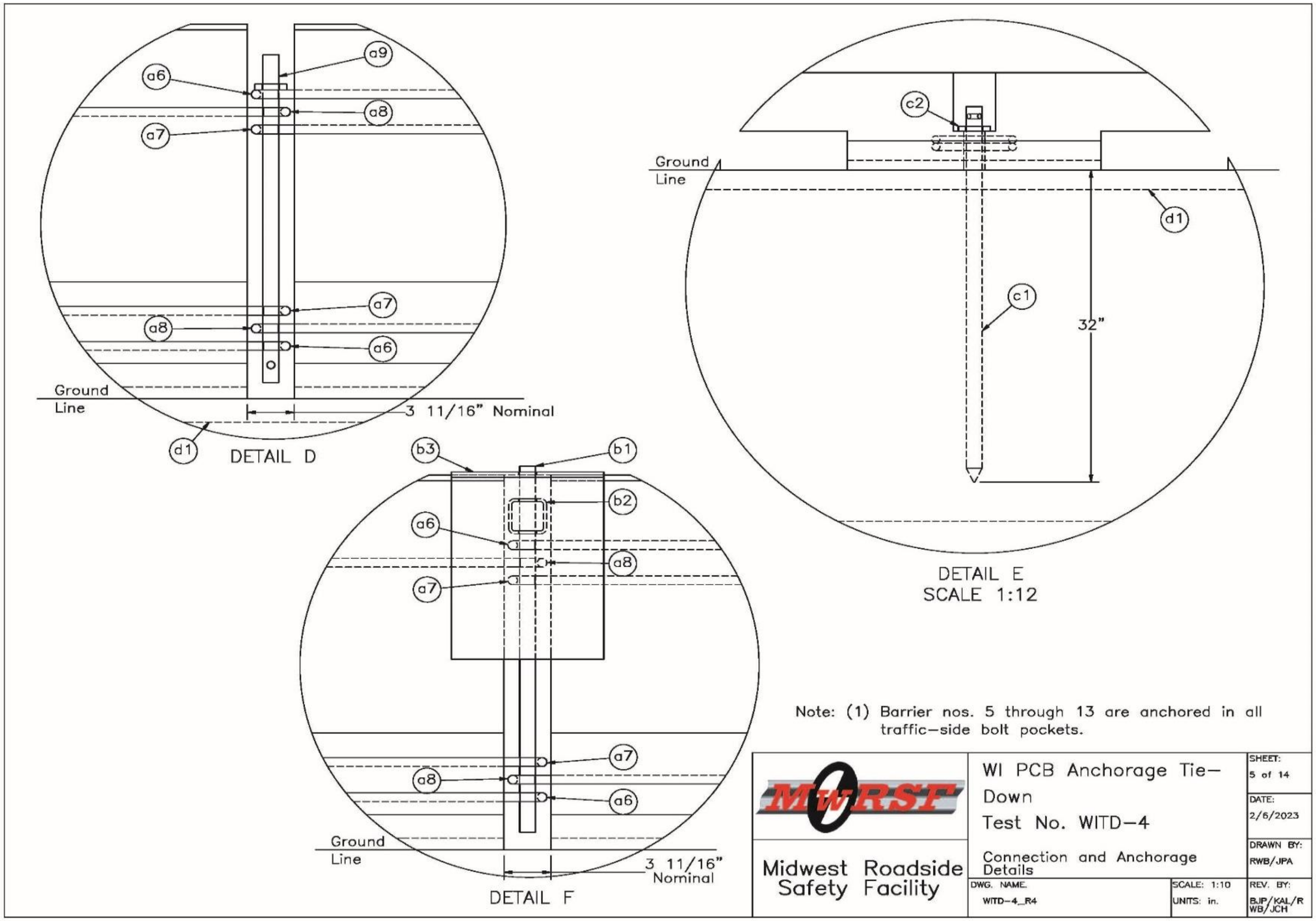

Figure 49. Connection and Anchorage Details, Test No. WITD-4

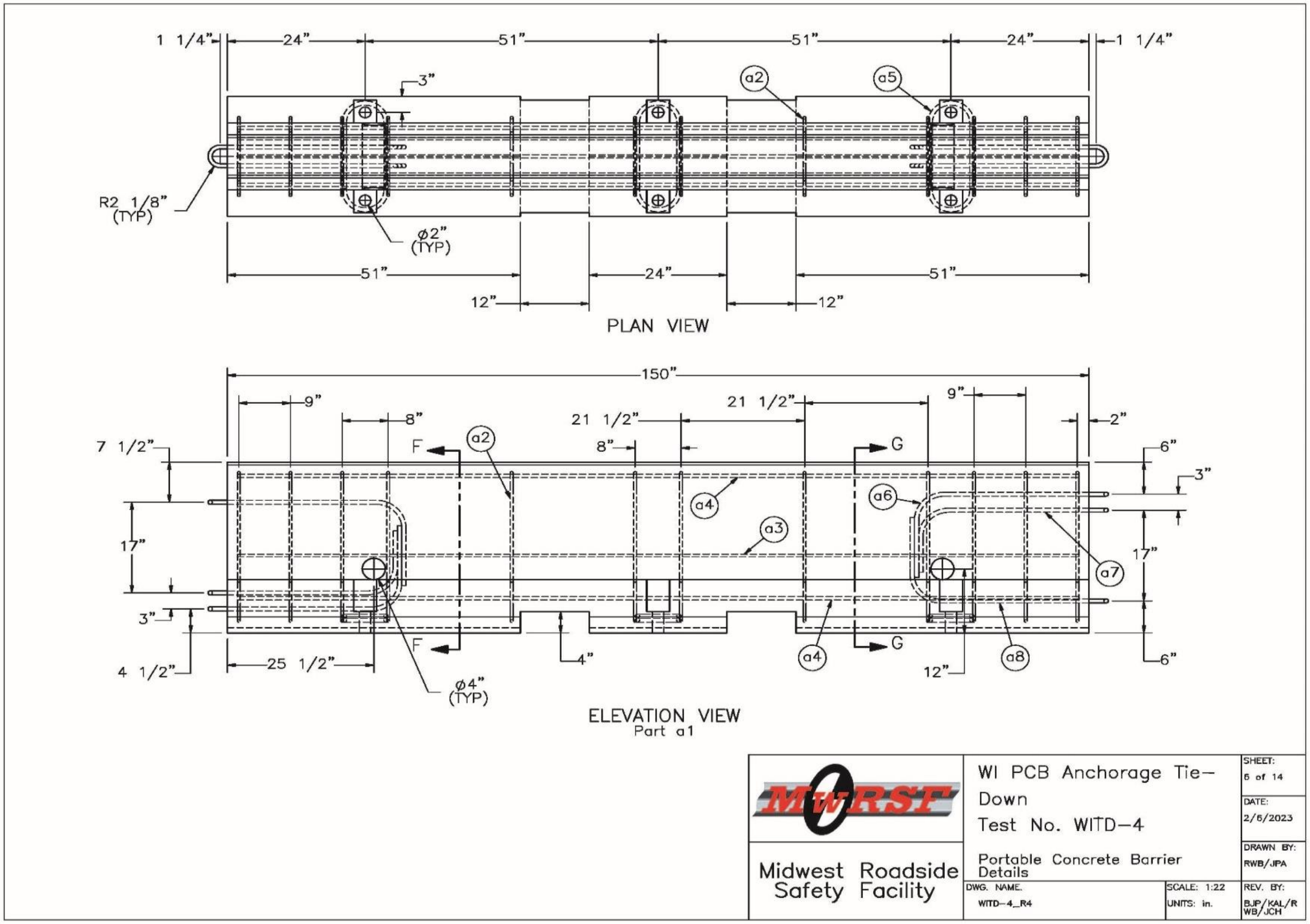

Figure 50. PCB Details, Test No. WITD-4

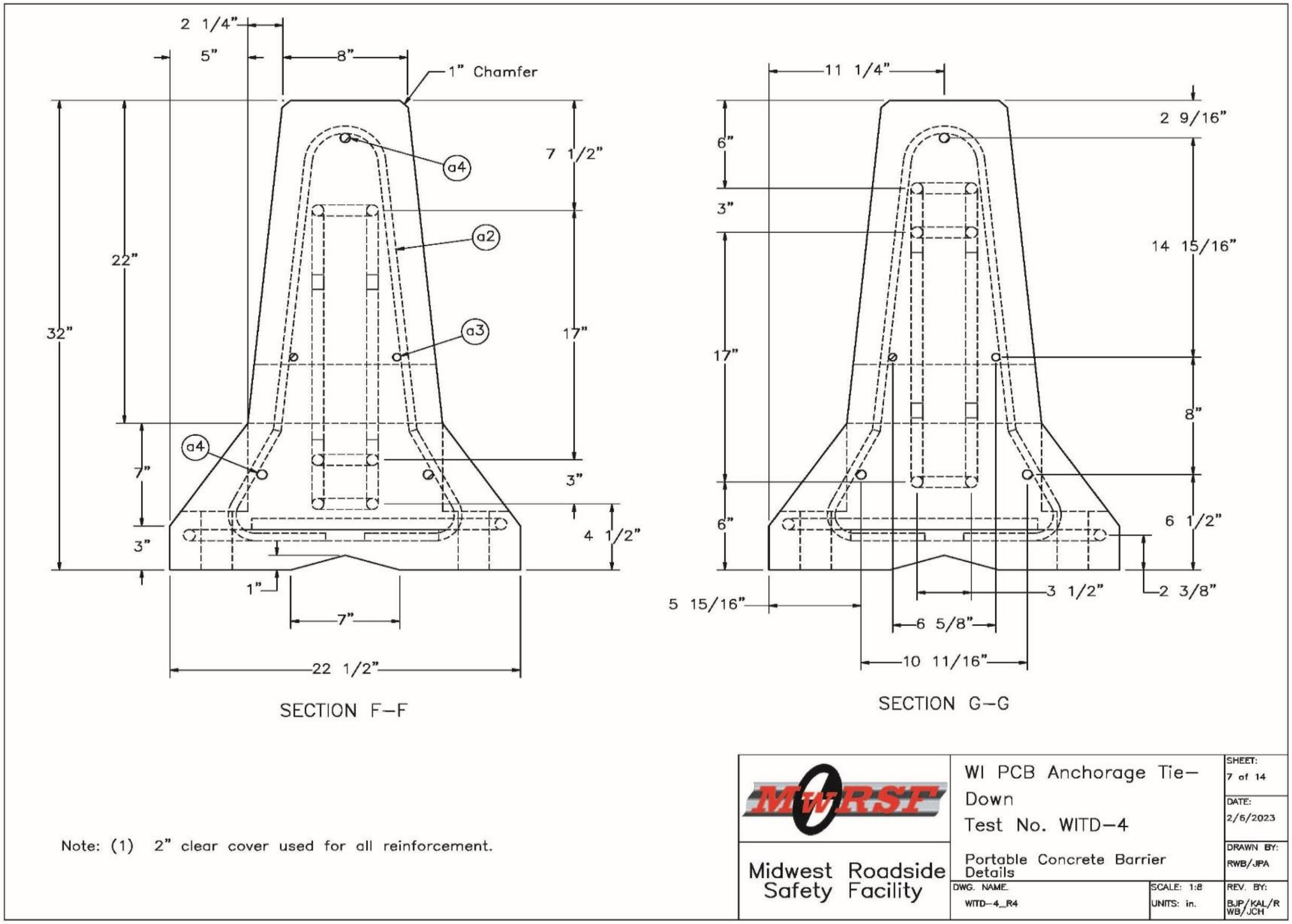

Figure 51. PCB Details, Test No. WITD-4

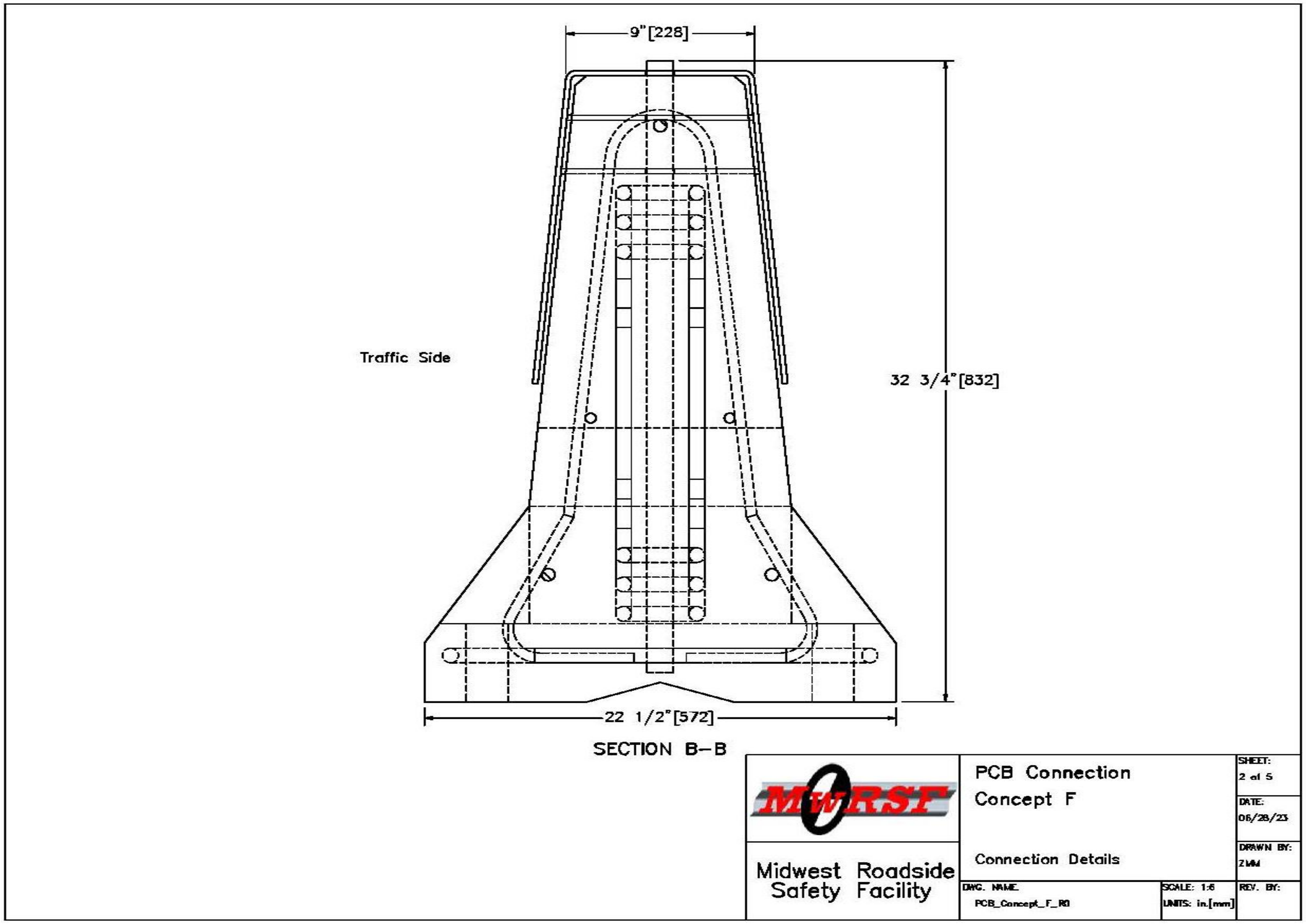

Figure 52. PCB with Saddle Cap, Test No. WITD-4

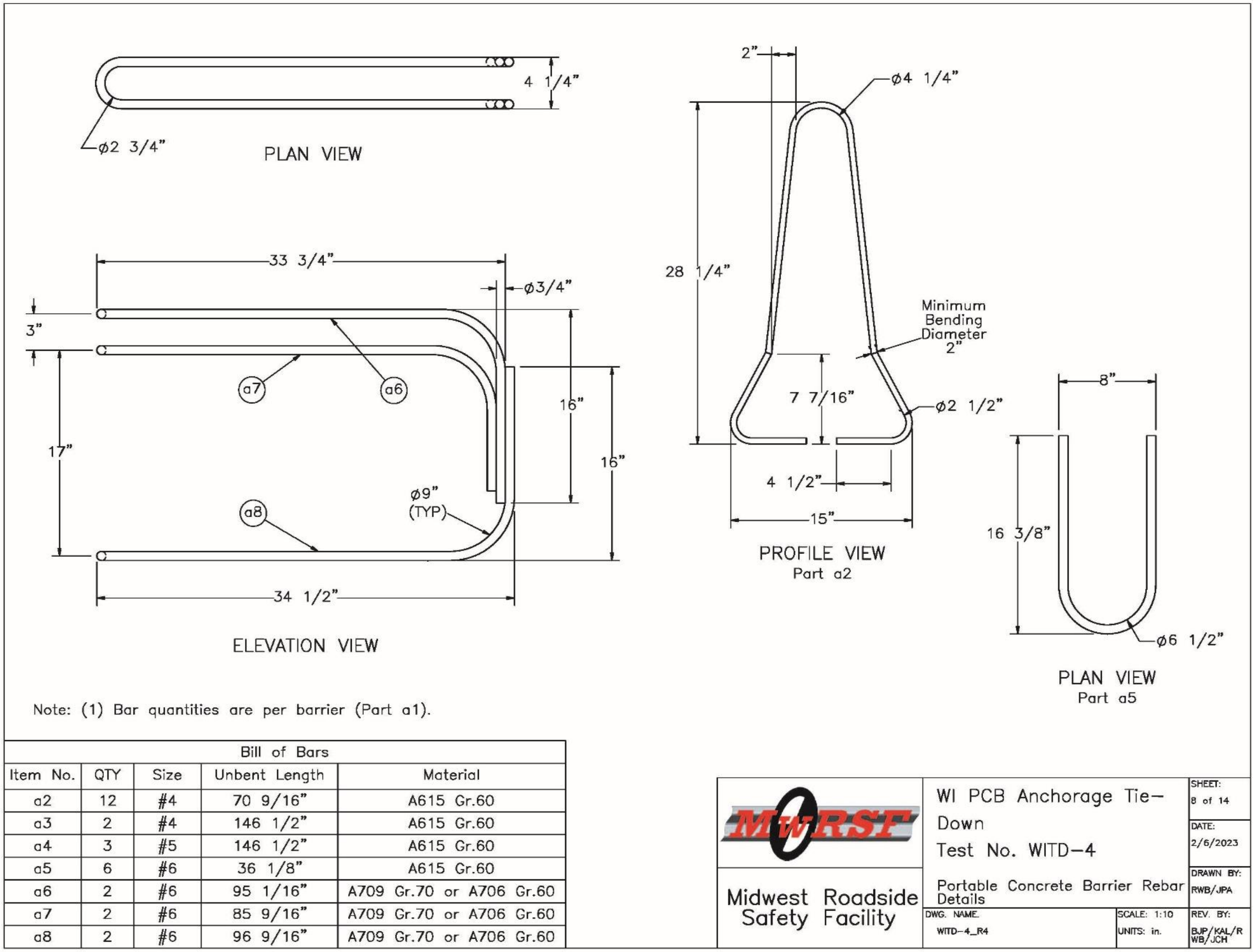

Note: (1) Bar quantities are per barrier (Part a1).

Bill of Bars

Item No.	QTY	Size	Unbent Length	Material
a2	12	#4	70 9/16"	A615 Gr.60
a3	2	#4	146 1/2"	A615 Gr.60
a4	3	#5	146 1/2"	A615 Gr.60
a5	6	#6	36 1/8"	A615 Gr.60
a6	2	#6	95 1/16"	A709 Gr.70 or A706 Gr.60
a7	2	#6	85 9/16"	A709 Gr.70 or A706 Gr.60
a8	2	#6	96 9/16"	A709 Gr.70 or A706 Gr.60

WI PCB Anchorage Tie-Down
Test No. WITD-4

Portable Concrete Barrier Rebar Details

SHEET: 8 of 14
DATE: 2/6/2023
DRAWN BY: RWB/JPA
DWG. NAME. WITD-4_R4
SCALE: 1:10
UNITS: in.
REV. BY: BJP/KAL/RWB/JCH

Figure 53. PCB Rebar Details, Test No. WITD-4

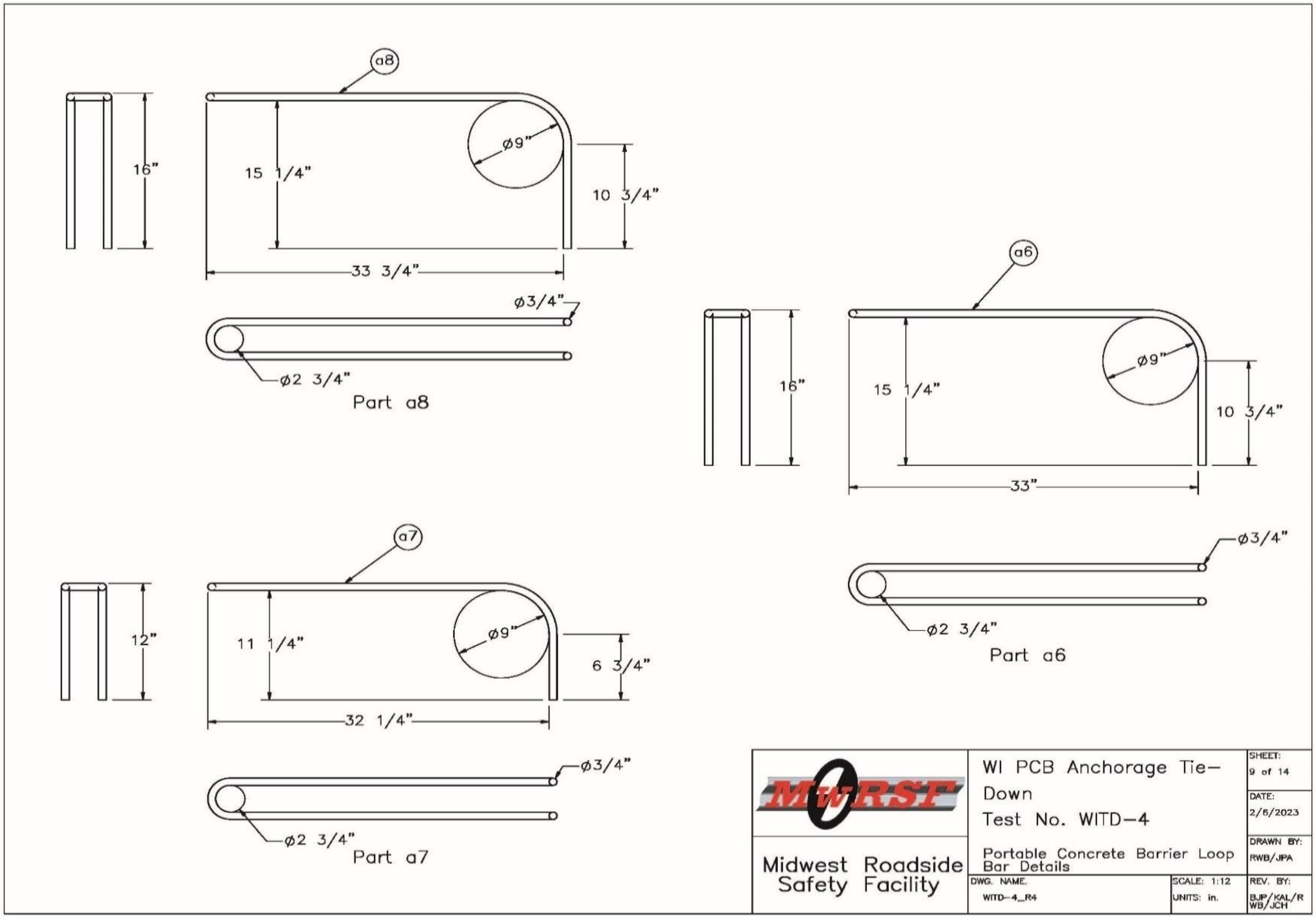

Figure 54. PCB Loop Bar Details, Test No. WITD-4

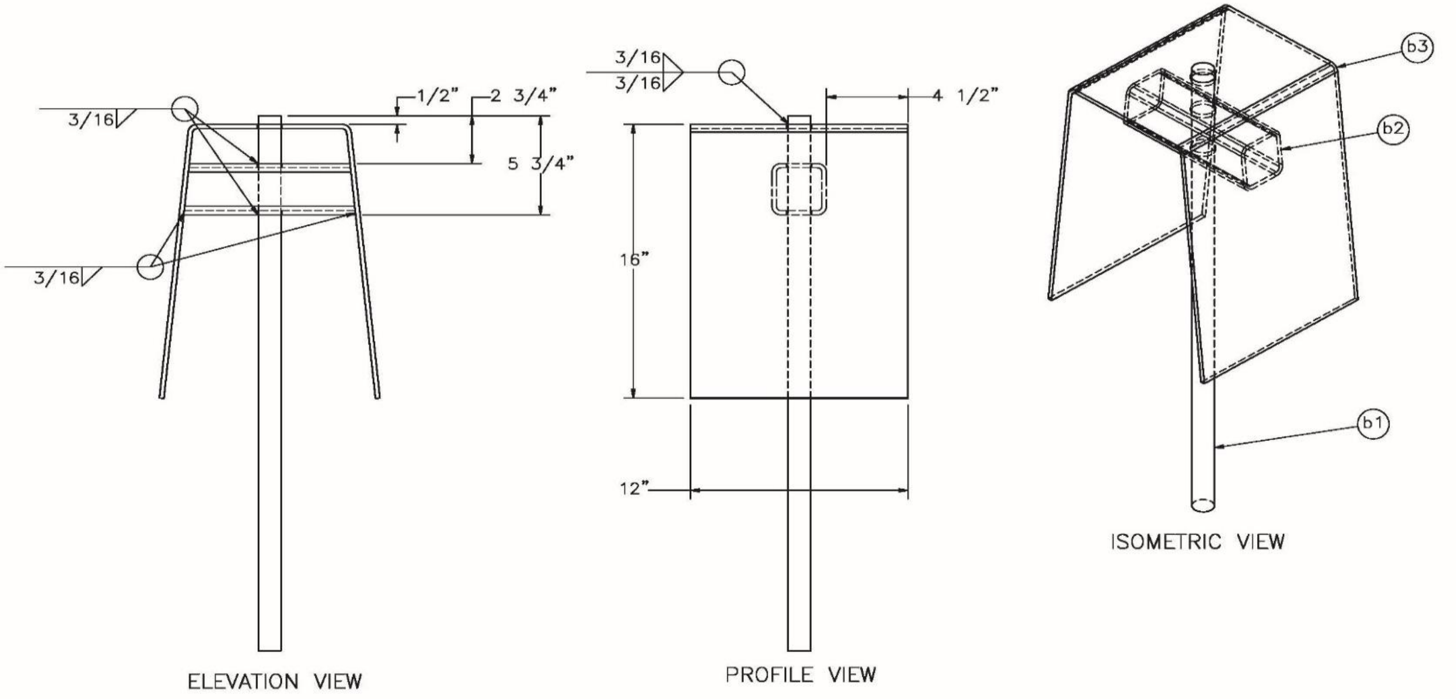

Notes: (1) Complete as many of the welds shown as possible.
(2) Saddle Cap Assemblies only used between barrier nos. 5–13.
(3) Saddle Cap Assembly does not need to be galvanized for testing purposes.

Item No.	QTY.	Description	Material Specification	Treatment Specification
–	8	Saddle Cap Assembly	–	ASTM A123
b1	1	1 1/4" Dia., 31 1/4" Long Connector Pin	ASTM A36	–
b2	1	HSS 3"x3"x1/4", 9 1/2" Long Stiffening Tube	ASTM A1085	–
b3	1	40 5/16"x12"x1/4" Saddle Cap	A572 Gr. 50	–

Midwest Roadside Safety Facility

WI PCB Anchorage Tie-Down
Test No. WITD-4
Saddle Cap Assembly Details

SHEET: 10 of 14
DATE: 2/6/2023
DRAWN BY: RWB/JPA
DWG. NAME. WITD-4_R4
SCALE: 1:8
UNITS: in.
REV. BY: BJP/KAL/RWB/JCH

Figure 55. Saddle Cap Assembly Details, Test No. WITD-4

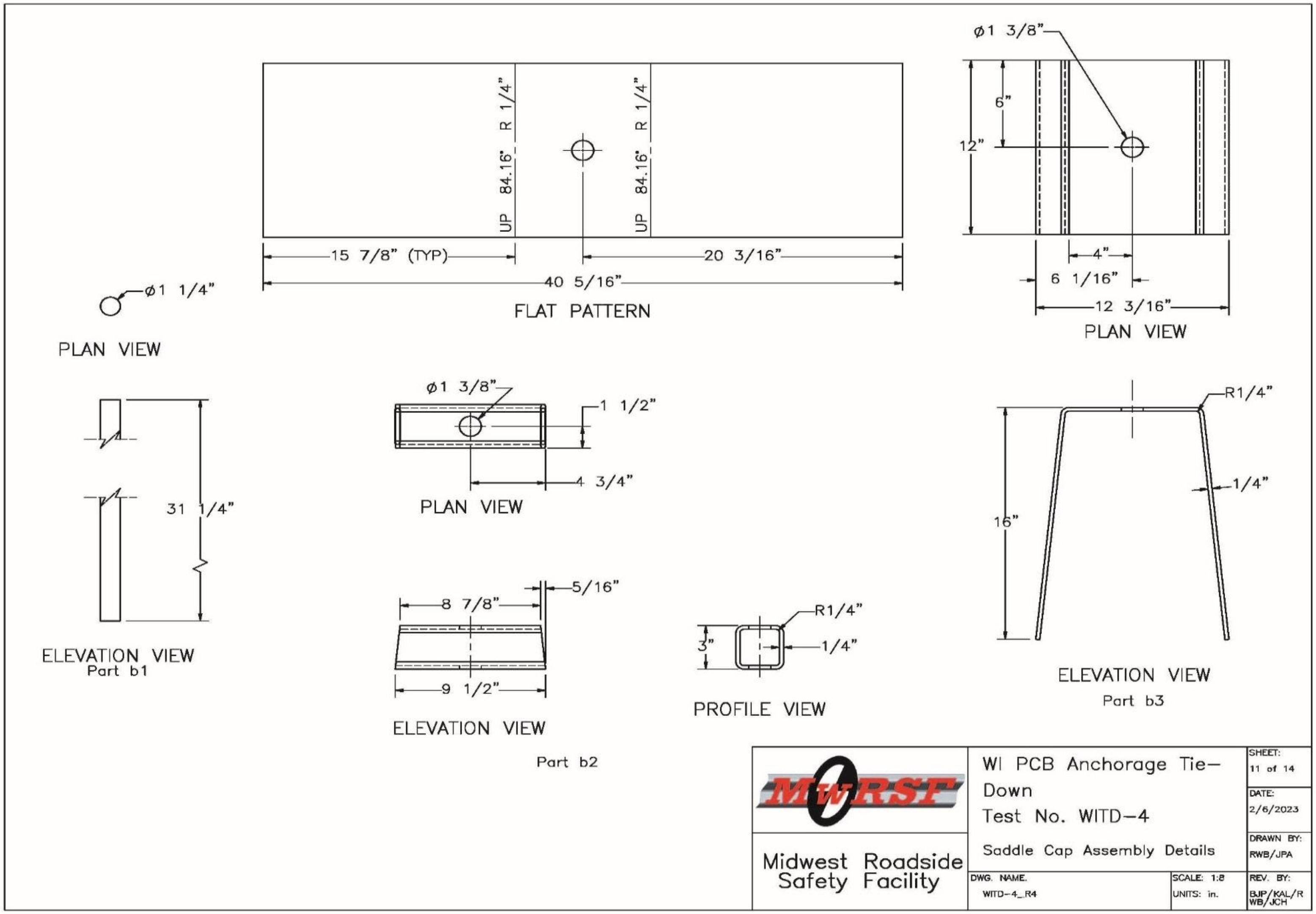

Figure 56. Saddle Cap Assembly Details, Test No. WITD-4

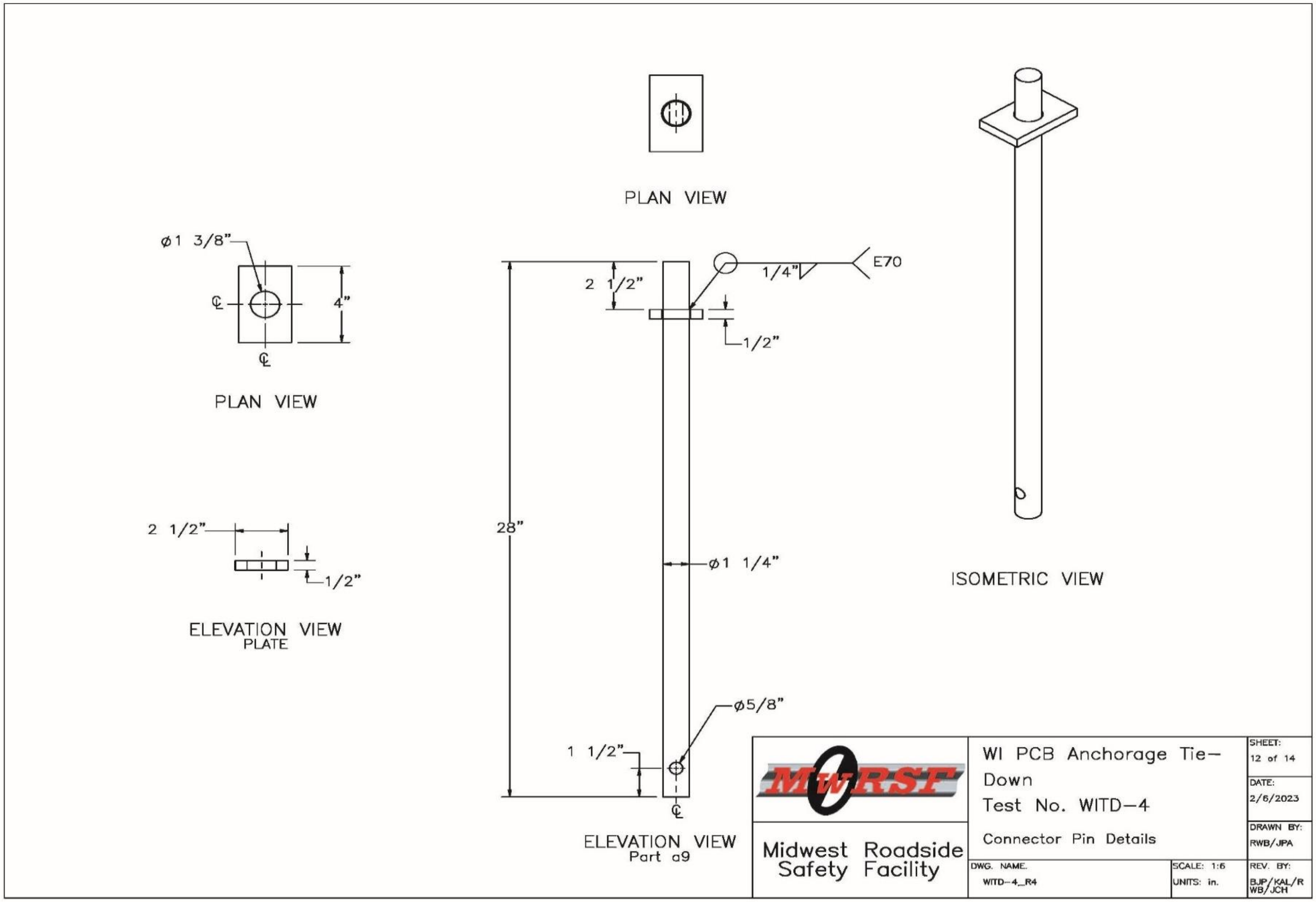

Figure 57. Connector Pin Details, Test No. WITD-4

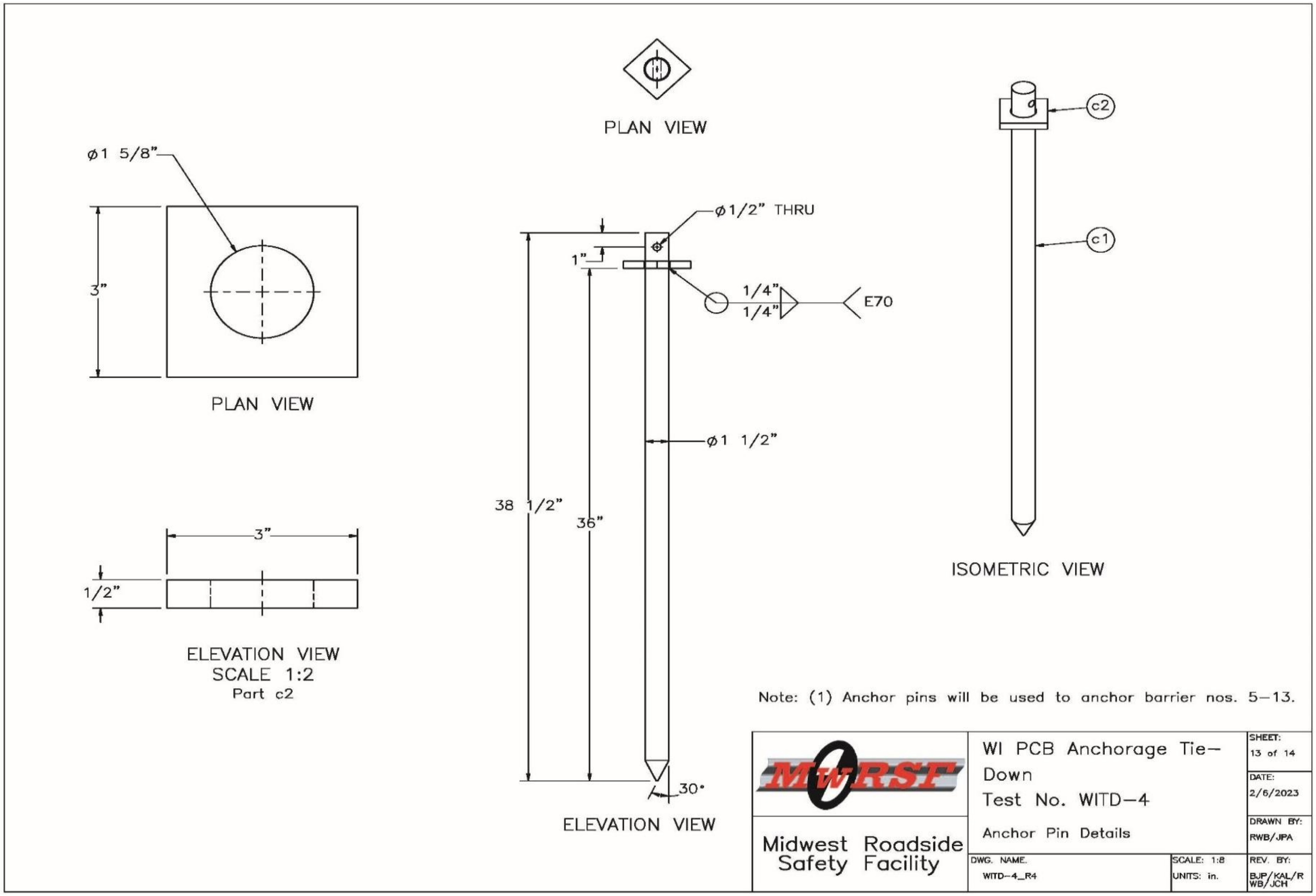

Figure 58. Anchor Pin Details, Test No. WITD-4

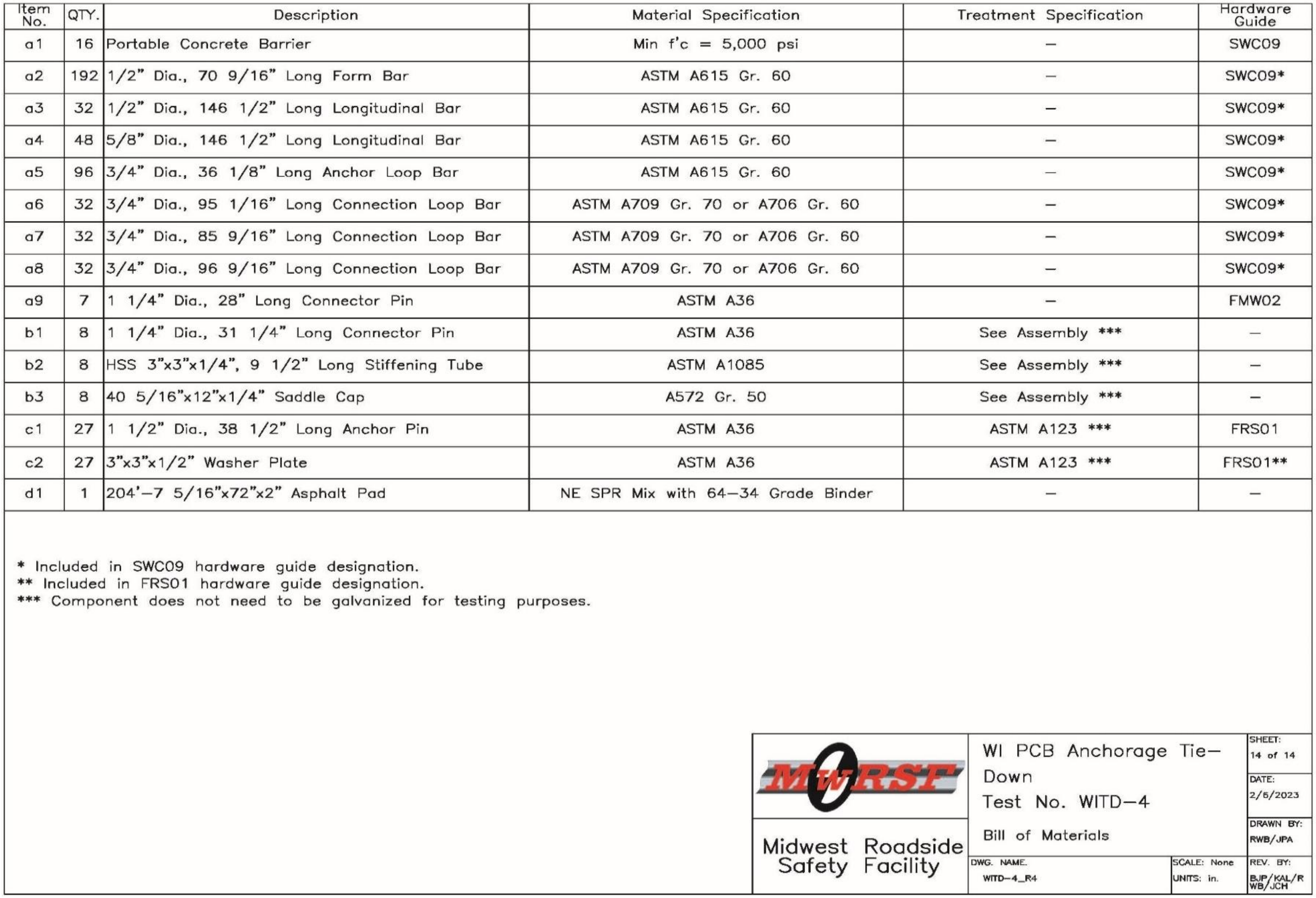

Item No.	QTY.	Description	Material Specification	Treatment Specification	Hardware Guide
a1	16	Portable Concrete Barrier	Min f'c = 5,000 psi	–	SWC09
a2	192	1/2" Dia., 70 9/16" Long Form Bar	ASTM A615 Gr. 60	–	SWC09*
a3	32	1/2" Dia., 146 1/2" Long Longitudinal Bar	ASTM A615 Gr. 60	–	SWC09*
a4	48	5/8" Dia., 146 1/2" Long Longitudinal Bar	ASTM A615 Gr. 60	–	SWC09*
a5	96	3/4" Dia., 36 1/8" Long Anchor Loop Bar	ASTM A615 Gr. 60	–	SWC09*
a6	32	3/4" Dia., 95 1/16" Long Connection Loop Bar	ASTM A709 Gr. 70 or A706 Gr. 60	–	SWC09*
a7	32	3/4" Dia., 85 9/16" Long Connection Loop Bar	ASTM A709 Gr. 70 or A706 Gr. 60	–	SWC09*
a8	32	3/4" Dia., 96 9/16" Long Connection Loop Bar	ASTM A709 Gr. 70 or A706 Gr. 60	–	SWC09*
a9	7	1 1/4" Dia., 28" Long Connector Pin	ASTM A36	–	FMW02
b1	8	1 1/4" Dia., 31 1/4" Long Connector Pin	ASTM A36	See Assembly ***	–
b2	8	HSS 3"x3"x1/4", 9 1/2" Long Stiffening Tube	ASTM A1085	See Assembly ***	–
b3	8	40 5/16"x12"x1/4" Saddle Cap	A572 Gr. 50	See Assembly ***	–
c1	27	1 1/2" Dia., 38 1/2" Long Anchor Pin	ASTM A36	ASTM A123 ***	FRS01
c2	27	3"x3"x1/2" Washer Plate	ASTM A36	ASTM A123 ***	FRS01**
d1	1	204'–7 5/16"x72"x2" Asphalt Pad	NE SPR Mix with 64–34 Grade Binder	–	–

* Included in SWC09 hardware guide designation.
** Included in FRS01 hardware guide designation.
*** Component does not need to be galvanized for testing purposes.

Midwest Roadside Safety Facility

WI PCB Anchorage Tie–Down
Test No. WITD–4
Bill of Materials

SHEET: 14 of 14
DATE: 2/6/2023
DRAWN BY: RWB/JPA
REV. BY: BJP/KAL/RWB/JCH
DWG. NAME. WITD–4_R4
SCALE: None
UNITS: in.

Figure 59. Bill of Materials. Test No. WITD-4

Figure 60. Test Installation Photographs, Test No. WITD-4

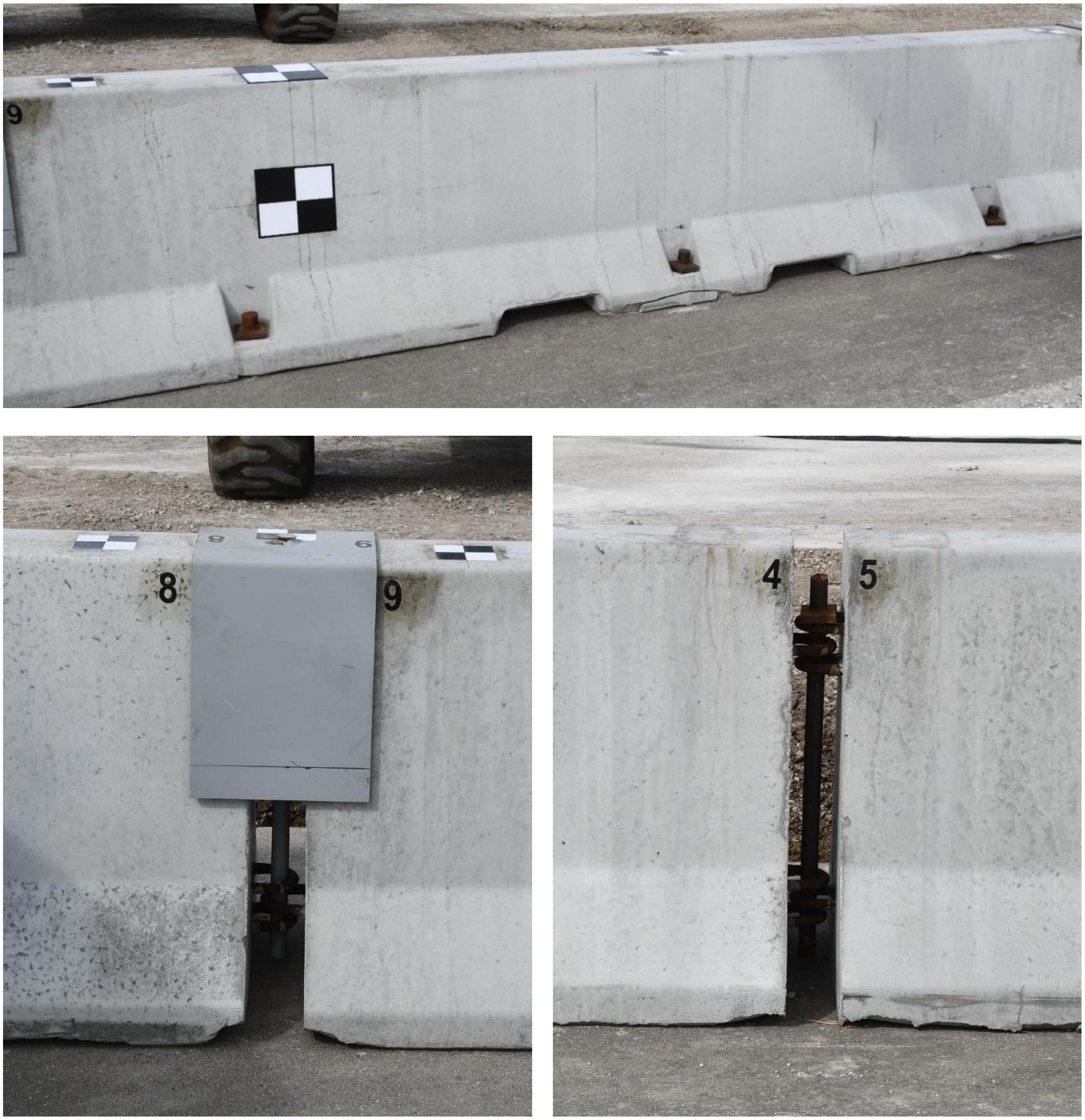

Figure 61. Test Installation Photographs: Anchor (top), Saddle Cap (bottom left) and Connection Pin (bottom right) Details, Test No. WITD-4

7 FULL-SCALE CRASH TEST NO. WITD-4

7.1 Weather Conditions

Test no. WITD-4 was conducted on March 15, 2023, at approximately 2:30 p.m. The weather conditions as reported by the National Oceanic and Atmospheric Administration (station 14939/KLNK) are shown in Table 5.

Table 5. Weather Conditions, Test No. WITD-4

Temperature	69°F
Humidity	39 %
Wind Speed	29 mph
Wind Direction	210° from True North
Sky Conditions	Broken Clouds
Visibility	9 Statute Miles
Pavement Surface	Dry
Previous 3-Day Precipitation	0.0 in.
Previous 7-Day Precipitation	0.36 in.

7.2 Test Description

Initial vehicle impact was to occur 51⅝ in. upstream from the centerline of the joint between barrier nos. 8 and 9, as shown in Figure 62, which was selected using Table 2.7 of MASH. The 5,019-lb crew cab pickup truck impacted the anchored PCB system at a speed of 61.9 mph and at an angle of 25.0 degrees. The actual point of impact was 1.7 in. downstream from the target impact location, as shown in Figure 62. During the test, the vehicle was captured and redirected by the anchored F-shape PCB system. As the vehicle was redirected, the lower leading edge of the left-front door snagged on the saddle cap and was displaced rearward and outward. There was little deformation to the saddle cap. After brakes were applied, the vehicle came to rest 200.7 ft downstream from the impact point and 27.2 ft laterally in front of the traffic side of the barrier.

A detailed description of the sequential impact events is contained in Table 6. Sequential photographs are shown in Figures 63 and 64. Documentary photographs of the crash test are shown in Figures 65 and 66. The vehicle trajectory and final position are shown in Figure 67.

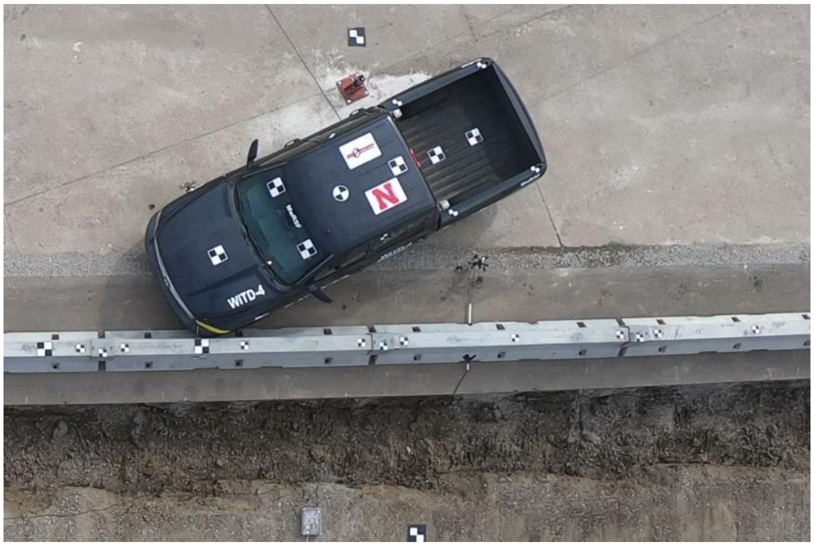

Figure 62. Impact Location, Test No. WITD-4

Table 6. Sequential Description of Impact Events, Test No. WITD-4

Time sec	Event
0.000	Vehicle's front bumper and left-front tire contacted barrier no. 8 and deformed.
0.006	Vehicle's left headlight contacted barrier no. 8 and disengaged. Vehicle's left fender contacted barrier no. 8 and deformed.
0.020	Vehicle's grille contacted barrier and disengaged. Vehicle's left-front tire deflated. Vehicle pitched upward.
0.028	Vehicle yawed away from barrier.
0.044	Vehicle's left-front door contacted barrier no. 8 and deformed. Vehicle rolled toward barrier.
0.074	Vehicle's right headlight disengaged.
0.098	Vehicle's right-front tire became airborne.
0.146	Vehicle's right-rear tire became airborne.
0.160	Vehicle's left-rear door contacted barrier no. 9 and deformed.
0.178	Vehicle's left quarter panel contacted barrier no. 8 and deformed.
0.182	Vehicle's left-rear tire contacted barrier no. 8 and deflated. Vehicle's left taillight contacted barrier no. 8 and shattered.
0.190	Vehicle was parallel to system at a speed of 49.9 mph. Vehicle's bumper cover detached.
0.212	Vehicle pitched downward.
0.270	Vehicle's left-front tire became airborne.
0.362	Vehicle's left-rear tire became airborne.
0.414	Vehicle exited system at a speed of 50.5 mph and an angle of 1.5 degrees.
0.546	Vehicle's left-front tire contacted ground.
0.682	Vehicle's front bumper contacted ground.
0.706	Vehicle rolled away from barrier.
0.734	Vehicle pitched upward.
0.914	Vehicle's left-rear tire contacted ground.
1.110	Vehicle yawed toward barrier.
1.302	Vehicle's right-front tire contacted ground.
1.366	Vehicle's right-rear tire contacted ground.
1.686	Vehicle's right-rear tire became airborne.
2.070	Vehicle's right-rear tire contacted ground.
4.250	Vehicle came to rest.

0.000 sec

0.000 sec

0.100 sec

0.100 sec

0.200 sec

0.200 sec

0.300 sec

0.300 sec

0.400 sec

0.400 sec

0.500 sec

0.500 sec

Figure 63. Sequential Photographs, Test No. WITD-4

0.000 sec

0.000 sec

0.100 sec

0.100 sec

0.200 sec

0.200 sec

0.300 sec

0.300 sec

0.400 sec

0.400 sec

0.500 sec

0.500 sec

Figure 64. Sequential Photographs, Test No. WITD-4

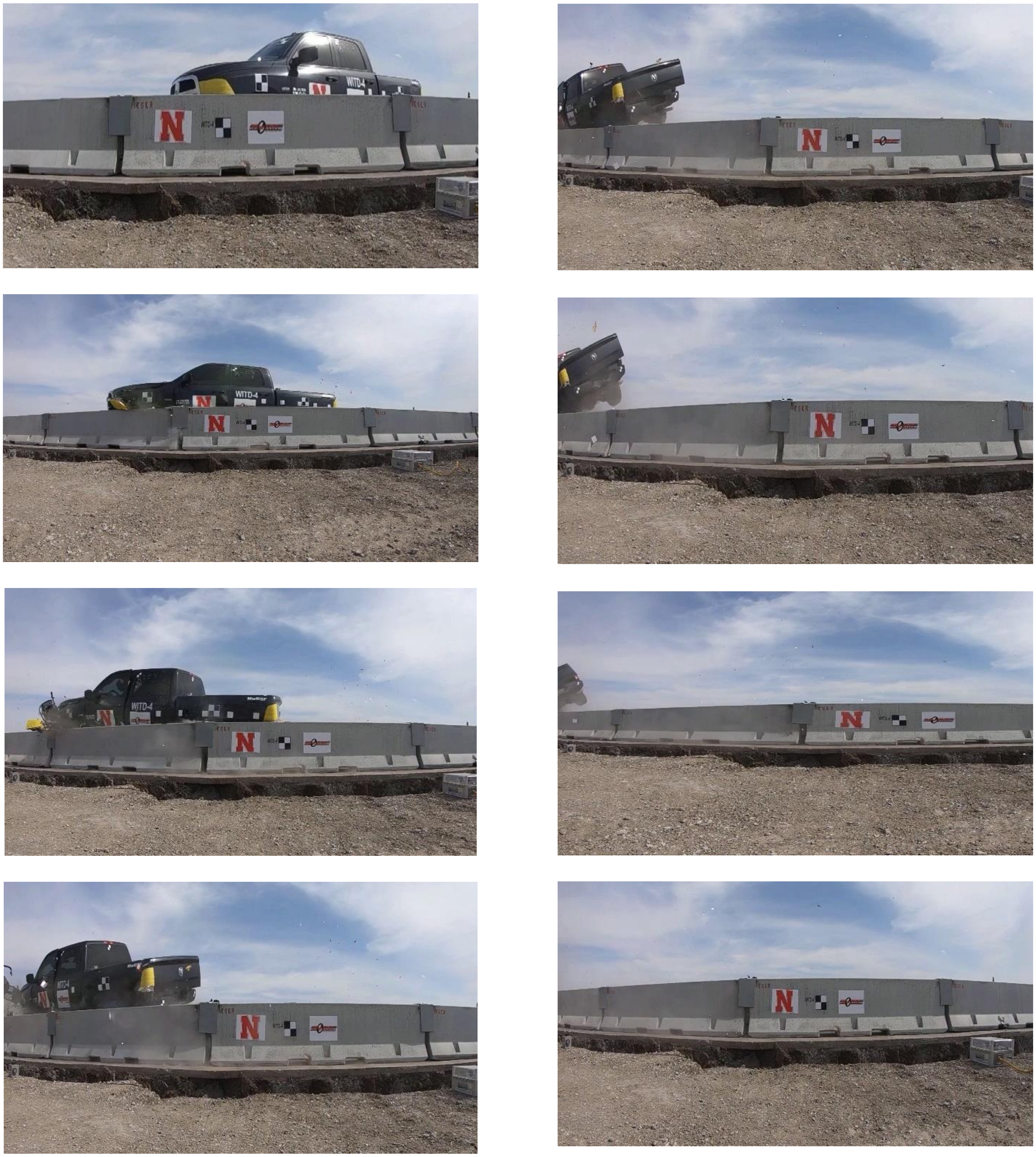

Figure 65. Documentary Photographs, Test No. WITD-4

Figure 66. Documentary Photographs, Test No. WITD-4

Figure 67. Vehicle Final Position and Trajectory Marks, Test No. WITD-4

7.3 Barrier Damage

Damage to the barrier was moderate, as shown in Figures 68 through 71. Barrier damage consisted of contact marks on the front face of the concrete segments and concrete spalling, cracking, and fracture. The length of vehicle contact along the barrier was approximately 20 ft – 1¾ in., which began 74¼ in. upstream from the joint of barrier nos. 8 and 9.

Tire marks were visible on the front face of barrier nos. 8 and 9. Concrete spalling and breakout occurred on the front side at each anchor pocket of barrier no. 8, at the upstream and middle anchor pockets of barrier no. 9, and at the middle anchor pocket of barrier no. 10. Dimensions of concrete that disengaged from barrier no. 8 at the upstream, middle, and downstream anchor pockets were 11-in. long x 1½-in. wide x ½-in. deep, 24-in. long x 4-in. wide x 3-in. deep, and 20¾-in. long x ½-in. wide x 3¼-in. deep, respectively. There was a vertical crack originating at the downstream drainage slot of barrier no. 8 that extended through the top of the barrier. There was cracking local to the upstream edge of the upstream drainage slot on the back side of barrier no. 8. Dimensions of concrete that disengaged from barrier no. 9 at the upstream and middle anchor pockets were 19¾-in. long x 10-in. wide x 2-in. deep, 24½-in. long x 3½-in. wide x 2½-in. deep, respectively. There was cracking at the barrier no. 9 downstream anchor pocket that measured 15¾-in. long x 6-in. wide. There was a vertical crack originating at the upstream drainage slot of barrier no. 9 that extended through the top of the barrier. Dimensions of concrete that disengaged from barrier no. 10 at the middle anchor pocket were 19½-in. long x 4-in. wide x 2½-in deep. Slight cracking was caused at barrier no. 8 upstream, barrier no. 9 middle, and barrier no. 10 middle anchor pockets during pre-test anchor bolt installation. All anchor pins in barrier nos. 8 through 10 were displaced vertically.

There were contact marks and scrapes on the saddle cap at the joint of barrier nos. 8 and 9 and contact marks on the saddle cap at the joint of barrier nos. 9 and 10. Slight outward bulging of the saddle cap at the joint between barrier nos. 8 and 9 was observed. There was a segment of the vehicle door panel sheet metal that snagged and wrapped around the saddle cap that wedged between the saddle cap and barrier. There was a crack in the asphalt pad beginning at the downstream anchor pin of barrier no. 8 and extended laterally through the pad up to the trench. The lateral end of the asphalt pad on the front side of the barrier was heaved upwards. Soil and asphalt disengagement adjacent to the trench did not occur.

Figure 68. Overall System Damage, Test No. WITD-4

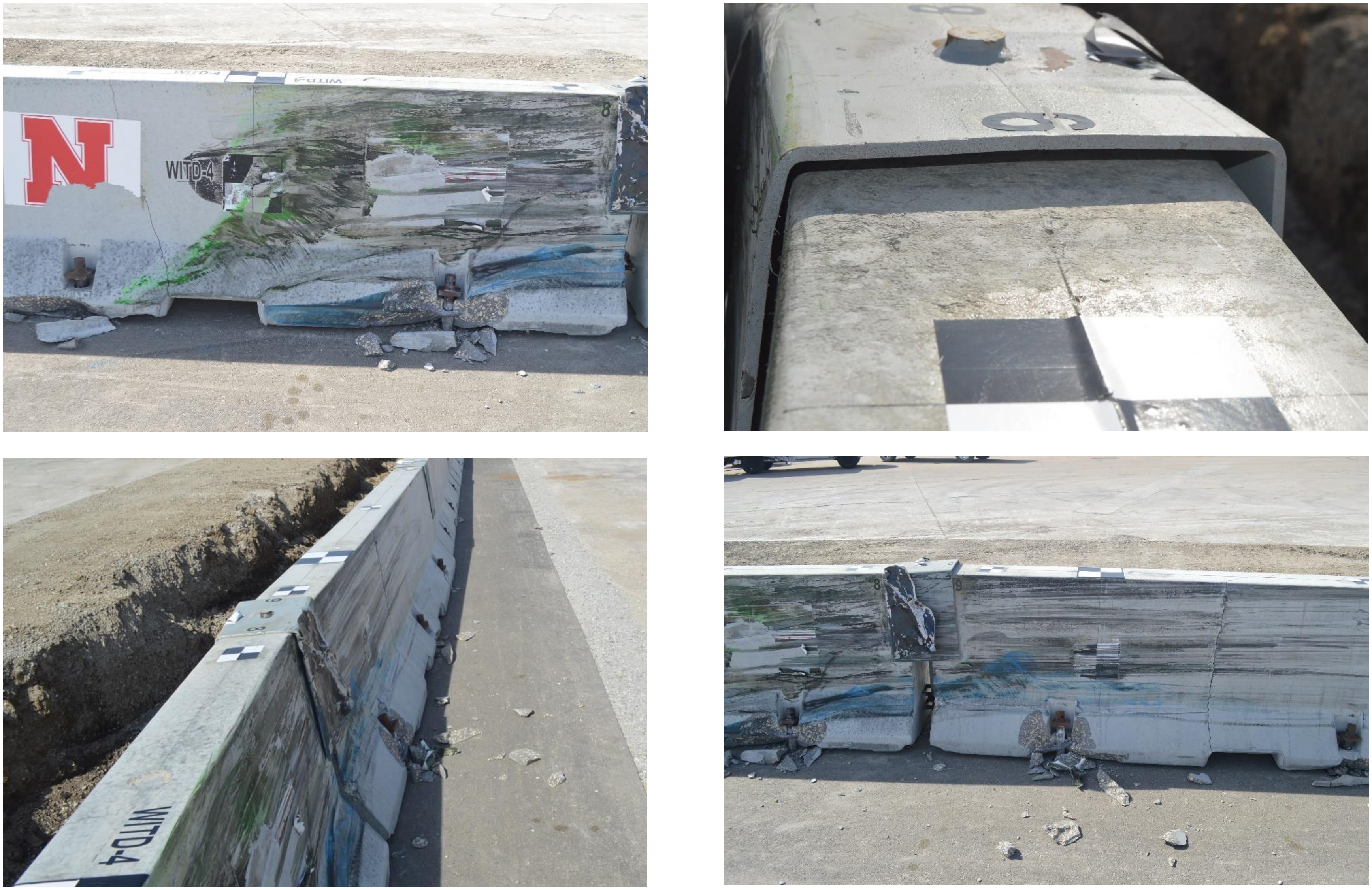

Figure 69. System Damage at Impact Location, Barrier Nos. 8 and 9, Test No. WITD-4

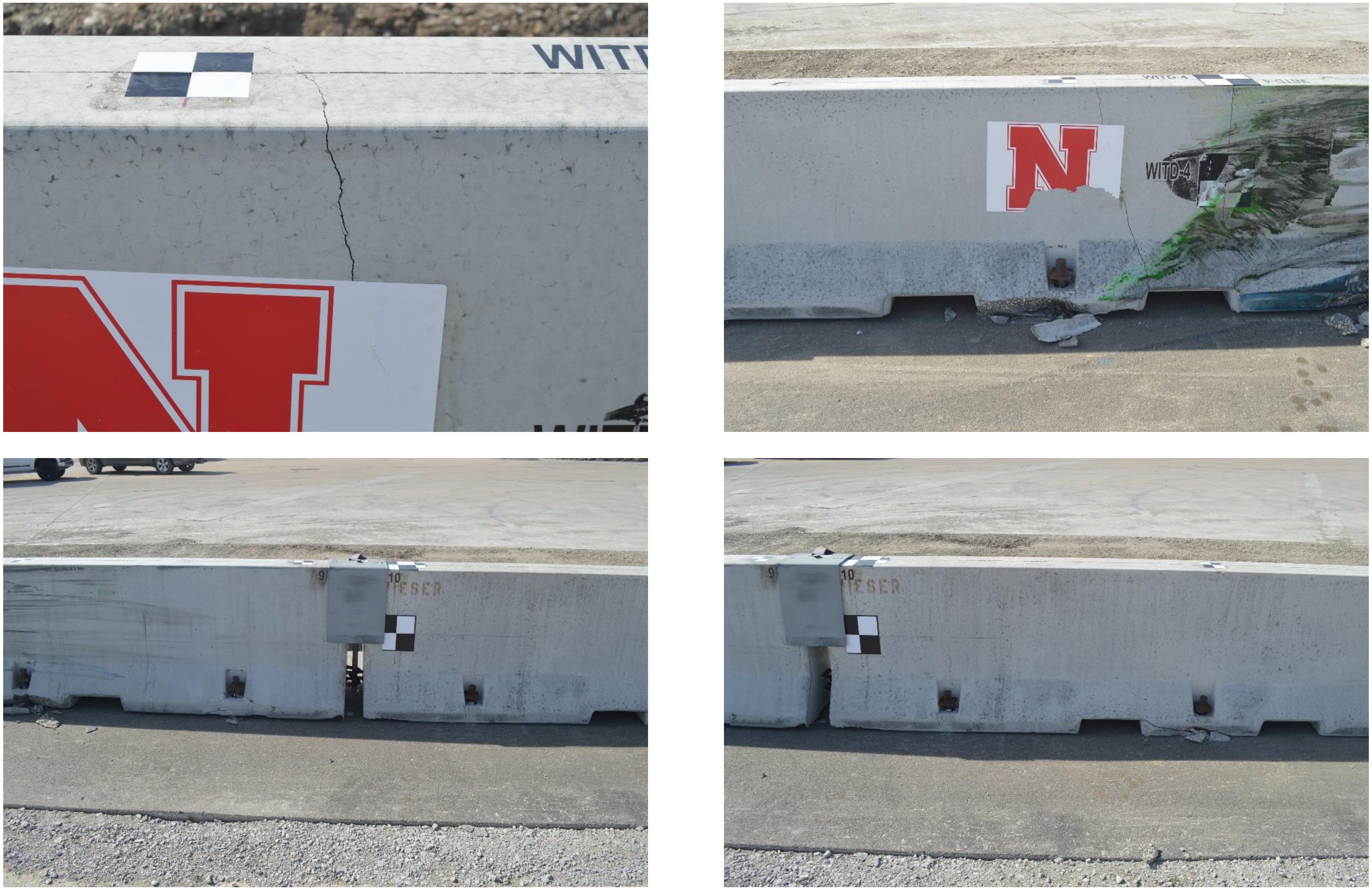

Figure 70. System Damage, Barrier Nos. 9 and 10, Test No. WITD-4

Figure 71. System Damage, Non-Traffic Side, Barrier Nos. 7 through 11, Test No. WITD-4

The maximum lateral permanent set of the barrier system was 4.4 in. at the downstream end of barrier no. 8, as measured in the field. The maximum lateral dynamic deflection was 9.9 in. at the upstream end of barrier no. 9, as determined from high-speed digital video analysis. The working width of the system was 32.4 in., also determined from high-speed digital video analysis. A schematic of the permanent set deflection, dynamic deflection, and working width is shown in Figure 72.

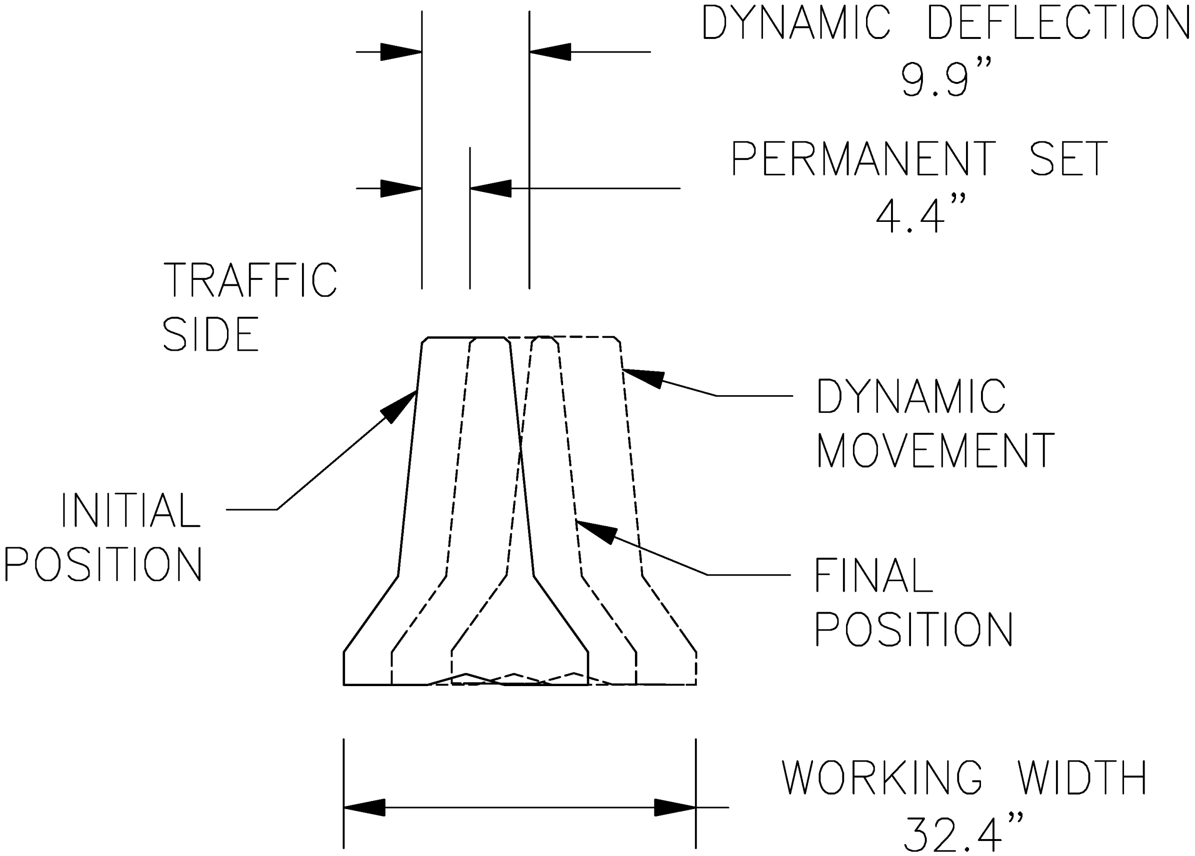

Figure 72. Permanent Set, Dynamic Deflection, and Working Width, Test No. WITD-4

7.4 Vehicle Damage

Damage to the vehicle was moderate, as shown in Figures 73 through 76. The maximum occupant compartment intrusions are listed in Table 7 along with the intrusion limits established in MASH for various areas of the occupant compartment. Complete occupant compartment and vehicle deformations, as well as the corresponding locations are provided in Appendix E. MASH defines intrusion or deformation as the occupant compartment being deformed and reduced in size with no observed penetration. Outward deformations, which are denoted as negative numbers in Appendix E, are not considered crush toward the occupant, and are not evaluated by MASH criteria.

The majority of damage was concentrated on the left side of the vehicle. The left-front corner of the vehicle was crushed inward and the left-front door was torn. The grille disengaged and the left-front bumper was crushed and scraped. The headlights were disengaged from the vehicle. Damage to the left fender included the leading edge being crushed rearward at the headlight opening and the area behind the left tire was scraped and crushed. The left-front and left-rear tires were punctured, and the left-front wheel was deformed and scraped. The lower leading edge of the left-front outer door panel was torn rearward approximately 17 in., opening a 7-in. tall x 1½-in. wide hole at the leading edge that was peeled outward 2 in. A dent spanned from the middle to the rear of the left-front door, causing the door to wrinkle by the handle. Scrapes followed the rearward tear, and the door was shifted rearward. The left-rear door was scraped along its entire width and scrapes and dents were found on the rear of the door frame. Dents were also found behind the left-rear wheel well and at the left side of the rear bumper. The tailgate was detached.

Underneath the vehicle, the left-front shocks were bent backward, the bump stop was disengaged, the bump stop housing was bent rearward, the bump stop of the left-rear shocks was disengaged, and the axle was bent. The sway bars were shifted laterally, the end links of the left-front sway bars were bent rearward at both connection points, and the bottom connection disengaged from the control arm. The steering knuckle assemblies were scraped on the left side and the control arm at the ball joint was disconnected from the steering knuckle. The left-lower control arm was broken at both mounts on the cross members and at the steering knuckle, along with a small nick on the right lower control arm. The panhard bar in the rear suspension was severely bent and the tie rod on the left side was bent rearward. The rear axle of the drivetrain was bent and the overall frame of the chassis had a bow in the middle of both frame rails. The middle cross member was slightly twisted, and the frame horn on the left side was bent into the middle of the vehicle.

Figure 73. Vehicle Damage, Test No. WITD-4

Figure 74. Vehicle Damage, Test No. WITD-4

Figure 75. Vehicle Occupant Compartment Damage, Test No. WITD-4

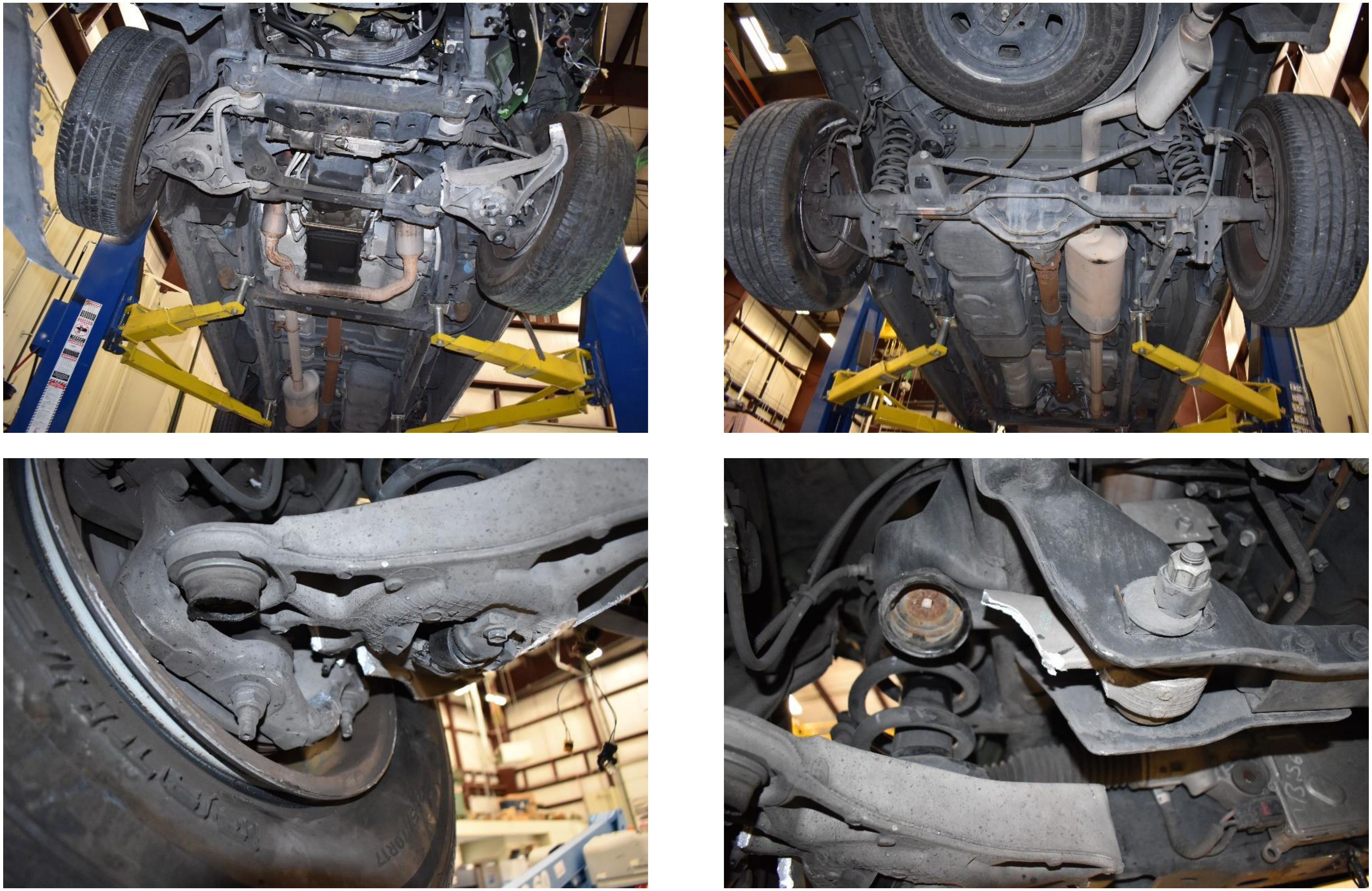

Figure 76. Vehicle Undercarriage Damage, Test No. WITD-4

Table 7. Maximum Occupant Compartment Intrusion by Location, Test No. WITD-4

Location	Maximum Intrusion in.	MASH Allowable Intrusion in.
Wheel Well & Toe Pan	1.7	≤ 9
Floor Pan & Transmission Tunnel	0.0*	≤ 12
A-Pillar	0.5	≤ 5
A-Pillar (Lateral)	0.0*	≤ 3
B-Pillar	0.3	≤ 5
B-Pillar (Lateral)	0.0*	≤ 3
Side Front Panel (in Front of A-Pillar)	0.2	≤ 12
Side Door (Above Seat)	0.0*	≤ 9
Side Door (Below Seat)	0.0*	≤ 12
Roof	0.3	≤ 4
Windshield	0.0	≤ 3
Side Window	Intact	No shattering resulting from contact with structural member of test article
Dash	0.4	N/A

N/A – No MASH criteria exist for this location.
*Negative value reported as 0.0. See Appendix E for further information.

7.5 Occupant Risk

The calculated occupant impact velocities (OIVs) and maximum 0.010-sec average occupant ride down accelerations (ORAs) in both the longitudinal and lateral direction, as determined from accelerometer data, are shown in Table 8. Note that the OIVs and ORAs were within suggested limits, as provided in MASH. The calculated THIV, PHD, and ASI values are also shown in Table 8. The recorded data from the accelerometers and rate transducers are shown graphically in Appendix F.

Table 8. Summary of Occupant Risk Values, Test No. WITD-4

Evaluation Criteria		Transducer		MASH Limits
		SLICE-1	SLICE-2 (primary)	
OIV ft/s	Longitudinal	-14.98	-13.61	±40
	Lateral	20.98	21.93	±40
ORA g's	Longitudinal	-6.29	-6.60	±20.49
	Lateral	13.65	11.71	±20.49
Maximum Angular Displacement degrees	Roll	-44.3	-37.6	±75
	Pitch	-10.4	-13.4	±75
	Yaw	58.5	57.8	not required
THIV – ft/s		24.77	25.36	not required
PHD – g's		13.90	11.94	not required
ASI		1.21	1.36	not required

7.6 Discussion

The analysis of the test results for test no. WITD-4 showed that the system adequately contained and redirected the 2270P vehicle with controlled lateral displacements of the barrier. The test vehicle did not penetrate nor ride over the barrier and remained upright during and after the collision. Vehicle roll, pitch, and yaw angular displacements, as shown in Appendix F, were deemed acceptable because they did not adversely influence occupant risk nor cause rollover. In test no. WITD-4, the impact point was selected to maximize vehicle snag and loading of the barrier joint. Although the vehicle was captured and redirected successfully, the lower leading edge of the left-front door snagged on the saddle cap between barrier nos. 8 and 9. Snagging caused the outer door panel to peel away and wedge between the saddle cap and barrier no. 8. This snag also caused the lower corner of the door to separate and pull away from the door frame while displacing outward and rearward. The snag and pull on the lower door created a 7-in. tall x 1½-in. wide gap at the lower corner of the door and disengaged a portion of the outer panel of the door, as shown in Figure 77. There was little deformation to the saddle cap at the joint between barrier nos. 8 and 9. MASH defines penetration as occurring when a component of the test article penetrates into the occupant compartment. As the lower edge of the door displaced outward and not toward the occupant compartment, and the upstream edge of the saddle cap was not bent outward from the barrier segment and towards the vehicle, the snag on the saddle cap was not considered penetration and was deemed acceptable. After impact, the vehicle exited the barrier at an angle of 1.5 degrees, and its trajectory did not violate the bounds of the exit box. Therefore, test no. WITD-4 was determined to be acceptable according to the MASH safety performance criteria for test designation no. 3-11. A summary of test results and sequential photographs are in Figure 78.

Figure 77. Left-Front Door Snag, Test No. WITD-4

0.000 sec 0.150 sec 0.300 sec 0.450 sec 0.600 sec

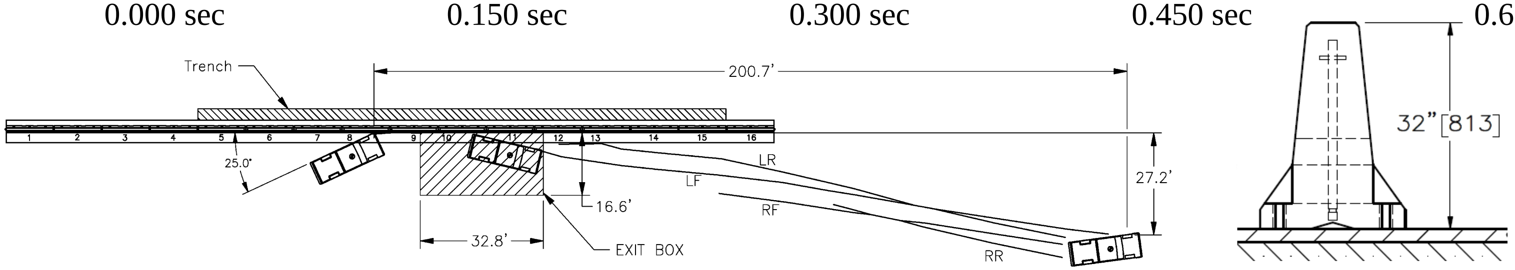

- Test Agency ... MwRSF
- Test Number ... WITD-4
- Date ... 3/15/23
- MASH Test Designation ... 3-11
- Test Article ... Anchored F-Shape PCB
- Total Length ... 204 ft – 7 5/16 in.
- Key Component – F-Shape PCB
  - Length ... 12 ft – 6 in.
  - Width ... 22½ in.
  - Height ... 32 in.
- Key Component – Anchor Bolts
  - Pin Size ... 1½-in. diameter
  - Pin Material ... ASTM A36
  - Pin Length ... 38½ in.
  - Embedment Depth ... 32 in.
  - Number of Pins per Barrier ... 3
  - Pinned Barrier Nos. ... 5 through 13
- Type of Support Surface ... 2-in. thick asphalt
- Vehicle Make /Model ... 2017 Dodge Ram 1500
  - Curb ... 5,242 lb
  - Test Inertial ... 5,019 lb (MASH Limit 5,000 ± 110 lb)
  - Gross Static ... 5,183 lb (MASH Limit 5,165 ± 110 lb)
- Impact Conditions
  - Speed ... 61.9 mph (MASH Limit 62.0 ± 2.5 mph)
  - Angle ... 25.0 deg. (MASH Limit 25 ± 1.5 deg.)
  - Impact Location ... 49.9 in. upstream from the joint center of barrier nos. 8 and 9
- Impact Severity ... 114.8 kip-ft > 106 kip-ft limit from MASH
- Exit Conditions
  - Speed ... 50.5 mph
  - Angle ... 1.5 deg
- Exit Box Criterion ... Pass
- Vehicle Stability ... Satisfactory
- Vehicle Stopping Distance ... 200.7 ft downstream, 27.2 ft laterally in front
- Vehicle Damage ... Moderate
  - VDS [22] ... 01-RFQ-3
  - CDC [23] ... 01-RYEW-3
- Maximum Interior Deformation ... 1.7 in. at wheel well and toe pan ≤ MASH limit
- Test Article Damage ... Moderate
- Maximum Test Article Deflections
  - Permanent Set ... 4.4 in.
  - Dynamic ... 9.9 in.
  - Working Width ... 32.4 in.
- Transducer Data

Evaluation Criteria		Transducer		MASH Limit
		SLICE-1	SLICE-2 (primary)	
OIV ft/s	Longitudinal	-14.98	-13.61	±40
	Lateral	-20.98	-21.93	±40
ORA g's	Longitudinal	-6.29	-6.60	±20.49
	Lateral	-13.65	11.71	±20.49
Maximum Angular Displacement deg.	Roll	-44.3	-37.6	±75
	Pitch	-10.4	-13.4	±75
	Yaw	58.5	57.8	not required
THIV – ft/s		24.77	25.36	not required
PHD – g's		13.90	11.94	not required
ASI		1.21	1.36	not required

Figure 78. Summary of Test Results and Sequential Photographs, Test No. WITD-4

A comparison of relevant metrics from test nos. WITD-2, WITD-3, and WITD-4 are shown in Table 9. There was a significant decrease in toe pan deformation in test no. WITD-4 when compared to test nos. WITD-2 and WITD-3. Dynamic and permanent set deflections were also decreased in test no. WITD-4. Relative lateral barrier displacement decreased from 3.44 in. and 3.28 in., in test nos. WITD-2 and WITD-3, respectively, to 1.19 in. in test no. WITD-4. Longitudinal OIV and ORA decreased in test no. WITD-4, while lateral OIV and ORA increased slightly. Note that OIVs and ORAs were within MASH limits in test no. WITD-4.

Table 9. Barrier Performance Metrics, Test Nos.WITD-2, WITD-3, and WITD-4

Performance Metric		Test		
		Test No. WITD-2	Test No. WITD-3	Test No. WITD-4
Dynamic Deflection (in.)		24.5	16.3	9.9
Permanent Set Deflection (in.)		14.6	10.9	4.4
Toe Pan Deformation (in.)		13.5	10.4	1.7
Relative Lateral Barrier Displacement (in.)		3.44	3.28	1.19
OIV (ft/s)	Longitudinal	-23.9	-17.6	-13.6
	Lateral	19.1	17.1	-21.9
ORA (g’s)	Longitudinal	-9.7	-8.8	-6.6
	Lateral	8.7	-6.4	11.7
Soil/Asphalt Disengagement		Multiple areas of soil and asphalt fracture beneath impacted barrier segments	None	None

Visual comparisons of test no. WITD-4 and the FEA model, as shown in Figures 79 and 80, demonstrate that the behavior of the vehicle and barrier were similar between the full-scale test and the baseline simulation. A comparison of OIVs, ORAs, and dynamic deflection are in Table 10. There was good agreement between test no. WITD-4 and model OIVs and ORAs. Although the baseline model accurately predicted test no. WITD-3 dynamic deflection, the model with the saddle cap underpredicted test no. WITD-4 dynamic deflection by 3 in. Moreover, the final saddle cap model did not predict door snag on the saddle cap and underestimated the relative lateral barrier displacement by approximately 0.3 in. Exclusion of concrete damage from the model potentially contributed to the underprediction of model dynamic deflection and door snag.

Since the final saddle cap model with the 2270P vehicle failed to predict door snag on the saddle cap, an additional model with the 1100C vehicle model was simulated for further evaluation of the system, shown in Figure 81. Occupant risk measures were acceptable, and the wheel did not snag at the joint, however, the saddle cap gouged the bumper. Although the 1100C vehicle door did not snag on the saddle cap, the model displayed more potential for door snag than the 2270P vehicle model. Given the door snag in test no. WITD-4 and the potential snag displayed in the 1100C vehicle model, a small car test on the system developed herein is recommended.

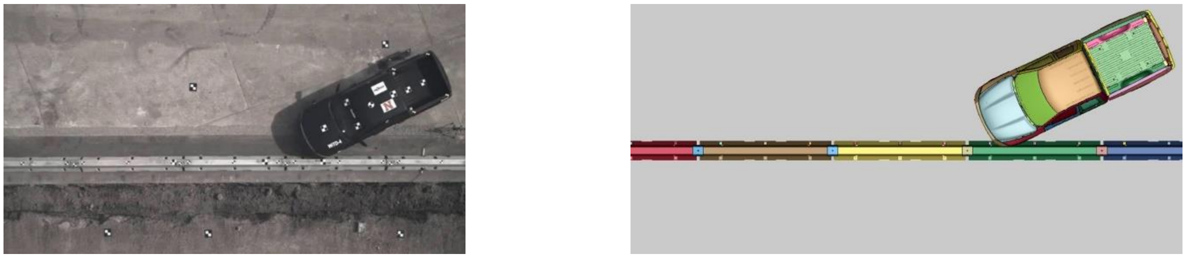

0.000 sec

0.000 sec

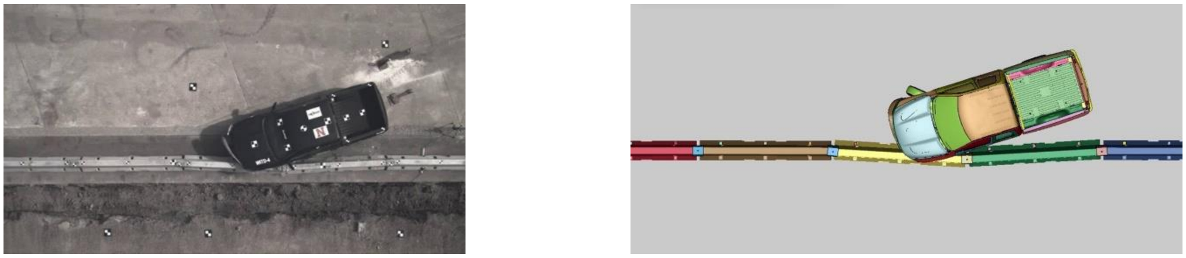

0.100 sec

0.100 sec

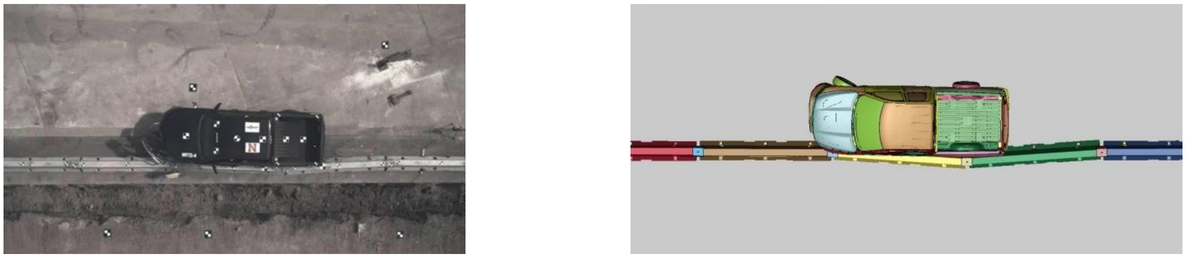

0.200 sec

0.200 sec

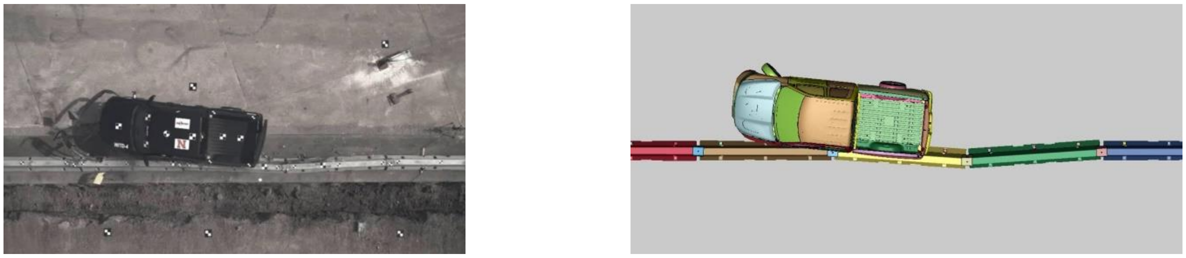

0.300 sec

0.300 sec

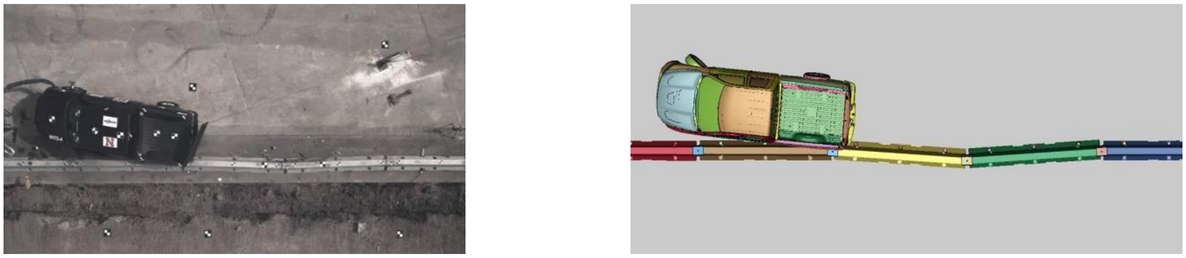

0.400 sec

0.400 sec

Figure 79. Overhead Sequential Photographs, Test No. WITD-4 (left) and FEA Model (right)

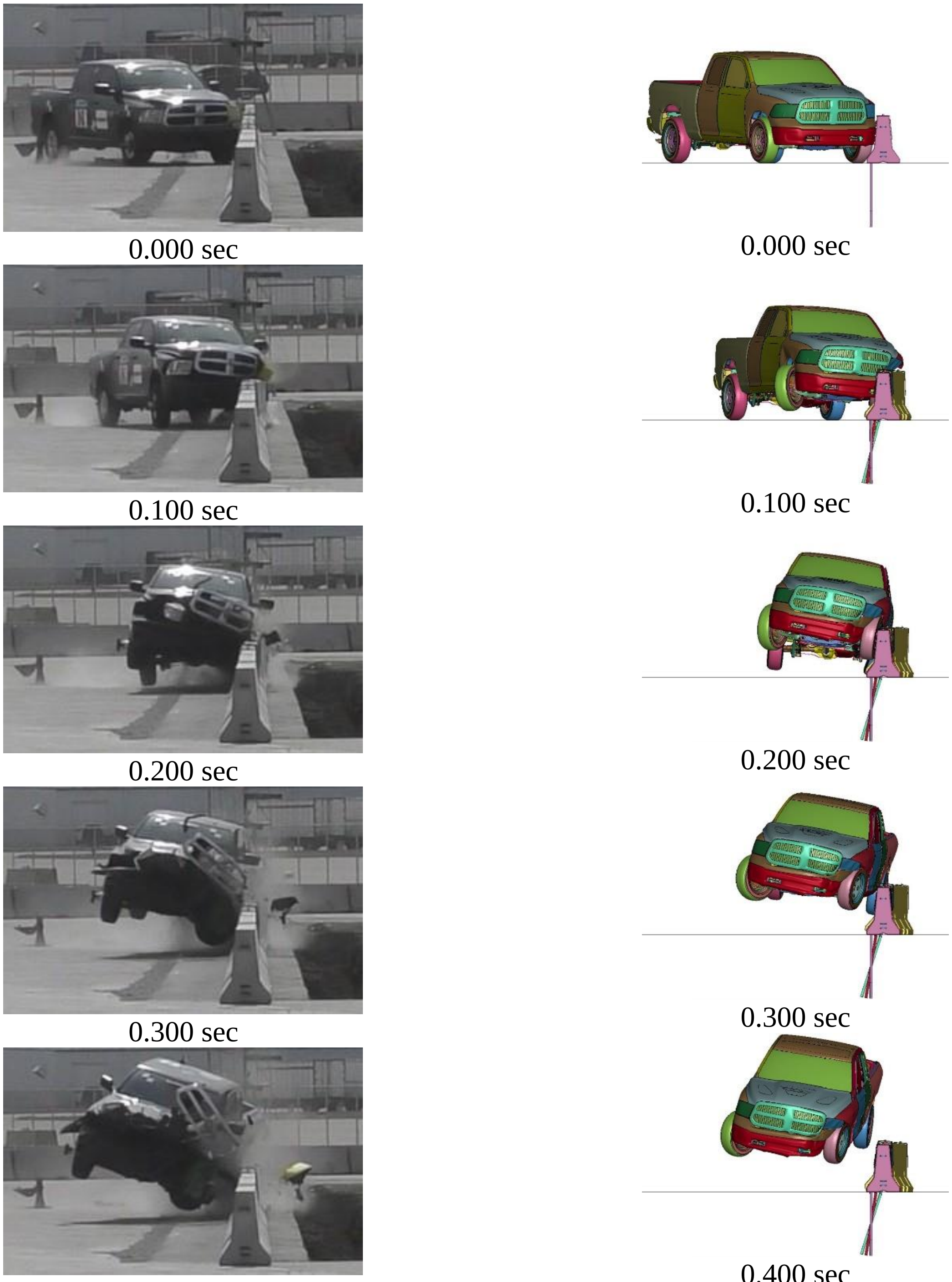

0.000 sec

0.000 sec

0.100 sec

0.100 sec

0.200 sec

0.200 sec

0.300 sec

0.300 sec

0.400 sec

0.400 sec

Figure 80. Downstream Sequential Photographs, Test No. WITD-4 (left) and FEA Model (right)

Table 10. OIV, ORA, and Dynamic Deflection Comparison, Test No. WITD-4 and FEA Model

Metric		Test No. WITD-4	FEA Model
OIV (ft/s)	Longitudinal	-13.6	-13.3
	Lateral	-21.9	-20.6
ORA (g's)	Longitudinal	-6.6	-5.7
	Lateral	11.7	12.0
Dynamic Deflection (in.)		9.9	13.5
Relative Lateral Barrier Displacement (in.)		1.19	0.90

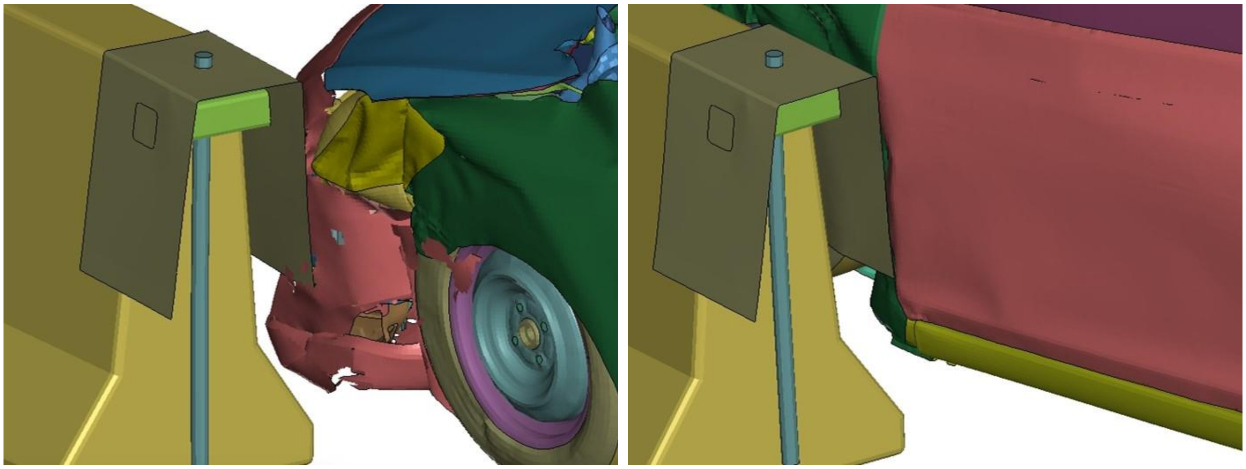

Figure 81. 1100C Vehicle Gouge (left) and Door-Saddle Cap Interaction (right)

8 SUMMARY, CONCLUSIONS, AND RECOMMENDATIONS

This research effort developed and assessed the crashworthiness of a modified, steel pin tie-down anchorage for F-shape PCBs installed on asphalt road surfaces adjacent to a vertical drop off in accordance with MASH TL-3 evaluation criteria. The study began with the development of potential design concepts to improve the safety performance of the steel pin tie-down system. The researchers brainstormed design concepts and evaluated their potential to reduce joint separation and wheel snag. A total of six design concepts were presented to the sponsors for review and selection of a preferred design concept. The sponsors preferred a concept that did not require concrete anchors for ease of installation. As such, the sponsors selected a saddle cap without concrete anchors for design development using LS-DYNA and eventual full-scale crash testing. The saddle cap design concept was evaluated and refined using engineering analysis and LS-DYNA computer simulation. The final saddle cap design was then implemented in a full-scale crash test.

The test installation utilized 32-in. tall x 22½-in. wide x 12-ft 6-in. long F-shape PCBs with a pin and loop connection and anchor pockets in the toes of the barriers. The steel pin tie-down for use on asphalt road surfaces used 1½-in. diameter steel pins installed through the anchor pockets on the traffic-side face of each PCB segment. The pins were driven through a 2-in. thick layer of asphalt and into the soil to a depth of 32 in. The PCB segments for the asphalt tie-down anchorage were installed with the back of the barrier 18 in. from the edge of a 36-in. wide by 36-in. deep trench. A saddle cap assembly was attached to the joints between barrier nos. 5 through 13. The assembly consisted of a 16-in. tall x 12-in. wide x ¼-in. thick saddle cap, a 31¼-in. long x 1¼-in. diameter connection pin, and a 3-in. tall x 3-in. wide x ¼-in. thick stiffening tube. Test no. WITD-4 was conducted according to MASH test designation no. 3-11 on the steel pin tie-down PCB anchorage to evaluate its performance. A summary of the test results is shown in Table 11.

In test no. WITD-4, the 2270P pickup truck impacted the barrier 49.9 in. upstream from the center of the joint between barrier nos. 8 and 9 at a speed of 61.9 mph and at an angle of 25.0 degrees, resulting in an impact severity of 114.8 kip-ft. During the test, the vehicle was contained and redirected by the anchored F-shape PCB system. As the vehicle was redirected, the leading edge of the left-front door snagged on the saddle cap between barrier nos. 8 and 9, causing the outer door panel to peel away and wedge between the saddle cap and barrier no. 8. This snag also caused the door to separate from the door frame, displacing outward and reward, leaving a 7-in. tall x 1½-in. wide gap. There was little deformation to the saddle cap at the joint between barrier nos. 8 and 9. As the lower edge of the door displaced outward and not toward the occupant, and the upstream edge of the saddle cap was not bent outward, the snag on the saddle cap was not considered penetration and was deemed acceptable. After impacting the barrier system, the vehicle exited the system at a speed of 50.5 mph and an angle of 1.5 degrees. The maximum lateral dynamic barrier deflection was 9.9 in. at the upstream end of barrier no. 9, while the working width of the system was 32.4 in. The maximum occupant deformation was 1.7 in. at the toe pan, which was within MASH limits. Subsequently, test no. WITD-4 was determined to be acceptable according to the safety performance criteria for MASH test designation no. 3-11.

Previous 1100C small car tests have indicated that safety shape barriers are capable of successfully capturing and redirecting the vehicle in both free-standing PCB and permanent concrete parapet applications. As such, the anchored F-shape PCB evaluated in this study was expected to perform similarly to these previous MASH 1100C vehicle tests in terms of capture and redirection. Therefore, test designation no. 3-10 with the 1100C vehicle was initially deemed non-critical for the evaluation of the asphalt tie-down anchorage and saddle caps for use with F-shape PCBs. However, because of the door snag that occurred in the 2270P vehicle test and the potential for snag shown in the 1100C vehicle model, concerns arose regarding crashworthiness of the system in MASH test designation no. 3-10. In a small car test, it is possible that snagging which is similar to or more severe than that observed in test no. WITD-4 could occur, potentially violating MASH occupant risk criteria. Accordingly, an 1100C vehicle test was recommended to the sponsors and will be funded by the Wisconsin Department of Transportation and documented in a subsequent report.

Table 11. Summary of Safety Performance Evaluation

<table>
<tr><th>Evaluation Factors</th><th colspan="4">Evaluation Criteria</th><th>Test No. WITD-4</th></tr>
<tr><td>Structural Adequacy</td><td>A.</td><td colspan="3">Test article should contain and redirect the vehicle or bring the vehicle to a controlled stop; the vehicle should not penetrate, underride, or override the installation although controlled lateral deflection of the test article is acceptable.</td><td>S</td></tr>
<tr><td rowspan="11">Occupant Risk</td><td rowspan="2">D.</td><td colspan="3">1. Detached elements, fragments or other debris from the test article should not penetrate or show potential for penetrating the occupant compartment, or present an undue hazard to other traffic, pedestrians, or personnel in a work zone.</td><td>S</td></tr>
<tr><td colspan="3">2. Deformations of, or intrusions into, the occupant compartment should not exceed limits set forth in Section 5.2.2 and Appendix E of MASH.</td><td>S</td></tr>
<tr><td>F.</td><td colspan="3">The vehicle should remain upright during and after collision. The maximum roll and pitch angles are not to exceed 75 degrees.</td><td>S</td></tr>
<tr><td rowspan="4">H.</td><td colspan="3">Occupant Impact Velocity (OIV) (see Appendix A, Section A5.2.2 of MASH for calculation procedure) should satisfy the following limits:</td><td rowspan="4">S</td></tr>
<tr><td colspan="3">Occupant Impact Velocity Limits</td></tr>
<tr><td>Component</td><td>Preferred</td><td>Maximum</td></tr>
<tr><td>Longitudinal and Lateral</td><td>30 ft/s</td><td>40 ft/s</td></tr>
<tr><td rowspan="4">I.</td><td colspan="3">The Occupant Ride down Acceleration (ORA) (see Appendix A, Section A5.2.2 of MASH for calculation procedure) should satisfy the following limits:</td><td rowspan="4">S</td></tr>
<tr><td colspan="3">Occupant Ride down Acceleration Limits</td></tr>
<tr><td>Component</td><td>Preferred</td><td>Maximum</td></tr>
<tr><td>Longitudinal and Lateral</td><td>15.0 g’s</td><td>20.49 g’s</td></tr>
<tr><td colspan="5">MASH Test Designation No.</td><td>3-11</td></tr>
<tr><td colspan="5">Final Evaluation (Pass or Fail)</td><td>Pass</td></tr>
</table>

S – Satisfactory U – Unsatisfactory NA – Not Applicable

9 REFERENCES

1. *Manual for Assessing Safety Hardware*, Second Edition, American Association of State Highway and Transportation Officials (AASHTO), Washington, D.C., 2016.

2. Polivka, K.A., Faller, R.K., Sicking, D.L., Rohde, J.R., Bielenberg, R.W., Reid, J.D., and Coon, B.A., *Performance Evaluation of the Free-Standing Temporary Barrier – Update to NCHRP 350 Test No. 3-11 with 28" C.G. Height (2214TB-2),* Report No. TRP-03-174-06, Midwest Roadside Safety Facility, University of Nebraska-Lincoln, Lincoln, Nebraska, October 2006.

3. Bielenberg, R.W., Faller, R.K., Rohde, J.R., Reid, J.D., Sicking, D.L., and Holloway, J.C., *Development of Tie-Down and Transition Systems for Temporary Concrete Barrier on Asphalt Road Surfaces*, Report No. TRP-03-180-06, Midwest Roadside Safety Facility, University of Nebraska-Lincoln, Lincoln, Nebraska, February 2007.

4. Ross, H.E., Sicking, D.L., Zimmer, R.A., and Michie, J.D., *Recommended Procedures for the Safety Performance Evaluation of Highway Features*, National Cooperative Highway Research Program (NCHRP) Report 350, Transportation Research Board, Washington, D.C., 1993.

5. Bielenberg, R.W., Asselin, N.M., and Faller, R.K., *MASH TL-3 Evaluation of Concrete and Asphalt Tied-Down Anchorage for Portable Concrete Barrier*, Report No. TRP-03-386-19, Midwest Roadside Safety Facility, University of Nebraska-Lincoln, Lincoln, Nebraska, February 2019.

6. Stolle, C.J., Polivka, K.A., Faller, R.K., Sicking, D.L., Bielenberg, R.W., Reid, J.D., Rohde, J.R., Allison, E.M., and Terpsma, R.J., *Evaluation of Box Beam Stiffening of Unanchored Temporary Concrete Barriers*, Report No. TRP-03-202-08, Midwest Roadside Safety Facility, University of Nebraska-Lincoln, Lincoln, Nebraska, 2008.

7. Wiebelhaus, M.J., Terpsma, R.J., Lechtenberg, K.A., Faller, R.K., Sicking, D.L., Bielenberg, R.W., Reid, J.D., and Rohde, J.R., *Development of a Temporary Concrete Barrier to Permanent Concrete Median Barrier Approach Transition,* Report No. TRP-03-208-10, Midwest Roadside Safety Facility, University of Nebraska-Lincoln, Lincoln, Nebraska, 2010.

8. Bielenberg, R.W., Quinn, T.E., Faller, R.K., Sicking, D.L., and Reid, J.D., *Development of a Retrofit, Low-Deflection, Temporary Concrete Barrier System,* Report No. TRP-03-295-14, Midwest Roadside Safety Facility, University of Nebraska-Lincoln, Lincoln, Nebraska, 2014.

9. LS-DYNA Keyword User's Manual R13, Livermore Software Technology Company (LSTC), Livermore, California, 2021.

10. Bielenberg, R.W., Meyer, T.M., Faller, R.K., and Reid, J.R., *Length of Need and Minimum System Length for F-Shape Portable Concrete Barrier,* Report No. TRP-03-337-17, Midwest Roadside Safety Facility, University of Nebraska-Lincoln, Lincoln, Nebraska, May 2017.

11. Bligh, R.P., Sheikh, N.M., Menges, W.L., and Haug., R.R., *Development of Low-Deflection Precast Concrete Barrier*, Report No. 0-4162-3, Texas Transportation Institute, College Station, TX, January 2005.

12. Bielenberg, R.W., Quinn, T.E., Faller, R.K., Sicking, D.L., and Reid, J.D., *Development of a Retrofit, Low-Deflection, Temporary Concrete Barrier System*, Final Report to the Wisconsin Department of Transportation, Report No. TRP 03-295-14, Midwest Roadside Safety Facility, University of Nebraska-Lincoln, Lincoln, Nebraska, March 31, 2014.

13. Dhafer, M., *Update on New MASH Pickup Truck Model*, Center for Collision Safety and Analysis, TRB 98th Annual Meeting (2019) Roadside Safety Design Computational Mechanics Subcommittee, AFB20(1), Washington, D.C., January 14, 2019, Obtained on February 12, 2019.

14. Mongiardini, M., Ray, M.H., Plaxico, C.A., and Anghileri, M., *Procedures for Verification and Validation of Computer Simulations Used for Roadside Safety Applications*, Final Report to the National Cooperative Highway Research Program (NCHRP) Report No. W179, Project No. 22-24, Worcester Polytechnic Institute, March 2010.

15. Buth, C.E., Hirsch, T.J., and Menges, W.L., *Testing of New Bridge Rail and Transition Designs—Volume I: Technical Report*, Report FHWA-RD-93-058, Federal Highway Administration, 1993.

16. Buth, C.E., Hirsch, T.J., and Menges, W.L., *Testing of New Bridge Rail and Transition Designs—Volume IIV: Appendix F*, Report FHWA-RD-93-064, Federal Highway Administration, 1997.

17. Polivka, K.A., Faller, R.K., Sicking, D.L., Rohde, J.R., Bielenberg, R.W., Reid, J.D., and Coon, B.A., *Performance Evaluation of the Permanent New Jersey Safety Shape Barrier - Update to NCHRP 350 Test No. 3-10 (2214NJ-1)*, Report No. TRP-03-177-06, Midwest Roadside Safety Facility, University of Nebraska-Lincoln, Lincoln, Nebraska, October 13, 2006.

18. Sheikh, N.M., Menges, W.L., Kuhn, D.L., *MASH TL-3 Testing and Evaluation of Free-Standing Portable Concrete Barrier*, Test Report No. 607911-1&2, Texas A&M Transportation Institute, Texas A&M University, College Station, Texas, May 2017.

19. Hinch, J., Yang, T.L., and Owings, R., *Guidance Systems for Vehicle Testing*, ENSCO, Inc., Springfield, Virginia, 1986.

20. *Center of Gravity Test Code - SAE J874 March 1981*, SAE Handbook Vol. 4, Society of Automotive Engineers, Inc., Warrendale, Pennsylvania, 1986.

21. Society of Automotive Engineers (SAE), *Instrumentation for Impact Test – Part 1 – Electronic Instrumentation*, SAE J211/1 MAR95, New York, New York, July 2007.

22. *Vehicle Damage Scale for Traffic Investigators*, Second Edition, Technical Bulletin No. 1, Traffic Accident Data (TAD) Project, National Safety Council, Chicago, Illinois, 1971.

23. *Collision Deformation Classification – Recommended Practice J224 March 1980*, Handbook Volume 4, Society of Automotive Engineers (SAE), Warrendale, Pennsylvania, 1985.

10 APPENDICES

Appendix A. Omitted Design Concepts

Concept 1

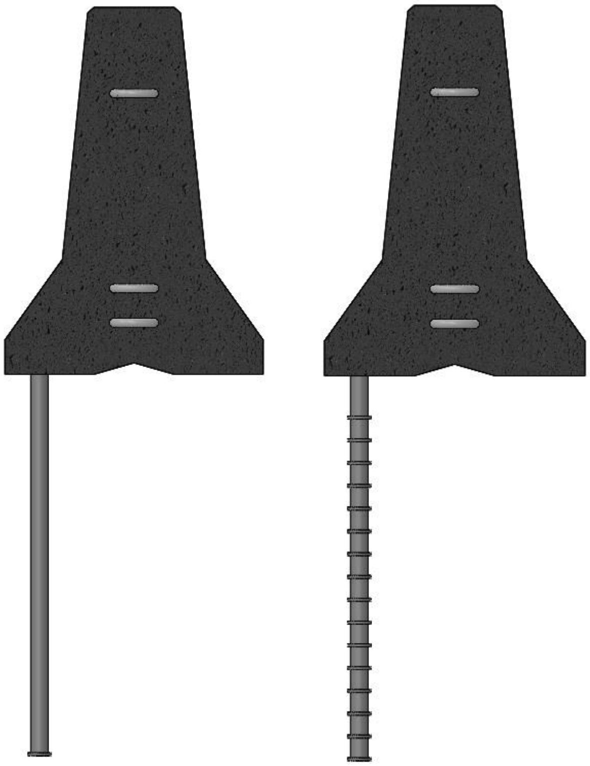

Figure A-1. Anchor Pins Embedded in Grout

Concept description: drill holes through the asphalt and soil, place barriers, fill holes with grout, and sink pins through anchor pockets and into the grout. This concept was intended to increase vertical resistance.

Reason(s) for omission: required a hole to be drilled prior to PCB placement; leave in the ground or break asphalt to remove.

Concept 2

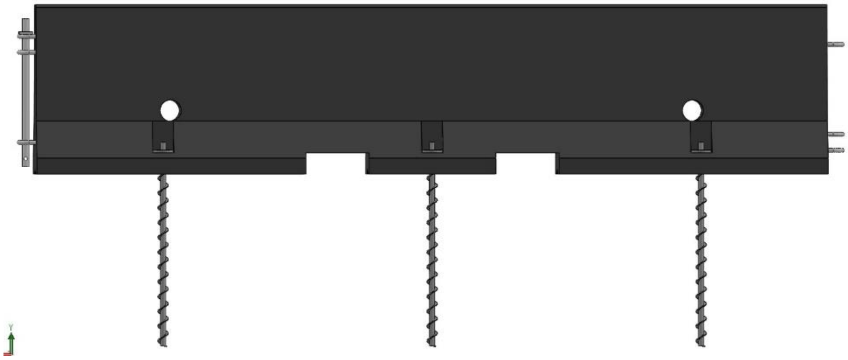

American Earth Anchors

The best screw you will have in the dirt™

americanearthanchors.com

QUICK REFERENCE

PE46-Hex | Specifications

46" Penetrator™
with hex head

- Aircraft-quality cast aluminum 356 alloy
- Heat-treated to T6 specification
- Install with 2" or 51 mm socket
- Removable

10.5 lb (4.8 kg)

6-point socket (instead of 12-point socket) will minimize wear and rounding of hex head for repeated installation/removal

LOAD CAPACITY
Pullout strength with flight fully embedded

Soil Class 1 Hardpan Asphalt	Soil Class 2 Sandy gravel Very dense sand	Soil Class 3 Silty/clayey sand Silty gravel	Soil Class 4 Loose/med dense sands Loose sands Firm clays	Soil Class 4 Loose fine un-compacted sand
14,000 lb 62.3 kN	9,500 lb 42.3 kN	3,300 lb 14.7 kN	2,000 lb 8.90 kN	750 lb 3.34 kN

Soil classification per ASTM D-2487/2488

American Earth Anchors
info@americanea.com
americanearthanchors.com

Contact us for CUSTOM WORK
Size, length, shape, material, prototypes, cable assemblies

866-520-8511
+1 508-520-8511

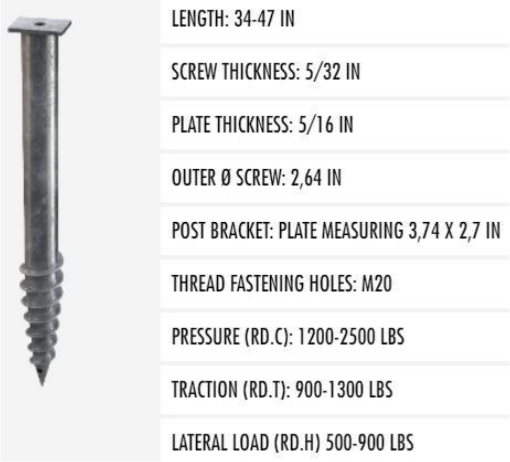

LENGTH: 34-47 IN

SCREW THICKNESS: 5/32 IN

PLATE THICKNESS: 5/16 IN

OUTER Ø SCREW: 2,64 IN

POST BRACKET: PLATE MEASURING 3,74 X 2,7 IN

THREAD FASTENING HOLES: M20

PRESSURE (RD.C): 1200-2500 LBS

TRACTION (RD.T): 900-1300 LBS

LATERAL LOAD (RD.H) 500-900 LBS

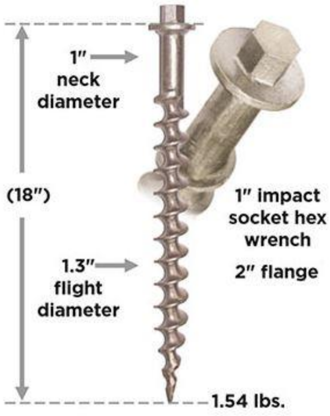

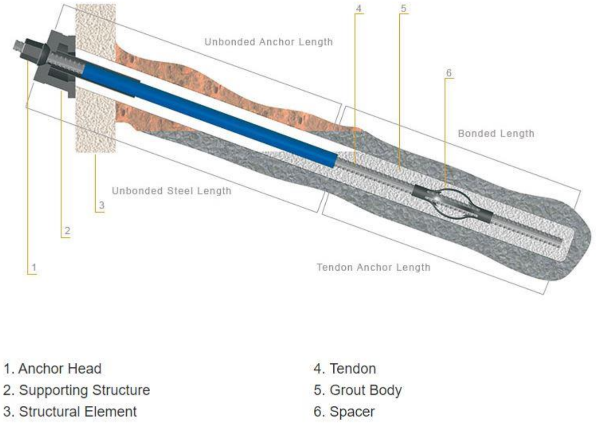

Figure A-2. Soil/Earth Anchors

Concept description: use soil/earth anchors with or without pre-drilled holes to increase vertical resistance.

Reason(s) for omission: required a hole to be drilled prior to PCB placement; lacked sufficient lateral or vertical load capacity; cost; leave in place or break asphalt to remove.

Concept 3

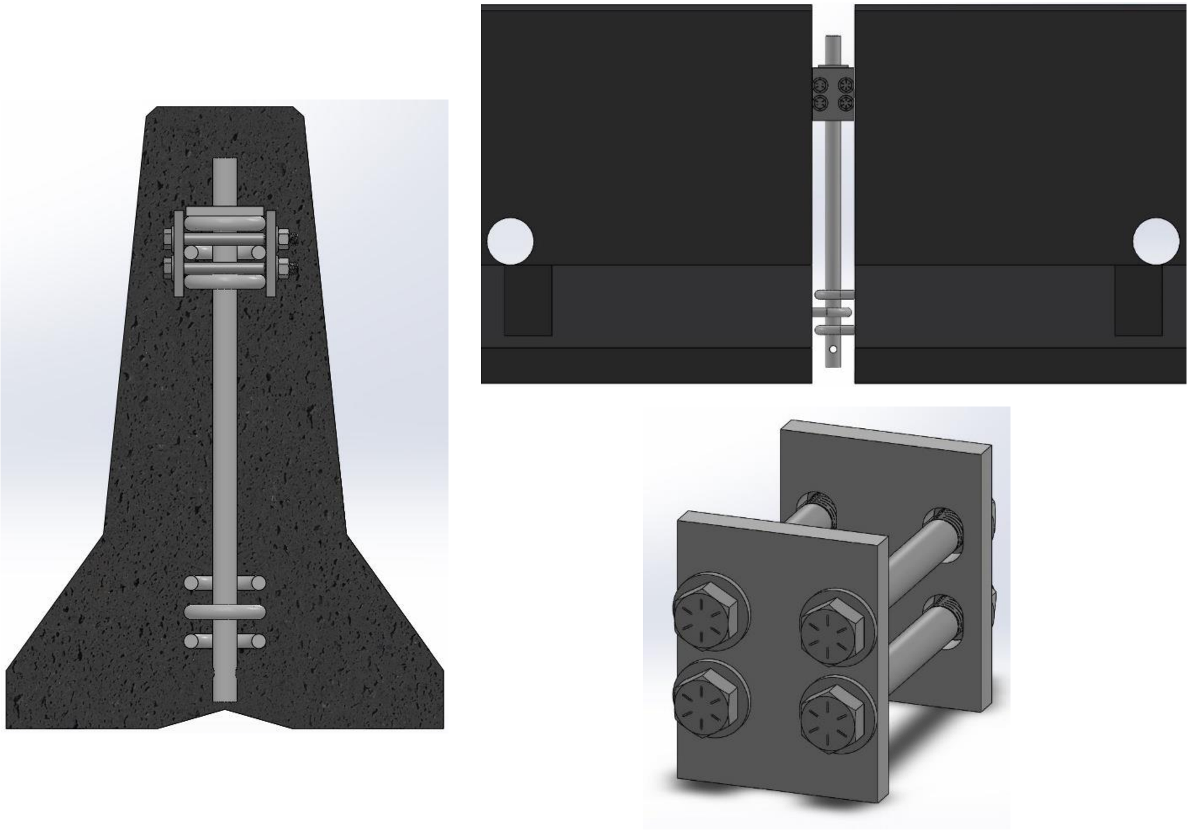

Figure A-3. Loop-Locking Mechanism

Concept description: lock connection loops together laterally and vertically to promote shear transfer and decrease relative lateral barrier displacements.

Reason(s) for omission: concerns that the connecting loops would yield, allowing relative lateral barrier displacement and rotation; difficult to install.

Concept 4

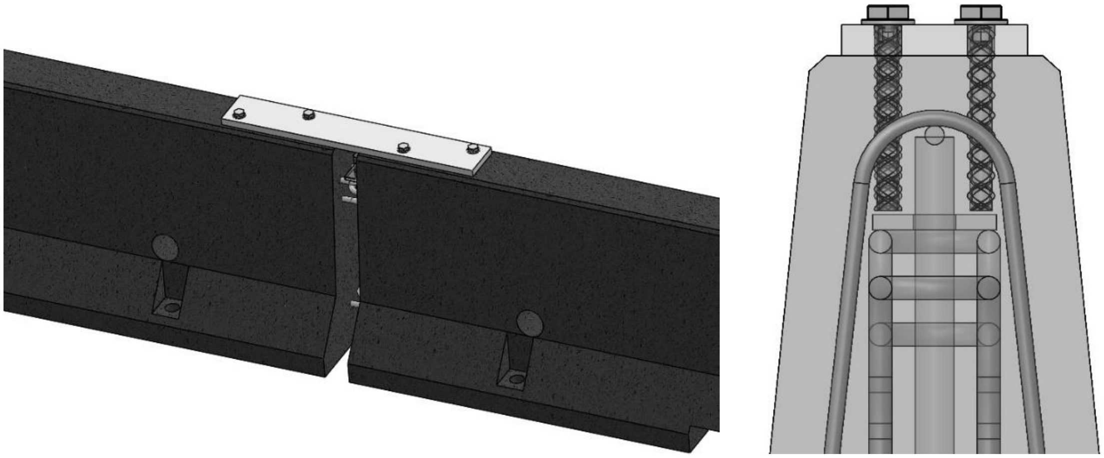

Figure A-4. Top-Mounted Shear Plate

<u>Concept description</u>: robust shear plate bolted to the top of barriers to provide shear transfer.

<u>Reason(s) for omission</u>: due to lack of rebar between the wedge anchor and the face of the PCB, there were concerns that the wedge bolt would cause concrete fracture upon impact, eliminating shear transfer capabilities.

Concept 5

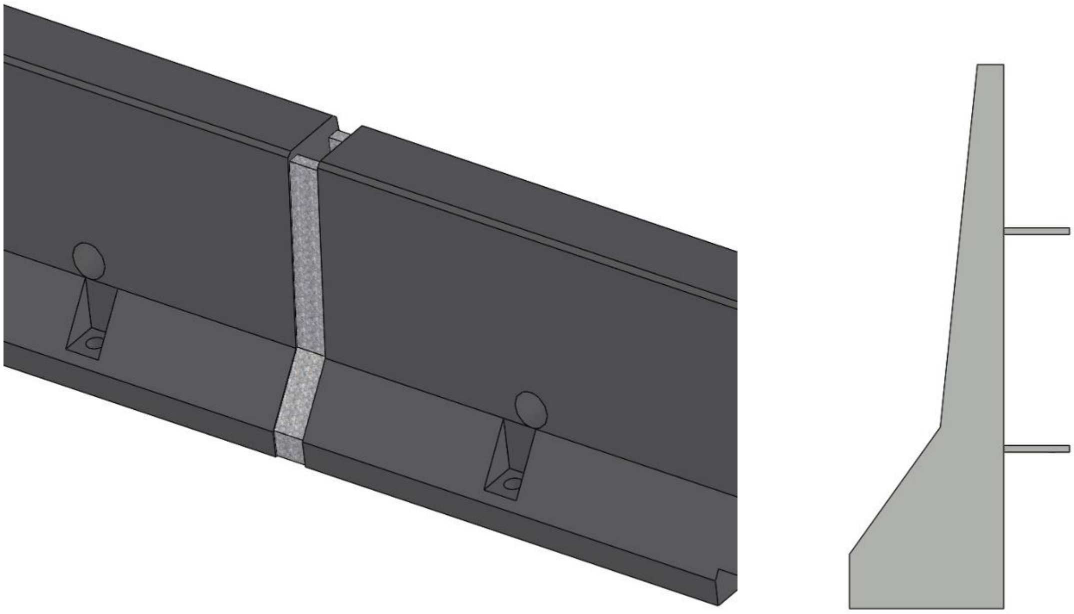

Figure A-5. Gap-Filling Mechanism

Concept description: shield the gap by filling the joint.

Reason(s) for omission: although this design limits relative PCB rotation about the vertical axis, this design drew concerns that the gap filler would provide a snag face rather than shielding the gap.

Appendix B. RSVVP Results

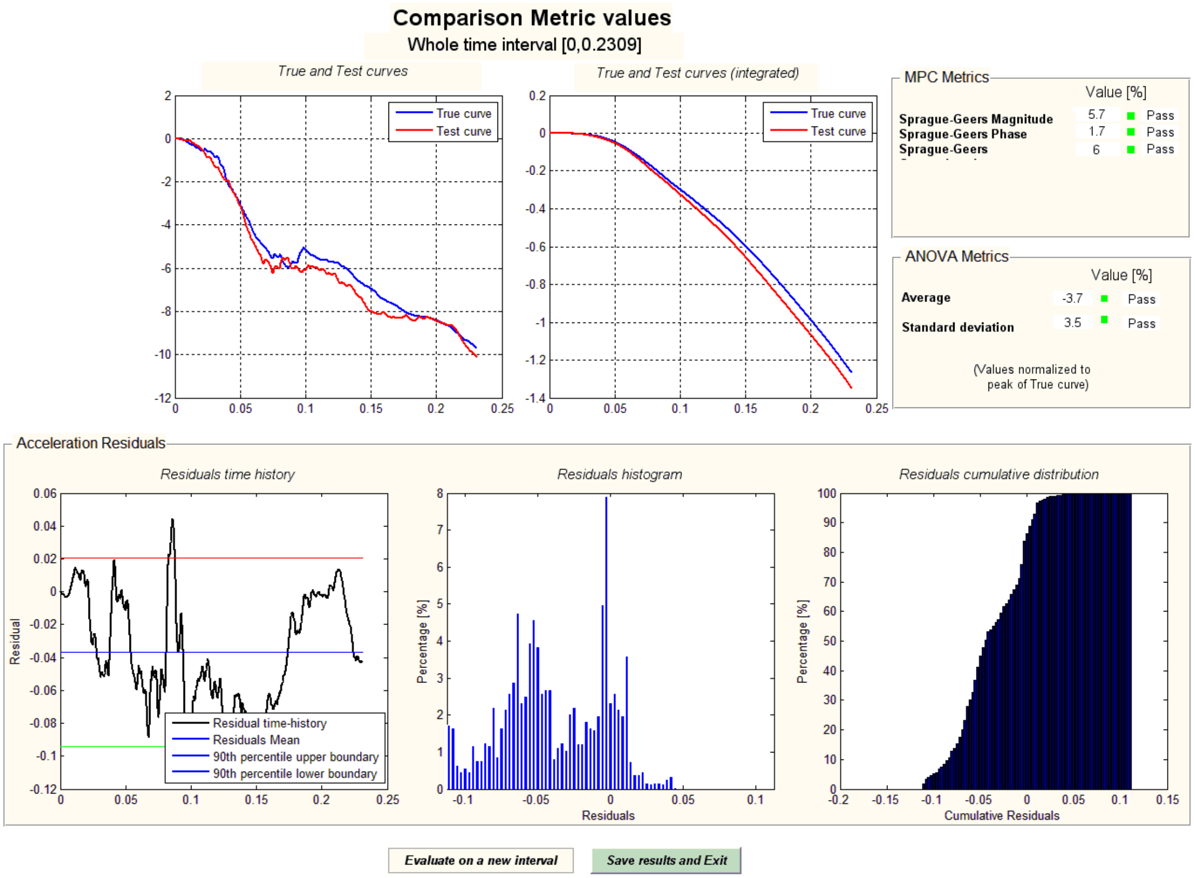

Comparison Metric values

Whole time interval [0,0.2309]

MPC Metrics

	Value [%]		
Sprague-Geers Magnitude	5.7	🟩	Pass
Sprague-Geers Phase	1.7	🟩	Pass
Sprague-Geers	6	🟩	Pass

ANOVA Metrics

	Value [%]		
Average	-3.7	🟩	Pass
Standard deviation	3.5	🟩	Pass

(Values normalized to peak of True curve)

Figure B-1. WITD-3 Model with 4-in. Gap Spacing Lateral Vehicle CG RSVVP Results

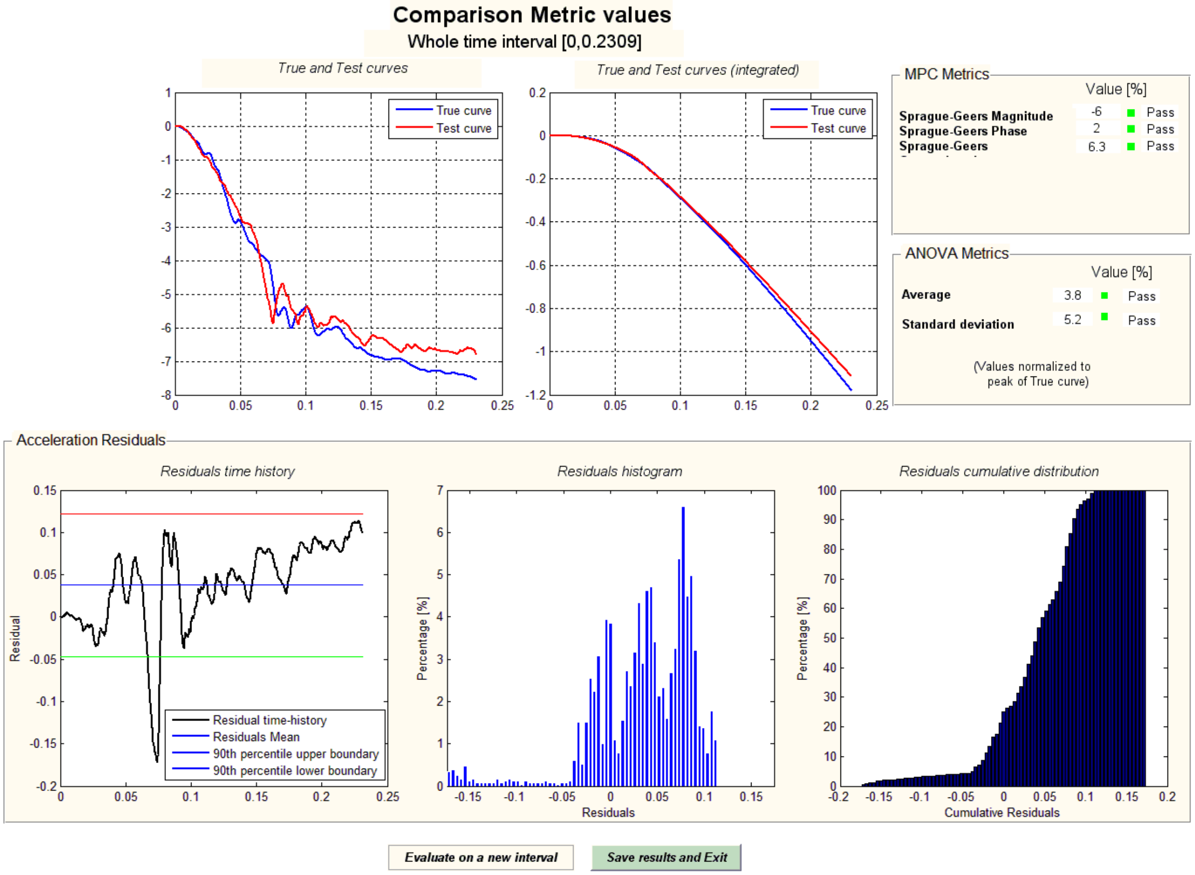

Comparison Metric values

Whole time interval [0,0.2309]

MPC Metrics

	Value [%]		
Sprague-Geers Magnitude	-6	🟩	Pass
Sprague-Geers Phase	2	🟩	Pass
Sprague-Geers	6.3	🟩	Pass

ANOVA Metrics

	Value [%]		
Average	3.8	🟩	Pass
Standard deviation	5.2	🟩	Pass

(Values normalized to peak of True curve)

Figure B-2. WITD-3 Model with 4-in. Gap Spacing Longitudinal Vehicle CG RSVVP Results

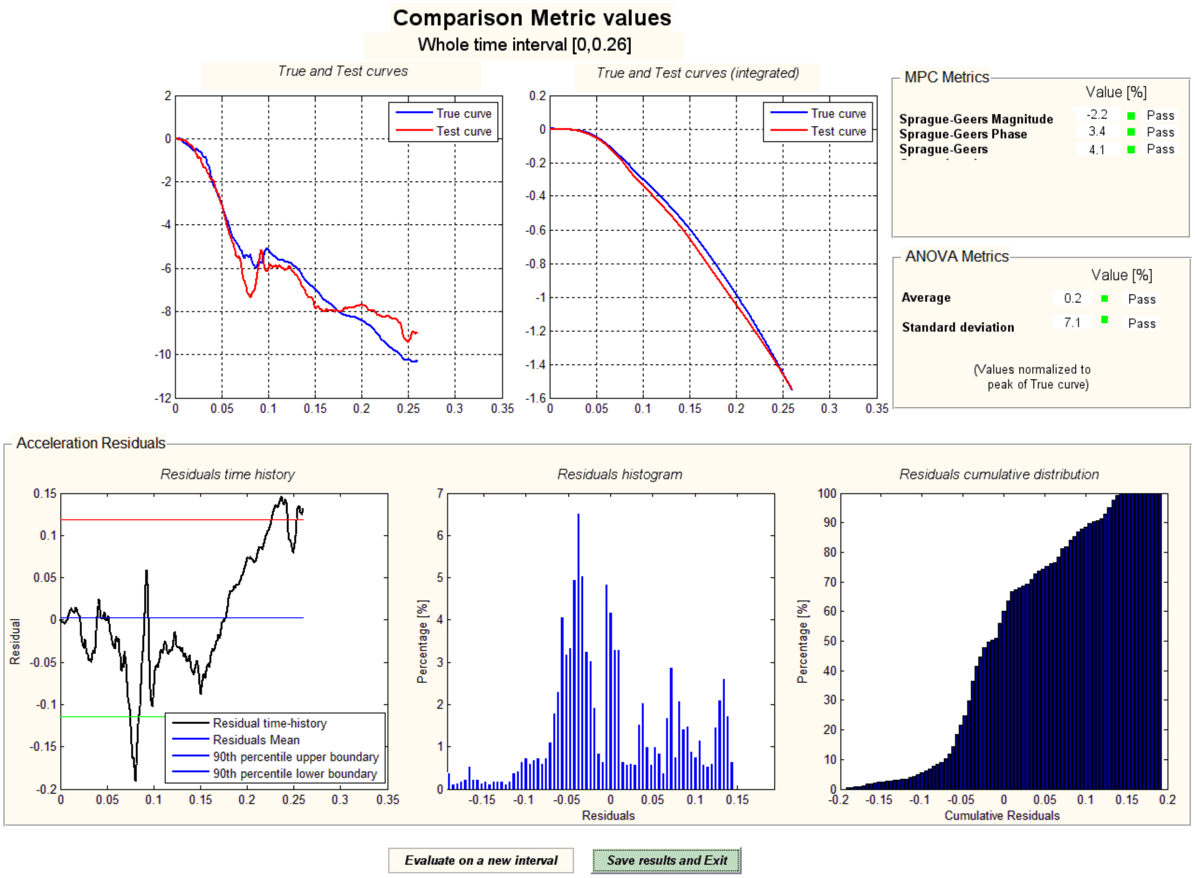

MPC Metrics

	Value [%]		
Sprague-Geers Magnitude	-2.2	🟩	Pass
Sprague-Geers Phase	3.4	🟩	Pass
Sprague-Geers	4.1	🟩	Pass

ANOVA Metrics

	Value [%]		
Average	0.2	🟩	Pass
Standard deviation	7.1	🟩	Pass

(Values normalized to peak of True curve)

Figure B-3. WITD-3 Model with 3.5-in. Gap Spacing Lateral Vehicle CG RSVVP Results

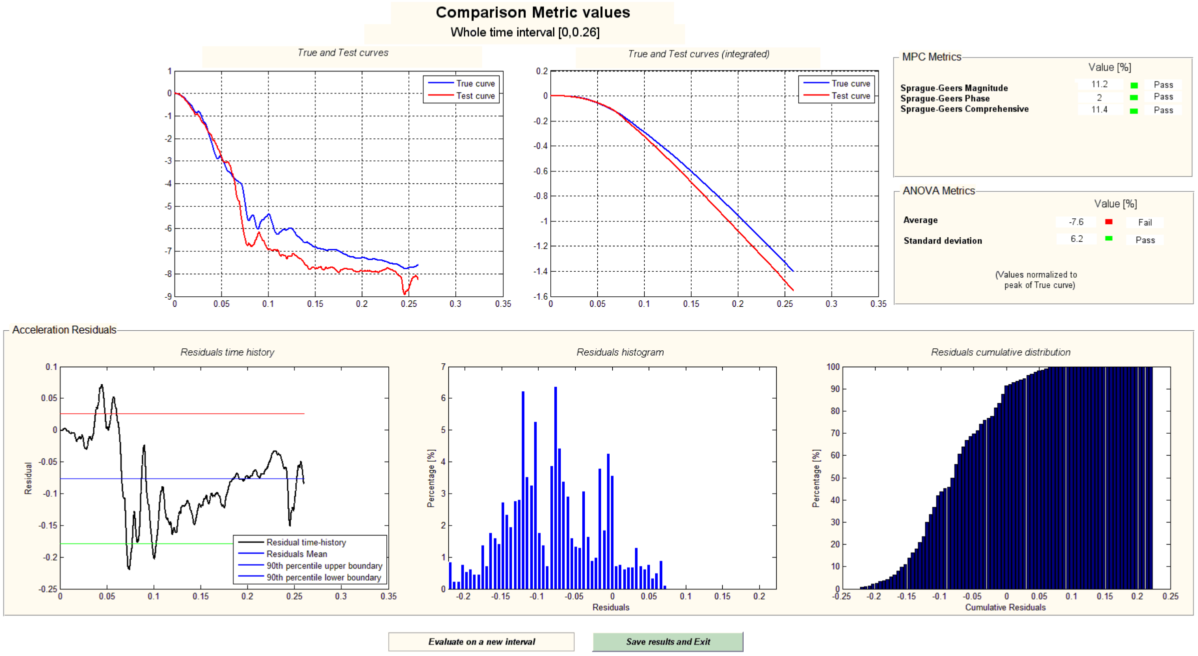

Comparison Metric values

Whole time interval [0,0.26]

MPC Metrics

	Value [%]		
Sprague-Geers Magnitude	11.2	🟩	Pass
Sprague-Geers Phase	2	🟩	Pass
Sprague-Geers Comprehensive	11.4	🟩	Pass

ANOVA Metrics

	Value [%]		
Average	-7.6	🟥	Fail
Standard deviation	6.2	🟩	Pass

(Values normalized to peak of True curve)

Figure B-4. WITD-3 Model with 3.5-in. Gap Spacing Longitudinal Vehicle CG RSVVP Result

Appendix C. Vehicle Center of Gravity Determination

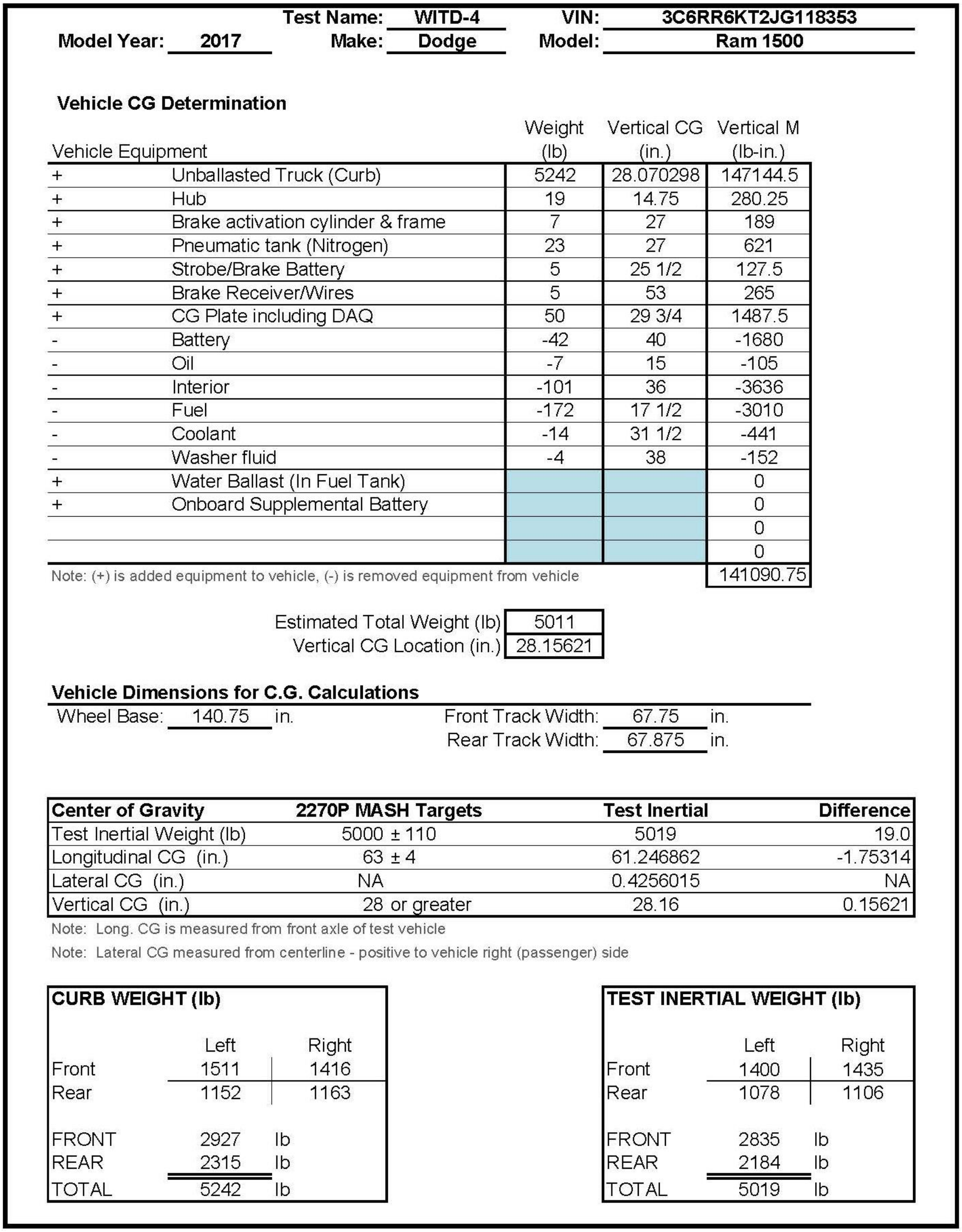

Test Name: WITD-4
VIN: 3C6RR6KT2JG118353
Model Year: 2017
Make: Dodge
Model: Ram 1500

Vehicle CG Determination

	Vehicle Equipment	Weight (lb)	Vertical CG (in.)	Vertical M (lb-in.)
+	Unballasted Truck (Curb)	5242	28.070298	147144.5
+	Hub	19	14.75	280.25
+	Brake activation cylinder & frame	7	27	189
+	Pneumatic tank (Nitrogen)	23	27	621
+	Strobe/Brake Battery	5	25 1/2	127.5
+	Brake Receiver/Wires	5	53	265
+	CG Plate including DAQ	50	29 3/4	1487.5
-	Battery	-42	40	-1680
-	Oil	-7	15	-105
-	Interior	-101	36	-3636
-	Fuel	-172	17 1/2	-3010
-	Coolant	-14	31 1/2	-441
-	Washer fluid	-4	38	-152
+	Water Ballast (In Fuel Tank)			0
+	Onboard Supplemental Battery			0
				0
				0
				141090.75

Note: (+) is added equipment to vehicle, (-) is removed equipment from vehicle

Estimated Total Weight (lb) 5011
Vertical CG Location (in.) 28.15621

Vehicle Dimensions for C.G. Calculations

Wheel Base: 140.75 in.
Front Track Width: 67.75 in.
Rear Track Width: 67.875 in.

Center of Gravity	**2270P MASH Targets**	**Test Inertial**	**Difference**
Test Inertial Weight (lb)	5000 ± 110	5019	19.0
Longitudinal CG (in.)	63 ± 4	61.246862	-1.75314
Lateral CG (in.)	NA	0.4256015	NA
Vertical CG (in.)	28 or greater	28.16	0.15621

Note: Long. CG is measured from front axle of test vehicle

Note: Lateral CG measured from centerline - positive to vehicle right (passenger) side

CURB WEIGHT (lb)

	Left	Right
Front	1511	1416
Rear	1152	1163

FRONT 2927 lb
REAR 2315 lb
TOTAL 5242 lb

TEST INERTIAL WEIGHT (lb)

	Left	Right
Front	1400	1435
Rear	1078	1106

FRONT 2835 lb
REAR 2184 lb
TOTAL 5019 lb

Figure C-1. Vehicle Mass Distribution, Test No. WITD-4

Appendix D. Material Specifications

Table B-1. Bill of Materials, Test No. WITD-4

Item No.	Description	Material Specification	Reference
a1	Portable Concrete Barrier	Min f'c = 5,000 psi [34.5 MPa]	Concrete Test Reports: 7031/7582
a2	½" Dia., 70$^{9}/_{16}$" Long Form Bar	ASTM A615 Gr. 60	H#5716717603
a3	½" Dia., 146½" Long Longitudinal Bar	ASTM A615 Gr. 60	H#5716717603
a4	⅝" Dia., 146½" Long Longitudinal Bar	ASTM A615 Gr. 60	H#5717263002
a5	¾" Dia., 36$^{1}/_{8}$" Long Anchor Loop Bar	ASTM A615 Gr. 60	H#5717147402
a6	¾" Dia., 95$^{1}/_{16}$" Long Connection Loop Bar	ASTM A709 Gr. 70 or A706 Gr. 60	H#KN17102927 H#KN17102928
a7	¾" Dia., 85$^{9}/_{16}$" Long Connection Loop Bar	ASTM A709 Gr. 70 or A706 Gr. 60	H#KN17102927 H#KN17102928
a8	¾" Dia., 96$^{9}/_{16}$" Long Connection Loop Bar	ASTM A709 Gr. 70 or A706 Gr. 60	H#KN17102927 H#KN17102928
a9	1¼" Dia., 28" Long Connector Pin	ASTM A36	H#5415671902
b1	1¼" Dia., 31¼" Long Connector Pin	ASTM A36	H#2068693
b2	HSS 3"x3"x¼", 9½" Long Stiffening Tube	ASTM A36	H#19013461
b3	40$^{5}/_{16}$"x12"x¼" Saddle Cap	A572 Gr. 50	H# B2205590
c1	1½" Dia., 38½" Long Anchor Pin	NE SPS Mix with 52-34 Grade Binder	H#2068693
c2	3"x3"x½" Washer Plate	ASTM A36	H#19013461
d1	2400"x72 "x2" Asphalt Pad	NE SPS Mix with 52-34 Grade Binder	Lab#43224

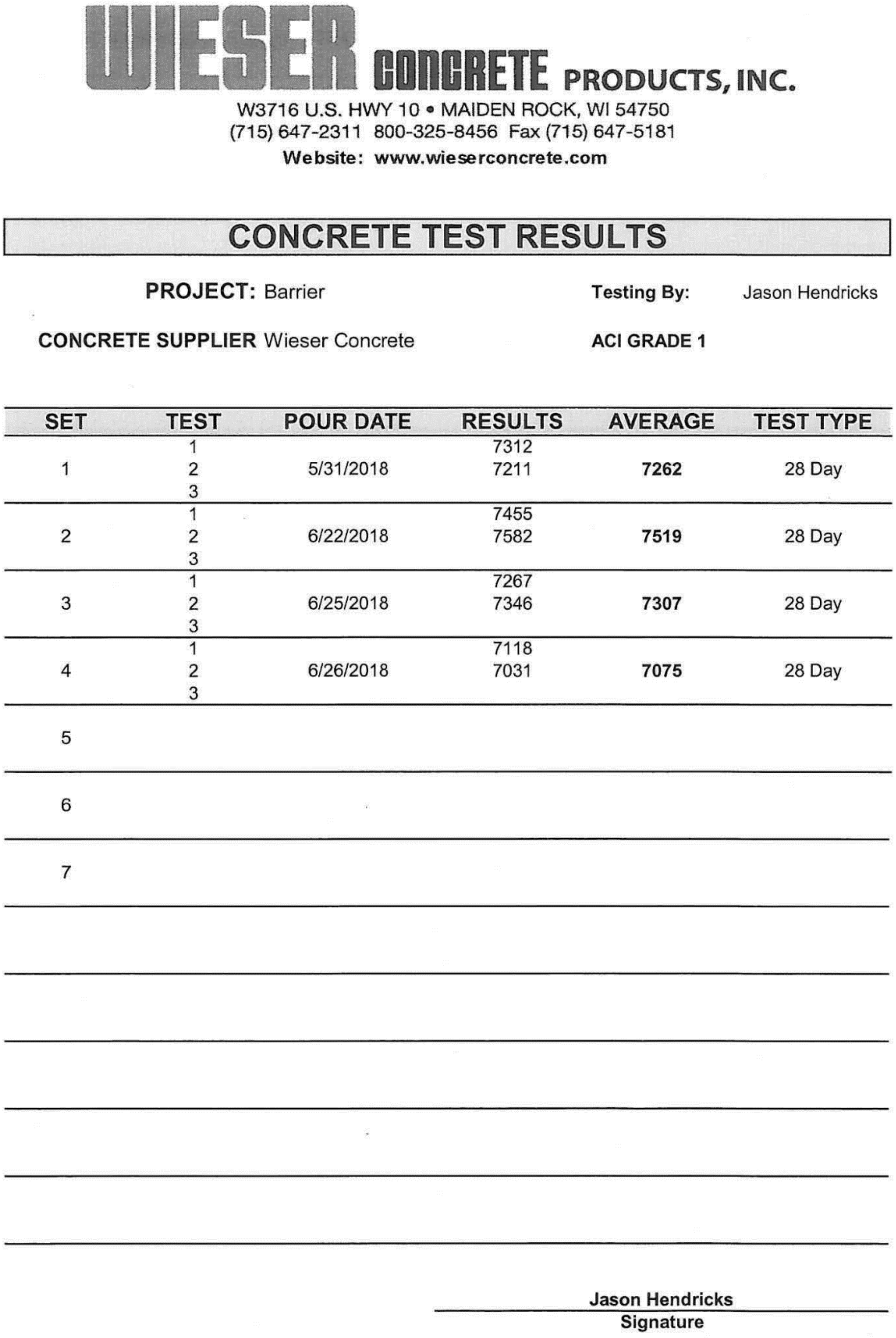

WIESER CONCRETE PRODUCTS, INC.

W3716 U.S. HWY 10 • MAIDEN ROCK, WI 54750
(715) 647-2311 800-325-8456 Fax (715) 647-5181
Website: www.wieserconcrete.com

CONCRETE TEST RESULTS

PROJECT: Barrier

Testing By: Jason Hendricks

CONCRETE SUPPLIER Wieser Concrete

ACI GRADE 1

SET	TEST	POUR DATE	RESULTS	AVERAGE	TEST TYPE
1	1	5/31/2018	7312	**7262**	28 Day
	2		7211		
	3				
2	1	6/22/2018	7455	**7519**	28 Day
	2		7582		
	3				
3	1	6/25/2018	7267	**7307**	28 Day
	2		7346		
	3				
4	1	6/26/2018	7118	**7075**	28 Day
	2		7031		
	3				
5					
6					
7					

Jason Hendricks
Signature

Figure D-1. Portable Concrete Barrier, Test No. WITD-4 (Item No. a1)

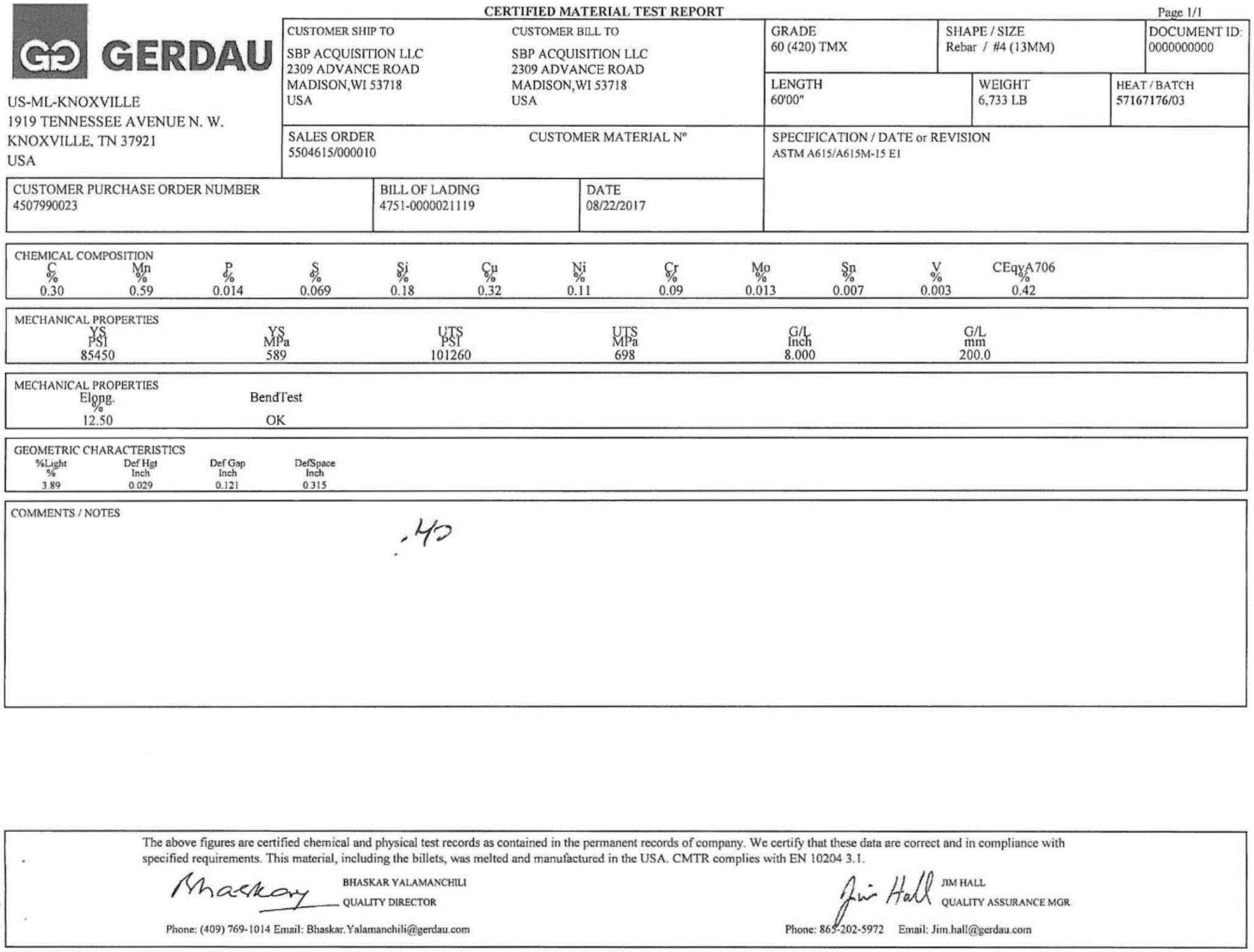

GERDAU

CERTIFIED MATERIAL TEST REPORT

Page 1/1

US-ML-KNOXVILLE
1919 TENNESSEE AVENUE N. W.
KNOXVILLE, TN 37921
USA

CUSTOMER SHIP TO
SBP ACQUISITION LLC
2309 ADVANCE ROAD
MADISON,WI 53718
USA

CUSTOMER BILL TO
SBP ACQUISITION LLC
2309 ADVANCE ROAD
MADISON,WI 53718
USA

GRADE: 60 (420) TMX
SHAPE / SIZE: Rebar / #4 (13MM)
DOCUMENT ID: 0000000000
LENGTH: 60'00"
WEIGHT: 6,733 LB
HEAT / BATCH: 57167176/03
SALES ORDER: 5504615/000010
CUSTOMER MATERIAL N°:
SPECIFICATION / DATE or REVISION: ASTM A615/A615M-15 E1
CUSTOMER PURCHASE ORDER NUMBER: 4507990023
BILL OF LADING: 4751-0000021119
DATE: 08/22/2017

CHEMICAL COMPOSITION

C %	Mn %	P %	S %	Si %	Cu %	Ni %	Cr %	Mo %	Sn %	V %	CEqyA706 %
0.30	0.59	0.014	0.069	0.18	0.32	0.11	0.09	0.013	0.007	0.003	0.42

MECHANICAL PROPERTIES

YS PSI	YS MPa	UTS PSI	UTS MPa	G/L Inch	G/L mm
85450	589	101260	698	8.000	200.0

MECHANICAL PROPERTIES

Elong. %	BendTest
12.50	OK

GEOMETRIC CHARACTERISTICS

%Light %	Def Hgt Inch	Def Gap Inch	DefSpace Inch
3.89	0.029	0.121	0.315

COMMENTS / NOTES

.40

The above figures are certified chemical and physical test records as contained in the permanent records of company. We certify that these data are correct and in compliance with specified requirements. This material, including the billets, was melted and manufactured in the USA. CMTR complies with EN 10204 3.1.

Bhaskary
BHASKAR YALAMANCHILI
QUALITY DIRECTOR
Phone: (409) 769-1014 Email: Bhaskar.Yalamanchili@gerdau.com

Jim Hall
JIM HALL
QUALITY ASSURANCE MGR
Phone: 865-202-5972 Email: Jim.hall@gerdau.com

Figure D-2. ½-in. Diameter Bar, Test No. WITD-4 (Item Nos. a2 and a3)

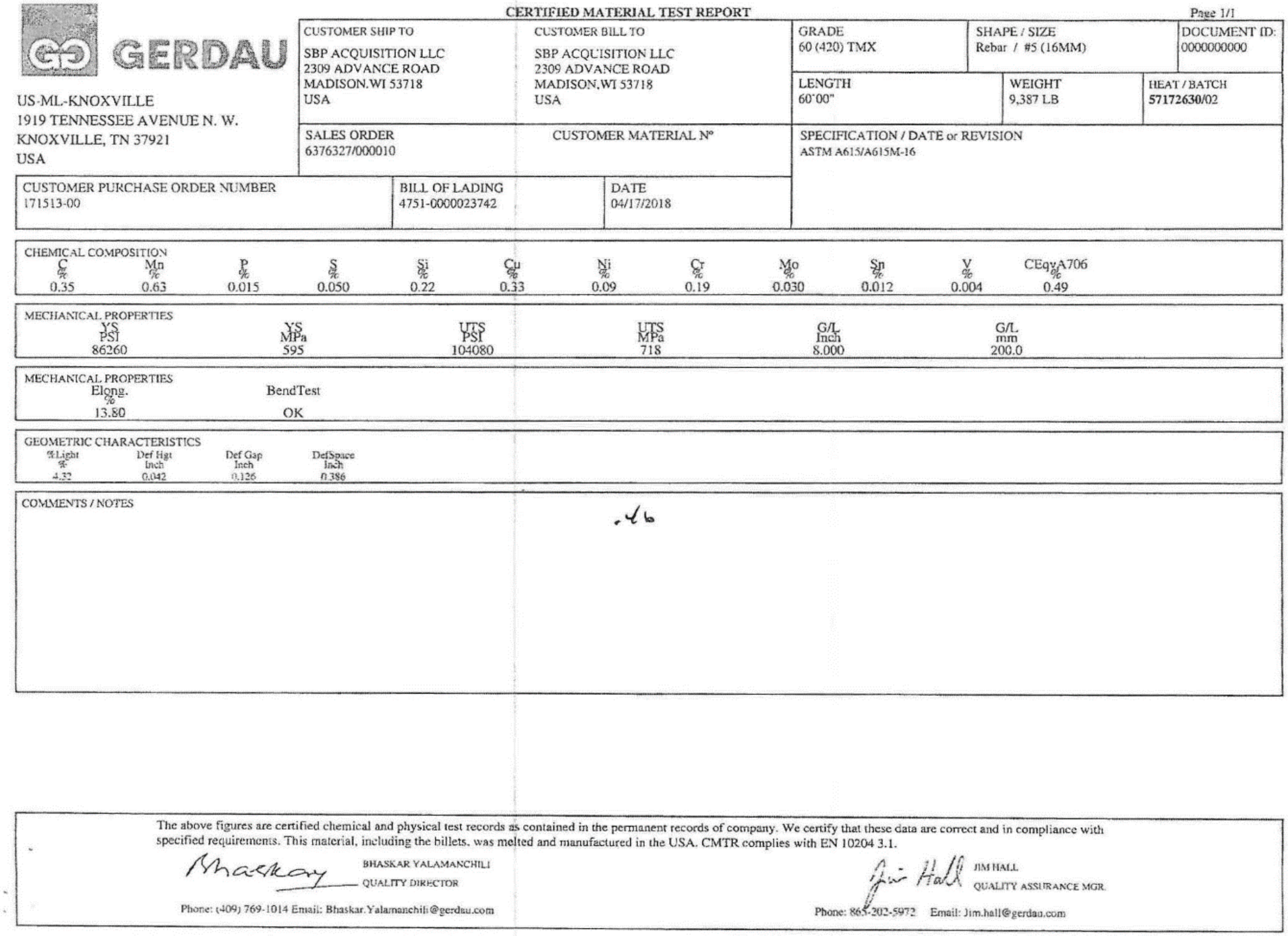

GERDAU

US-ML-KNOXVILLE
1919 TENNESSEE AVENUE N. W.
KNOXVILLE, TN 37921
USA

CERTIFIED MATERIAL TEST REPORT

Page 1/1

CUSTOMER SHIP TO SBP ACQUISITION LLC 2309 ADVANCE ROAD MADISON,WI 53718 USA	CUSTOMER BILL TO SBP ACQUISITION LLC 2309 ADVANCE ROAD MADISON,WI 53718 USA	GRADE 60 (420) TMX	SHAPE / SIZE Rebar / #5 (16MM)	DOCUMENT ID: 0000000000
		LENGTH 60'00"	WEIGHT 9,387 LB	HEAT / BATCH **57172630/02**
SALES ORDER 6376327/000010	CUSTOMER MATERIAL Nº	SPECIFICATION / DATE or REVISION ASTM A615/A615M-16		

CUSTOMER PURCHASE ORDER NUMBER 171513-00	BILL OF LADING 4751-0000023742	DATE 04/17/2018

CHEMICAL COMPOSITION

C %	Mn %	P %	S %	Si %	Cu %	Ni %	Cr %	Mo %	Sn %	V %	CEqvA706 %
0.35	0.63	0.015	0.050	0.22	0.33	0.09	0.19	0.030	0.012	0.004	0.49

MECHANICAL PROPERTIES

YS PSI	YS MPa	UTS PSI	UTS MPa	G/L Inch	G/L mm
86260	595	104080	718	8.000	200.0

MECHANICAL PROPERTIES

Elong. %	BendTest
13.80	OK

GEOMETRIC CHARACTERISTICS

%Light %	Def Hgt Inch	Def Gap Inch	DefSpace Inch
4.32	0.042	0.126	0.386

COMMENTS / NOTES

.46

The above figures are certified chemical and physical test records as contained in the permanent records of company. We certify that these data are correct and in compliance with specified requirements. This material, including the billets, was melted and manufactured in the USA. CMTR complies with EN 10204 3.1.

Bhaskar
BHASKAR YALAMANCHILI
QUALITY DIRECTOR
Phone: (409) 769-1014 Email: Bhaskar.Yalamanchili@gerdau.com

Jim Hall
JIM HALL
QUALITY ASSURANCE MGR.
Phone: 865-202-5972 Email: Jim.hall@gerdau.com

Figure D-3. ⅝-in. Diameter, 146½-in. Long Longitudinal Bar, Test No. WITD-4 (Item No. a4)

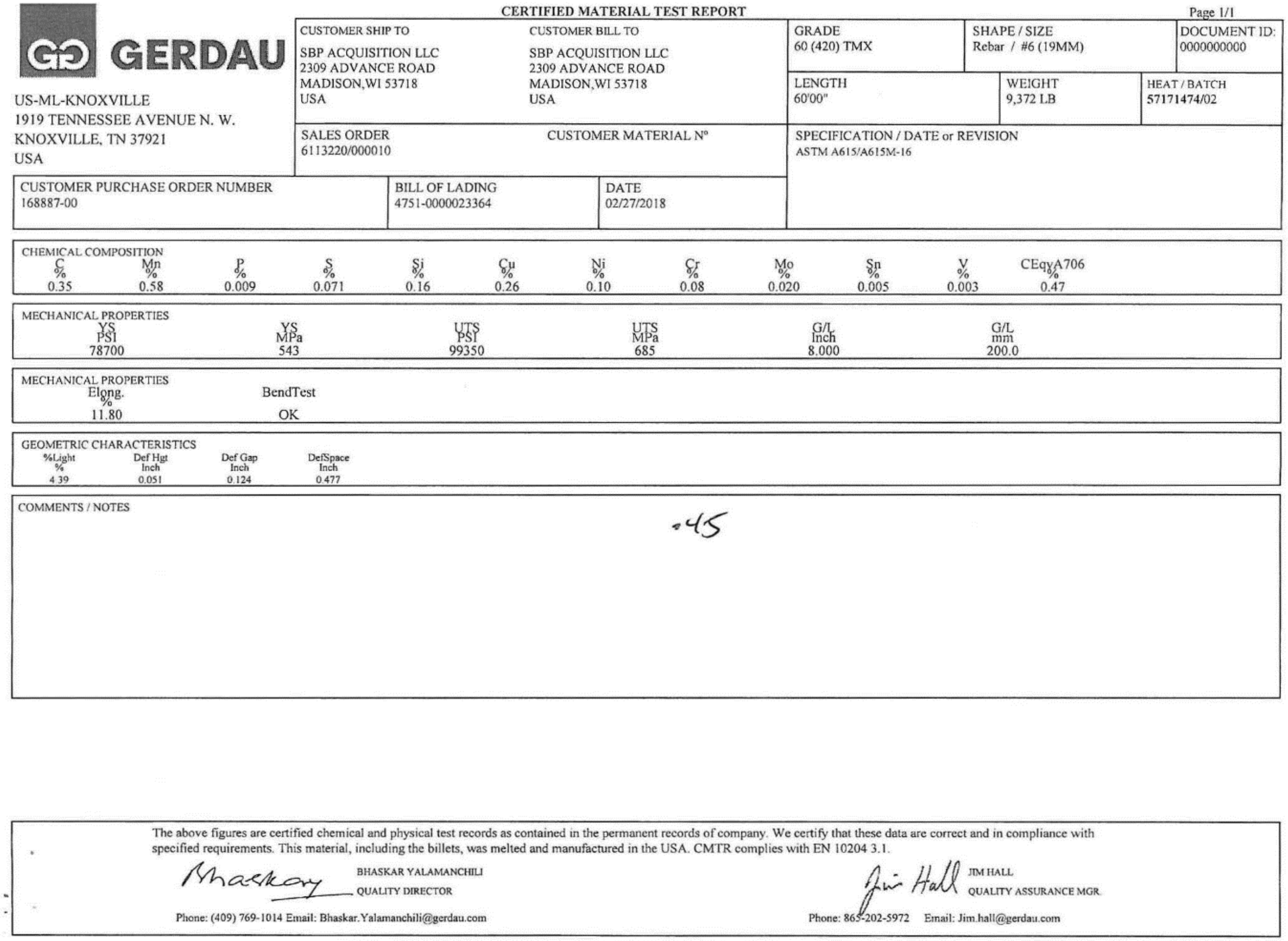

GERDAU

US-ML-KNOXVILLE
1919 TENNESSEE AVENUE N. W.
KNOXVILLE, TN 37921
USA

CERTIFIED MATERIAL TEST REPORT

Page 1/1

CUSTOMER SHIP TO SBP ACQUISITION LLC 2309 ADVANCE ROAD MADISON,WI 53718 USA	CUSTOMER BILL TO SBP ACQUISITION LLC 2309 ADVANCE ROAD MADISON,WI 53718 USA	GRADE 60 (420) TMX	SHAPE / SIZE Rebar / #6 (19MM)	DOCUMENT ID: 0000000000	
		LENGTH 60'00"	WEIGHT 9,372 LB	HEAT / BATCH 57171474/02	
SALES ORDER 6113220/000010	CUSTOMER MATERIAL N°	SPECIFICATION / DATE or REVISION ASTM A615/A615M-16			

CUSTOMER PURCHASE ORDER NUMBER	BILL OF LADING	DATE
168887-00	4751-0000023364	02/27/2018

CHEMICAL COMPOSITION

C %	Mn %	P %	S %	Si %	Cu %	Ni %	Cr %	Mo %	Sn %	V %	CEqyA706 %
0.35	0.58	0.009	0.071	0.16	0.26	0.10	0.08	0.020	0.005	0.003	0.47

MECHANICAL PROPERTIES

YS PSI	YS MPa	UTS PSI	UTS MPa	G/L Inch	G/L mm
78700	543	99350	685	8.000	200.0

MECHANICAL PROPERTIES

Elong. %	BendTest
11.80	OK

GEOMETRIC CHARACTERISTICS

%Light %	Def Hgt Inch	Def Gap Inch	DefSpace Inch
4.39	0.051	0.124	0.477

COMMENTS / NOTES

.45

The above figures are certified chemical and physical test records as contained in the permanent records of company. We certify that these data are correct and in compliance with specified requirements. This material, including the billets, was melted and manufactured in the USA. CMTR complies with EN 10204 3.1.

Bhaskar
BHASKAR YALAMANCHILI
QUALITY DIRECTOR
Phone: (409) 769-1014 Email: Bhaskar.Yalamanchili@gerdau.com

Jim Hall
JIM HALL
QUALITY ASSURANCE MGR.
Phone: 865-202-5972 Email: Jim.hall@gerdau.com

Figure D-4. ¾-in. Diameter, 36⅛-in. Long Anchor Loop Bar, Test No. WITD-4 (Item No. a5)

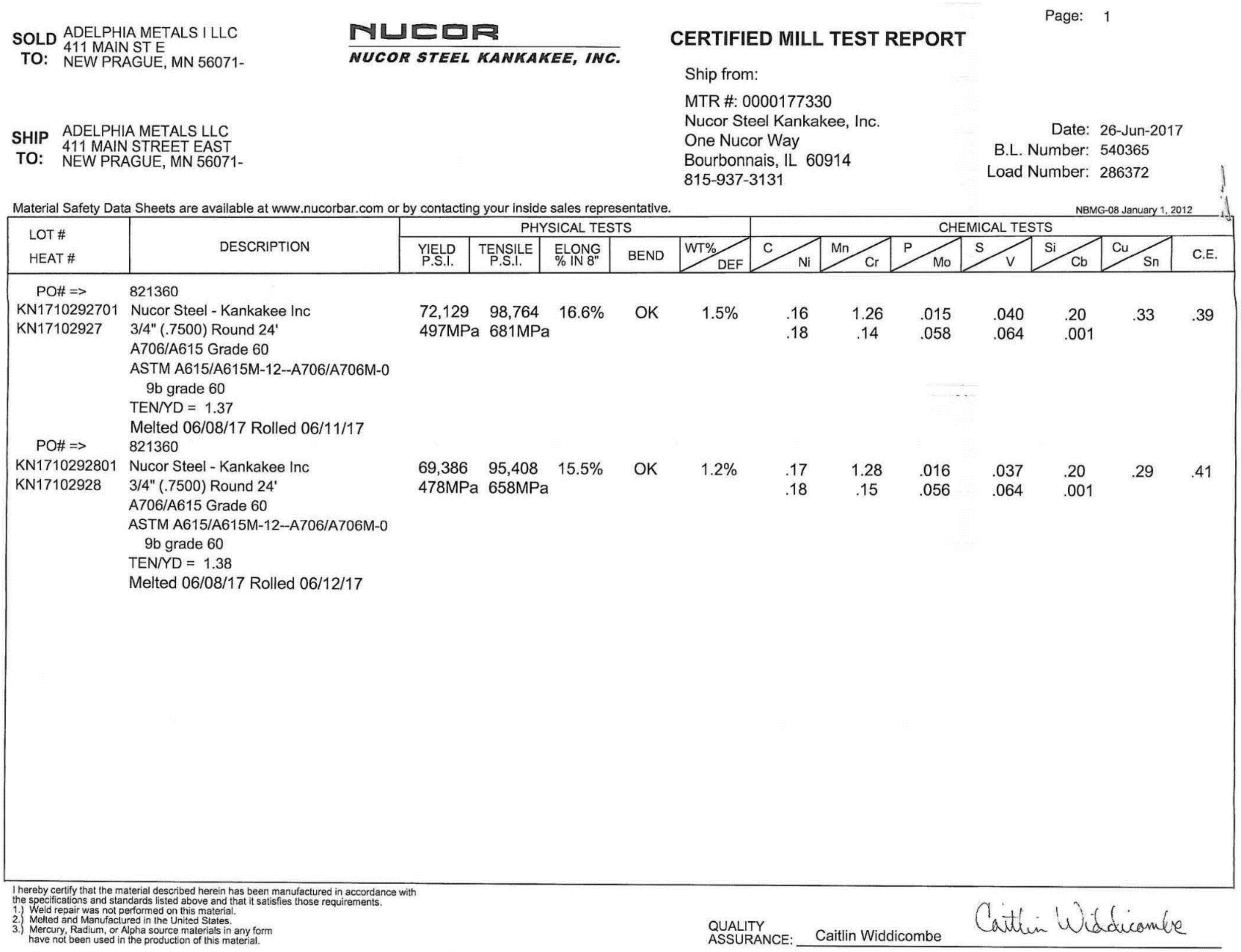

SOLD TO:
ADELPHIA METALS I LLC
411 MAIN ST E
NEW PRAGUE, MN 56071-

NUCOR
NUCOR STEEL KANKAKEE, INC.

CERTIFIED MILL TEST REPORT

Page: 1

Ship from:

MTR #: 0000177330
Nucor Steel Kankakee, Inc.
One Nucor Way
Bourbonnais, IL 60914
815-937-3131

SHIP TO:
ADELPHIA METALS LLC
411 MAIN STREET EAST
NEW PRAGUE, MN 56071-

Date: 26-Jun-2017
B.L. Number: 540365
Load Number: 286372

Material Safety Data Sheets are available at www.nucorbar.com or by contacting your inside sales representative.

NBMG-08 January 1, 2012

LOT # HEAT #	DESCRIPTION	PHYSICAL TESTS					CHEMICAL TESTS						
		YIELD P.S.I.	TENSILE P.S.I.	ELONG % IN 8"	BEND	WT% / DEF	C / Ni	Mn / Cr	P / Mo	S / V	Si / Cb	Cu / Sn	C.E.
PO# => KN1710292701 KN17102927	821360 Nucor Steel - Kankakee Inc 3/4" (.7500) Round 24' A706/A615 Grade 60 ASTM A615/A615M-12--A706/A706M-0 9b grade 60 TEN/YD = 1.37 Melted 06/08/17 Rolled 06/11/17	72,129 497MPa	98,764 681MPa	16.6%	OK	1.5%	.16 .18	1.26 .14	.015 .058	.040 .064	.20 .001	.33	.39
PO# => KN1710292801 KN17102928	821360 Nucor Steel - Kankakee Inc 3/4" (.7500) Round 24' A706/A615 Grade 60 ASTM A615/A615M-12--A706/A706M-0 9b grade 60 TEN/YD = 1.38 Melted 06/08/17 Rolled 06/12/17	69,386 478MPa	95,408 658MPa	15.5%	OK	1.2%	.17 .18	1.28 .15	.016 .056	.037 .064	.20 .001	.29	.41

I hereby certify that the material described herein has been manufactured in accordance with the specifications and standards listed above and that it satisfies those requirements.
1.) Weld repair was not performed on this material.
2.) Melted and Manufactured in the United States.
3.) Mercury, Radium, or Alpha source materials in any form have not been used in the production of this material.

QUALITY ASSURANCE: Caitlin Widdicombe Caitlin Widdicombe

Figure D-5. ¾-in. Diameter, Connection Loop Bar, Test No. WITD-4 (Item Nos. a6, a7, and a8)

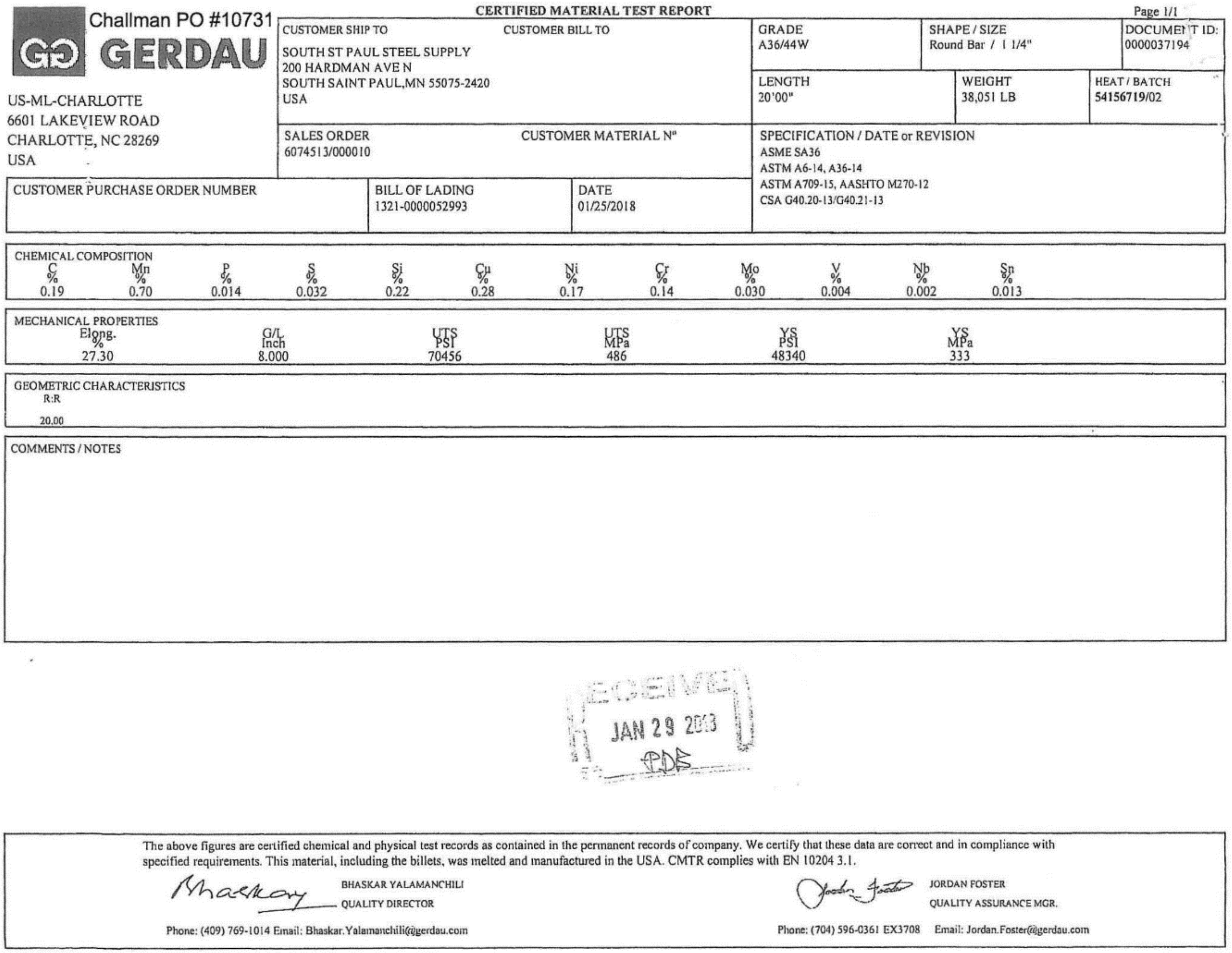

Challman PO #10731

GERDAU

US-ML-CHARLOTTE
6601 LAKEVIEW ROAD
CHARLOTTE, NC 28269
USA

CERTIFIED MATERIAL TEST REPORT

Page 1/1

CUSTOMER SHIP TO SOUTH ST PAUL STEEL SUPPLY 200 HARDMAN AVE N SOUTH SAINT PAUL,MN 55075-2420 USA	CUSTOMER BILL TO	GRADE A36/44W	SHAPE / SIZE Round Bar / 1 1/4"	DOCUMENT ID: 0000037194
		LENGTH 20'00"	WEIGHT 38,051 LB	HEAT / BATCH 54156719/02
SALES ORDER 6074513/000010	CUSTOMER MATERIAL N°	SPECIFICATION / DATE or REVISION ASME SA36 ASTM A6-14, A36-14 ASTM A709-15, AASHTO M270-12 CSA G40.20-13/G40.21-13		

CUSTOMER PURCHASE ORDER NUMBER	BILL OF LADING	DATE
	1321-0000052993	01/25/2018

CHEMICAL COMPOSITION

C %	Mn %	P %	S %	Si %	Cu %	Ni %	Cr %	Mo %	V %	Nb %	Sn %
0.19	0.70	0.014	0.032	0.22	0.28	0.17	0.14	0.030	0.004	0.002	0.013

MECHANICAL PROPERTIES

Elong. %	G/L Inch	UTS PSI	UTS MPa	YS PSI	YS MPa
27.30	8.000	70456	486	48340	333

GEOMETRIC CHARACTERISTICS

R:R
20.00

COMMENTS / NOTES

The above figures are certified chemical and physical test records as contained in the permanent records of company. We certify that these data are correct and in compliance with specified requirements. This material, including the billets, was melted and manufactured in the USA. CMTR complies with EN 10204 3.1.

Bhaskar
BHASKAR YALAMANCHILI
QUALITY DIRECTOR
Phone: (409) 769-1014 Email: Bhaskar.Yalamanchili@gerdau.com

Jordan Foster
JORDAN FOSTER
QUALITY ASSURANCE MGR.
Phone: (704) 596-0361 EX3708 Email: Jordan.Foster@gerdau.com

Figure D-6. 1¼-in. Diameter, 28-in. Long Connector Pin, Test No. WITD-4 (Item No. a9)

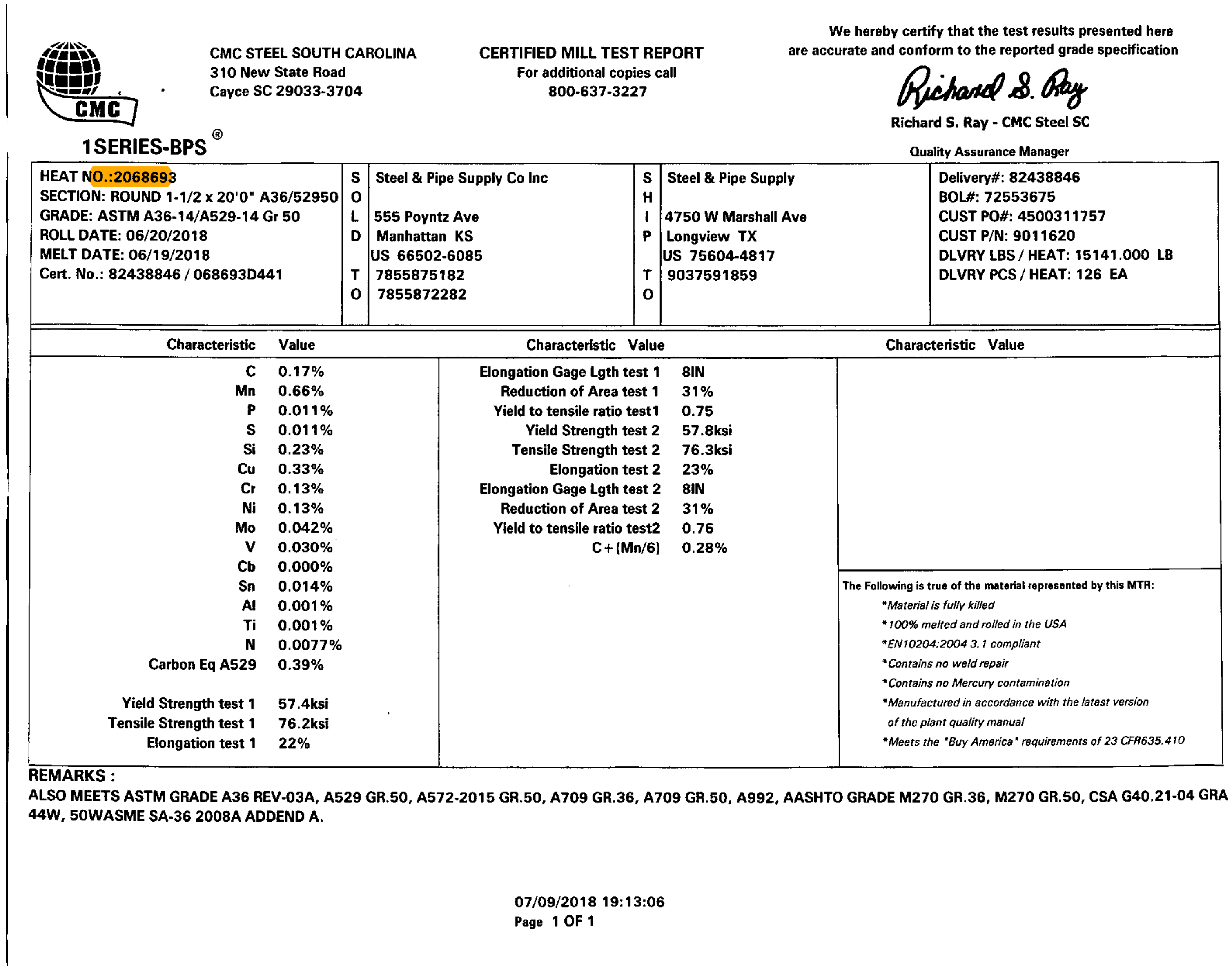

CMC STEEL SOUTH CAROLINA
310 New State Road
Cayce SC 29033-3704

CERTIFIED MILL TEST REPORT
For additional copies call
800-637-3227

We hereby certify that the test results presented here are accurate and conform to the reported grade specification

Richard S. Ray
Richard S. Ray - CMC Steel SC
Quality Assurance Manager

1SERIES-BPS ®

HEAT NO.:2068693
SECTION: ROUND 1-1/2 x 20'0" A36/52950
GRADE: ASTM A36-14/A529-14 Gr 50
ROLL DATE: 06/20/2018
MELT DATE: 06/19/2018
Cert. No.: 82438846 / 068693D441

SOLD TO:
Steel & Pipe Supply Co Inc
555 Poyntz Ave
Manhattan KS
US 66502-6085
7855875182
7855872282

SHIP TO:
Steel & Pipe Supply
4750 W Marshall Ave
Longview TX
US 75604-4817
9037591859

Delivery#: 82438846
BOL#: 72553675
CUST PO#: 4500311757
CUST P/N: 9011620
DLVRY LBS / HEAT: 15141.000 LB
DLVRY PCS / HEAT: 126 EA

Characteristic	Value	Characteristic	Value	Characteristic	Value
C	0.17%	Elongation Gage Lgth test 1	8IN		
Mn	0.66%	Reduction of Area test 1	31%		
P	0.011%	Yield to tensile ratio test1	0.75		
S	0.011%	Yield Strength test 2	57.8ksi		
Si	0.23%	Tensile Strength test 2	76.3ksi		
Cu	0.33%	Elongation test 2	23%		
Cr	0.13%	Elongation Gage Lgth test 2	8IN		
Ni	0.13%	Reduction of Area test 2	31%		
Mo	0.042%	Yield to tensile ratio test2	0.76		
V	0.030%	C+(Mn/6)	0.28%		
Cb	0.000%				
Sn	0.014%				
Al	0.001%				
Ti	0.001%				
N	0.0077%				
Carbon Eq A529	0.39%				
Yield Strength test 1	57.4ksi				
Tensile Strength test 1	76.2ksi				
Elongation test 1	22%				

The Following is true of the material represented by this MTR:

**Material is fully killed*
**100% melted and rolled in the USA*
**EN10204:2004 3.1 compliant*
**Contains no weld repair*
**Contains no Mercury contamination*
**Manufactured in accordance with the latest version of the plant quality manual*
**Meets the "Buy America" requirements of 23 CFR635.410*

REMARKS :
ALSO MEETS ASTM GRADE A36 REV-03A, A529 GR.50, A572-2015 GR.50, A709 GR.36, A709 GR.50, A992, AASHTO GRADE M270 GR.36, M270 GR.50, CSA G40.21-04 GRA 44W, 50WASME SA-36 2008A ADDEND A.

07/09/2018 19:13:06
Page 1 OF 1

Figure D-7. 1¼-in. Diameter, 31¼-in. Long Anchor Pin, Test No. WITD-4 (Item No. b1)

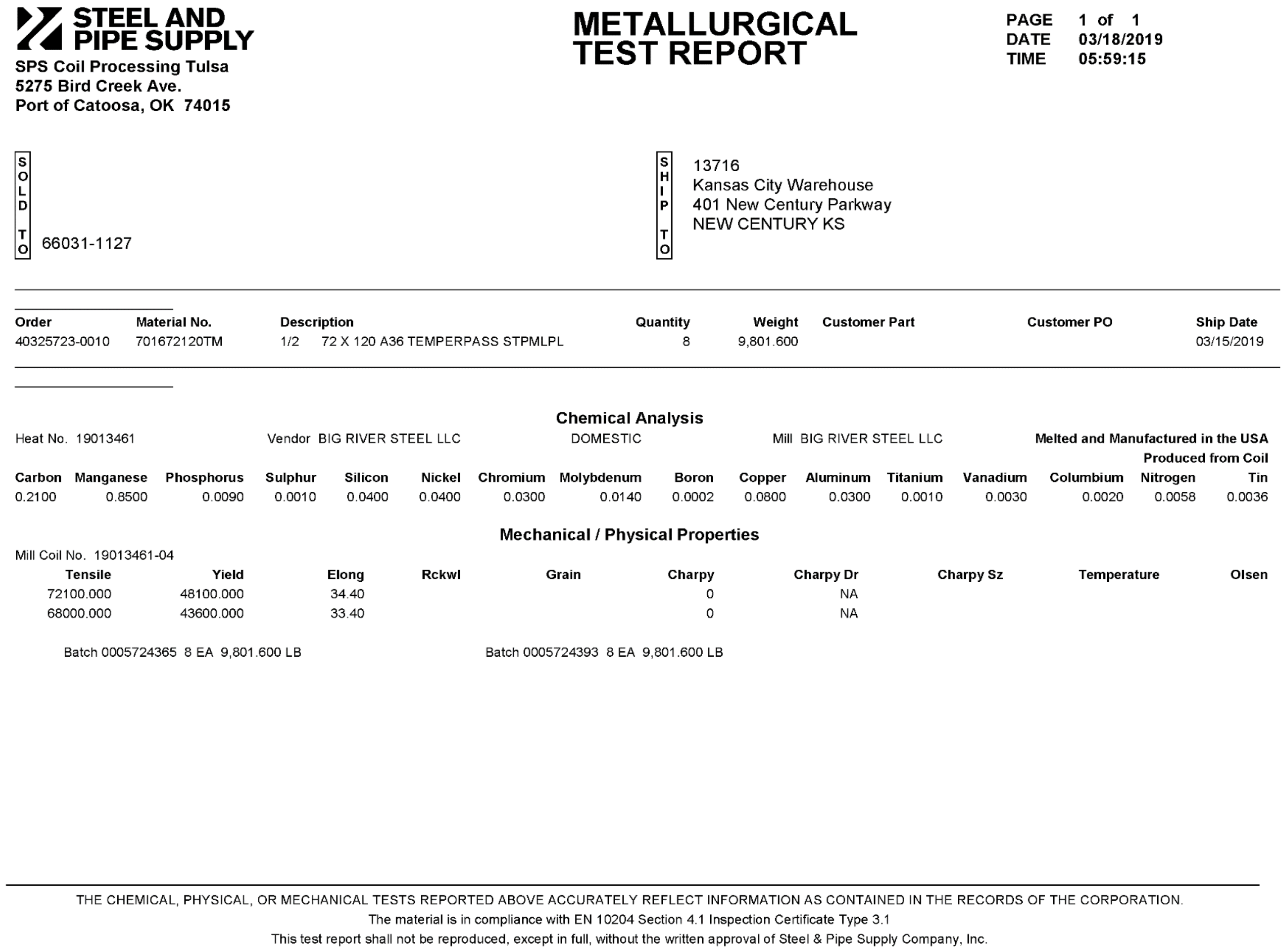

STEEL AND PIPE SUPPLY
SPS Coil Processing Tulsa
5275 Bird Creek Ave.
Port of Catoosa, OK 74015

METALLURGICAL TEST REPORT

PAGE 1 of 1
DATE 03/18/2019
TIME 05:59:15

SOLD TO
66031-1127

SHIP TO
13716
Kansas City Warehouse
401 New Century Parkway
NEW CENTURY KS

Order	Material No.	Description	Quantity	Weight	Customer Part	Customer PO	Ship Date
40325723-0010	701672120TM	1/2 72 X 120 A36 TEMPERPASS STPMLPL	8	9,801.600			03/15/2019

Chemical Analysis

Heat No. 19013461 Vendor BIG RIVER STEEL LLC DOMESTIC Mill BIG RIVER STEEL LLC **Melted and Manufactured in the USA**
Produced from Coil

Carbon	Manganese	Phosphorus	Sulphur	Silicon	Nickel	Chromium	Molybdenum	Boron	Copper	Aluminum	Titanium	Vanadium	Columbium	Nitrogen	Tin
0.2100	0.8500	0.0090	0.0010	0.0400	0.0400	0.0300	0.0140	0.0002	0.0800	0.0300	0.0010	0.0030	0.0020	0.0058	0.0036

Mechanical / Physical Properties

Mill Coil No. 19013461-04

Tensile	Yield	Elong	Rckwl	Grain	Charpy	Charpy Dr	Charpy Sz	Temperature	Olsen
72100.000	48100.000	34.40			0	NA			
68000.000	43600.000	33.40			0	NA			

Batch 0005724365 8 EA 9,801.600 LB Batch 0005724393 8 EA 9,801.600 LB

THE CHEMICAL, PHYSICAL, OR MECHANICAL TESTS REPORTED ABOVE ACCURATELY REFLECT INFORMATION AS CONTAINED IN THE RECORDS OF THE CORPORATION.
The material is in compliance with EN 10204 Section 4.1 Inspection Certificate Type 3.1
This test report shall not be reproduced, except in full, without the written approval of Steel & Pipe Supply Company, Inc.

Figure D-8. 3-in. x 3-in. x ½-in. Washer Plate, Test No. WITD-3 (Item No. b2)

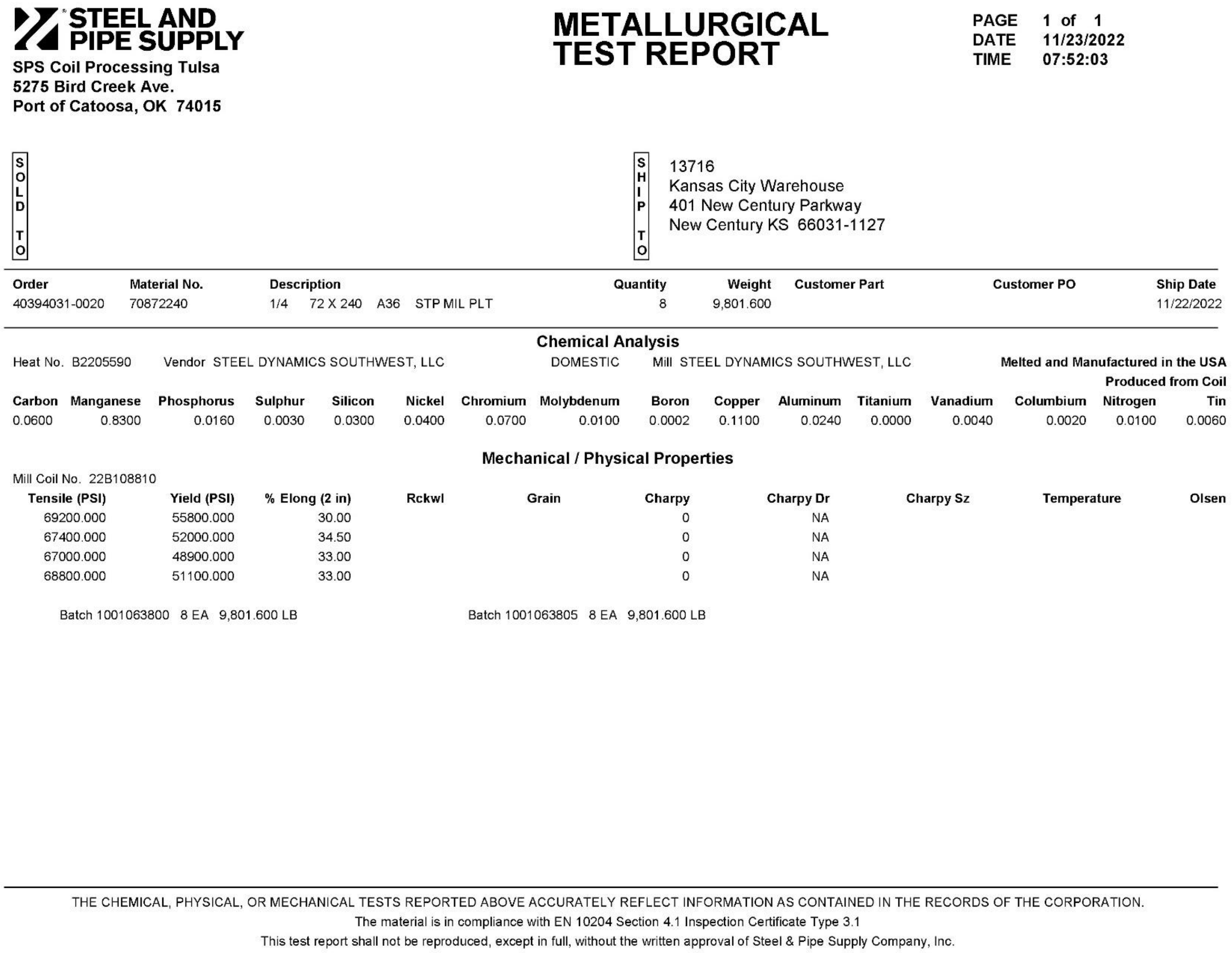

STEEL AND PIPE SUPPLY
SPS Coil Processing Tulsa
5275 Bird Creek Ave.
Port of Catoosa, OK 74015

METALLURGICAL TEST REPORT

PAGE 1 of 1
DATE 11/23/2022
TIME 07:52:03

SOLD TO

SHIP TO
13716
Kansas City Warehouse
401 New Century Parkway
New Century KS 66031-1127

Order	Material No.	Description	Quantity	Weight	Customer Part	Customer PO	Ship Date
40394031-0020	70872240	1/4 72 X 240 A36 STP MIL PLT	8	9,801.600			11/22/2022

Chemical Analysis

Heat No. B2205590 Vendor STEEL DYNAMICS SOUTHWEST, LLC DOMESTIC Mill STEEL DYNAMICS SOUTHWEST, LLC **Melted and Manufactured in the USA**
Produced from Coil

Carbon	Manganese	Phosphorus	Sulphur	Silicon	Nickel	Chromium	Molybdenum	Boron	Copper	Aluminum	Titanium	Vanadium	Columbium	Nitrogen	Tin
0.0600	0.8300	0.0160	0.0030	0.0300	0.0400	0.0700	0.0100	0.0002	0.1100	0.0240	0.0000	0.0040	0.0020	0.0100	0.0060

Mechanical / Physical Properties

Mill Coil No. 22B108810

Tensile (PSI)	Yield (PSI)	% Elong (2 in)	Rckwl	Grain	Charpy	Charpy Dr	Charpy Sz	Temperature	Olsen
69200.000	55800.000	30.00			0	NA			
67400.000	52000.000	34.50			0	NA			
67000.000	48900.000	33.00			0	NA			
68800.000	51100.000	33.00			0	NA			

Batch 1001063800 8 EA 9,801.600 LB

Batch 1001063805 8 EA 9,801.600 LB

THE CHEMICAL, PHYSICAL, OR MECHANICAL TESTS REPORTED ABOVE ACCURATELY REFLECT INFORMATION AS CONTAINED IN THE RECORDS OF THE CORPORATION.
The material is in compliance with EN 10204 Section 4.1 Inspection Certificate Type 3.1
This test report shall not be reproduced, except in full, without the written approval of Steel & Pipe Supply Company, Inc.

Figure D-9. 40$^{5}/_{16}$-in. x 12-in. x ¼-in. Saddle Cap, Test No. WITD-4 (Item No. b3)

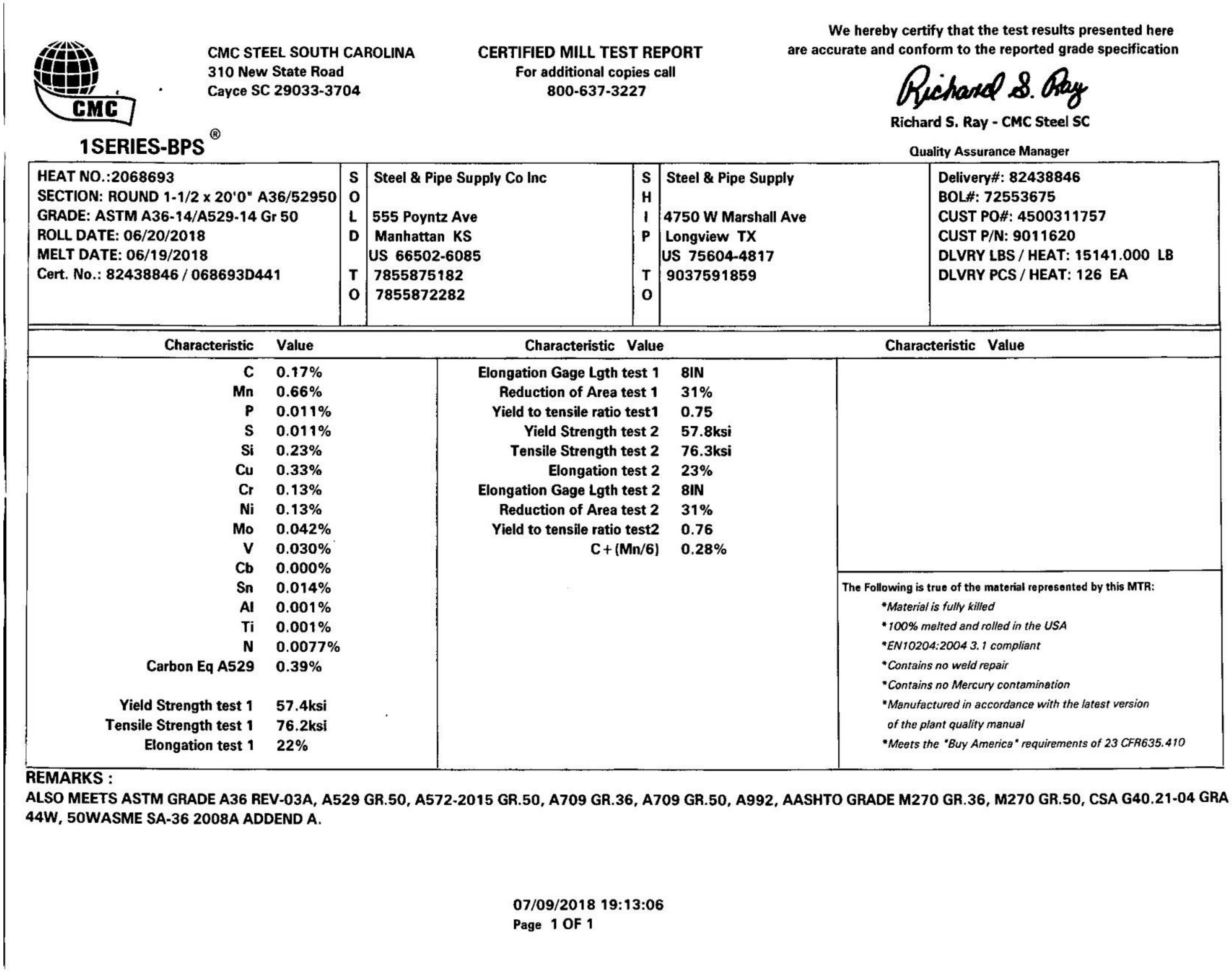

CMC

CMC STEEL SOUTH CAROLINA
310 New State Road
Cayce SC 29033-3704

CERTIFIED MILL TEST REPORT
For additional copies call
800-637-3227

We hereby certify that the test results presented here are accurate and conform to the reported grade specification

Richard S. Ray
Richard S. Ray - CMC Steel SC
Quality Assurance Manager

1SERIES-BPS®

HEAT NO.:2068693 SECTION: ROUND 1-1/2 x 20'0" A36/52950 GRADE: ASTM A36-14/A529-14 Gr 50 ROLL DATE: 06/20/2018 MELT DATE: 06/19/2018 Cert. No.: 82438846 / 068693D441	SOLD TO Steel & Pipe Supply Co Inc 555 Poyntz Ave Manhattan KS US 66502-6085 7855875182 7855872282	SHIP TO Steel & Pipe Supply 4750 W Marshall Ave Longview TX US 75604-4817 9037591859	Delivery#: 82438846 BOL#: 72553675 CUST PO#: 4500311757 CUST P/N: 9011620 DLVRY LBS / HEAT: 15141.000 LB DLVRY PCS / HEAT: 126 EA

Characteristic	Value	Characteristic	Value	Characteristic	Value
C	0.17%	Elongation Gage Lgth test 1	8IN		
Mn	0.66%	Reduction of Area test 1	31%		
P	0.011%	Yield to tensile ratio test1	0.75		
S	0.011%	Yield Strength test 2	57.8ksi		
Si	0.23%	Tensile Strength test 2	76.3ksi		
Cu	0.33%	Elongation test 2	23%		
Cr	0.13%	Elongation Gage Lgth test 2	8IN		
Ni	0.13%	Reduction of Area test 2	31%		
Mo	0.042%	Yield to tensile ratio test2	0.76		
V	0.030%	C+(Mn/6)	0.28%		
Cb	0.000%				
Sn	0.014%				
Al	0.001%				
Ti	0.001%				
N	0.0077%				
Carbon Eq A529	0.39%				
Yield Strength test 1	57.4ksi				
Tensile Strength test 1	76.2ksi				
Elongation test 1	22%				

The Following is true of the material represented by this MTR:
**Material is fully killed*
**100% melted and rolled in the USA*
**EN10204:2004 3.1 compliant*
**Contains no weld repair*
**Contains no Mercury contamination*
**Manufactured in accordance with the latest version of the plant quality manual*
**Meets the "Buy America" requirements of 23 CFR635.410*

REMARKS :
ALSO MEETS ASTM GRADE A36 REV-03A, A529 GR.50, A572-2015 GR.50, A709 GR.36, A709 GR.50, A992, AASHTO GRADE M270 GR.36, M270 GR.50, CSA G40.21-04 GRA 44W, 50WASME SA-36 2008A ADDEND A.

07/09/2018 19:13:06
Page 1 OF 1

Figure D-10. 1½-in. Dia., 38½-in. Long Anchor Pin, Test No. WITD-4 (Item No. c1)

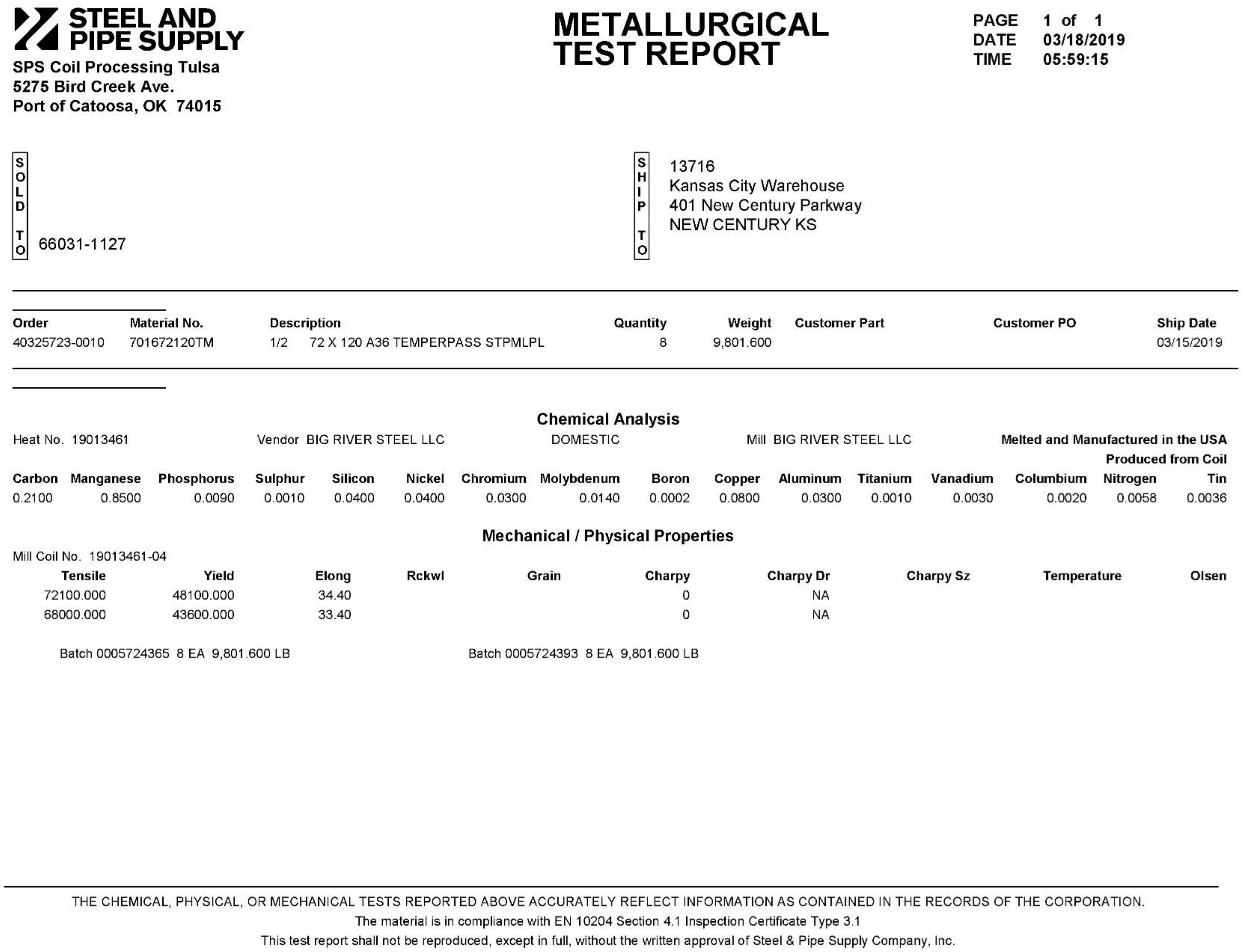

STEEL AND PIPE SUPPLY
SPS Coil Processing Tulsa
5275 Bird Creek Ave.
Port of Catoosa, OK 74015

METALLURGICAL TEST REPORT

PAGE 1 of 1
DATE 03/18/2019
TIME 05:59:15

SOLD TO
66031-1127

SHIP TO
13716
Kansas City Warehouse
401 New Century Parkway
NEW CENTURY KS

Order	Material No.	Description	Quantity	Weight	Customer Part	Customer PO	Ship Date
40325723-0010	701672120TM	1/2 72 X 120 A36 TEMPERPASS STPMLPL	8	9,801.600			03/15/2019

Chemical Analysis

Heat No. 19013461 Vendor BIG RIVER STEEL LLC DOMESTIC Mill BIG RIVER STEEL LLC **Melted and Manufactured in the USA**
Produced from Coil

Carbon	Manganese	Phosphorus	Sulphur	Silicon	Nickel	Chromium	Molybdenum	Boron	Copper	Aluminum	Titanium	Vanadium	Columbium	Nitrogen	Tin
0.2100	0.8500	0.0090	0.0010	0.0400	0.0400	0.0300	0.0140	0.0002	0.0800	0.0300	0.0010	0.0030	0.0020	0.0058	0.0036

Mechanical / Physical Properties

Mill Coil No. 19013461-04

Tensile	Yield	Elong	Rckwl	Grain	Charpy	Charpy Dr	Charpy Sz	Temperature	Olsen
72100.000	48100.000	34.40			0	NA			
68000.000	43600.000	33.40			0	NA			

Batch 0005724365 8 EA 9,801.600 LB Batch 0005724393 8 EA 9,801.600 LB

THE CHEMICAL, PHYSICAL, OR MECHANICAL TESTS REPORTED ABOVE ACCURATELY REFLECT INFORMATION AS CONTAINED IN THE RECORDS OF THE CORPORATION.
The material is in compliance with EN 10204 Section 4.1 Inspection Certificate Type 3.1
This test report shall not be reproduced, except in full, without the written approval of Steel & Pipe Supply Company, Inc.

Figure D-11. 3-in. x 3-in. x ½-in. Washer Plate, Test No. WITD-4 (Item No. c2)

Project: City of Lincoln 84th & Havelock
Date: April 5, 2019
Type Mix: SLX
Sample ID: Cather SLX Field Verification Testing
Lab No. 43224
Date Produced:
N initial ☐ N design 50 N Max. ☐

Maximum Specific Gravity (Gmm)

Laboratory Number			
Sample + pycometer in Air	a	4019.0	
Pycometer in Air	b	2018.8	
Dry Wt. Sample **(A)** **(a-b)**	A	2000.2	
Test Temperature	d	77	***Must be 77 F***
Sample + pycometer under Water, gms	C	2458.7	
Pycometer under water, gm.	B	1274.83	
Theoretical Maximum Specific Gravity **(Gmm)**	Gmm	2.450	

Gyratory Specimen Data (Gmb)

Sample ID		#1	#2	#3
Weight in Air	L	4,754.0		
Weight in Water	M	2,749.2		
Weight SSD in Air	N	4,758.5		
Volume (N-M)	O	2,009.3	-	-
Gmb Measured (L/O)	P	2.366	#DIV/0!	#DIV/0!
Height @ N ini	Q	115.40		
Height @ N des	R	115.40		
Height @ N Max	S	115.40		

	Avg			
Gmb @ Nini	2.366	2.366	-	-
Gmb @Ndes	2.366	2.366	-	-
Gmb @ Nmax	2.366	2.366	-	-

Bulk Specific Gravity of Asphalt Cement **(Gb)**	1.028	
Bulk Specific Gravity of Combined Aggregate **(Gsb)**	2.577	
Bulk Specific Gravity of Coarse Aggregate **(Gsb)**	2.644	
Bulk Specific Gravity of Fine Aggregate **(Gsb)**	2.558	
Bulk Specific Gravity of FAA **(Gsb)**	2.580	

		Spec.
Avg % Voids @ Nini	3.4	
Avg % Voids @ Ndes	3.4	3% +/- 1%
Avg % Voids @ Nmax	3.4	
VMA	13.16	16min
VFA	73.88	n/a
Fine Aggregate Angularity (2.580 Gsb)	43.40	43min
Coarse Aggregate Angularity (1 Face / 2 Face)	99/98	n/a
Sand Equivalent	75	45min

Mix Correction	0	
Total Sample + Trays before Ignition	4880.8	
Weight of Trays	2860.2	
Total Weight of Sample before Ignition	2020.6	
Total Weight of Sample after Ignition	4771	
Corrected Weight of Sample after Ignition	1910.8	
Percent Asphalt Cement by Mixture	**5.43**	5.3min
Weight of Seive anslysis sample prior to washing	1905.5	

Design:

22% 3/8" LS Chips
33% 3A CSG
10% LS Man Sand
30% RAP
5% RAS
5.7% PG 64-34

Sieve Designation	1"	3/4"	1/2'	3/8"	#4	#8	#16	#30	#50	#100	#200
Weight Retained	0	0	11.5	41.3	499.8	1045	1363.4	1530.6	1594.2	1712.9	1758.1
% Retained		0.0	0.6	2.2	26.2	54.8	71.6	80.3	83.7	89.9	92.3
% Passing		100.0	99.4	97.8	73.8	45.2	28.4	19.7	16.3	10.1	7.7
Specifications			**98-100**	**93-100**	**70-87**	**45-65**	**25-41**	**15-31**	**10-21**		**4-10**

Figure D-12. Asphalt Pad, Test No. WITD-4 (Item No. d1)

Appendix E. Vehicle Deformation Records

The following figures and tables describe all occupant compartment measurements taken on the test vehicles used in full-scale crash testing herein. MASH defines intrusion as the occupant compartment being deformed and reduced in size with no penetration. Outward deformations, which are denoted as negative numbers within this appendix, are not considered as crush toward the occupant, and are not subject to evaluation by MASH criteria.

Model Year: 2017

Test Name: WITD-4

Make: Dodge

VIN: 3C6RR6KT2JG118353

Model: Ram 1500

VEHICLE DEFORMATION
DRIVER SIDE FLOOR PAN - SET 1

	POINT	Pretest X (in.)	Pretest Y (in.)	Pretest Z (in.)	Posttest X (in.)	Posttest Y (in.)	Posttest Z (in.)	ΔX[A] (in.)	ΔY[A] (in.)	ΔZ[A] (in.)	Total Δ (in.)	Crush[B] (in.)	Directions for Crush[C]
TOE PAN - WHEEL WELL (X, Z)	1	61.7729	-42.8584	-5.1653	60.8762	-42.7960	-5.2851	0.8967	0.0624	0.1198	0.9068	0.9047	X, Z
	2	62.9726	-39.5201	-4.4080	61.3869	-39.1448	-5.1332	1.5857	0.3753	0.7252	1.7836	1.7437	X, Z
	3	60.7753	-34.5490	-2.7415	60.1938	-34.3916	-2.6673	0.5815	0.1574	-0.0742	0.6070	0.5815	X
	4	60.7337	-29.0372	-2.6034	60.7168	-28.8504	-2.2061	0.0169	0.1868	-0.3973	0.4393	0.0169	X
	5	58.5261	-23.0966	-3.5451	58.5170	-23.0764	-3.3112	0.0091	0.0202	-0.2339	0.2349	0.0091	X
	6	56.1832	-43.5459	-0.1761	56.1285	-43.3760	0.1840	0.0547	0.1699	-0.3601	0.4019	0.0547	X
	7	56.3235	-38.3185	-0.1852	56.2270	-38.1459	0.0693	0.0965	0.1726	-0.2545	0.3223	0.0965	X
	8	56.3893	-33.0187	-0.1335	56.3534	-32.8810	0.2045	0.0359	0.1377	-0.3380	0.3667	0.0359	X
	9	56.6585	-27.8688	-0.1855	56.6454	-27.7805	0.1239	0.0131	0.0883	-0.3094	0.3220	0.0131	X
	10	55.0510	-23.4873	-2.0948	54.9764	-23.4506	-1.8669	0.0746	0.0367	-0.2279	0.2426	0.0746	X
FLOOR PAN (Z)	11	52.1258	-42.8556	0.6846	52.0685	-42.7060	1.0694	0.0573	0.1496	-0.3848	0.4168	-0.3848	Z
	12	52.6462	-38.2909	0.7405	52.6259	-38.1235	1.1365	0.0203	0.1674	-0.3960	0.4304	-0.3960	Z
	13	52.2999	-33.3283	0.8251	52.2400	-33.1727	1.1454	0.0599	0.1556	-0.3203	0.3611	-0.3203	Z
	14	52.2581	-27.9115	0.8933	52.1845	-27.7213	1.1872	0.0736	0.1902	-0.2939	0.3577	-0.2939	Z
	15	51.1419	-23.7533	-1.3807	51.0930	-23.6884	-1.1991	0.0489	0.0649	-0.1816	0.1990	-0.1816	Z
	16	47.9783	-42.7274	0.7072	47.9442	-42.6323	1.0802	0.0341	0.0951	-0.3730	0.3864	-0.3730	Z
	17	47.8758	-38.1354	0.7362	47.8293	-38.0414	1.1013	0.0465	0.0940	-0.3651	0.3799	-0.3651	Z
	18	48.3270	-33.9815	0.8027	48.2997	-33.8514	1.1102	0.0273	0.1301	-0.3075	0.3350	-0.3075	Z
	19	47.6276	-28.3601	0.8863	47.5656	-28.2261	1.1705	0.0620	0.1340	-0.2842	0.3203	-0.2842	Z
	20	48.0216	-23.7094	-1.4676	47.9727	-23.6470	-1.3062	0.0489	0.0624	-0.1614	0.1798	-0.1614	Z
	21	42.1156	-42.7347	0.7044	42.1315	-42.5832	1.0291	-0.0159	0.1515	-0.3247	0.3587	-0.3247	Z
	22	43.0951	-37.8101	0.7580	43.0452	-37.7296	1.0861	0.0499	0.0805	-0.3281	0.3415	-0.3281	Z
	23	43.4813	-32.9966	0.8156	43.1630	-32.7631	1.0952	0.3183	0.2335	-0.2796	0.4837	-0.2796	Z
	24	43.2028	-28.2219	0.8954	43.1231	-28.1699	1.1546	0.0797	0.0520	-0.2592	0.2761	-0.2592	Z
	25	43.7566	-23.7689	-1.9107	43.6758	-23.7724	-1.5970	0.0808	-0.0035	-0.3137	0.3240	-0.3137	Z
	26	38.2727	-43.2893	-0.2829	38.2454	-43.1322	0.0652	0.0273	0.1571	-0.3481	0.3829	-0.3481	Z
	27	38.3019	-38.2150	-0.2237	38.2821	-38.1022	0.0833	0.0198	0.1128	-0.3070	0.3277	-0.3070	Z
	28	38.3571	-33.7866	-0.1688	38.3448	-33.6561	0.1001	0.0123	0.1305	-0.2689	0.2991	-0.2689	Z
	29	38.2391	-27.8611	0.1216	38.1809	-27.7560	0.3479	0.0582	0.1051	-0.2263	0.2562	-0.2263	Z
	30	38.4733	-23.7701	-1.4412	38.3729	-23.7409	-1.1931	0.1004	0.0292	-0.2481	0.2692	-0.2481	Z

[A] Positive values denote deformation as inward toward the occupant compartment, negative values denote deformations outward away from the occupant compartment.

[B] Crush calculations that use multiple directional components will disregard components that are negative and only include positive values where the component is deforming inward toward the occupant compartment.

[C] Direction for Crush column denotes which directions are included in the crush calculations. If "NA" then no intrusion is recorded, and Crush will be 0.

Pretest Floor Pan

Posttest Floor Pan

Figure E-1. Floor Pan Deformation Data – Set 1, Test No. WITD-4

Test Name: WITD-4
VIN: 3C6RR6KT2JG118353
Model Year: 2017
Make: Dodge
Model: Ram 1500

VEHICLE DEFORMATION
DRIVER SIDE FLOOR PAN - SET 2

	POINT	Pretest X (in.)	Pretest Y (in.)	Pretest Z (in.)	Posttest X (in.)	Posttest Y (in.)	Posttest Z (in.)	ΔX[A] (in.)	ΔY[A] (in.)	ΔZ[A] (in.)	Total Δ (in.)	Crush[B] (in.)	Directions for Crush[C]
TOE PAN - WHEEL WELL (X, Z)	1	60.1843	-28.6800	-0.2064	59.2406	-28.7744	-0.3470	0.9437	-0.0944	0.1406	0.9588	0.9541	X, Z
	2	61.3711	-25.3399	0.5633	59.7529	-25.1244	-0.1735	1.6182	0.2155	0.7368	1.7911	1.7780	X, Z
	3	59.1486	-20.3711	2.2035	58.5325	-20.3799	2.2958	0.6161	-0.0088	-0.0923	0.6230	0.6161	X
	4	59.0982	-14.8593	2.3395	59.0551	-14.8412	2.7864	0.0431	0.0181	-0.4469	0.4493	0.0431	X
	5	56.8935	-8.9219	1.3711	56.8760	-9.0604	1.6760	0.0175	-0.1385	-0.3049	0.3353	0.0175	X
	6	54.5398	-29.3734	4.7199	54.4209	-29.3714	5.0569	0.1189	0.0020	-0.3370	0.3574	0.1189	X
	7	54.6733	-24.1458	4.7107	54.5262	-24.1410	4.9648	0.1471	0.0048	-0.2541	0.2936	0.1471	X
	8	54.7316	-18.8459	4.7616	54.6563	-18.8768	5.1231	0.0753	-0.0309	-0.3615	0.3705	0.0753	X
	9	54.9945	-13.6956	4.7110	54.9546	-13.7763	5.0671	0.0399	-0.0807	-0.3561	0.3673	0.0399	X
	10	53.4028	-9.3169	2.7824	53.3163	-9.4366	3.0723	0.0865	-0.1197	-0.2899	0.3253	0.0865	X
FLOOR PAN (Z)	11	50.4721	-28.6882	5.5347	50.3503	-28.7006	5.8917	0.1218	-0.0124	-0.3570	0.3774	-0.3570	Z
	12	50.9858	-24.1228	5.5951	50.9115	-24.1190	5.9847	0.0743	0.0038	-0.3896	0.3966	-0.3896	Z
	13	50.6320	-19.1606	5.6742	50.5306	-19.1679	6.0088	0.1014	-0.0073	-0.3346	0.3497	-0.3346	Z
	14	50.5823	-13.7438	5.7403	50.4802	-13.7166	6.0720	0.1021	0.0272	-0.3317	0.3481	-0.3317	Z
	15	49.4862	-9.5878	3.4525	49.4242	-9.6729	3.6880	0.0620	-0.0851	-0.2355	0.2580	-0.2355	Z
	16	46.3245	-28.5655	5.5106	46.2262	-28.6224	5.8486	0.0983	-0.0569	-0.3380	0.3566	-0.3380	Z
	17	46.2156	-23.9736	5.5371	46.1159	-24.0315	5.8870	0.0997	-0.0579	-0.3499	0.3684	-0.3499	Z
	18	46.6605	-19.8191	5.6073	46.5904	-19.8422	5.9191	0.0701	-0.0231	-0.3118	0.3204	-0.3118	Z
	19	45.9528	-14.1986	5.6813	45.8613	-14.2163	5.9927	0.0915	-0.0177	-0.3114	0.3250	-0.3114	Z
	20	46.3671	-9.5480	3.3306	46.3056	-9.6277	3.5402	0.0615	-0.0797	-0.2096	0.2325	-0.2096	Z
	21	40.4621	-28.5805	5.4419	40.4147	-28.5668	5.7215	0.0474	0.0137	-0.2796	0.2839	-0.2796	Z
	22	41.4345	-23.6546	5.5050	41.3327	-23.7145	5.8103	0.1018	-0.0599	-0.3053	0.3274	-0.3053	Z
	23	41.8136	-18.8406	5.5655	41.4555	-18.7482	5.8411	0.3581	0.0924	-0.2756	0.4612	-0.2756	Z
	24	41.5279	-14.0662	5.6406	41.4196	-14.1552	5.9187	0.1083	-0.0890	-0.2781	0.3114	-0.2781	Z
	25	42.1074	-9.6133	2.8395	42.0129	-9.7473	3.1926	0.0945	-0.1340	-0.3531	0.3893	-0.3531	Z
	26	36.6314	-29.1405	4.4116	36.5411	-29.1077	4.7044	0.0903	0.0328	-0.2928	0.3082	-0.2928	Z
	27	36.6531	-24.0662	4.4696	36.5828	-24.0779	4.7435	0.0703	-0.0117	-0.2739	0.2830	-0.2739	Z
	28	36.7019	-19.6376	4.5237	36.6498	-19.6320	4.7793	0.0521	0.0056	-0.2556	0.2609	-0.2556	Z
	29	36.5728	-13.7122	4.8110	36.4888	-13.7327	5.0489	0.0840	-0.0205	-0.2379	0.2531	-0.2379	Z
	30	36.8192	-9.6214	3.2496	36.7051	-9.7116	3.5269	0.1141	-0.0902	-0.2773	0.3131	-0.2773	Z

[A] Positive values denote deformation as inward toward the occupant compartment, negative values denote deformations outward away from the occupant compartment.

[B] Crush calculations that use multiple directional components will disregard components that are negative and only include positive values where the component is deforming inward toward the occupant compartment.

[C] Direction for Crush column denotes which directions are included in the crush calculations. If "NA" then no intrusion is recorded, and Crush will be 0.

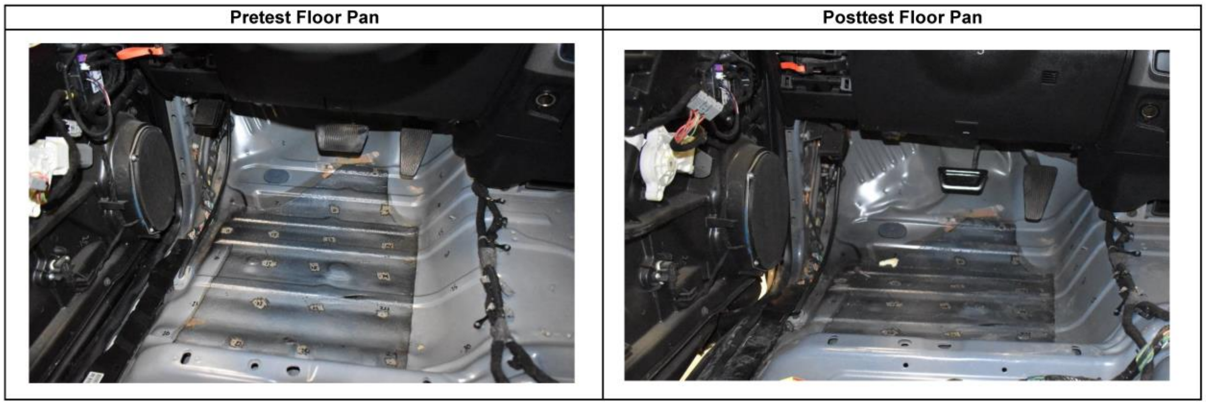

Pretest Floor Pan

Posttest Floor Pan

Figure E-2. Floor Pan Deformation Data – Set 2, Test No. WITD-4

Test Name: WITD-4
VIN: 3C6RR6KT2JG118353
Model Year: 2017
Make: Dodge
Model: Ram 1500

VEHICLE DEFORMATION
DRIVER SIDE INTERIOR CRUSH - SET 1

	POINT	Pretest X (in.)	Pretest Y (in.)	Pretest Z (in.)	Posttest X (in.)	Posttest Y (in.)	Posttest Z (in.)	ΔX[A] (in.)	ΔY[A] (in.)	ΔZ[A] (in.)	Total Δ (in.)	Crush[B] (in.)	Directions for Crush[C]
DASH (X, Y, Z)	1	49.0450	-44.1983	-30.1721	49.0571	-44.3955	-29.8435	-0.0121	-0.1972	0.3286	0.3834	0.3834	X, Y, Z
	2	46.9401	-32.9849	-33.8220	47.0049	-33.2176	-33.5172	-0.0648	-0.2327	0.3048	0.3889	0.3889	X, Y, Z
	3	45.9552	-16.2263	-31.1779	46.0214	-16.4646	-30.9264	-0.0662	-0.2383	0.2515	0.3527	0.3527	X, Y, Z
	4	46.1752	-44.2560	-20.5912	46.1591	-44.3575	-20.2191	0.0161	-0.1015	0.3721	0.3860	0.3860	X, Y, Z
	5	44.1677	-32.9536	-19.8942	44.1641	-33.1745	-19.6959	0.0036	-0.2209	0.1983	0.2969	0.2969	X, Y, Z
	6	43.1394	-17.5564	-20.5409	43.1931	-17.7504	-20.3043	-0.0537	-0.1940	0.2366	0.3106	0.3106	X, Y, Z
SIDE PANEL (Y)	7	55.0952	-46.0081	-8.6337	55.0395	-45.8453	-8.2587	0.0557	0.1628	0.3750	0.4126	0.1628	Y
	8	59.6098	-46.1000	-9.0181	59.6213	-46.0488	-8.6686	-0.0115	0.0512	0.3495	0.3534	0.0512	Y
	9	56.4850	-46.0461	-4.0076	56.4978	-45.8564	-3.7175	-0.0128	0.1897	0.2901	0.3469	0.1897	Y
IMPACT SIDE DOOR (Y)	10	20.6026	-47.8753	-27.2277	20.1182	-48.8738	-27.3685	0.4844	-0.9985	-0.1408	1.1187	-0.9985	Y
	11	30.7555	-47.7773	-27.1420	30.2832	-48.7701	-27.0611	0.4723	-0.9928	0.0809	1.1024	-0.9928	Y
	12	40.7087	-47.5633	-27.1159	40.3010	-48.5335	-26.8787	0.4077	-0.9702	0.2372	1.0788	-0.9702	Y
	13	20.6588	-48.3891	-7.6922	19.7267	-49.2478	-8.1081	0.9321	-0.8587	-0.4159	1.3338	-0.8587	Y
	14	31.2517	-48.8857	-5.6808	30.2757	-49.8022	-5.8913	0.9760	-0.9165	-0.2105	1.3553	-0.9165	Y
	15	41.1073	-49.5862	-5.1302	40.0140	-50.2937	-4.9021	1.0933	-0.7075	0.2281	1.3221	-0.7075	Y
ROOF - (Z)	16	37.3697	-38.7910	-46.5437	37.3543	-39.1585	-46.2947	0.0154	-0.3675	0.2490	0.4442	0.2490	Z
	17	40.0130	-28.7570	-47.1914	40.0533	-29.1428	-46.9651	-0.0403	-0.3858	0.2263	0.4491	0.2263	Z
	18	41.8093	-15.3427	-47.2756	41.8071	-15.7213	-47.1437	0.0022	-0.3786	0.1319	0.4009	0.1319	Z
	19	28.1054	-37.0331	-49.9644	28.1042	-37.4054	-49.6982	0.0012	-0.3723	0.2662	0.4577	0.2662	Z
	20	29.2150	-26.8055	-50.6206	29.2359	-27.1365	-50.3969	-0.0209	-0.3310	0.2237	0.4000	0.2237	Z
	21	30.1348	-17.4675	-50.8118	30.1826	-17.7628	-50.6209	-0.0478	-0.2953	0.1909	0.3549	0.1909	Z
	22	15.3228	-35.6668	-50.8145	15.4357	-35.9627	-50.5759	-0.1129	-0.2959	0.2386	0.3965	0.2386	Z
	23	15.1972	-23.0926	-51.4855	15.2197	-23.3432	-51.3073	-0.0225	-0.2506	0.1782	0.3083	0.1782	Z
	24	15.1261	-15.4643	-51.6106	15.2506	-15.7971	-51.4651	-0.1245	-0.3328	0.1455	0.3840	0.1455	Z
	25	-5.5060	-35.8060	-50.9679	-5.3901	-36.0573	-50.7553	-0.1159	-0.2513	0.2126	0.3490	0.2126	Z
	26	-5.7557	-24.8509	-51.4692	-5.6982	-25.1002	-51.3009	-0.0575	-0.2493	0.1683	0.3062	0.1683	Z
	27	-5.8872	-16.2657	-51.5836	-5.7663	-16.5934	-51.4715	-0.1209	-0.3277	0.1121	0.3668	0.1121	Z
	28	-21.9601	-36.6650	-50.3498	-21.9010	-36.8697	-50.1613	-0.0591	-0.2047	0.1885	0.2845	0.1885	Z
	29	-22.6247	-23.7477	-50.8137	-22.5350	-23.9549	-50.6800	-0.0897	-0.2072	0.1337	0.2624	0.1337	Z
	30	-22.5555	-16.0080	-50.8795	-22.4649	-16.2539	-50.7830	-0.0906	-0.2459	0.0965	0.2793	0.0965	Z
A-PILLAR Maximum (X, Y, Z)	31	53.6022	-44.6584	-33.0451	53.8443	-44.8948	-32.5775	-0.2421	-0.2364	0.4676	0.5772	0.4676	Z
	32	50.1592	-44.0167	-35.4870	50.2833	-44.2833	-35.0828	-0.1241	-0.2666	0.4042	0.4999	0.4042	Z
	33	47.0005	-42.3443	-37.0932	47.0989	-42.5652	-36.7636	-0.0984	-0.2209	0.3296	0.4088	0.3296	Z
	34	43.2716	-41.8631	-40.1430	43.3855	-42.1100	-39.8009	-0.1139	-0.2469	0.3421	0.4370	0.3421	Z
	35	40.3102	-40.7860	-41.6060	40.4970	-40.9943	-41.2763	-0.1868	-0.2083	0.3297	0.4324	0.3297	Z
	36	37.7931	-41.0477	-44.4934	37.9580	-41.3120	-44.1201	-0.1649	-0.2643	0.3733	0.4862	0.3733	Z
A-PILLAR Lateral (Y)	31	53.6022	-44.6584	-33.0451	53.8443	-44.8948	-32.5775	-0.2421	-0.2364	0.4676	0.5772	-0.2364	Y
	32	50.1592	-44.0167	-35.4870	50.2833	-44.2833	-35.0828	-0.1241	-0.2666	0.4042	0.4999	-0.2666	Y
	33	47.0005	-42.3443	-37.0932	47.0989	-42.5652	-36.7636	-0.0984	-0.2209	0.3296	0.4088	-0.2209	Y
	34	43.2716	-41.8631	-40.1430	43.3855	-42.1100	-39.8009	-0.1139	-0.2469	0.3421	0.4370	-0.2469	Y
	35	40.3102	-40.7860	-41.6060	40.4970	-40.9943	-41.2763	-0.1868	-0.2083	0.3297	0.4324	-0.2083	Y
	36	37.7931	-41.0477	-44.4934	37.9580	-41.3120	-44.1201	-0.1649	-0.2643	0.3733	0.4862	-0.2643	Y
B-PILLAR Maximum (X, Y, Z)	37	10.1326	-40.9626	-45.8616	10.1268	-41.1939	-45.6595	0.0058	-0.2313	0.2021	0.3072	0.2022	X, Z
	38	13.6948	-43.0645	-40.0993	13.6956	-43.2657	-39.8370	-0.0008	-0.2012	0.2623	0.3306	0.2623	Z
	39	11.0811	-45.6473	-30.0983	11.0669	-45.6909	-29.8054	0.0142	-0.0436	0.2929	0.2965	0.2932	X, Z
	40	14.9359	-45.8115	-27.4906	14.9136	-45.8592	-27.1563	0.0223	-0.0477	0.3343	0.3384	0.3350	X, Z
B-PILLAR Lateral (Y)	37	10.1326	-40.9626	-45.8616	10.1268	-41.1939	-45.6595	0.0058	-0.2313	0.2021	0.3072	-0.2313	Y
	38	13.6948	-43.0645	-40.0993	13.6956	-43.2657	-39.8370	-0.0008	-0.2012	0.2623	0.3306	-0.2012	Y
	39	11.0811	-45.6473	-30.0983	11.0669	-45.6909	-29.8054	0.0142	-0.0436	0.2929	0.2965	-0.0436	Y
	40	14.9359	-45.8115	-27.4906	14.9136	-45.8592	-27.1563	0.0223	-0.0477	0.3343	0.3384	-0.0477	Y

[A] Positive values denote deformation as inward toward the occupant compartment, negative values denote deformations outward away from the occupant compartment.

[B] Crush calculations that use multiple directional components will disregard components that are negative and only include positive values where the component is deforming inward toward the occupant compartment.

[C] Direction for Crush column denotes which directions are included in the crush calculations. If "NA" then no intrusion is recorded, and Crush will be 0.

Figure E-3. Occupant Compartment Deformation Data – Set 1, Test No. WITD-4

Test Name: WITD-4
VIN: 3C6RR6KT2JG118353
Model Year: 2017
Make: Dodge
Model: Ram 1500

VEHICLE DEFORMATION
DRIVER SIDE INTERIOR CRUSH - SET 2

	POINT	Pretest X (in.)	Pretest Y (in.)	Pretest Z (in.)	Posttest X (in.)	Posttest Y (in.)	Posttest Z (in.)	ΔX[A] (in.)	ΔY[A] (in.)	ΔZ[A] (in.)	Total Δ (in.)	Crush[B] (in.)	Directions for Crush[C]
DASH (X, Y, Z)	1	47.7544	-30.0293	-25.3580	47.7451	-30.2657	-25.0562	0.0093	-0.2364	0.3018	0.3835	0.3835	X, Y, Z
	2	45.6731	-18.8201	-29.0344	45.7516	-19.0722	-28.7147	-0.0785	-0.2521	0.3197	0.4146	0.4146	X, Y, Z
	3	44.6318	-2.0624	-26.4060	44.7496	-2.3281	-26.0744	-0.1178	-0.2657	0.3316	0.4409	0.4409	X, Y, Z
	4	44.7767	-30.0891	-15.8101	44.7210	-30.2607	-15.4706	0.0557	-0.1716	0.3395	0.3845	0.3845	X, Y, Z
	5	42.7436	-18.7898	-15.1387	42.7297	-19.0779	-14.9318	0.0139	-0.2881	0.2069	0.3550	0.3550	X, Y, Z
	6	41.6983	-3.3944	-15.8011	41.7808	-3.6507	-15.4953	-0.0825	-0.2563	0.3058	0.4074	0.4074	X, Y, Z
SIDE PANEL (Y)	7	53.5640	-31.8242	-3.7522	53.4423	-31.8017	-3.4003	0.1217	0.0225	0.3519	0.3730	0.0225	Y
	8	58.0828	-31.9090	-4.0856	58.0289	-32.0082	-3.7507	0.0539	-0.0992	0.3349	0.3534	-0.0992	Y
	9	54.9015	-31.8588	0.8893	54.8408	-31.8312	1.1597	0.0607	0.0276	0.2704	0.2785	0.0276	Y
IMPACT SIDE DOOR (Y)	10	19.2863	-33.7507	-22.7337	18.7721	-34.7252	-22.9780	0.5142	-0.9745	-0.2443	1.1286	-0.9745	Y
	11	29.4375	-33.6365	-22.5335	28.9323	-34.6325	-22.5368	0.5052	-0.9960	-0.0033	1.1168	-0.9960	Y
	12	39.3894	-33.4067	-22.3952	38.9471	-34.4063	-22.2220	0.4423	-0.9996	0.1732	1.1067	-0.9996	Y
	13	19.1230	-34.2594	-3.1987	18.1274	-35.1705	-3.7259	0.9956	-0.9111	-0.5272	1.4489	-0.9111	Y
	14	29.6933	-34.7388	-1.0677	28.6459	-35.7435	-1.3730	1.0474	-1.0047	-0.3053	1.4831	-1.0047	Y
	15	39.5431	-35.4235	-0.4058	38.3699	-36.2481	-0.2578	1.1732	-0.8246	0.1480	1.4416	-0.8246	Y
ROOF - (Z)	16	36.2560	-24.6445	-41.8618	36.2641	-24.9562	-41.6399	-0.0081	-0.3117	0.2219	0.3827	0.2219	Z
	17	38.8905	-14.6065	-42.4822	38.9809	-14.9407	-42.2373	-0.0904	-0.3342	0.2449	0.4241	0.2449	Z
	18	40.6664	-1.1894	-42.5497	40.7493	-1.5203	-42.3428	-0.0829	-0.3309	0.2069	0.3990	0.2069	Z
	19	27.0281	-22.9022	-45.3872	27.0612	-23.1815	-45.1579	-0.0331	-0.2793	0.2293	0.3629	0.2293	Z
	20	28.1289	-12.6730	-46.0336	28.2114	-12.9111	-45.8033	-0.0825	-0.2381	0.2303	0.3414	0.2303	Z
	21	29.0359	-3.3335	-46.2168	29.1696	-3.5375	-45.9798	-0.1337	-0.2040	0.2370	0.3401	0.2370	Z
	22	14.2538	-21.5563	-46.3819	14.4066	-21.7232	-46.1965	-0.1528	-0.1669	0.1854	0.2925	0.1854	Z
	23	14.1159	-8.9825	-47.0576	14.2118	-9.1008	-46.8834	-0.0959	-0.1183	0.1742	0.2314	0.1742	Z
	24	14.0341	-1.3544	-47.1855	14.2518	-1.5543	-47.0127	-0.2177	-0.1999	0.1728	0.3424	0.1728	Z
	25	-6.5717	-21.7285	-46.7702	-6.4151	-21.7970	-46.6496	-0.1566	-0.0685	0.1206	0.2092	0.1206	Z
	26	-6.8331	-10.7740	-47.2772	-6.7060	-10.8376	-47.1582	-0.1271	-0.0636	0.1190	0.1854	0.1190	Z
	27	-6.9769	-2.1891	-47.3953	-6.7640	-2.3301	-47.2979	-0.2129	-0.1410	0.0974	0.2733	0.0974	Z
	28	-23.0303	-22.6135	-46.3375	-22.9331	-22.5956	-46.2753	-0.0972	0.0179	0.0622	0.1168	0.0622	Z
	29	-23.7101	-9.6974	-46.8124	-23.5484	-9.6783	-46.7541	-0.1617	0.0191	0.0583	0.1729	0.0583	Z
	30	-23.6525	-1.9576	-46.8795	-23.4699	-1.9771	-46.8274	-0.1826	-0.0195	0.0521	0.1909	0.0521	Z
A-PILLAR Maximum (X, Y, Z)	31	52.3444	-30.4829	-28.1792	52.5674	-30.7595	-27.7289	-0.2230	-0.2766	0.4503	0.5736	0.4503	Z
	32	48.9281	-29.8472	-30.6600	49.0401	-30.1352	-30.2785	-0.1120	-0.2880	0.3815	0.4909	0.3815	Z
	33	45.7851	-28.1803	-32.3022	45.8796	-28.4078	-31.9945	-0.0945	-0.2275	0.3077	0.3942	0.3077	Z
	34	42.0902	-27.7057	-35.3940	42.2069	-27.9377	-35.0786	-0.1167	-0.2320	0.3154	0.4086	0.3154	Z
	35	39.1437	-26.6337	-36.8907	39.3390	-26.8137	-36.5875	-0.1953	-0.1800	0.3032	0.4031	0.3032	Z
	36	36.6598	-26.9000	-39.8062	36.8373	-27.1183	-39.4656	-0.1775	-0.2183	0.3406	0.4418	0.3406	Z
A-PILLAR Lateral (Y)	31	52.3444	-30.4829	-28.1792	52.5674	-30.7595	-27.7289	-0.2230	-0.2766	0.4503	0.5736	-0.2766	Y
	32	48.9281	-29.8472	-30.6600	49.0401	-30.1352	-30.2785	-0.1120	-0.2880	0.3815	0.4909	-0.2880	Y
	33	45.7851	-28.1803	-32.3022	45.8796	-28.4078	-31.9945	-0.0945	-0.2275	0.3077	0.3942	-0.2275	Y
	34	42.0902	-27.7057	-35.3940	42.2069	-27.9377	-35.0786	-0.1167	-0.2320	0.3154	0.4086	-0.2320	Y
	35	39.1437	-26.6337	-36.8907	39.3390	-26.8137	-36.5875	-0.1953	-0.1800	0.3032	0.4031	-0.1800	Y
	36	36.6598	-26.9000	-39.8062	36.8373	-27.1183	-39.4656	-0.1775	-0.2183	0.3406	0.4418	-0.2183	Y
B-PILLAR Maximum (X, Y, Z)	37	9.0164	-26.8591	-41.4864	9.0288	-26.9676	-41.3697	-0.0124	-0.1085	0.1167	0.1598	0.1167	Z
	38	12.5167	-28.9539	-35.6837	12.5190	-29.0645	-35.5087	-0.0023	-0.1106	0.1750	0.2070	0.1750	Z
	39	9.7944	-31.5384	-25.7121	9.7565	-31.5245	-25.5216	0.0379	0.0139	0.1905	0.1947	0.1947	X, Y, Z
	40	13.6198	-31.6958	-23.0611	13.5680	-31.7063	-22.8229	0.0518	-0.0105	0.2382	0.2440	0.2438	X, Z
B-PILLAR Lateral (Y)	37	9.0164	-26.8591	-41.4864	9.0288	-26.9676	-41.3697	-0.0124	-0.1085	0.1167	0.1598	-0.1085	Y
	38	12.5167	-28.9539	-35.6837	12.5190	-29.0645	-35.5087	-0.0023	-0.1106	0.1750	0.2070	-0.1106	Y
	39	9.7944	-31.5384	-25.7121	9.7565	-31.5245	-25.5216	0.0379	0.0139	0.1905	0.1947	0.0139	Y
	40	13.6198	-31.6958	-23.0611	13.5680	-31.7063	-22.8229	0.0518	-0.0105	0.2382	0.2440	-0.0105	Y

[A] Positive values denote deformation as inward toward the occupant compartment, negative values denote deformations outward away from the occupant compartment.

[B] Crush calculations that use multiple directional components will disregard components that are negative and only include positive values where the component is deforming inward toward the occupant compartment.

[C] Direction for Crush column denotes which directions are included in the crush calculations. If "NA" then no intrusion is recorded, and Crush will be 0.

Figure E-4. Occupant Compartment Deformation Data – Set 2, Test No. WITD-4

Test Name: WITD-4
VIN: 3C6RR6KT2JG118353
Model Year: 2017
Make: Dodge
Model: Ram 1500

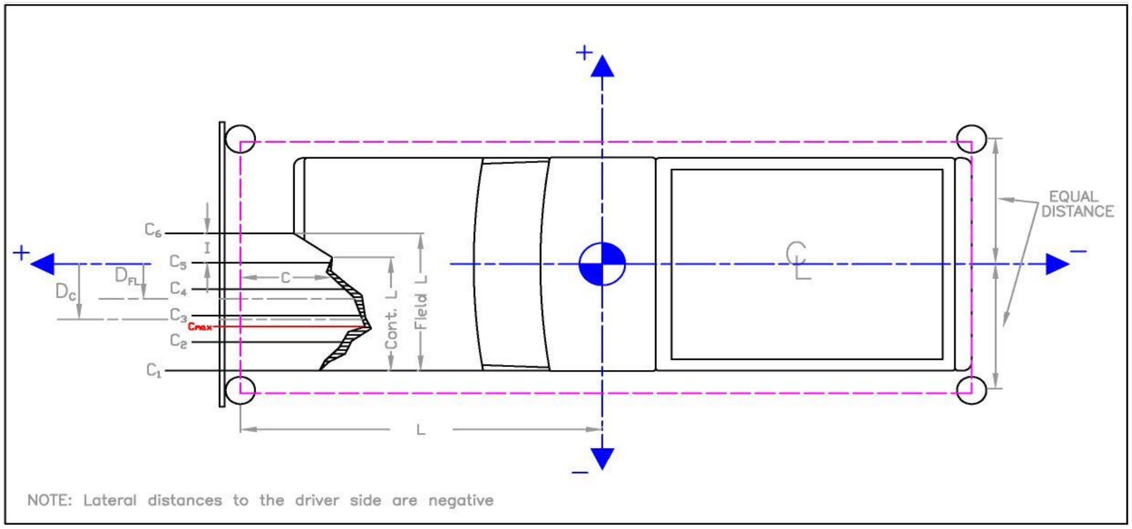

NOTE: Lateral distances to the driver side are negative

	in.	(mm)
Distance from C.G. to reference line - L_{REF}:	117	(2972)
Total Vehicle Width:	77 1/2	(1969)
Width of contact and induced crush - Field L:	77 1/2	(1969)
Crush measurement spacing interval (L/5) - I:	15 1/2	(394)
Distance from center of vehicle to center of Field L - D_{FL}:	0	()
Width of Contact Damage:	23 1/4	(591)
Distance from center of vehicle to center of contact damage - D_C:	-27 1/8	-(689)

NOTE: Enter "NA" for crush measurement if distance can not be measured (i.e., side of vehicle has been pushed inward)
NOTE: All values must be filled out above before crush measurements are filled out.

	Crush Measurement		Lateral Location		Original Profile Measurement		Dist. Between Ref. Lines		Actual Crush	
	in.	(mm)	in.	(mm)	in.	(mm)	in.	(mm)	in.	(mm)
C_1	N/a	N/A	-38 3/4	-(984)	22 1/2	(572)	12	(305)	N/A	N/A
C_2	35 1/4	(895)	-23 1/4	-(591)	6 1/2	(165)			16 3/4	(425)
C_3	16	(406)	-7 3/4	-(197)	4 1/4	(108)			- 1/4	-(6)
C_4	15 5/8	(397)	7 3/4	(197)	4 1/4	(108)			- 5/8	-(16)
C_5	17 3/4	(451)	23 1/4	(591)	6 1/4	(159)			- 1/2	-(13)
C_6	N/a	N/A	38 3/4	(984)	20 1/2	(521)			N/A	N/A
C_{MAX}	35 1/4	(895)	-23 1/4	-(591)	6 1/2	(165)			16 3/4	(425)

Figure E-5. Exterior Vehicle Crush (NASS) – Front, Test No. WITD-4

Test Name: WITD-4 **VIN:** 3C6RR6KT2JG118353

Model Year: 2017 **Make:** Dodge **Model:** Ram 1500

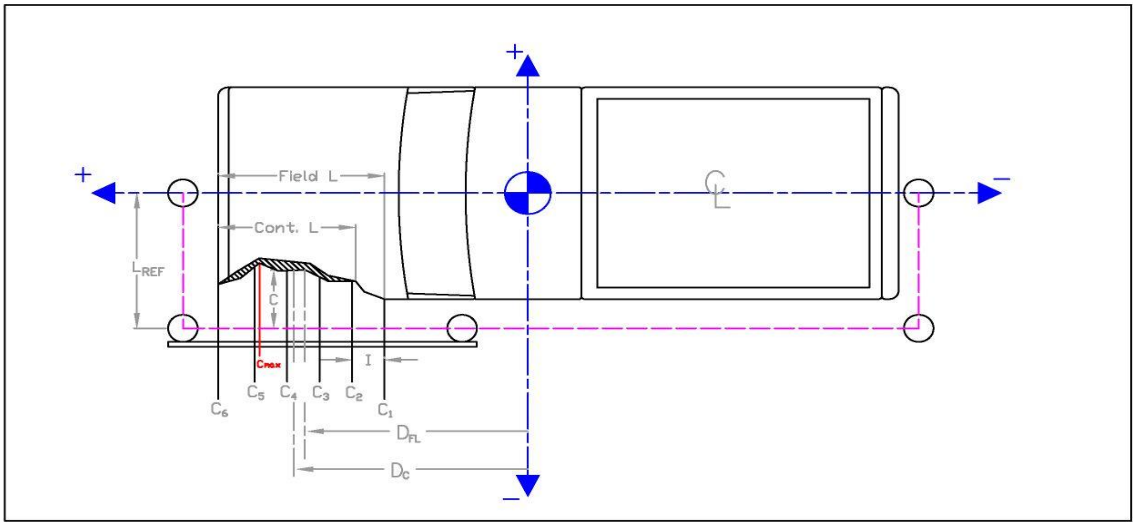

	in.	(mm)
Distance from centerline to reference line - L_{REF}:	50 1/2	(1283)
Total Vehicle Length:	228 1/4	(5798)
Distance from vehicle c.g. to 1/2 of Vehicle total length:	-14 7/8	-(378)
Width of contact and induced crush - Field L:	228 1/4	(5798)
Crush measurement spacing interval (L/5) - I:	45 5/8	(1159)
Distance from vehicle c.g. to center of Field L - D_{FL}:	-14 7/8	-(378)
Width of Contact Damage:	228 1/4	(5798)
Distance from vehicle c.g. to center of contact damage - D_C:	-14 7/8	-(378)

NOTE: Enter "NA" for crush measurement if distance can not be measured (i.e., front of vehicle has been pushed inward or tire has been removed)

NOTE: All values must be filled out above before crush measurements are filled out.

	Crush Measurement		Longitudinal Location		Original Profile Measurement		Dist. Between Ref. Lines		Actual	Crush
	in.	(mm)	in.	(mm)	in.	(mm)	in.	(mm)	in.	(mm)
C_1	N/a	N/A	-129	-(3277)	33 1/2	(851)	6 1/2	(165)	N/A	N/A
C_2	N/a	N/A	-83 3/8	-(2118)	5 1/2	(140)			N/A	N/A
C_3	11 7/8	(302)	-37 3/4	-(959)	5 3/4	(146)			- 3/8	-(10)
C_4	10 3/4	(273)	7 7/8	(200)	5	(127)			- 3/4	-(19)
C_5	N/a	N/A	53 1/2	(1359)	5 3/8	(137)			N/A	N/A
C_6	35 1/4	(895)	99 1/8	(2518)	7 1/4	(184)			21 1/2	(546)
C_{MAX}	28 3/4	(730)	87	(2210)	5 3/4	(146)			16 1/2	(419)

Figure E-6. Exterior Vehicle Crush (NASS) – Side, Test No. WITD-4

Test Name: WITD-4
VIN: 3C6RR6KT2JG118353
Model Year: 2017
Make: Dodge
Model: Ram 1500

Driver Side Maximum Deformation							
Reference Set 1				Reference Set 2			
Location	Maximum Deformation^{A,B} (in.)	MASH Allowable Deformation (in.)	Directions of Deformation^{C}	Location	Maximum Deformation^{A,B} (in.)	MASH Allowable Deformation (in.)	Directions of Deformation^{C}
Roof	0.3	≤ 4	Z	Roof	0.2	≤ 4	Z
Windshield^{D}	0.0	≤ 3	X, Z	Windshield^{D}	NA	≤ 3	X, Z
A-Pillar Maximum	0.5	≤ 5	Z	A-Pillar Maximum	0.5	≤ 5	Z
A-Pillar Lateral	-0.3	≤ 3	Y	A-Pillar Lateral	-0.3	≤ 3	Y
B-Pillar Maximum	0.3	≤ 5	X, Z	B-Pillar Maximum	0.2	≤ 5	X, Z
B-Pillar Lateral	-0.3	≤ 3	Y	B-Pillar Lateral	0.0	≤ 3	Y
Toe Pan - Wheel Well	1.7	≤ 9	X, Z	Toe Pan - Wheel Well	1.8	≤ 9	X, Z
Side Front Panel	0.2	≤ 12	Y	Side Front Panel	0.0	≤ 12	Y
Side Door (above seat)	-1.0	≤ 9	Y	Side Door (above seat)	-1.0	≤ 9	Y
Side Door (below seat)	-0.9	≤ 12	Y	Side Door (below seat)	-1.0	≤ 12	Y
Floor Pan	-0.4	≤ 12	Z	Floor Pan	-0.4	≤ 12	Z
Dash - no MASH requirement	0.4	NA	X, Y, Z	Dash - no MASH requirement	0.4	NA	X, Y, Z

[A] Items highlighted in red do not meet MASH allowable deformations.

[B] Positive values denote deformation as inward toward the occupant compartment, negative values denote deformations outward away from the occupant compartment.

[C] For Toe Pan - Wheel Well the direction of defromation may include X and Z direction. For A-Pillar Maximum and B-Pillar Maximum the direction of deformation may include X, Y, and Z directions. The direction of deformation for Toe Pan -Wheel Well, A-Pillar Maximum, and B-Pillar Maximum only include components where the deformation is positive and intruding into the occupant compartment. If direction of deformation is "NA" then no intrusion is recorded and deformation will be 0.

[D] If deformation is observered for the windshield then the windshield deformation is measured posttest with an examplar vehicle, therefore only one set of reference is measured and recorded.

Notes on vehicle interior crush:

Figure E-7. Driver Side Maximum Deformation, Test No. WITD-4

Appendix F. Accelerometer and Rate Transducer Data Plots, Test No. WITD-4

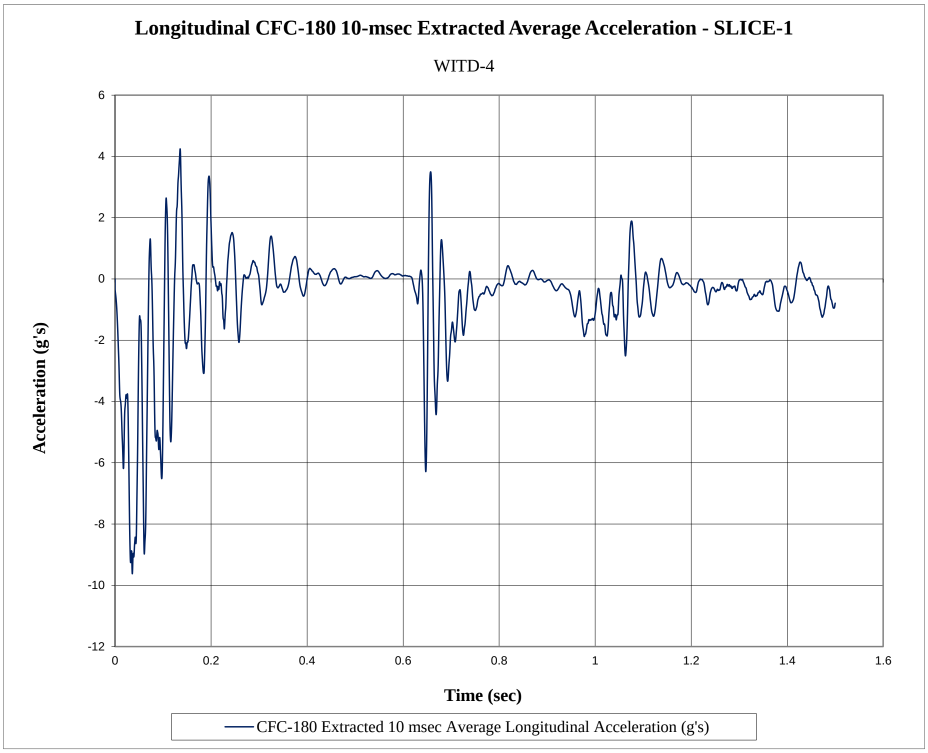

Figure F-1. 10-ms Average Longitudinal Deceleration (SLICE-1), Test No. WITD-4

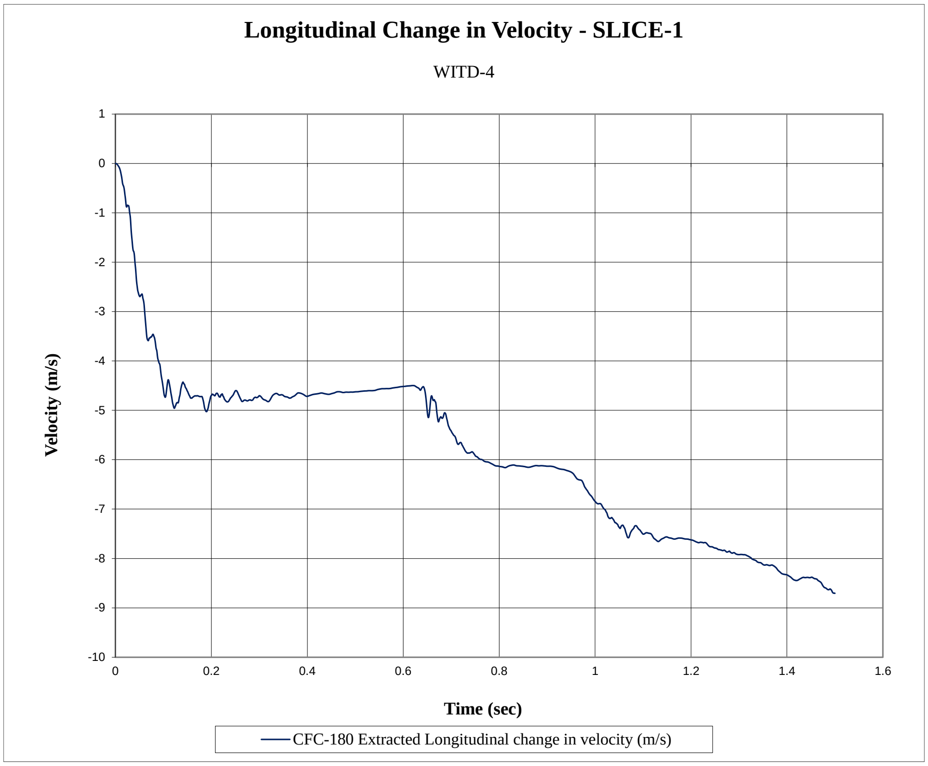

Figure F-2. Longitudinal Occupant Impact Velocity (SLICE-1), Test No. WITD-4

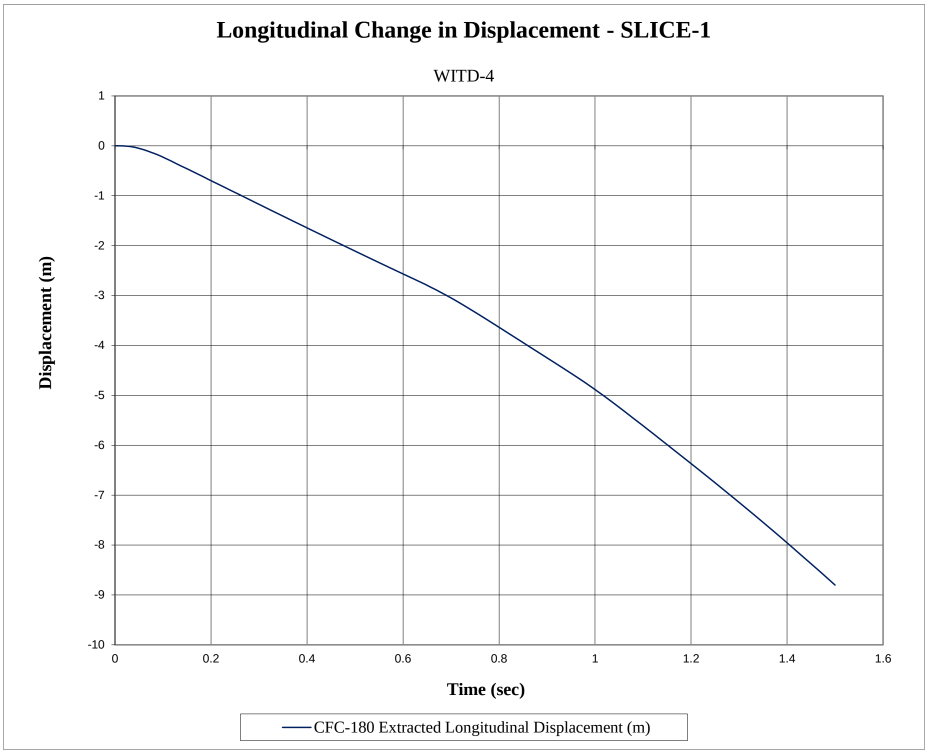

Figure F-3. Longitudinal Occupant Displacement (SLICE-1), Test No. WITD-4

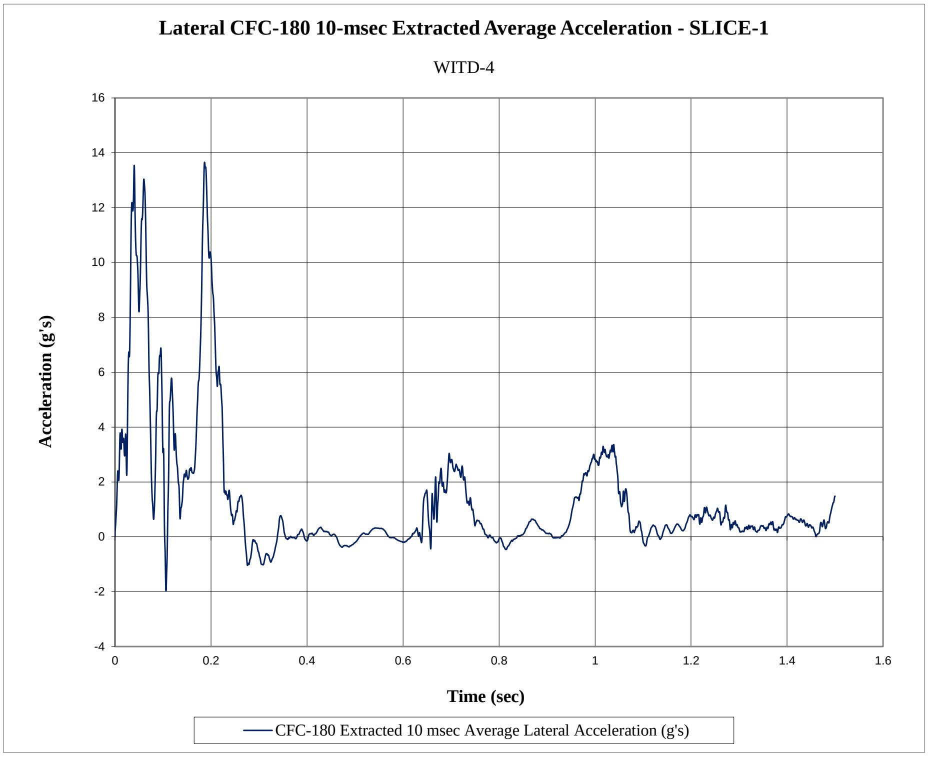

Figure F-4. 10-ms Average Lateral Deceleration (SLICE-1), Test No. WITD-4

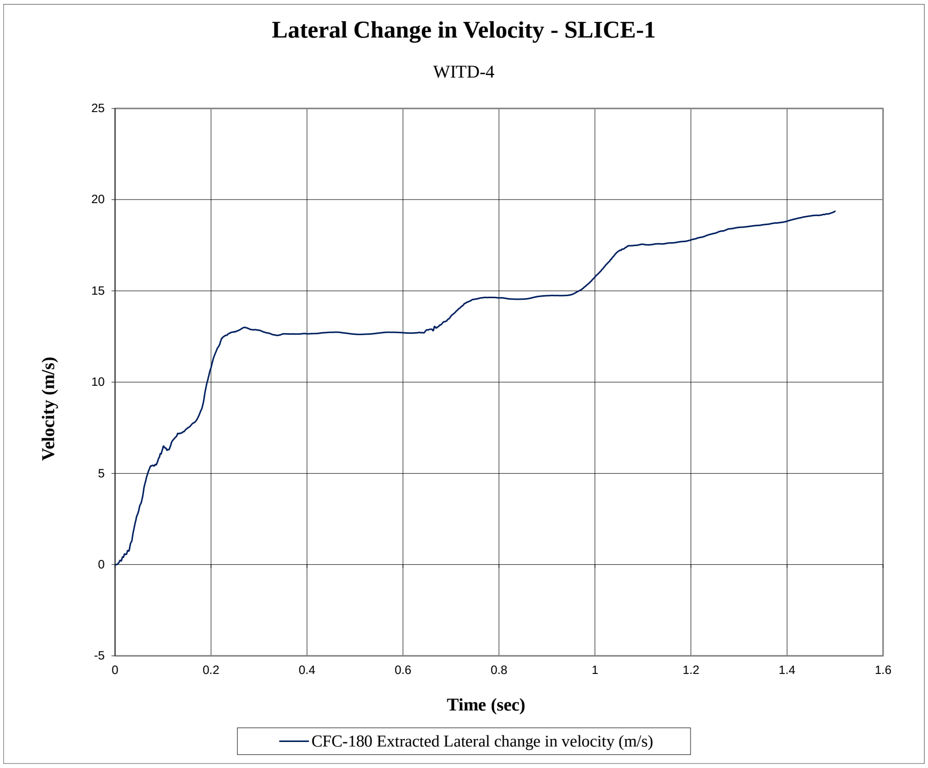

Figure F-5. Lateral Occupant Impact Velocity (SLICE-1), Test No. WITD-4

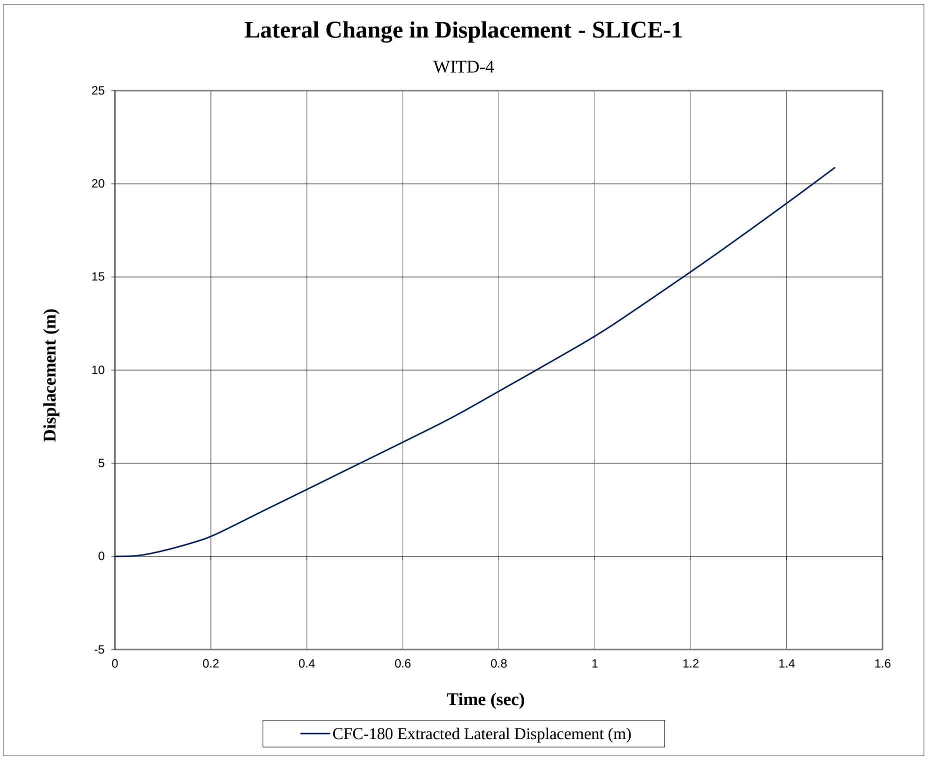

Figure F-6. Lateral Occupant Displacement (SLICE 1), Test No. WITD-4

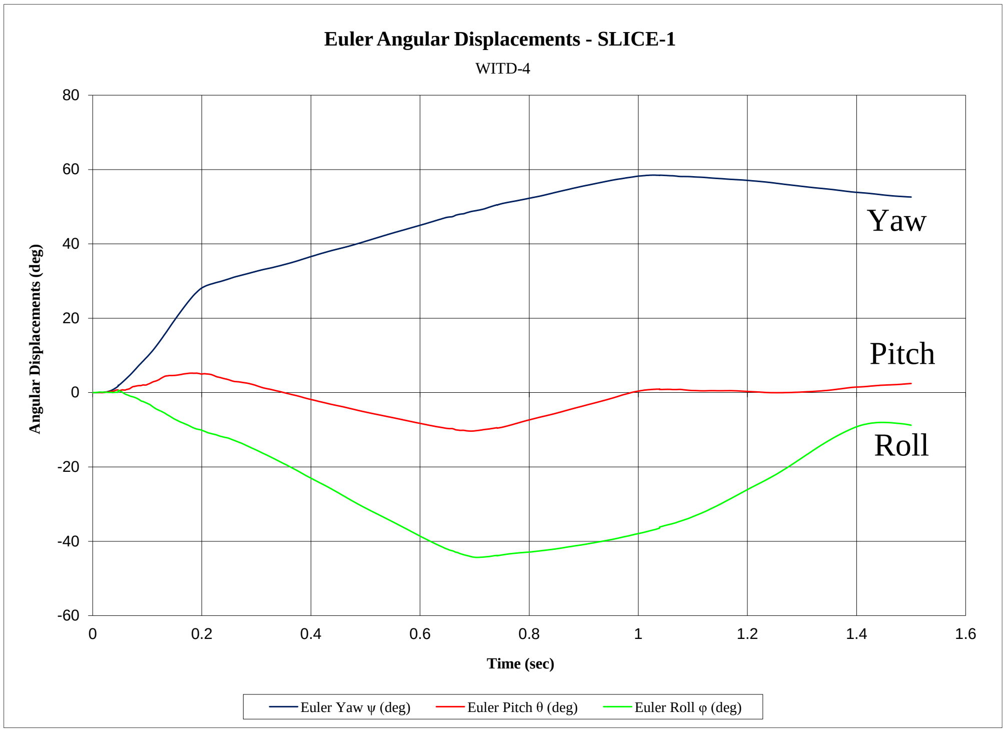

Figure F-7. Vehicle Angular Displacements (SLICE-1), Test No. WITD-4

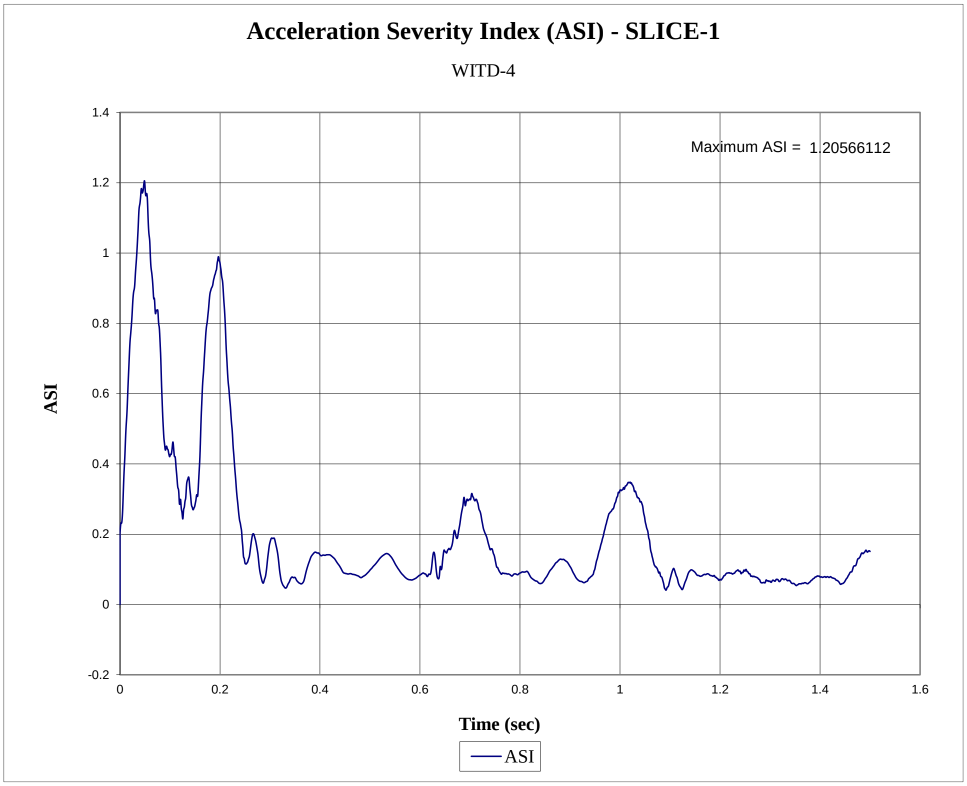

Figure F-8. Acceleration Severity Index (SLICE-1), Test No. WITD-4

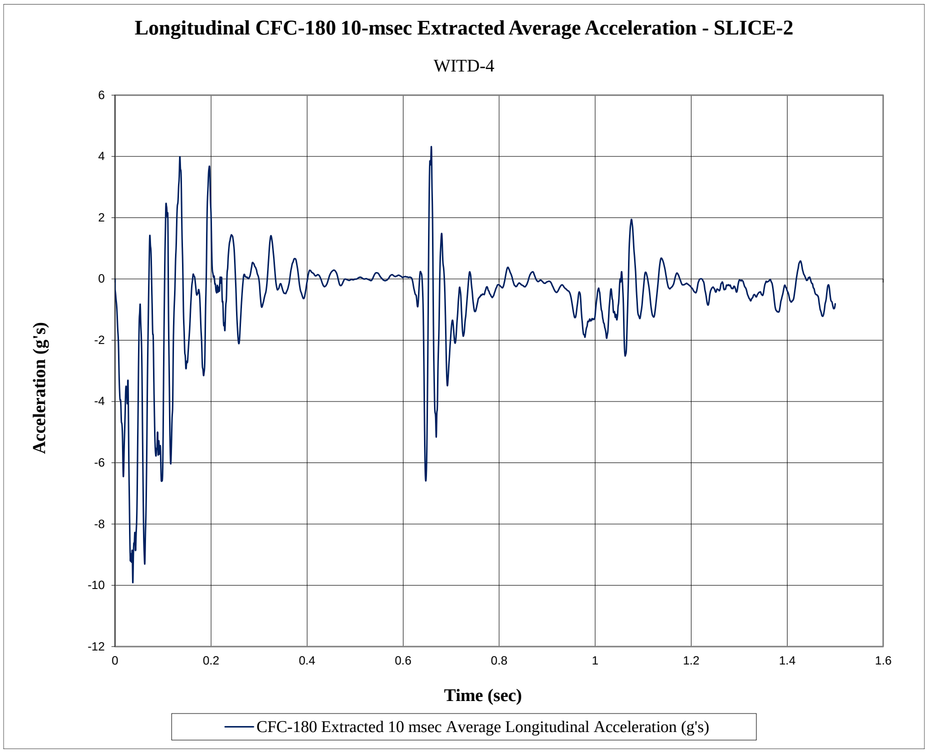

Figure F-9. 10-ms Average Longitudinal Deceleration (SLICE-2), Test No. WITD-4

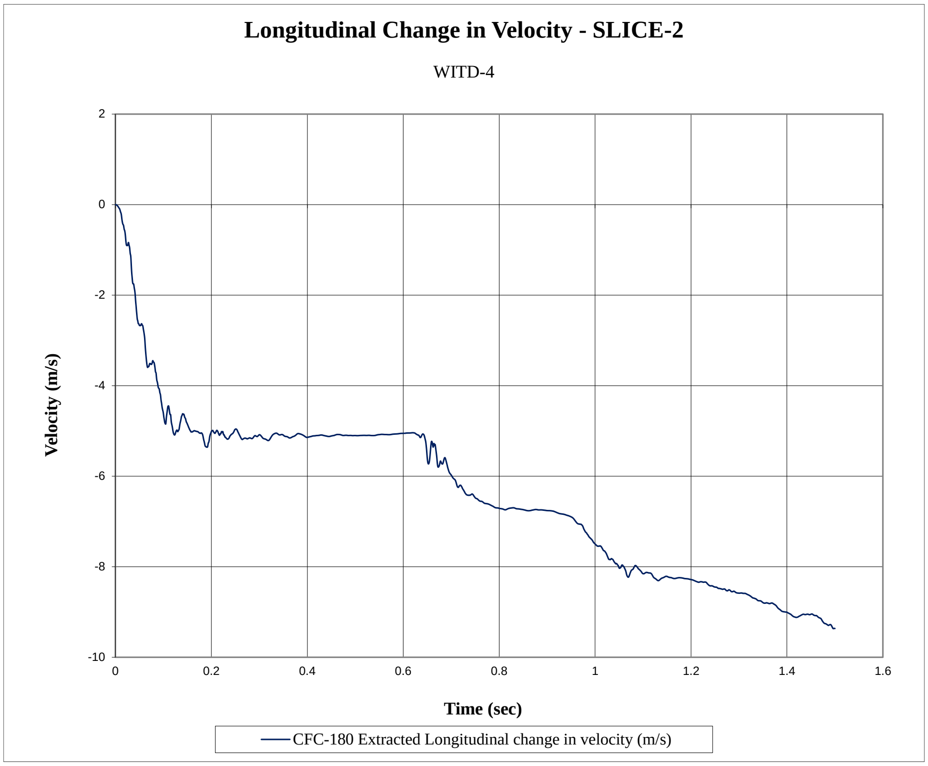

Figure F-10. Longitudinal Occupant Impact Velocity (SLICE-2), Test No. WITD-4

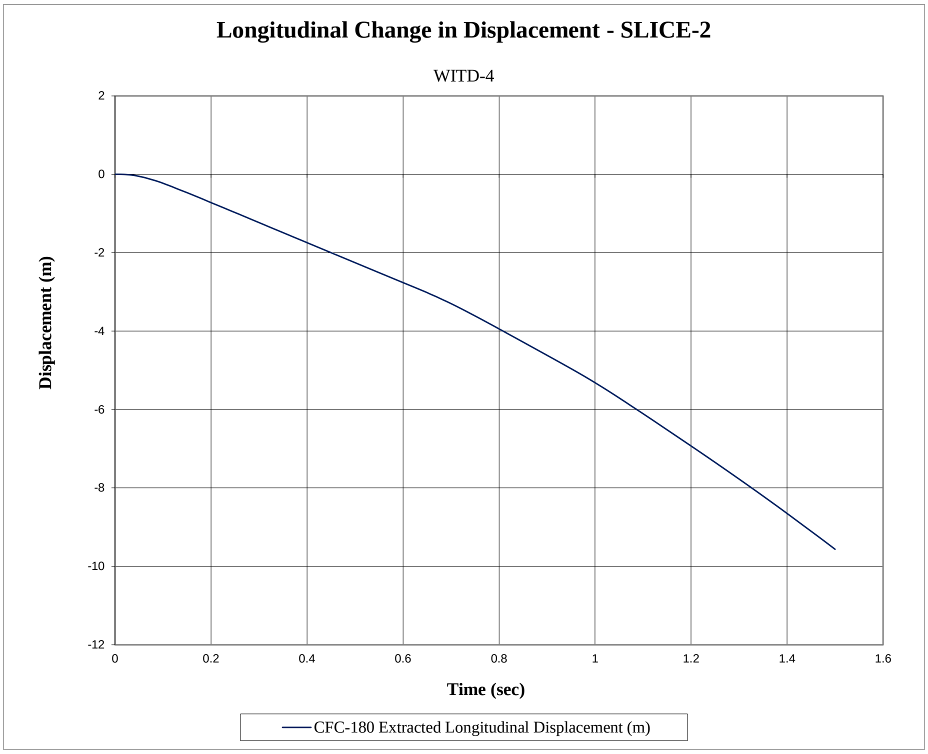

Figure F-11. Longitudinal Occupant Displacement (SLICE 2), Test No. WITD-4

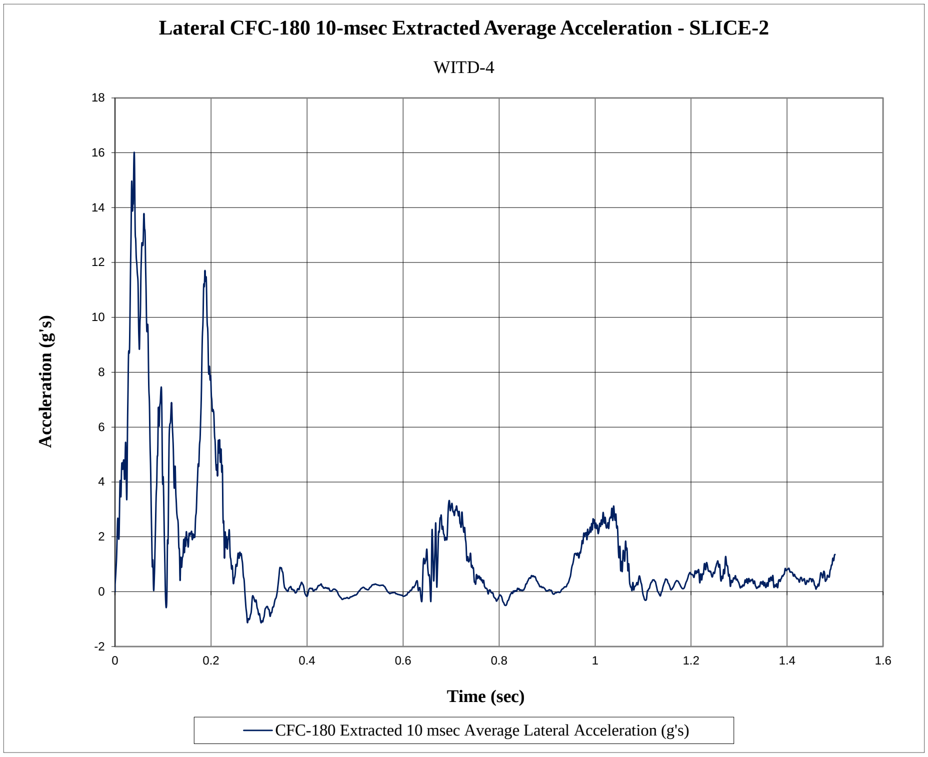

Figure F-12. 10-ms Average Longitudinal Deceleration (SLICE-2), Test No. WITD-4

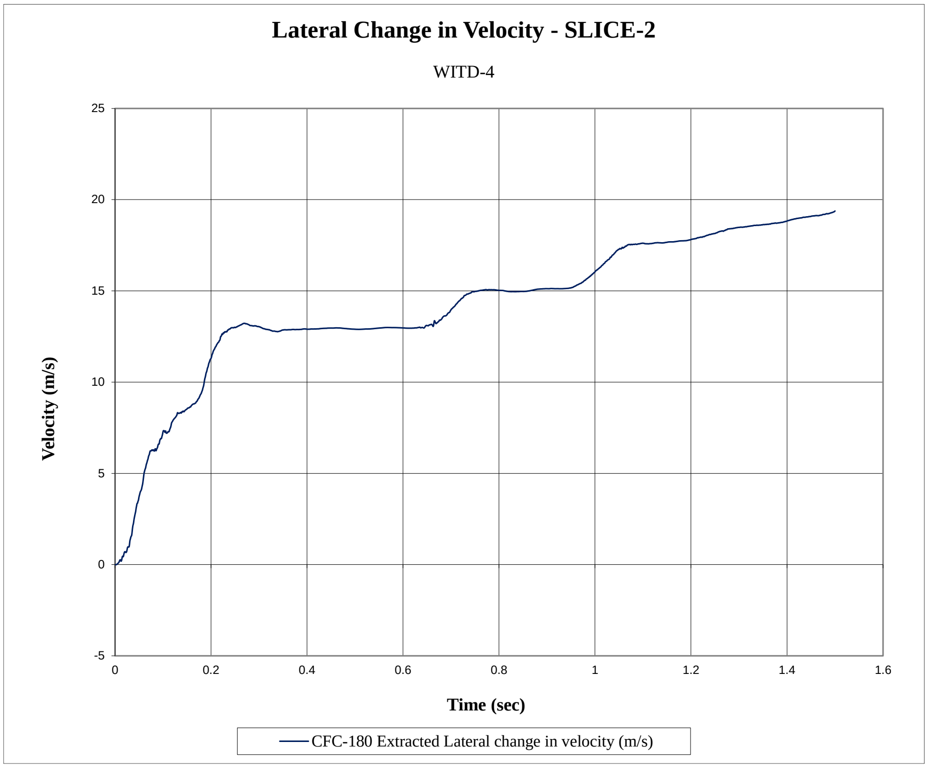

Figure F-13. Lateral Occupant Impact Velocity (SLICE-2), Test No. WITD-4

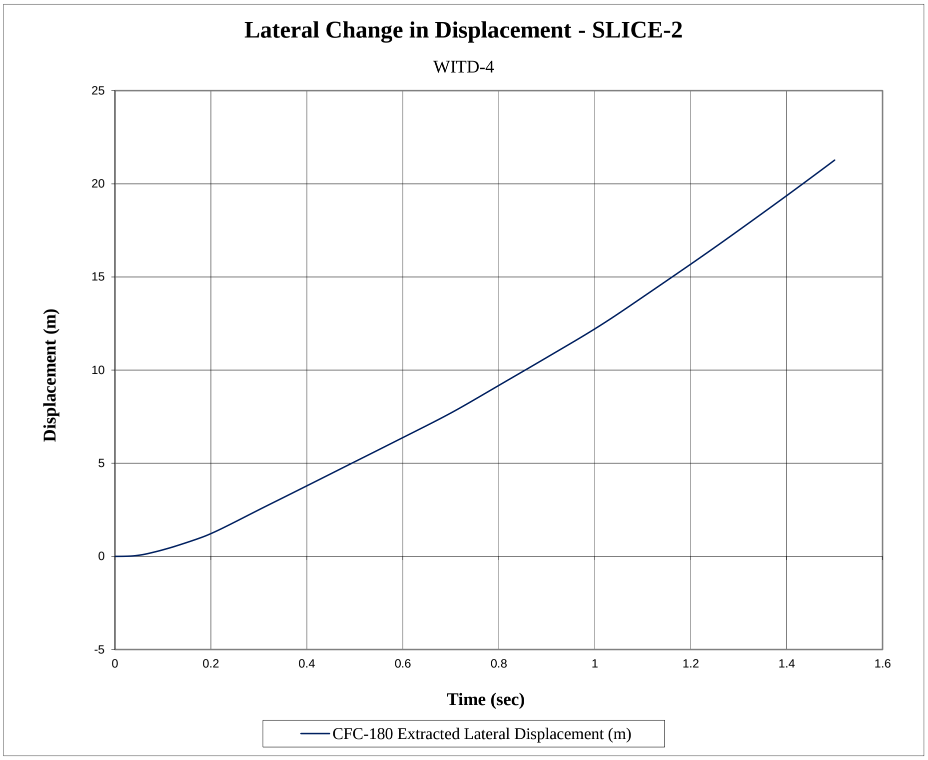

Figure F-14. Lateral Occupant Displacement (SLICE 2), Test No. WITD-4

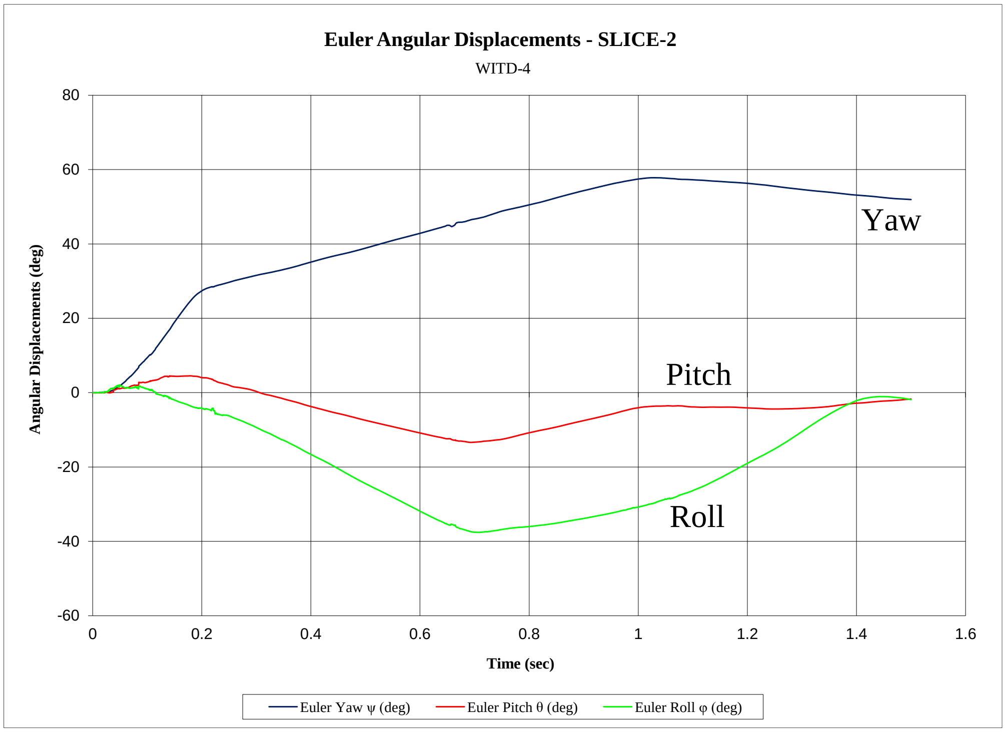

Figure F-15. Vehicle Angular Displacements (SLICE-1), Test No. WITD-4

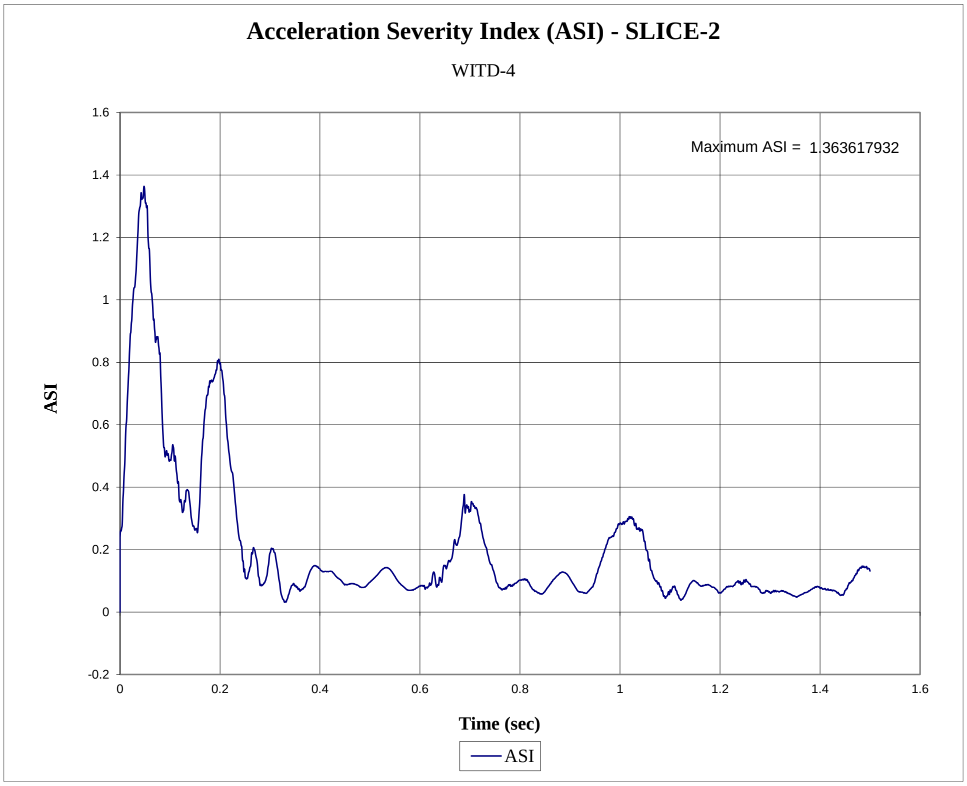

Figure F-16. Acceleration Severity Index (SLICE-1), Test No. WITD-4

END OF DOCUMENT